CECÍLIA PARDO BELLVER

ANATOMICAL AND ELECTROPHYSIOLOGICAL STUDY OF THE VOMERONASAL CIRCUITS: AMYGDALOID RESPONSE TO ODOURS AND PHEROMONES

ANATOMICAL AND ELECTROPHYSIOLOGICAL STUDY OF THE VOMERONASAL CIRCUITS: AMYGDALOID RESPONSE TO ODOURS AND PHEROMONES

CECÍLIA PARDO BELLVER

Estudi anatòmic i electrofisiològic dels circuits vomeronasals: resposta amigdalina a olors i feromones

Doctorat en Neurociències
Dept. de Biologia Cel·lular i Dept. d'Anatomia i Embriologia Humana
Facultat de Biologia i Facultat de Medicina
Universitat de València

2017

VNIVERSITAT ID VALÈNCIA

N'Enrique Lanuza Navarro i En Vicent Teruel Martí, doctors per la Universitat de València i Professors dels Departaments de Biologia Cel·lular i Anatomia i Embriologia Humana de la Universitat de València

CERTIFIQUEN

Que Na Cecília Pardo Bellver, llicenciada en Biologia i Màster en Neurociències Bàsiques i Aplicades per la Universitat de València, ha realitzat sota la seua direcció el treball titulat: **Estudi anatòmic i electrofisiològic dels circuits vomeronasals: resposta amigdalina a olors i feromones**.

Per tal que conste, en compliment de la legislació, signem el present certificat a:

València a 26 de Maig de 2017,

Dr. Enrique Lanuza Navarro   Dr. Vicent Teruel Martí

Small though it is, the human brain can be quite effective when used properly.

The Doctor.

"Pero sí, pero sí, usted está viendo solamente la mitad de la verdad. Y recuerde esto: hemos de empezar de nuevo, dado que nuestra primera lectura de la historia estaba totalmente equivocada."

Race hizo una ligera mueca.

"Ya estoy acostumbrado a esto. A menudo me parece que ese es todo el trabajo de un detective: borrar los falsos comienzos y volver a empezar."

"Sí, esto es muy cierto. Esto es lo que algunas personas no quieren hacer. Conciben una hipótesis y quieren que todo encaje en ella. Si algún dato o pormenor no encaja en la hipótesis, lo rechazan. Pero siempre los hechos que no encajan son los significativos."

Muerte en el Nilo, **Agatha Christie**.

If I go insane, please don't put your wires in my brain.

If, **Pink Floyd**.

ABSTRACT

Rodents detect information concerning the world around them mainly through two chemosensory systems: the olfactory and the vomeronasal systems. In order to develop an appropriate behavioural response to their environment, these systems exhibit both functional and physiological convergence. Further understanding of the organization and function of the olfactory systems would allow us to comprehend how their information is integrated in the brain. In a first approach we performed a thorough analysis of the connections of key structures involved in the processing of vomeronasal information: the medial (Me) and the posteromedial cortical (PMCo) amygdaloid nucleus. Then, we enquire the population activity elicited by olfactory and vomeronasal stimuli in three main structures of the vomeronasal system: the accessory olfactory bulb (AOB), Me and PMCo; and, simultaneously, the activity in the main olfactory bulb (MOB). This will allow us to investigate both the neural circuitry processing olfactory and vomeronasal information and the basic principles of integration of these stimuli.

The PMCo is the unique cortical target of the AOB and should therefore be considered the primary vomeronasal cortex. It coordinates the neural processing of vomeronasal cues, as it receives information from and projects back to each of the structures of the vomeronasal system and shows significant interconnections with the main olfactory system. Also, through its projections to the Me, the ventral hippocampus and the ventral striatum, PMCo directs behavioural responses and contributes to the spatial map of the chemical environment. The Me coordinates the behavioural response to olfactory and vomeronasal cues. It shows a high connectivity among its subdivisions, with the other nuclei of the chemosensory amygdala and with structures of the olfactory system (especially the anterior Me), thus suggesting that the information from these systems is subjected to a complex intrinsic processing before being relayed to other structures. Aside from these, the main efferences of the Me are the bed nucleus of the *stria terminalis* (BST) and the hypothalamus, through which the subdivisions of the Me mediate different behavioural responses. The anterior and posteroventral subdivisions of the Me are mainly involved in defensive behaviours through its connections with the medial posterointermediate BST and the defensive hypothalamic circuit; and, although less dense, they also innervate reproductive-related nuclei per-

haps controlling the inhibition of sexual behaviours. The postero-dorsal subdivision of the Me mediates reproductive behaviours through its projections to the medial posteromedial BST and the hypothalamic reproductive circuit, although some projections to defensive-related nuclei also exist. The emergence of a coherent behaviour relies on the communication between brain regions that are functionally and anatomically specialised. Communication between the AOB and the other nuclei is mediated by theta oscillations, as the AOB shows high phase coupling with the MOB, Me and PMCo. Furthermore, the circuit responds with different oscillatory rhythms depending on the perceived stimulus. The exploration of a neutral stimulus (absence of vomeronasal cues) induces a prominent theta activity with a peak at $4 - 6$ Hz in both olfactory bulbs, the Me and the PMCo; while conspecific-derived stimuli (containing both olfactory and vomeronasal cues) induce oscillatory activity at ≈ 7 Hz. The correlated activation of the bulbs suggests a coupling between the stimuli internalization in the nasal cavity (sniffing) and the vomeronasal pumping. Moreover, the Me shows a characteristic theta peak elicited by male-soiled bedding and the PMCo shows a similar theta peak in response to female-derived stimuli, thus indicating a differential processing within the amygdala related to the sex of the conspecific. During the exploration epochs, the AOB and the amygdaloid nuclei show fast-gamma frequency segments ($90 - 120$ Hz) modulated by the theta waves in AOB; whereas the MOB evidences an increase in the high-gamma band ($60 - 80$ Hz) that were also modulated by the theta in AOB. Thus, particular theta-gamma patterns in the olfactory network modulate the integration of chemosensory information in the amygdala, allowing the selection of an appropriate behaviour.

In summary, the present results show the different levels of convergence of the olfactory and vomeronasal information. We describe the wiring of the amygdaloid structures receiving information from the olfactory bulbs and transferring it to hypothalamic and striatal targets. The different nodes show coupled activity and effective communication, that allow the system to work together as a network for the integration and response to chemosensory cues.

AGRAÏMENTS

"L'Univers ens posa en llocs on podem aprendre, mai són llocs fàcils, però sí els indicats. Estiguem on estiguem, és el moment i el lloc indicat." Aquestes paraules de Delenn, ambaixadora en la Babylon 5, són molt adequades quan pense en el que ha estat fer un doctorat. L'oportunitat d'arribar a aquest moment me la van oferir els meus directors de tesi Quique i Vicent. Fèiem broma en començar el doctorat dient que els doctorands ens assemblem als nostres directors com els fills es pareixen als pares. Ara sé que és veritat i jo he tingut dos directors excel·lents dels que m'he quedat moltes coses bones. De Quique una infinita paciència i la convicció de que quan més pressa tens amb més calma has d'anar, i de Vicent una especial atenció al detall i que l'Office no és suficient. Amb vosaltres he après molt i encara continue aprenent, sou uns professors magnífics i espere haver estat a l'altura, gràcies sempre.

Una altra cosa que he tingut la sort de tenir són els vostres laboratoris. Durant els anys de tesi es creen moltes relacions i el laboratori acaba convertint-se en una família. Gràcies a vosaltres he tingut dos famílies, una a Biologia i una altra a Medicina. En Biologia he tingut uns companys pacients i comprensius, que m'han anat ensenyant com treballar a un laboratori, que han discutit els meus resultats per millorar-los i que mai han perdut el somriure. Beña, treballes més que ningú i ha estat un plaer treballar amb tu; Marcos, m'has renyit sempre amb raó i això m'ha fet millor experimentadora. María i Hugo, vosaltres més que companys sou amics, espere poder compartir més temps amb vosaltres i, per cert, vos dec una partida al Time Stories. A tots els que estàveu i a tots els que esteu: gràcies.

A Medicina he trobat un laboratori nou i ple d'idees. Ana i Joana ha segut un plaer estar amb vosaltres, teníeu molt a en-senyar i jo molt a aprendre. Aina, Arantxa i Sergio, hem tingut que superar el repte de fer un doctorat i ho hem superat junts, gràcies per fer-lo més assolible.

Sens dubte mereix un agraïment especial la meua família. La paciència necessaria per sentir-me parlar durant tants anys d'anatomia i electrofisiologia no es pot pagar. Sóc molt afortu-nada per tenir-vos. I, especialment, volia agrair al meus pares el suport que incondicionalment m'han donat, que ha generat totes les oportunitats i tots els encontres que m'han fet ser qui ara sóc i, més que res, les abraçades que encara em donen.

Per últim, a Sergio. No hi ha paraules suficients per expressar el que significa per a mi que formes part de la meua vida. Hem anat creixent junts des de que ens coneguérem en primer de carrera i once anys després encara em sorprens. Gràcies per compartir la teua vida amb mi. Espere que continues fent-ho. Per tot el que ens espera et diré: *Sunrise on the road behind. Sunset on the road ahead. There's nothing to stop* us *now.*

A tots vosaltres, gràcies.

CONTENTS

LIST OF FIGURES

LIST OF TABLES

ABBREVIATIONS

3V	3rd ventricle
I	layer 1
II	layer 2
III	layer 3
AAA	anterior amygdaloid area
AAD	anterior amygdaloid area, dorsal part
AAV	anterior amygdaloid area, ventral part
ac	anterior commissure
Acb	accumbens nucleus
AcbC	accumbens nucleus, core
AcbSh	accumbens nucleus, shell
ACo	anterior cortical amygdaloid nucleus
AH	anterior hypothalamic area
AHA	anterior hypothalamic area, anterior part
AHi	amygdalohippocampal area
AHP	anterior hypothalamic area, posterior part
AI	agranular insular cortex
AIP	agranular insular cortex, posterior part
AOB	accessory olfactory bulb
AOM	anterior olfactory nucleus, medial part
AON	anterior olfactory nucleus
AOP	anterior olfactory nucleus, posterior part
APir	amygdalopiriform transition area
Arc	arcuate hypothalamic nucleus
AStr	amygdalostriatal transition area
AVPe	anteroventral periventricular nucleus
BAOT	bed nucleus of the accessory tract olfactory
BDA	biotinylated dextranamine
BLA	basolateral amygdaloid nucleus, anterior part
BLP	basolateral amygdaloid nucleus, posterior part
BLV	basolateral amygdaloid nucleus, ventral part

BMA	basomedial amygdaloid nucleus, anterior part
BMP	basomedial amygdaloid nucleus, posterior part
BST	bed nucleus of the *stria terminalis*
BSTIA	BST, intraamygdaloid division
BSTL	BST, lateral division
BSTLD	BST, lateral division, dorsal part
BSTLI	BST, lateral division, intermediate part
BSTLP	BST, lateral division, posterior part
BSTLV	BST, lateral division, ventral part
BSTMA	BST, medial division, anterior part
BSTMPI	BST, medial division, posterointermediate part
BSTMPL	BST, medial division, posterolateral part
BSTMPM	BST, medial division, posteromedial part
BSTMV	BST, medial division, ventral part
CA1	field CA1 of hippocampus
cc	*corpus callosum*
Ce	central amygdaloid nucleus
CeC	central amygdaloid nucleus, capsular part
CeL	central amygdaloid nucleus, lateral division
CeM	central amygdaloid nucleus, medial division
Cl	claustrum
cp	cerebral peduncle
CPu	*caudate putamen*
CxA	cortex-amygdala transition zone
DB	diagonal band
DEn	dorsal endopiriform nucleus
dlo	olfactory tract, dorsal part
DM	dorsomedial hypothalamic nucleus
DTT	dorsal *tenia tecta*
DR	dorsal raphe nucleus
ec	external capsule
Ent	entorhinal cortex
f	fornix
FG	fluorogold
fi	fimbria of the hippocampus
fmi	forceps minor of the *corpus callosum*
Gl	glomerular layer of the MOB
GlA	glomerular layer of the AOB

GrA	granule cell layer of the AOB
GrO	granular cell layer of the MOB
HDB	nucleus of the horizontal limb of the DB
I	intercalated nuclei of the amygdala
ic	internal capsule
ICj	islands of Calleja
ICjM	major island of Calleja
ICjvm	ventromedial island of Calleja
IL	infralimbic cortex
IPAC	interstitial nucleus of the posterior limb of the *ac*
IPl	internal plexiform layer of the MOB
LA	lateroanterior hypothalamic nucleus
La	lateral amygdaloid nucleus
LFP	local field potential
LGP	lateral globus pallidus
LH	lateral hypothalamic area
LHb	lateral habenular nucleus
LMol	*stratum lacumosum moleculare* of hippocampal CA1
lo	lateral olfactory tract
LOT	nucleus of the lateral olfactory tract
LPO	lateral preoptic area
LSD	lateral septal nucleus, dorsal part
LSI	lateral septal nucleus, intermediate part
LSV	lateral septal nucleus, ventral part
LV	lateral ventricle
MD	mediodorsal thalamic nucleus
Me	medial amygdaloid nucleus
MeA	medial amygdaloid nucleus, anterior part
MePD	medial amygdaloid nucleus, posterodorsal part
MePV	medial amygdaloid nucleus, posteroventral part
MGP	medial globus pallidus
Mi	mitral cell layer of the MOB
MI	modulation index
MiA	mitral cell layer of the AOB
ML	medial mammillary nucleus, lateral part
MM	medial mammillary nucleus, medial part
MO	medial orbital cortex
MOB	main olfactory bulb

MPA	medial preoptic area
MPO	medial preoptic nucleus
MS	medial septal nucleus
MTu	medial tuberal nucleus
nfft	nonequispaced fast *Fourier* transform
opt	optic tract
Or	oriens layer of the hippocampus
Pa	paraventricular hypothalamic nucleus
PAG	periaqueductal gray
PB	phosphate buffer
Pe	periventricular hypothalamic nucleus
PH	posterior hypothalamic area
Pir	piriform cortex
PLCo	posterolateral cortical amygdaloid nucleus
PLV	phase-locking value
PMCo	posteromedial cortical amygdaloid nucleus
PMD	premammillary nucleus, dorsal part
PMV	premammillary nucleus, ventral part
Po	posterior thalamic nuclear group
PRh	perhirinal cortex
PrL	prelimbic cortex
PSTh	parasubthalamic nucleus
PT	paratenial thalamic nucleus
PV	paraventricular thalamic nucleus
Py	pyramidal cell layer of the hippocampus
Rad	*stratum radiatum* of hippocampal CA1
Re	reuniens thalamic nucleus
RLi	rostral linear nucleus of the raphe
Rt	reticular thalamic nucleus
S	subiculum
SCh	suprachiasmatic nucleus
SFi	septofimbrial nucleus
SHi	septohippocampal nucleus
SHy	septohypothalamic nucleus
SI	*substantia innominata*
SM	nucleus of the *stria medullaris*
sm	*stria medullaris*
SN	*substantia nigra*

sox	supraoptic decussation
st	*stria terminalis*
STh	subthalamic nucleus
SuM	supramammillary nucleus
TC	*tuber cinereum* area
Tu	olfactory tubercle
VDB	nucleus of the vertical limb of the diagonal band
VEn	ventral endopiriform nucleus
VMH	ventromedial hypothalamic nucleus
VMHC	ventromedial hypothalamic nucleus, central part
VMHDM	ventromedial hypothalamic nucleus, dorsomedial part
VMHVL	ventromedial hypothalamic nucleus, ventrolateral part
VP	ventral pallidum
VTA	ventral tegmental area
VTT	ventral *tenia tecta*
ZI	*zona incerta*

Part I

INTRODUCTION AND OBJECTIVES

1

INTRODUCTION

The perception of the environment is an active process that requires sensory systems to detect, gather and process information about the everchanging world. Active sensing allows an animal to selectively sample regions in space during specific time epochs and this environmental input gives valuable information about the external conditions in which the organism is living, thus enabling it to generate proper behavioural responses for its survival.

In rodents, as macrosmatic mammals, olfactory stimuli play an essential role in the acquisition of information about conspecifics, possible predators and food. Most tetrapods possess two olfactory systems: the main olfactory system and the accessory or vomeronasal system (Ubeda-Bañón et al., 2011). These systems have been identified in some teleost fishes (lungfishes: González et al. 2010), in amphibians (Herrick, 1921; Taniguchi et al., 2008), in reptiles (lizards: Martinez-Garcia et al. 1991; Lohman and Smeets 1993; snakes: Lanuza and Halpern 1998), in marsupials (opossum: McCotter 1912; Scalia and Winans 1975; Martínez-Marcos and Halpern 1999a, 2006) and in placental mammals (first described by Jacobson in 1813, for an English translation see Trotier and Doving 1998; also Ramón y Cajal 1901; McCotter 1912; Scalia and Winans 1975). However, birds do not have a vomeronasal system (Ubeda-Bañón et al., 2011), while in primates the vomeronasal system is poorly developed (platyrrhini), vestigial (hominidae) or lost (catarrhini; Ubeda-Bañón et al. 2011).

The main olfactory system is activated mainly by volatile chemicals (Buck, 1996; Gutiérrez-Castellanos et al., 2010). Odour molecules enter the nasal cavity reaching the main olfactory epithelium, which contains the sensory neurons, and projects to the main olfactory bulb (MOB) for further olfactory information processing. The MOB then projects primarily to the anterior olfactory nucleus, piriform cortex and some cortical amygdaloid nuclei (Martínez-Marcos, 2009). Therefore, the main olfactory system allows the animal to respond to chemical changes in the environment. On the other hand, the accessory olfactory system

is activated by non-volatile chemicals with biological relevance to the individual (Gutiérrez-Castellanos et al., 2010; Chamero et al., 2012). Such chemicals include sexual pheromones (Kimoto et al., 2005; Roberts et al., 2010), chemical signals eliciting aggressive behaviour (Chamero et al., 2007, 2011), predator cues (Takahashi, 2014), illness-derived cues (Rivière et al., 2009), and stress-related signals (Nodari et al., 2008). The chemoreceptive structure of this system, the vomeronasal organ, is located at the base of the nasal septum and sends projections to the accessory olfactory bulb (AOB), which serves as the first processing center of vomeronasal information and mainly projects to the medial and posteromedial cortical nuclei of the amygdala, and the posterior bed nucleus of the *stria terminalis* (Martínez-Marcos, 2009). Therefore, the accessory olfactory system is mainly involved in the detection and response to conspecific and predator cues.

However, even though on anatomical grounds olfactory and vomeronasal information are processed mainly in separated structures, information from both the olfactory and vomeronasal systems should be integrated to allow the generation of a complete picture of the chemical cues present in the environment and the generation of appropriate behavioural responses (Baum and Kelliher, 2009; Keller et al., 2009; Martínez-García et al., 2009). Understanding the performance of these systems requires a dual approach, since knowing the connections and wiring patterns of the brain would not be enough to understand how they give rise to the behaviour of an animal. Even so, revealing the connectivity of a nucleus can lead our reasoning about its function. Thus, we need to know the basic circuitry and then, we must understand how neurons and neuronal systems interact in order to give rise to appropiate behaviours.

From an anatomical perspective, as briefly explained before, the organisation of these sensory systems has been extensively studied (for a review see Martínez-Marcos 2009). Noteworthy, there is a relatively minor, but relevant, direct convergence of olfactory and vomeronasal information in some amygdaloid structures. The amygdaloid complex is an heterogeneous structure both from the anatomical and functional points of view (Swanson and Petrovich, 1998). Within the amygdala, we can roughly outline two functional subsystems, namely the central/ basolateral subsystem and the medial/ cortical subsystem involved in managing two different, but closely related, functions (Martínez-García et al., 2007). The central/ basolateral subsystem coordinates innate and learned reactions of fear/ anxiety/ aversion or of attraction/ reward-directed behaviours to virtually any stimulus. The medial/ cortical subsystem is primarily involved in the coordination of species-specific behavioural responses to chemo-

sensory stimuli (olfactory and vomeronasal) with a strong emotional component. Furthermore, the amygdala includes portions of the pallium: basolateral and cortical; and the subpallium: central (Martínez-García et al., 2007) and medial, the later also has some cell groups derived from the ventral pallidum (García-López et al., 2008). Among these nuclei, those with direct inputs from the MOB are grouped as the "olfactory amygdala" and those with direct inputs from the AOB constitute the "vomeronasal amygdala" (Kevetter and Winans, 1981a,b). Moreover, the term "chemosensory amygdala" refers to both the olfactory and the vomeronasal amygdala (Gutiérrez-Castellanos et al., 2010).

A further examination of the convergent projections of the MOB and the AOB reveals that the anterior division of the medial amygdaloid nucleus receives substantial inputs from both bulbs (Scalia and Winans, 1975; Pro-Sistiaga et al., 2007; Kang et al., 2009, 2011; Cádiz-Moretti et al., 2013). Among the secondary vomeronasal centres, the medial amygdaloid nucleus (Me) is a key structure in the network of neural nuclei controlling sociosexual behaviours in rodents (Swann et al., 2009). This network is composed of a number of interconnected nuclei rich in neurons expressing receptors for sexual steroids, including the Me, the posterior bed nucleus of the *stria terminalis*, the lateral ventral septum and the medial preoptic area (Newman, 1999). Among these structures, only the Me receives convergent projections from both olfactory bulbs. The efferent connections of the Me have been previously studied in male rats (Canteras et al., 1995) and male hamsters (Gomez and Newman, 1992; Coolen and Wood, 1998; Maras and Petrulis, 2010a).

These studies have revealed that the Me is a heterogeneous structure in which at least three subdivisions can be clearly recognised by means of their anatomical connections with different functional systems and their embriological origin. Regarding the neuroanatomical data, the anterior division of the medial amygdaloid nucleus (MeA) is connected with structures implicated in defensive, agonistic as well as in reproductive behaviours. The posterodorsal subdivision (MePD) contains the highest density of androgen and estrogen receptors (Simerly et al., 1990; Cooke, 2006) and is connected mainly with structures implicated in reproductive behaviours (Canteras et al., 1995). And finally, the posteroventral subdivision (MePV) projects preferentially to structures suggested being involved in defensive behaviours (Canteras, 2002). These anatomical subdivisions also fit the expression pattern of genes of the Lhx family of transcription factors. Thus, the MeA expresses mainly Lhx5, the MePD Lhx6, and the MePV Lhx9 (Choi et al., 2005). Recent studies on the developmental origins of the Me cells (García-López

et al., 2008; García-Moreno et al., 2010; Bupesh et al., 2011) have shown that the Lhx9-expressing cells of the MePV originate in the ventral pallium, and consequently are glutamatergic projection neurons (Choi et al., 2005). In contrast, the Lhx6 neurons of the MePD are GABAergic cells originated in the caudoventral medial ganglionic eminence (and therefore they are neurons of pallidal nature). Finally, the MeA contains a population of Lhx5-expressing neurons originated in the hypothalamic supraopto-paraventricular domain (Abellán et al., 2010) and also abundant nitrergic cells originated from the commissural preoptic area (Hirata et al., 2009; Bupesh et al., 2011). The neuroanatomical and developmental data discussed are consistent with a number of functional studies in several rodent species. In mice and hamsters, the MeA has been shown to be activated by sexual and non-sexual social odours and also by chemicals derived from hetero-specific individuals (Meredith and Westberry, 2004; Samuelsen and Meredith, 2009). Thus, the MeA seems to categorise the detected chemical stimuli and then relay sex-related information to the MePD (Petrulis, 2009; Maras and Petrulis, 2010b), which consequently is mainly activated by sexually related chemical signals (hamsters: Fernandez-Fewell and Meredith 1994; Kollack-Walker and Newman 1997; mice: Choi et al. 2005; rats: Bressler and Baum 1996; gerbils: Heeb and Yahr 1996). Accordingly, electrolytic lesions of the transition between the MeA and the MePD are most effective in abolishing the attraction of female mice for sex-derived chemical signals (DiBenedictis et al., 2012). Similar results have been obtained in male hamsters with lesions that functionally disconnect the MeA and the MePD (Maras and Petrulis, 2010c). On the other hand, the MePV displays a strong response when mice are exposed to predator (cat) odours (Choi et al., 2005; Samuelsen and Meredith, 2009), a response that has been also reported in rats exposed to cat odours (Dielenberg et al., 2001).

Surprisingly, the efferent connections of the Me in mice have been only partially examined in a single study, which reports data in males mainly regarding the MePD (Usunoff et al., 2009). Given that mice are widely use in behavioural neuroscience studies, due to the availability of genetically modified animals that allow exploring the molecular basis of behaviour, it is of interest to obtain direct anatomical data in this species.

On the other hand, among the secondary vomeronasal structures, the posteromedial amygdaloid nucleus (PMCo), which receives direct projections from the AOB (Winans and Scalia, 1970; Scalia and Winans, 1975; Von Campenhausen and Mori, 2000), is the only one with a pallial origin (Martínez-García et al., 2007; Medina et al., 2004). In fact, the PMCo displays a characteristic

cortical lamination, which depends on Reelin (Boyle et al., 2011). In this laminar organization we can distinguish a molecular layer I, receiving vomeronasal projections (Von Campenhausen and Mori, 2000), that is positive for calretinin, neuropilin and acetyl cholinesterase (Kemppainen et al., 2002; Gutiérrez-Castellanos et al., 2010). Calretinin appears to be a marker of chemosensory inputs (Wouterlood and Härtig, 1995), whereas neuropilin and acetyl cholinesterase appear to be specific markers for the vomeronasal pathway (Gutiérrez-Castellanos et al., 2010). Deep to the molecular layer I, an outer cell layer II is present, which shows a relatively dense amount of packed cells with small cell bodies. Finally, a deep cell layer III can be observed, composed of neurons with larger cell bodies quite polymorphic and with inner limits, which are not easy to delineate. The histochemical detection of vesicular zinc is helpful to trace the boundary between layers II and III (Kemppainen et al., 2002). To our knowledge, only partial data about its afferent and efferent projections is available (hamsters: Kevetter and Winans 1981a; rats: Canteras et al. 1992; Kemppainen et al. 2002; sheep: Meurisse et al. 2009). Among the main projections of the PMCo described in the rat, it is worth mentioning a massive glutamatergic projection to the granular layer of the AOB, which provides a feedback loop at the sensory level and modulates the pheromone signal processing (Fan and Luo, 2009; Martínez-Marcos and Halpern, 1999b). This feedback projection, together with its laminar organisation and its pallial origin, suggest the idea that the PMCo should be considered the primary vomeronasal cortex. Therefore, the PMCo is the only case of a mammalian primary sensory cortex in which hodological information is incomplete.

Very few studies have tackled the behavioural or functional role of the PMCo. Romero et al. (1990) reported that lesions of the PMCo of female rats decreased the time that they spent in the proximity of a caged intact male as compared to a castrated male. However, a study on the effects of lesions of the PMCo in sexual behaviour of hamsters (Maras and Petrulis, 2008) reported no alterations of the preference for the urine of a conspecific of the opposite sex, but showed a mild alteration in copulatory behaviour. Further anatomical and functional studies are therefore needed to clarify the function of this nucleus. Moreover, recent studies in genetically modified mice have revealed important aspects of how vomeronasal information drives sociosexual behaviour (Chamero et al., 2012). In addition, several male sexual pheromones (Leinders-Zufall et al., 2000; Haga et al., 2010), as well as predator signals (Papes et al., 2010; Isogai et al., 2011), have been identified as vomeronasal stimuli in mice. However, neuroanatomical data have not been obtained in mice in parallel

to this information about the vomeronasal system and its natural signals.

From the physiological perspective, oscillations, as evidenced by the local field potentials (LFP), reflect a functional condition of interconnected neuronal groups. In the olfactory system, the olfactory sensation depends on stimulus acquisition, an active mechamism known as sniffing, driven by the respiratory rhythm (Kepecs et al., 2006; Kay et al., 2009). The sniffing is a dynamic, animal-controlled behaviour (Welker, 1964; Youngentob et al., 1987; Kepecs et al., 2007; Wesson et al., 2008). During normal breathing, odorants are passively sampled at low frequency $1 - 4$ Hz, a behaviour typically observed in familiar environments (Welker, 1964; Kepecs et al., 2007). In the presence of a novel odorant, there is an increase in the respiration rate to active odour sampling (sniffing) at $4 - 12$ Hz (Youngentob et al., 1987; Kepecs et al., 2006; Verhagen et al., 2007; Wesson et al., 2008). Thus, sniffing imposes a temporal structure on olfactory input that shapes how odour information is conveyed from the periphery to the MOB (Kepecs et al., 2006; Verhagen et al., 2007). Many studies have characterised odour representation in the MOB, mainly in anesthetised animals (Adrian, 1950; Macrides and Chorover, 1972; Neville and Haberly, 2003; Lin et al., 2005), through single cell recordings (Lin et al., 2005; Bathellier et al., 2008), local field activity recordings (Ravel et al., 2003; Beshel et al., 2007) or through calcium imaging (Wachowiak and Cohen, 2001; Verhagen et al., 2007). The relationship between the neural activity in the MOB and the sniffing cycle has been extensively studied. The first studies reported a temporal coupling between the dynamics of neural activity and rhythmic odour sampling (Adrian, 1950; Macrides and Chorover, 1972), with frequencies within the theta band modulating higher frequencies (Adrian, 1950; Neville and Haberly, 2003; Kay et al., 2009), typically beta ($15 - 30$ Hz) and gamma ($30 - 120$ Hz) ranges. There is evidence indicating that these oscillations play a key role in the discrimination of odorants (Beshel et al., 2007; Rojas-Líbano and Kay, 2008; Kay and Beshel, 2010) and in olfactory learning (Ravel et al., 2003; Martin and Ravel, 2014).

However, little is known about the particular oscillatory activity in the vomeronasal system. As in the main olfactory system, the internalisation of the stimuli may drive an oscillatory pattern in the vomeronasal system. Since some of the vomeronasal stimuli are high molecular weight non-volatile molecules, the vomeronasal organ presents a particular mechanism to introduce these molecules into the organ. This mechanism, described as vomeronasal pumping (Meredith and O'Connell, 1979; Wysocki et al., 1980), relies on the control of the vasodilatation of a

blood vessel located in the lumen of the organ. Hypothetically, repeated contraction and dilatation of this blood vessel would generate successive negative and positive pressure able to suck stimuli into the vomeronasal organ and clear the lumen in a cyclic manner. However, not much information is available about the response of the vomeronasal system to such cycling activity. The exposure to novel stimuli induces an increase in the frequency of the vomeronasal pumping (Meredith, 1994) and the vomeronasal receptor neurons increase their firing rate (Holy et al., 2000; Meeks et al., 2010). In the AOB, the neurons respond with an increase in the firing rate (Luo et al., 2003; Ben-Shaul et al., 2010; Meeks et al., 2010), that corresponds with an increase in the population activity with a predominant peak in the theta frequency band (Binns and Brennan, 2005; Tendler and Wagner, 2015). This oscillatory pattern has been suggested to be specific for social stimuli (Tendler and Wagner, 2015) and appears to reflect a state that promotes neuronal communication between brain regions (Buzsáki, 2006).

The mechanisms of information processing in the medial and posteromedial cortical amygdaloid nuclei are still unknown. A few previous studies have approached the role of the medial amygdala in the context of a social recognition paradigm (Binns and Brennan, 2005; Bergan et al., 2014; Tendler and Wagner, 2015) or have described the nature of its neurons, as morphologically and physiologically heterogeneous (Niimi et al., 2012). In the case of the posteromedial cortical amygdaloid nucleus, to our knowledge, no comprehensive study of the response of the PMCo to vomeronasal stimuli has been performed. Although, there is a report about electrical stimulation of either the main olfactory bulb or the vomeronasal organ could drive some of the same units in the PMCo, thus suggesting the convergence of input from these systems onto single neurons in the vomeronasal amygdala (Licht and Meredith, 1987).

It is unknown whether sniffing behaviour and vomeronasal pumping mechanism are independent and, consequently, the cyclic activities generate different and independent patterns of oscillations in the centers of the main and accessory olfactory systems. Alternatively, olfactory sniffing and vomeronasal pumping could work in a synchronic fashion and, accordingly, activity in the vomeronasal system would be coupled to the theta, beta and gamma rhythms described in the main olfactory system. The descriptions of olfactory processing in the awake animals would facilitate understanding basic principles of the olfactory and vomeronasal systems function. Therefore, this thesis evaluates the neuronal population activity in the vomeronasal system, including key structures of the vomeronasal amygdala,

and the common aspects of the olfactory and vomeronasal oscillations that allow the integration of both types of chemosensory information.

2

OBJECTIVES

The general objective of this doctoral thesis is to expand our understanding of the organisation and function of the olfactory and vomeronasal systems, and how information from both systems is integrated to allow the generation of a complete picture of the chemical cues present in the environment and the generation of appropriate behavioural responses.

Understanding the performance of these systems requires a dual approach. First, we will elucidate the connectivity of key amygdaloid structures receiving projections from the main and the accessory olfactory bulbs. Second, we will try to understand how these neuronal systems interact.

There are several reasons to perform the present study in females. First, our previous behavioural studies have been focused on the sexual attraction that females display towards male pheromones (Martínez-García et al., 2009). Second, as most of the previous data in rats and hamsters have been obtained in males, with almost no information available in females, this will allow comparison of male and female projections. Finally, this work continues the analysis of the neural circuitry processing vomeronasal information in the brain of female mice (Cádiz-Moretti et al., 2013, 2016b).

The particular objectives are detailed below:

1. Description of the efferent connections of the medial amygdaloid nucleus in mice.

   As previously mentioned, prior descriptions in mice have been partially made in males, mainly regarding the MePD (Usunoff et al., 2009). Given that mice are widely use in behavioural neuroscience studies, it is of interest to obtain direct anatomical data in this species. In addition, there are relevant differences in distinct strains of mice regarding reproductive (Vale et al., 1973, 1974; Burns-Cusato et al., 2004; Dominguez-Salazar et al., 2004) and defensive (Belzung et al., 2001; Yang et al., 2004) behaviours, which are major functions of the Me. Thus, in the present study we compare

the efferent projections of the Me of the C57BL/6J and CD1 strains of mice.

2. Description of the afferent and efferent connections of the posteromedial cortical amygdaloid nucleus in mice.

   The PMCo, besides receiving projections from the AOB, has a feedback projection to the AOB that would modulate the processing of vomeronasal signals (Fan and Luo, 2009; Martínez-Marcos and Halpern, 1999b). This fact, together with its laminar organization and pallial origin, suggest that the PMCo could be the primary vomeronasal cortex. The connections of the PMCo have been partially described in male hamsters (Kevetter and Winans, 1981a), rats (Canteras et al., 1992; Kemppainen et al., 2002) or sheeps (Meurisse et al., 2009). In the present study, we aim to provide a comprehensive report of the afferent and efferent connections of the PMCo of female mice.

3. Evaluation of common aspects of the olfactory and vomeronasal oscillations that allow the integration of both types of chemosensory information.

   Therefore, we have performed recordings of neuronal population activity in awake, freely behaving female mice, to which we presented different chemical stimuli. These chemicals include two neutral odorants (clean and geraniol-scented bedding), detected by the main olfactory system, and three complex chemosensory stimuli (intact male- and female-soiled bedding and also bedding soiled by castrated males), which contain both olfactory and vomeronasal chemical signals. The male-soiled bedding contains attractive male sexual pheromones (Martínez-Ricós et al., 2007), which allows us to compare the activity of the different nodes of the vomeronasal system and the olfactory bulb in the context of sociosexual communication. In each animal, the recording electrodes were located in the MOB and AOB, as well as in the Me and the PMCo. These recording sites allow us to characterise the pattern of oscillatory activity in the main centers of the vomeronasal system and, at the same time, to evaluate to what extent they are different and independent from the sniffing-induced olfactory oscillations present in the MOB. The recording of local field activity in free-behaving animals would facilitate understanding basic principles of the integration of olfactory and vomeronasal information.

Part II

PROJECTIONS FROM THE MEDIAL
AMYGDALOID NUCLEUS

3

MATERIALS AND METHODS

3.1 ANIMALS

For the present study, we used 17 adult (at least 2 months of age) female mice (*Mus musculus*), from the C57BL/J6 (n = 9) and the CD1 (n = 6) strains (Charles River, France) with body weights between $18.1 - 25.1$ g and $37.5 - 45.1$ g, respectively. Animals were housed in cages with water and food available *ad libitum*, either in natural conditions or in a 12 h light: dark cycle, at $21 - 22°$C. We treated them according to the EEC guidelines for European Communities Council Directives of 24th November 1986 (86/609/EEC), and experimental procedures were approved by the Committee of Ethics on Animal Experimentation of the University of Valencia.

3.2 SURGICAL PROCEDURES

3.2.1 *Tracer injections*

To study the projections arising from the different divisions of the medial amygdaloid nucleus (anterior, posteroventral and posterodorsal), we performed iontophoretic injections of two different dextranamine conjugates as anterograde tracers. Biotin-conjugated dextranamine (BDA, 10000 MW, lysine fixable; Invitrogen, USA) was used diluted at 5% in phosphate buffer (PB, 0.01 M, pH 8.0), and tetrametylrhodamine-conjugated dextranamine (RDA, fluoro-ruby, 10000 MW, lysine fixable; Molecular Probes, USA) was used diluted at 10% in PB (0.01 M, pH 7.6). We delivered the tracers from glass micropipettes ($10 - 50$ μm diameter tips) by means of positive current pulses (7on/7off s, $3 - 5$ μA, $10 - 15$ min) using a current generator (Midgard Precision Courrent Source, Stoelting, USA). To reduce the leakage of tracer along the pipette track, a time lapse of $2 - 5$ minutes passed after the termination of each injection before the pipette was withdrawn. A continuous negative retentaining cur-

rent ($-0.8\ \mu$A) was applied during the entrance and withdrawal of the micropipette to avoid diffusion of the tracer.

3.2.2 *Surgery*

For surgery, 6 of the animals were anaesthetised with an intraperitoneal injection of a 3:2 ketamine (75 mg/kg; Merial laboratorios, Spain) and medotomedine (1 mg/kg; Pfizer, Spain) solution, complemented with atropine (0.04 mg/kg, iperitoneal; Sigma, USA) to reduce bronchial and salivary secretions and cardio-respiratory depression. The other 11 animals were anaesthetised through inhalation of isofluorane (1.5%) delivered in oxygen (0.9 L/min; MSS Isoflurane Vaporizer, Medical Supplies and Services Int'l Ltd, UK) using a mouse anaesthetic mask. All the animals received a butorfanol injection (5 mg/kg, subcutaneous; Fort Dodge Veterinaria, Spain) as analgesic. The depth of anaesthesia was monitored before the procedure by observing the loss of the righting, palpebral reflexes and pedal reflex (toe pinch), response to painful stimulation, and rate and depth of respiration; and during surgery, by monitoring the rate and depth of respiration, eye blinking and whisker movements. To maintain normal body temperature the animals were on top of a thermic blanket and to prevent eye desiccation eye-drops were applied (Siccafluid, Thea S.A Laboratories, Spain). After fixing the mouse head in the stereotaxic apparatus (963-A; David Kopf, USA) a small incision was made in the skin revealing the skull surface, then the skull landmarks (Lambda and Bregma) were set in the same horizontal plane and we drilled a small hole above the medial amygdala. Following tracer injection, we closed the wound with Histoacryl (1050052; B.Braun, Germany). After surgery, animals anaesthetised with the ketamine:medotomedine solution received then injections of atipamezol (1 ml/kg, subcutaneous; Pfizer) to revert the medotomedine effects.

In the first nine tracer injections (performed in C57 mice) we observed that labelled fibres in the contralateral hemibrain were absent or negligible (see 4), so we decided to perform one injection per hemisphere in the rest of the mice, to minimise the number of animals. Following Paxinos and Franklin (2004), in C57 mice we used coordinates shown in table 1 relative to Bregma. These were adapted to CD1 mice and the resulting coordinates are shown in table 1 as well.

3.3 HISTOLOGY

Six to eight days after the surgery, animals were deeply anaesthetised with an overdose of sodium pentobarbital (90 mg/kg,

Table 1: Coordinates of the injection sites (in mm) relative to Bregma.

		Antero Posterior	Lateral	Depth
C57BL/J6	MeA	−1.1	−2.0	−2.25
	MePD	−1.7	−2.2	−5.2
	MePV	−1.94	−2.1	−5.3
CD1	MeA	−1.4 to −1.7	±2.1	−5.1
	MePD	−1.9	±2.1	−5.1 to −5.3
	MePV	−1.9	±2.1	−5.1 to −5.48

intraperitoneal; Sigma). Then the animals were transcardially perfused with 20 ml of saline solution (0.9%, NaCl) followed by 60 ml of 4% paraformaldehyde diluted in PB (0.1 M, pH 7.6). Brains were removed from the skull, postfixed for 4 h in the same fixative and cryoprotected with 30% sucrose solution in PB (0.1 M, pH 7.6) at 4°C until they sank. Using a freezing microtome we obtained frontal sections (40 μm) through the brain that were collected in four matching series. In some animals, the olfactory bulbs were cut at 30 μm.

3.3.1 *Tracer detection*

For the detection of BDA, we inactivated the endogenous peroxidase with 1% H_2O_2 in Tris buffer saline (TBS, 0.05 M, pH 7.6) for 15 min and then the sections were incubated for 90 min in ABC complex (Vectastain ABC elite kit, Vector Labs, USA) diluted 1:50 in TBS-Tx (Triton X-100, 0.3%; in TBS 0.05 M, pH 7.6). After rinsing thoroughly with buffer, we developed the peroxidase activity with 0.025% diaminobenzidine in PB (0.1 M, pH 8.0), with 0.01% H_2O_2 and 0.1% nickel ammonium sulphate to darken the reaction product.

For the RDA immunohistochemical detection, we inactivated the endogenous peroxidase as previously described. Then, sections were incubated overnight in a specific primary antibody against tetrametylrhodamine raised in rabbit (Molecular Probes, Cat. #A-6397) diluted 1:4000 in TBS-Tx, followed by a standard peroxidase-antiperoxidase (PAP) method (goat anti-rabbit IgG, 1:100, Nordic Immunological Laboratories, The Netherlands; rabbit PAP, 1:800, Nordic Immunological Labs). Peroxidase activity was revealed as described before, but nickel was not used.

The sections were mounted onto gelatinised slides, dehydrated with graded alcohols, cleared with xylene and covers-

lipped with Entellan (Merck, Germany). To facilitate the identification of the neural structures containing the anterograde labelled fibres, before the tissue was coverslipped, it was counterstained with the Nissl method.

3.3.2 *Considerations regarding tracer injections*

Although dextranamines are commonly used as anterograde tracers, retrograde transport also occurs. Retrograde staining with BDA was visible as dark coloured cell bodies. These cells were mainly located around the injection site, which would not interfere with the anterograde tracing, or along the micropipette track. The later ones were carefully examined as non-restricted injections to confirm the labelling observed in the restricted ones.

3.4   IMAGE ACQUISITION AND PROCESSING

We observed the sections using an Olympus CX41RF-5 microscopy and photographed them using a digital Olympus XC50 camera. Brightness and contrast were adjusted, but no additional filtering or manSipulation of the images was performed. We arranged the pictures with Adobe Photoshop 7.0 (AdobeSystems, USA) and designed the line drawings and their labelling using Adobe Photoshop and Adobe Illustrator (Adobe Systems).

RESULTS

For the description of the distribution of anterograde labelling resulting from the different injections in the medial nucleus of the amygdala, we followed the nomenclature of the atlas of the mouse brain by Paxinos and Franklin (2004). To simplify the description of the intramygdaloid projections, the terms "olfactory amygdala" (Kevetter and Winans, 1981b) and "vomeronasal amygdala" (Kevetter and Winans, 1981a) are used. The first refers to amygdaloid structures that are direct targets of the main olfactory bulb and the second refers to amygdaloid structures that are direct targets of the accessory olfactory bulb. The term "chemosensory amygdala" includes both the olfactory and the vomeronasal amygdala (Gutiérrez-Castellanos et al., 2010).

The projection densities in the different targets of the medial amygdala subnuclei (anterior: MeA, posterodorsal: MePD and posteroventral: MePV), were subjectively classified as (see Table 2): very dense, dense, moderate, sparse and very sparse. We considered very dense the projection through the *stria teminalis* and very sparse the areas where we could observe only $2-5$ labelled fibres.

The injection sites obtained in the medial amygdala are described below. In addition, we obtained one injection located in the *substantia innominata* (SI) above the MeA, and another one restricted to the optic tract (*opt*) medial to the MeA (not shown). These injections were used as controls for the specificity of the anterograde labelling resulting from the medial amygdala injections (see below).

Table 2: Semiquantitative rating of the density of the anterograde labelling resulting after tracer injections in three subdivisions of the medial amygdaloid nucleus. IS = Injection site; nf = not found.

		MeA	MePD	MePD/MePV	MePV
Vomeronasal system and BST					
AOB	MiA	+++	-	+	+
	GrA/GlA	++/+	-	+++/-	+++/-
BST	BSTMA	++*	++*	+++	+++*
	BSTMV	++	++	++	+
	BSTMPI	++++*	++	+++	++
	BSTMPM	++	++++*	++++	++++*
	BSTMPL	+++	+++	+++	++
	BSTLD	++↑	-	+	+↓
	BSTLP	++	+↓	+	+↓
	BSTLV	++	+↓	+	+↓
Amygdala	BAOT	+++	+++	nf	+++
	MeA	IS	+++	++++	+++
	MePD	+++	IS	IS	++++
	MePV	+++	+++	IS	IS
	AAD/AAV	++	++	++	+/++
	PMCo	+++	++	++++	++++
Olfactory system					
MOB	GrO	+↓	-	-	-
Tenia tecta	DTT/VTT	++*	-	+	+
AON		+	-	+	+↓
Cortex	Pir	+	+	+	+
	DEn/VEn	+	+↓	+	+↓
	Ent	+	+↓	+↓	+↓
Amygdala	LOT	+	+	+	+↓
	CxA	+	+	++	+↓
	ACo	++	+++	+++	++
	PLCo	+++	++	+++	+++
	APir	+	+	+	+↓
Non-chemosensory amygdala					
	BMA	++	++	+++	++

	BMP	+	+	+	++
	BSTIA	+++	++	++	++
	AStr	++	-	-	-
	I	++	+	+	+
	CeM	++	++	++	+
	CeC	+++	+↓	+	-
	CeL	+	+↓	+	+↓
	BLA	+↓	+↓	+↓	-
	BLV/BLP	+	+	+	+
	La	+	+	+	+↓
	AHi	+++	++	++	++

Other cortical structures

Prefrontal cortex	PrL	+	-	-	-
	IL	+	-	-	-
	AI	+	-	+↓	+↓
	Cl	+	-	-	-
Hippocampus	CA1	+	++	+	++

Septum and Ventral striatum

Septum	LSD	+	+↓	+	+
	LSI	++↑*	+*	++	+
	LSV	++	+	++	++*
	MS	+	-	+	+↓
	HDB	++↑*	-	+	+
	VDB	++	-	+	+
	SHy	++	++	++	+++
	SHi	+	+↓	+	+↓
Ventral striatum	VP	+	+	+	-
	Acb	+	+	+	-
	Tu	++*	-	+↓	+↓
	ICj	+	-	+↓	+↓
	SI	++	++	++	++
	IPAC	++	-	+↓	+↓

Hypothalamus

Preoptic	MPA	++*	++*	++	+
	MPO	++	+++	++	++*
	LPO	+	+	+	+↓

	AVPe	-	++	+	-
Anterior	AHA/AHP	++	++	++	+
	Pa	+	+	+	+↓*
	Pe	+	+	+	+↓
	LA	+	+	+	+
	SCh	-	+	+	-
Tuberal	VMHDM	+++*	+	+++	++*
	VMHVL	++*	+++*	+++	++*
	DM	+	+	+	+↓
	LH	+	+	+	+
	Arc	+	+	+	+
Mammillary	PMD	+	+↓	+	+
	PMV	++*	+++*	+++	+++*
	MM/ML	+	+	+	+
	SuM	+	+	+	+
	PH	+	+	+	-
Thalamus					
	SM	+++	+++	+++	++
	Re	+↑*	+	+	+↓
	PV	+	+	+	+
	MD	+	-	-	-
	LHb	+	-	-	-
	PT	+	-	-	-
	ZI	+	-	-	-
	STh	+	+	+	+
	PSTh	+	+	+	-
Brainstem and midbrain					
	PAG	+	+	+	+
	VTA	+	+	+	+
	RLi	+↓	-	-	-
	DR	+↓	-	(not found)	-
	SN	-	+	+	-

Very dense: ++++; Dense: +++; Moderate: ++; Sparse: +; Very sparse: +↓; No labelling: -.

* Contralateral labelling.

4.1 ARCHITECTURE OF THE MEDIAL AMYGDALOID NUCLEUS

The medial amygdaloid nucleus (Me) is located in the medial superficial aspect of the amygdala. According to the atlas of the mouse brain by Paxinos and Franklin (2004), the Me is an heterogeneous structure comprised of four sunuclei: antoroventral, anterodorsal, posteroventral and posterodorsal. As Canteras et al. (1995) and Gomez and Newman (1992) suggested, projections from the anteroventral and anterodorsal subdivisions are described together, and will be referred as the anterior subdivision.

The begining of the MeA limits rostrally with the anterior amygdaloid area and laterally with the nucleus of the lateral olfactory tract. Then it extends caudally and runs adjacent to the bed nucleus of the accessory olfactory tract and the anterior cortical amygdaloid nucelus (Figure 1 A). Medially it limits with the *opt*, while the deeper part of the MeA limits with the anterior part of the basomedial amygdaloid nucleus. The MePD continuous with the dorsal aspect of the MeA and extends dorsally adjacent to the basomedial amygdaloid nucleus and the intraamygdaloid division of the bed nucleus of the *stria terminalis* (Figure 1 B). Regarding the MePV, is located ventral to the MePD and limits rostrally with the anterior cortical amygdaloid nucleus an caudally with the posteromedial cortical amygdaloid nucleus.

The Me shows a rough lamination (Martínez-García et al., 2012), specially in its posterior subdivisions, with a cell-free layer I (in which the projection from the accessory olfactory bulb terminates) and a high cell density layer II (that is not clearly defined) occupying the medial corner. Furthermore, the dorsal and ventral subdivisions of the posterior Me are not easily distinguishable in Nissl stained sections, except for their relative position.

4.2 INJECTIONS IN THE MEA

4.2.1 *Injection sites*

In eight experiments the injection affected the MeA, five of which have the tracer entirely confined to this subnucleus. Of the restricted injections (Figure 2 A,B), two correspond to single injections in the C57BL/6J strain and are used to describe both ipsilateral and contralateral projections of the MeA (Figure 2, injections M0331 and M1120); while the other three, which correspond to CD1 mice, are used to describe the ipsilateral projections. Injections M1143R and M1144L (Figure 2 A,B) show small
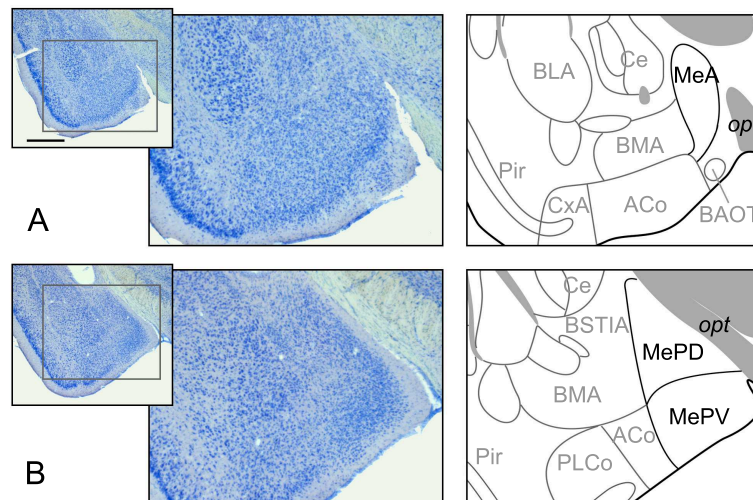
Figure 1: **Rostro-caudal organisation of the Me**. **A,** The anterior subdivision of the medial amygdaloid nucleous (MeA) and surrounding amygdaloid structures. Left: low-power photomicrographs of Nissl staining of coronal sections through the amygdala in mice and magnification to show the cytoarchitectonical organisation of the MeA. Right: Schematic representation showing the general organisation of the MeA and surrounding amygdaloid structures. **B,** Idem for the posterior subdivision of the medial amygdaloid nucleus. Scale bar in **A** (valid for **B**) = 500 μm.

tracer deposits along the micropipette track, which are located in the internal capsule (*ic*), medial globus pallidus (MGP), SI and the *opt*, and therefore are used only to check the labelling found in restricted injections. In the remining three cases the injections extended caudally and affected also the posterior subdivisions of the Me.

4.2.2   *Anterograde labelling resulting from injections in the MeA*

The injections of neural tracers in the anterior division of the medial amygdaloid nucleus (MeA) gave rise to anterograde labelling in a complex range of cerebral nuclei. Intra-amygdalar axons spread directly from MeA, while fibre labelling coursing outside the amygdala followed two main pathways: the *stria terminalis*, where labelled axons were located in the medial aspect, and the ventral amygdalofugal pathway (*ansa peduncularis*), where axons progressed across the SI. The output of the MeA appeared mostly ipsilateral, with scarce fibre labelling present in contralateral nuclei, as described below. Since no differences were observed in the anterograde labelling resulting from experiments in the C57BL/J6 and CD1 strains [except in the olfactory
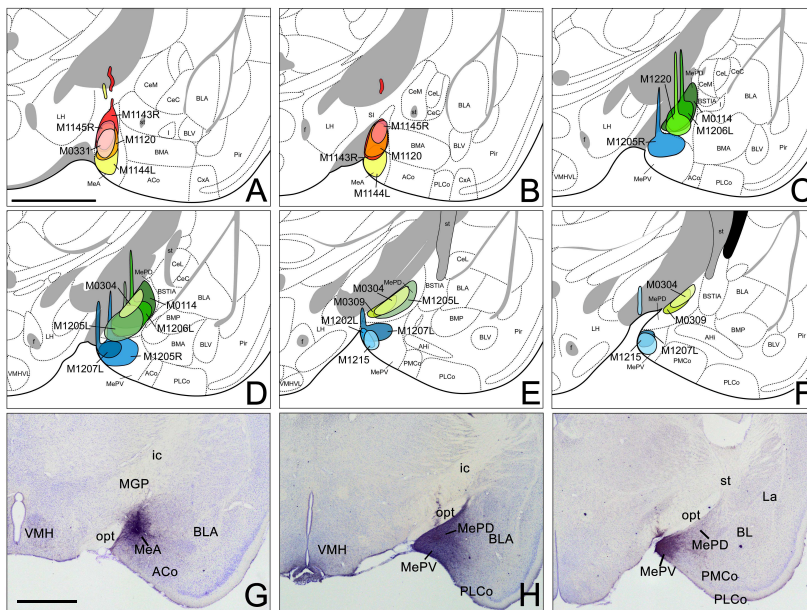
Figure 2: **Injection sites in the anterior, posterodorsal, and posteroventral subdivisions of the medial amygdaloid nucleus. A-F,** Schematic drawings representing the extent of the tracer injections in the anterior medial amygdaloid nucleus (MeA), the posterodorsal medial amygdaloid nucleus (MePD), and the posteroventral medial amygdaloid nucleus (MePV). MeA injections are represented in warm colours (**A, B**), MePD in green and MePV in blue (**C-F**). Coloured areas represent single injections and are identified with the animal code. For those animals with two injections, each one is identified with either an R (right hemisphere) or an L (left hemisphere). **G-I,** Photomicrographs of nissl-stained sections through the amygdala of the mouse showing representative injections sites. **G,** Injection site in the MeA of a CD1 mouse. **H,** Injection site in the MePD of a CD1 mouse. **I,** Injection site in the MePV of a CD1 mouse. For abbreviations, see list. Scale bar in **A** (valid for **B-I**) = 1 mm.

tubercle (Tu), see below], the results obtained in both strains are described together.

4.2.2.1 *Vomeronasal system*

Fibre labelling arising from the MeA injections extended rostrally through the accessory olfactory tract to end in the accessory olfactory bulb (AOB), were we observed dense anterograde labelling in the ventral aspect of the mitral cell layer, a moderate density of labelled fibres in the granular layer and few fibres in the glomerular layer, apparently in the posterior AOB (Figures 3 A,B and 4 A).

Anterograde labelling was also present in secondary vomeronasal structures. Fibres arriving to the bed nucleus of the *stria terminalis* (BST) mainly coursed through the *stria terminalis*, which

Figure 3: **Continued.**
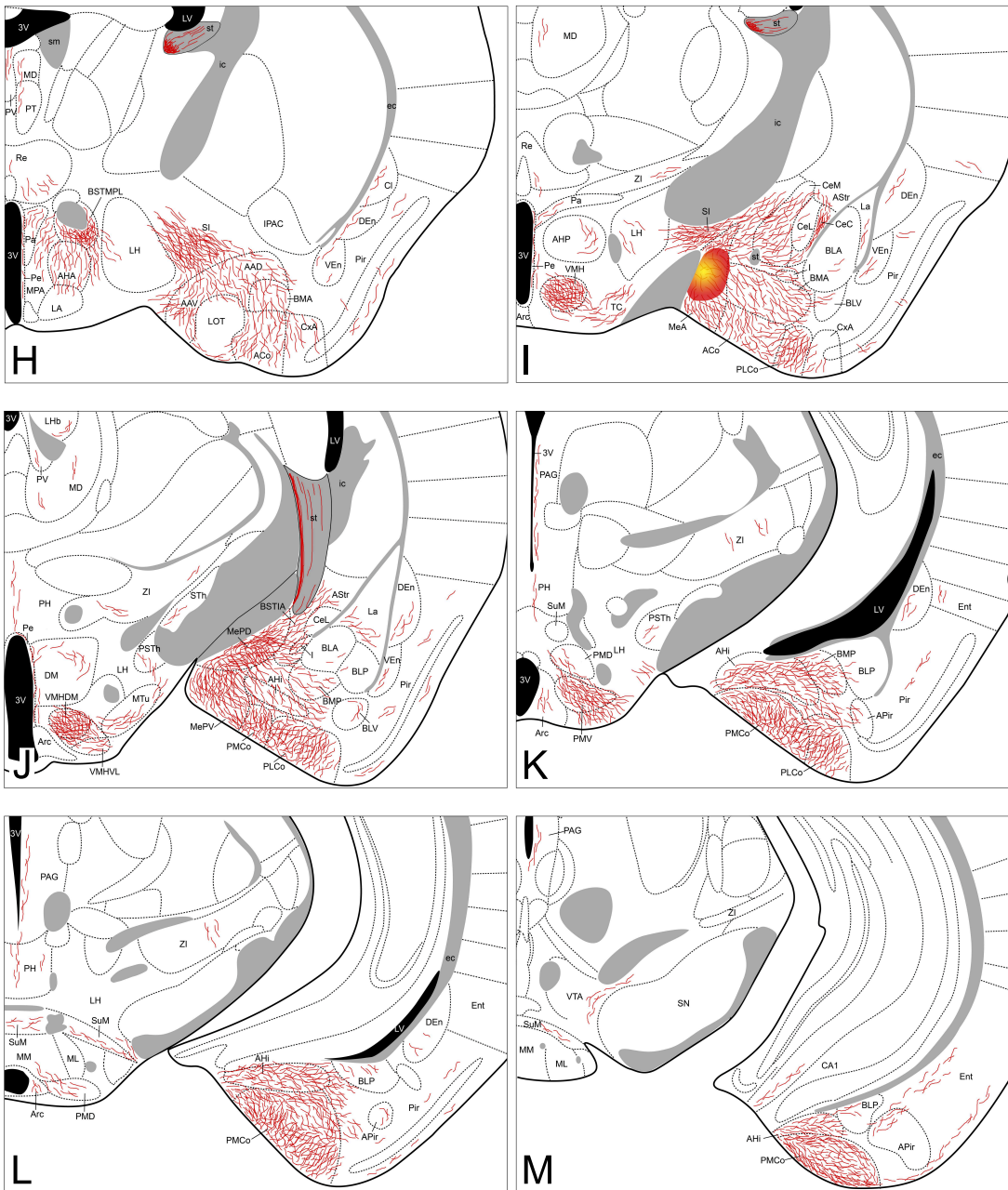
Figure 3: **Semi-schematic drawings of transverse sections through the mouse brain showing the distribution of anterogradely labelled fibres following a tracer injection in the MeA**. The injection site is depicted in panel **I**. **A** is rostral, **M** is caudal. The semi-schematic drawings were made based on an injection in a C57BL/J6 mouse. For abbreviations, see list. Scale bar = 1 mm.
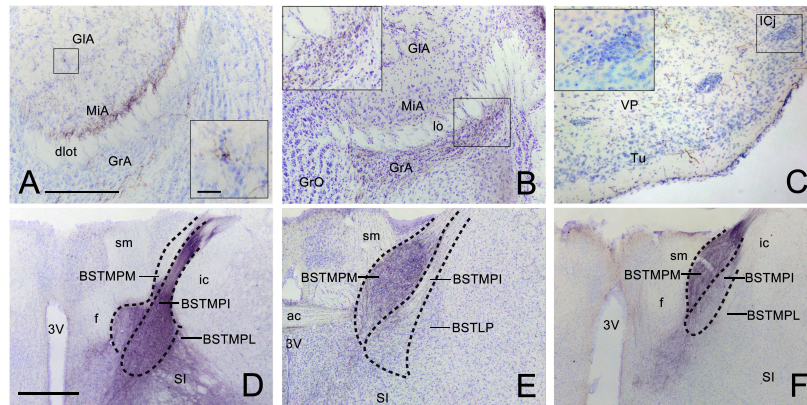
Figure 4: **Anterograde labelling in the accessory olfactory bulb (AOB), olfactory tubercle (Tu), and bed nucleus of the *stria terminalis* (BST) after tracer injections in the Me. A,** Nissl-stained transverse section through the AOB of a CD1 animal with a tracer injection in the MeA, showing the centrifugal projections to the deep aspect of the mitral cell layer. The inset shows a high magnification view of a labelled fibre next to a glomerulus. **B,** Nissl-stained transverse section through the AOB of a CD1 animal with a tracer injection in the MePV, showing the centrifugal projections to the granule cell layer. The inset shows a high magnification view of these labelled fibres. **C,** Photomicrograph of a transverse section through the ventromedial Tu of a C57BL/J6 animal with a tracer injection in the MeA. Note that some of the labelled fibres apparently innervate the islands of Calleja. **D-F,** Photomicrographs of Nissl-stained transverse sections through the BST of animals receiving tracer injections in the MeA (**D**), MePD (**E**), and MePV (**F**). Note that in **D** the densest labelling is in the medial posterointermediate division, whereas in **E** and **F** the densest labelling is in the medial posteromedial division. These photomicrographs correspond to a C57BL/J6 mouse injection (**D**) and CD1 mice injections (**E,F**). For abbreviations, see list. Scale bar in **A** (valid for **B,C**) = 250 μm. Scale bar in **D** (valid for **E,F**): = 500 μm. Inset scale bar in **A** (valid for **B,C**) = 20 μm.

showed a very dense fibre labelling (Figure 3 H-J). The injections in the MeA resulted in dense anterograde labelling in the BST, both in its medial and lateral divisions (see Table 2). A moderate, almost dense, terminal field was observed in the lateral BST, especially in the laterodorsal BST (Figure 3 F,G). Fibre labelling was also very dense in the posterointermediate medial BST (BST-MPI); dense in the posterolateral medial BST (BSTMPL); while moderate in the anteromedial BST (BSTMA), ventromedial BST (BSTMV) and medial posteromedial BST (BSTMPM; Figures 3 F-H and 4 D).

The injections in the MeA showed labelling in the rest of nuclei composing the vomeronasal amygdala. Dense terminal fields appeared in both the MePD and MePV (Figures 3 J and 5 A). Dense fibre labelling is also observed in the posteromedial cortical amygdaloid nucleus (PMCo; Figures 3 J-M and 5 A) and the
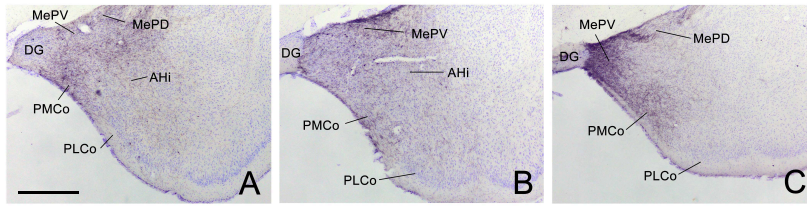
Figure 5: **Anterograde labelling in the amygdala after tracer injections in the different subdivisions of the Me**. Photomicrographs of transverse sections through the amygdala of CD1 animals receiving tracer injections in the MeA (**A**), MePD (**B**), and MePV (**C**). **A-C,** Note that in all cases dense anterograde labelling is observed in the vomeronasal amygdala. For abbreviations, see list. Scale bar in **A** (valid for **B** and **C**) = 500 μm.

bed nucleus of the accessory olfactory tract (BAOT; not shown, see Table 2). The anterior amygdaloid area showed a moderate density of fibre labelling, mainly in its ventral division (Figure 3 G,H).

4.2.2.2 *Olfactory system*

Injections in the MeA resulted in labelling in a number of olfactory-related structures. Some labeled axons apposed to the wall of the lateral ventricle ran dorsally to the AOB, crossing the granular cell layer of the dorsomedial olfactory bulb (Figure 3 B). A moderate amount of fibres was observed in the dorsal as well as ventral *tenia tecta* and the piriform cortex (Pir), which had more labelled fibres present in layers 1 and 3 (Figure 3 C,D). In addition, a sparse innervation was present in other cortical regions such as the anterior olfactory nucleus (mainly in the medial and ventral areas) and the endopiriform nucleus (Figure 3 C-L). Finally, a few axons extended caudally into the entorhinal cortex (Ent).

Whithin the olfactory amygdala, dense labelling was observed in the posterolateral cortical amygdaloid nucleus (PLCo; Figure 5 A) and moderate density in the anterior cortical nucleus (ACo). Other structures displayed only sparse anterograde labelling, such as the corticoamygdaloid transition area (CxA) and the amygdalopiriform transition area (APir), or were mostly devoid of labelled axons, such as the nucleus of the lateral olfactory tract (LOT), in which a small amount of fibres of passage were observed in layer 1 and a few labelled fibres were present in layer 3 (Figure 3 H,I).

4.2.2.3   *Non-chemosensory amygdala*

Among the non-chemosensory amygdala several nuclei showed anterograde labelling. In the central nucleus a moderate terminal field was observed in the medial (CeM) and capsular (CeC) parts, somewhat denser at the CeC, with sparse anterograde labelling in the lateral part (CeL; Figure 3 I,J). Dense anterograde labelling appeared also in the intra-amygdaloid division of the BST (BSTIA; Figure 3 J); while a moderate density was present in the amygdalostriatal transition area and the intercalated mass (I; Figure 3 I,J), located between the basolateral and basomedial nuclei. Within the basolateral amygdaloid complex, a moderate density of fibre labelling was observed in the anterior basomedial amygdaloid nucleus (BMA; Figure 3 H-K), and only sparse anterograde labelling appeared in the lateral (La) and basolateral nuclei (Figure 3 I-M).

4.2.2.4   *Other telencephalic structures*

After tracer injections in the MeA few other cortical structures showed anterograde labelling. In the prefrontal cortex, sparse labelling appeared in the prelimbic and infralimbic cortices (Figure 3 C,D). In addition, a sparse innervation was also observed in the agranular insular cortex and the claustrum (Figure 3 F-H). Finally, a few axons extended caudally into the *stratum lacunosum moleculare* of the CA1 field of the ventral hippocampus (Figure 3 M).

4.2.2.5   *Septum and ventral striatum*

The anterogradely labelled fibres reached the septum through the *stria terminalis*. At rostral levels a moderate axonal labelling was observed in the lateral septal complex, which appeared to be denser in its intermediate (LSI) than in its ventral division (LSV), with sparse labelling in its dorsal division (LSD; Figure 3 E,F). Some fibres were also observed in the medial septal nucleus (Figure 3 E,F). In addition, moderately dense anterograde labelling was present at the septohypothalamic nucleus (SHy), and a few fibres appeared in the septohippocampal nucleus (SHi; Figures 3 E,F). The nucleus of the diagonal band showed a moderate density of anterograde labelling both in the vertical and the horizontal limb, which was especially located in the anterolateral part of the horizontal limb (Figure 3 E-G), next to the boundary with the Tu. A number of fibres were also present next to the medial border of the major island of Calleja (Figure 3 E).

Within the ventral striatum, a small number of fibres were observed in the nucleus accumbens (Figure 3 D,E). The Tu showed a moderate labelling, with axons mainly surrounding the islands

of Calleja (Figure 3 D-F and 4 C). Only a few fibres enter both the ventromedial and the major islands. This anterograde labelling in the Tu appeared denser in the injections performed in the C57BL/6J than in the CD1 animals. The ventral pallidum showed sparse anterograde labelling (Figure 3 D,E). In addition, the SI displayed a moderate amount of anterogradely labelled axons and fibres of passage belonging to the ventral amygdalofugal pathway (Figure 3 F-I). Numerous fibres were also found in the interstitial nucleus of the posterior limb of the anterior commissure (IPAC; Figure 3 F,G).

4.2.2.6 *Hypothalamus*

Following injections in the MeA, abundant anterograde labelling appeared in many hypothalamic nuclei (Table 2). At preoptic levels, a moderate amount of anterograde labelling was observed in the medial preoptic nucleus (MPO) and medial preoptic area (MPA; Figure 3 F,G). Also, few labelled axons could be found in the lateral preoptic area (LPO; Figure 3 G).
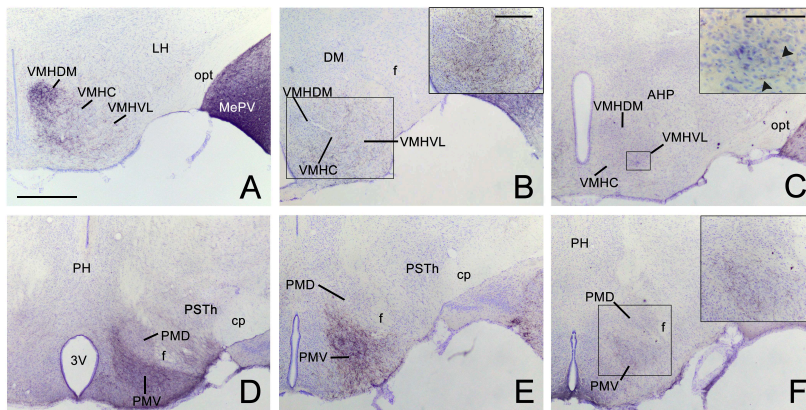
Figure 6: **Anterograde labelling in the hypothalamus following tracer injections in the Me**. Photomicrographs of transverse sections through the hypothalamus of animals receiving tracer injections in the MeA (**A,D**), MePD (**B,E**), and MePV (**C,F**). **A-C,** Pattern of anterograde labelling in the ventromedial hypothalamic nucleus (VMH) in CD1 animals. Injections in MeA resulted in dense fibre labelling in the dorsomedial VMH (**A**), whereas injections in MePD gave rise to dense labelling in the ventrolateral VMH (**B**). The MePV did not appear to innervate preferentially the dorsomedial or ventrolateral subdivision. **D-F,** Pattern of anterograde labelling in the premammillary hypothalamus. All three subdivisions of the Me mainly project to the ventral premammillary nucleus, with the densest labelling originated by the MeA (**D**) and the MePD (**E**). Premammillary hypothalamus photomicrographs correspond to a C57BL/J6 mouse injection (**D**) and CD1 mice injections (**E,F**). For abbreviations, see list. Scale bar in **A** (valid for **B-F**) = 500 μm. Inset scale bar in **B** (valid for **F**) = 50 μm. Inset scale bar in **C** = 20 μm.

At anterior levels, the anterior hypothalamic area had moderate labelling, which appeared less dense in its posterior part (Figure 3 H,I). A low density of labelled fibres was also observed in the lateroanterior hypothalamic nucleus (LA), the paraventricular hypothalamic nucleus (Pa), mainly in its anterior part, and the periventricular hypothalamic nucleus (Pe) (Figure 3 F-J).

In the tuberal region, the ventromedial hypothalamic nucleus showed a heterogeneous labelling. The central (VMHC) and dorsomedial (VMHDM) parts contained dense anterograde labelling, whereas the ventrolateral (VMHVL) part showed only a moderate density (Figure 3 I,J and 6 A). In addition, a few axons could be observed in the dorsomedial nucleus (DM) and the arcuate nucleus (Arc; Figure 3 J-L). Also, scarce fibre labelling was found in the lateral hypothalamic area (LH; Figure 3 H-K).

Finally at mammillary levels, a moderate anterograde labelling was observed in the ventral premammillary nucleus (PMV), with a few labelled fibres in its dorsal part (PMD; Figure 3 K,L and 6 D). The supramammillary nucleus (SuM) presented a sparse labelling, as did the medial mammillary nucleus (MM) and the posterior hypothalamic area (PH; Figure 3 J-M).

4.2.2.7 *Thalamus*

The injections in the MeA did not result in a wide distribution of labelling in the thalamus. Some axons progressed through the *stria medullaris* and apparently reached the paraventricular thalamic nucleus (PV) and the lateral habenula (LHb; Figure 3 H-J). A dense terminal field was observed in the nucleus of the *stria medullaris* (not shown). Sparse labelling was also found in the nucleus reuniens (Re; Figure 3 H,I), mediodorsal nucleus (MD) and parataenial thalamic nucleus (PT; Figure 3 H-J). Finally, a few labeled axons appeared in the zona incerta, subthalamic nucleus (STh) and parasubthalamic nucleus (PSTh; Figure 3 I-K).

4.2.2.8 *Brainstem and midbrain*

The injections in the MeA gave rise to scarce anterograde labelling in the periaqueductal gray (PAG) and the ventral tegmental area (VTA; Figures 3 K-M and 7). Moreover, a few fibres could be seen in the dorsal raphe nucleus and the rostral linear raphe nucleus (not shown).

4.2.3 *Contralateral labelling*

After tracer injections in the MeA we mainly observed labelling in the ipsilateral hemisphere, however a few axons crossed the midline in the anterior commissure, the supraoptic decussation
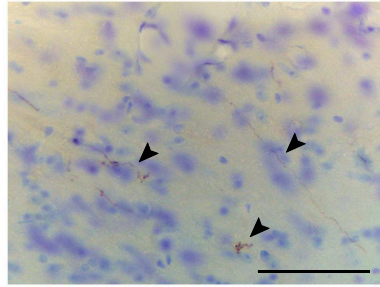
Figure 7: **Anterograde labelling in the ventral tegmental area following a tracer injections in the MeA**. Arrowheads point to scattered labelled fibres. Photomicrograph of a CD1 mice. Scale bar = 25 μm.

(*sox*) and the supramammilary decussation. Thus, in the contralateral hemisphere, scarce anterograde labelling was present generally in those structures that showed a dense ipsilateral projection (with the exception of the contralateral amygdala, which appeared devoid of labelling). A few fibres were observed in the contralateral *tenia tecta*, Tu, diagonal band, lateral septum, BST, Re and several parts of the hypothalamus, mainly in MPA, ventromedial hypothalamic nucleus, and PMV.

4.2.4 *Anterograde labelling following non-restricted injections*

The two non-restricted injections (Figure 2 A, injections M1143R and M1144L) showed some tracer contamination in the *ic*, MGP, SI, and *opt*. We observed fibres running through the forceps minor of the corpus callosum (*fmi*), the external capsule (*ec*), the basal part of the cerebral peduncle (*cp*), and *sox*. As a consequence, very scarce labelling was present in *substantia nigra* (SN), parafascicular thalamic nucleus and ventral posterior thalamic nuclei. Some sparse to moderate labelling was observed in the caudate-putamen (CPu), STh, supraoptic nucleus, and the lateral part of the LHb.

4.3 INJECTIONS IN THE MEPD

4.3.1 *Injection sites*

After tracer injection in the MePD, the experiments performed resulted in eight injections affecting this subnucleus. Six of them were confined almost entirely to this structure (Figure 2 C-F), while two of them affected both the MePD and MePV. Three of the restricted injections correspond to single tracer injections in the C57BL/6J strain and were used to describe the ipsilateral and contralateral projections of the MePD. The remaining restricted

injections were performed in CD1 mice that received injections in both hemispheres, and therefore were used to corroborate the ipsilateral labelling. One of the CD1 injections had the tracer extended beyond the boundary with the MePV (Figure 2 D, injection M1205L). In another case the injection involved the MeA (Figure 2 C,D, injection M1206L). In both cases, some of the nuclei or fibre tracts located along the micropipette track present small tracer deposits, including the primary somatosensory cortex, trunk region, the reticular thalamic nucleus (Rt), the *ic*, the MGP, and the *opt* (Figure 2 C,D, injections M1205L and M1206L).

4.3.2   *Anterograde labelling resulting from injections in the MePD*

As shown for the MeA, the efferents of the posterodorsal region of the Me (MePD) reached a complex range of cerebral nuclei. Axons originated from the MePD followed the same major pathways described for the MeA. However, in this case the majority of the labelled fibres coursed through the *stria terminalis*, with less anterogradely labelled axons found in the ventral amygdalofugal pathway. The output of the MePD was mostly ipsilateral, although a few axons appeared in contralateral nuclei (described below). As reported above, the anterograde labelling resulting from experiments in the C57BL/J6 and CD1 strains showed no difference.

4.3.2.1   *Vomeronasal system*

Injections in the MePD resulted in labelling in a number of secondary vomeronasal structures, but no labelling was observed in the AOB. Fibres coursing through the *stria terminalis* arrived to the BST, were they mainly labelled its medial division. Very dense anterograde labelling appeared in the BSTMPM, dense in the BSTMPL and a moderate labelling was present in the BSTMA, BSTMV and BSTMPI (Figure 8 B-D and 4 E). In contrast, the subnuclei composing the lateral division of the BST showed very scarce labelling.

Within the vomeronasal amygdala, a very dense anterograde labelling was observed in the rest of the Me (Figure 8 E-G). A dense field of fibres was found in the BAOT (Table 2); while, the PMCo and anterior amygdaloid area also showed a moderate density of labelling.

4.3.2.2   *Olfactory system*

The anterograde labelling observed in olfactory related structures following injections into the MePD is very scarce. Only a scarce amount of labelled fibres appeared in the Pir (with more

Figure 8: **Continued.**
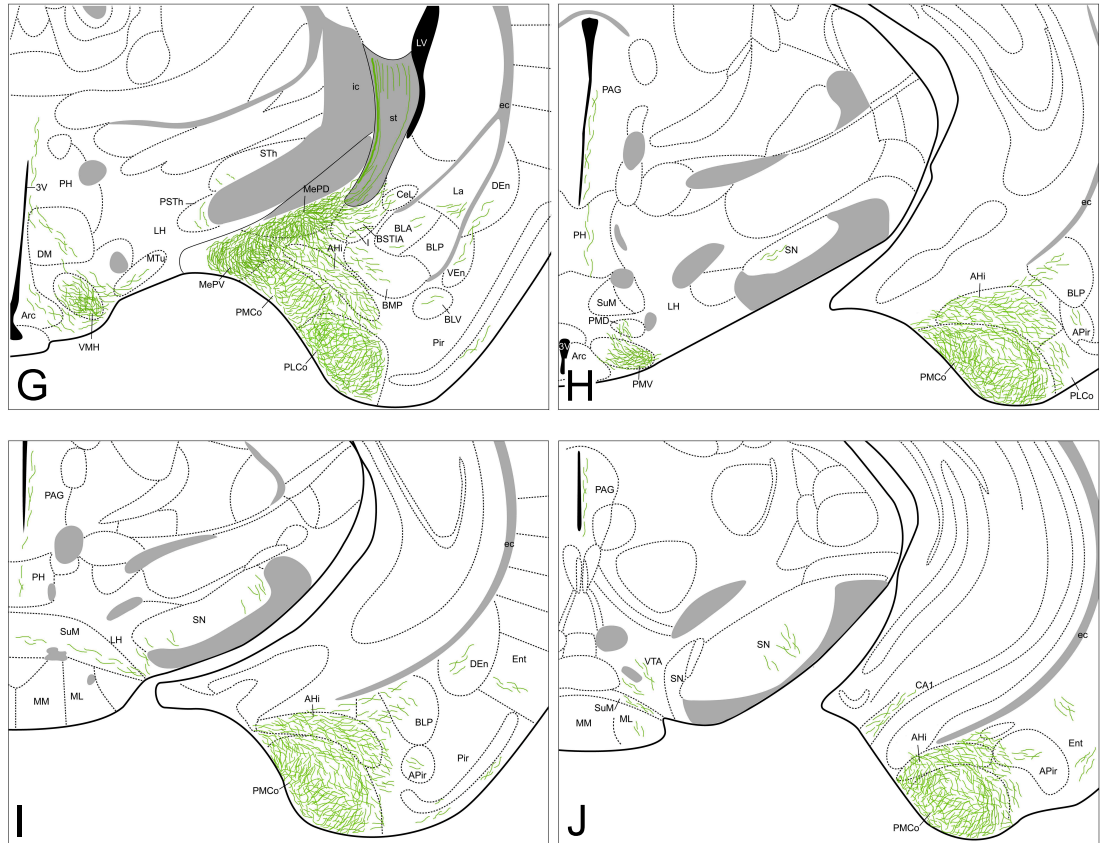
Figure 8: **Summary of the distribution of anterograde labelling following a tracer injection in the MePD, plotted onto semi-schematic drawings of transverse sections through the mouse brain**. The injection site is depicted in panel **F**. **A** is rostral, **J** is caudal. The semi-schematic drawings were made based on an injection in a C57BL/J6 mouse. For abbreviations, see list. Scale bar = 1 mm.

fibres in its posterior zone) and the endopiriform nucleus (Fgure 8 A-I); and at a caudal telencephalic levels in the Ent (Figure 8 I,J).

In the olfactory amygdala, a dense anterogrde labelling appered in the ACo, moderate density in the PLCo, whereas the cortex-amygdala transition zone displayed scarce labelling (Figure 8 D,E). The LOT was mostly devoid of axonal labelling, although some fibres could be observed in layer 1 (Figure 8 D). In the caudal amygdala, the APir area showed also a scarce labelling (Figure 8 H-J).

4.3.2.3   *Non-chemosensory amygdala*

The rest of the amygdala showed a heterogeneous labelling. In the central nucleus, a moderate density of labelled fibres was

observed in its medial division, whereas sparse fibre labelling appeared in the CeL and CeC (Figures 8 E-G). The BSTIA and the AHi showed moderate labelling and a scarce labelling was observed in the I. Within the basolateral amygdaloid complex, the basomedial nucleus showed moderately dense axonal labelling in the BMA (Figure 8 E,F). The posterior part of the basomedial nucleus, as well as the basolateral and La, presented sparse anterograde labelling (Figure 8 F-I).

4.3.2.4 *Other telencephalic structures*

The anterograde labelling in cortical structures after tracer injections in the MePD was very restricted. Aside from the labelling observed in the olfactory related nuclei, only a moderate terminal field was present in the CA1 field of the ventral hippocampus, specifically in the *stratum lacunosum moleculare* (Figure 8 J).

4.3.2.5 *Septum and ventral striatum*

In the septum, sparse anterograde labelling was present in the dorsal, intermediate, and ventral divisions of the lateral septal complex (Figure 8 A-C), but no fibres were observed in the medial septum/diagonal band complex. A moderate innervation was found in the SHy, while a few fibres were present in the SHi (Figure 8 A,B).

Within the ventral striatum, sparse innervation was present in the medial core and shell of the nucleus accumbens (Figure 8 A), but no labelling appeared in the Tu or the associated islands of Calleja. Anterograde labelling was also very scarce in the ventral pallidum (Figure 8 A). Finally, the SI showed a moderate labelling with fibres of passage coursing through the ventral amygdalofudal pathway (Figure 8 B-E).

4.3.2.6 *Hypothalamus*

In the preoptic hypothalamus, dense fibre labelling was observed in the MPO (Figure 8 C,D); while the anteroventral periventricular nucleus and the MPA show a moderately dense labelling, the caudal MPA showed a lower number of labelled fibres (Figure 8 B-D). A few fibres could also be found in the LPO (Figure 8 C).

At anterior levels, the anterior hypothalamic area had a moderate labelling, especially in its rostral part (Figure 8 D,E). In the rest of the anterior hypothalamus, only a sparse innervation was observed inthe LA, suprachiasmatic nucleus, Pa and Pe (Figure 8 D,E).

Within the tuberal region, labelled axons resulting after the MePD injections gave rise to a dense innervation in the shell around the ventromedial hypothalamic nucleus and the VM-HVL, whereas only a scarce density of labelled fibres was present in the VMHDM and VMHC (Figures 8 E-G and 6 B). In addition, a few axons were observed in the DM, Arc, and LH (Figure 8 D-G).

At mammillary levels, the PMV showed dense anterograde labelling, while the PMD had sparse labelling (Figures 8 H and 6 E). A few anterogradely labelled fibrer were also present in the SuM, MM, and PH (Figure 8 G-J).

4.3.2.7   *Thalamus*

The injections in the MePD resulted in scarce anterograde labelling in the thalamus. Only the axons coursing through the *stria medullaris* apparently gave rise to dense anterograde labelling in the nucleus of the *stria medullaris* (Figure 8 D). In addition, sparse fibre labelling was observed in the Re, PV, STh, and the PSTh (Figure 8 D-G).

4.3.2.8   *Brainstem and midbrain*

In animals with injections in the MePD, some labelled axons ran caudally to reach the PAG and to a lesser extent the VTA (Figure 8 H-J). Also, sparse labelling was observed in the SN (Figure 8 H-J), mainly in its reticular part.

4.3.3   *Contralateral labelling*

The anterograde labelling resulting from the injections in the MePD was mostly ipsilateral, but a few labelled axons were observed to cross the midline in the anterior commissure and the *sox*. Contralateral labelling was present in those nuclei that showed dense ipsilateral fibre labelling. Thus, sparse anterograde labelling appeared in the lateral septum, BST and the hypothalamus, mainly in MPA, ventromedial hypothalamic nucleus, and PMV.

4.3.4   *Anterograde labelling following non-restricted injections*

In the injections M1206L and M1205L (Figure 2 C-E), in which tracer contamination occurred in the somatosensory cortex (trunk region), Rt, *ic*, MGP, and *opt*, we observed sparse labelling in areas in which no fibre labelling appeared in the restricted injections in the MePD. Labelled fibres ran through the *ec*, optic chiasm and the *sox*. Thus, anterograde labelling was present in

the parietal insular cortex, CPu, the ventral posterior thalamic nuclei, posterior thalamic nuclear group (Po), SN and several structures in the visual thalamus. We also observed sparse to moderate fibre labelling in the lateral part of LHb .

4.4 INJECTIONS IN THE MEPV

4.4.1 *Injection sites*

We obtained four injections confined almost entirely to the MePV, two in the C57BL/6J strain (Figure 2 E,F, injections M1202L and M1215) and two in the CD1 strain (Figure 2 C-F, injections M1205R and M1207L). In the later ones, small tracer deposits were present along the micropipette track and some tracer could be found at the primary somatosensory cortex (trunk region), the *cp*, the *opt*, the STh (Figure 2 C-F), and caudally the SN, *pars reticulata*. In another case, small tracer deposits were present in the *cp*, STh and the pyramidal cell layer of the hippocampus (Figure 2 E,F, injection M1215). In addition, to describe the MePV projections we also studied the two injections encompassing the MePD and MePV (as described above) and an additional one that affected the caudal MePV and the medial aspect of the PMCo. In the case of the MePV, the contralateral projections were described based on a C57BL/J6 injection (Figure 2 E,F, injection M1215).

4.4.2 *Anterograde labelling resulting from injections in the MePV*

The labelled fibres resulting from the injections in the MePV course through the same pathways described above for the MeA and MePD injections, the *stria terminalis* and the ventral amygdalofudal pathway. In fact, a very dense group of axons leaving the injection site surrounded the MePD to reach the *stria terminalis* in their way out of the amygdala (Figure 9 I). As reported with MePD efferents, no differences between strains appeared in the anterograde labelling observed following tracer injections in the MePV. The output of the MePV was also mostly ipsilateral, although a few axons appeared in contralateral nuclei, as described below.

4.4.2.1 *Vomeronasal system*

Following injections in the MePV, labelled fibres coursed rostrally to innervate the AOB, where dense anterograde labelling was present in the granular layer and sparse labelling in the deep mitral cell layer (Figures 9 A and 4 B).
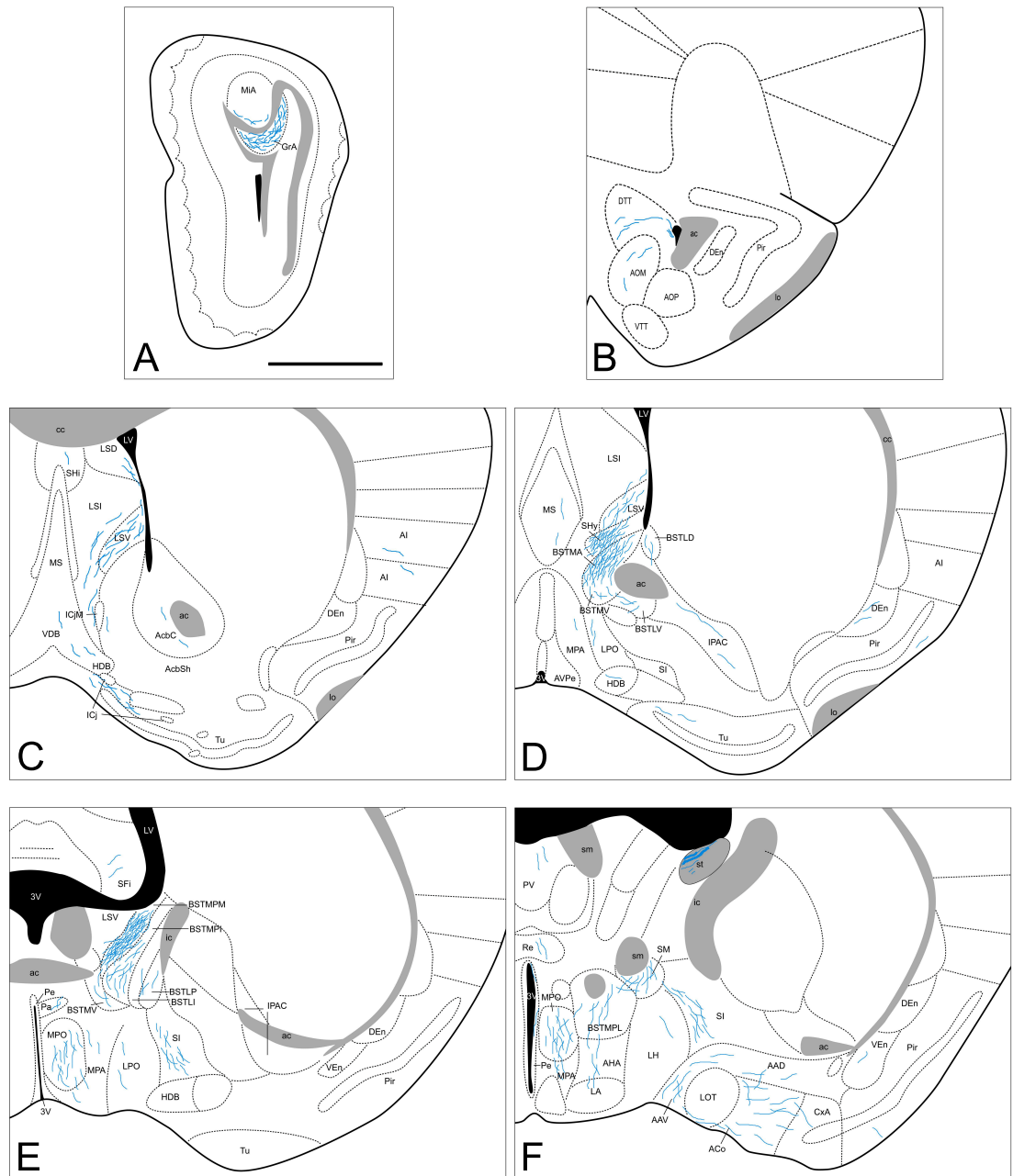
Figure 9: **Continued.**
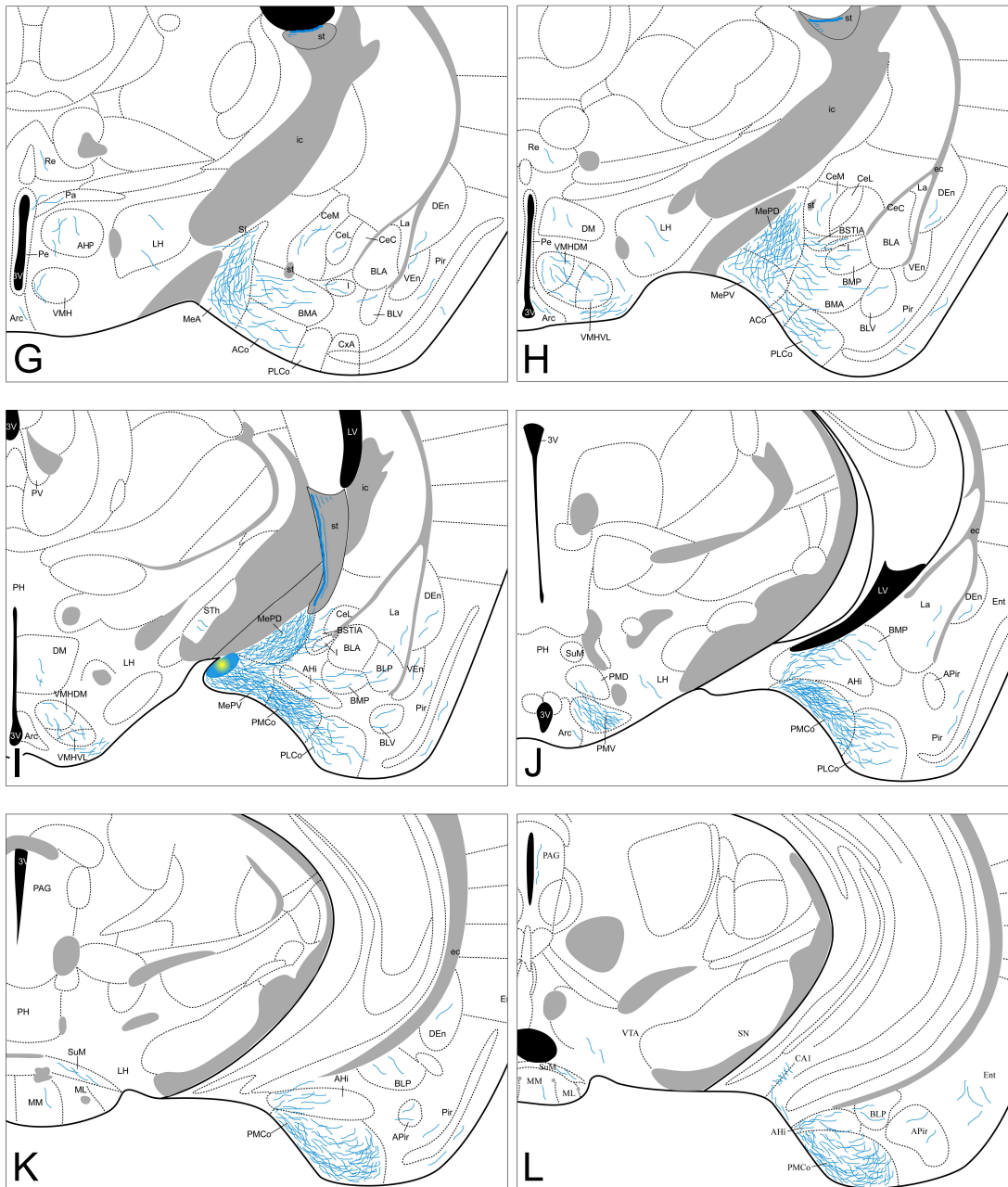
Figure 9: **Semi-schematic drawings of transverse sections through the mouse brain showing the distribution of anterogradely labelled fibres following tracer injections in the MePV**. The injection site is depicted in panel **I**. **A** is rostral, **L** is caudal. The drawings were made based on two injections, one in a C57BL/J6 mouse and another in a CD1 mouse. For abbreviations, see list. Scale bar = 1 mm.

Other secondary vomeronasal structures also received antero-grade labelling after tracer injecions in the MePV. The BST showed a heterogeneous pattern of anterograde labelling, from axons arriving through the *stria terminalis*. In the medial BST, la-belling was very dense in the BSTMPM, dense in the BSTMA, in-termediate in the BSTMPL and the BSTMPI, while the labelling was relatively light and diffuse in the BSTMV (Figures 9 D-F and 4 F). In contrast, all the subnuclei of the lateral BST showed very scarce anterograde labelling (Figure 9D,E; see Table 2).

The injections in the MePV resulted in dense anterograde la-belling in the other subnuclei of the Me (Figure 9 G-I). In the rest of the vomeronasal amygdala, there was very dense anterograde labelling in the PMCo (Figures 9 I-L and 5 C) and dense in the BAOT (not shown, see Table 2). In addition, the anterior amyg-daloid area showed moderate labelling in its ventral part (Figure 9 F).

4.4.2.2 *Olfactory system*

In the olfactory system, sparse innervation was observed in the Pir (with more labelled fibres present in its posterior zone) and dorsal *tenia tecta* (Figure 9 B-K). In addition, very scarce labelling was found in the endopiriform nucleus and the medial part of the anterior olfactory nucleus (Figure 9 B-K).

Within the olfactory amygdala, the ACo and the PLCo showed moderately dense axonal labelling (Figures 9 F-J and 5C), while the CxA (Figure 9 F,G) and the APir (Figure 9 K,L) had only a very sparse anterograde labelling. Finally, the LOT was mostly devoid of axons from the MePV, but some fibres could be ob-served in layer 1 (Figure 9 F).

4.4.2.3 *Non-chemosensory amygdala*

The central nucleus and associated intra-amygdaloid BST showed scarce and heterogeneous anterograde labelling follow-ing the MePV injections, with light labelling in the CeM, only a few fibres in the CeL and no labelling in the CeC (Figure 9 G-I). Scarce labelling was also observed in the I; but, in contrast, the BSTIA showed moderately dense labelling (Figure 9 G-I), as did the AHi (Figure 9 I-K). Finally, within the basolateral amyg-daloid complex, only the basomedial nucleus showed a moder-ate innervation both in its anterior and posterior parts (Figure 9 G-J), whereas sparse anterograde labelling was observed in the ventral basolateral amygdaloid nucleus. In the La only a few fibres were present (Figure 9 G-J).

4.4.2.4   *Other telencephalic structures*

After tracer injections in the MePV, few cortical structures (other than the olfactory related ones) showed anterograde labelling. A very scarce labelling was observed in the agranular insular cortex, and a moderate terminal field was present in the ventral hippocampus, in the *stratum lacunosum moleculare* of the CA1 field (Figure 9 J).

4.4.2.5   *Septum and ventral striatum*

At rostral levels the injections in the MePV resulted in anterograde labelling in the septal complex. The lateral septal nucleus showed moderate labelling in the LSV and scarce in the LSI and LSD divisions (Figure 9 C,D). In addition, the SHy had a dense innervation (Figure 9 D), while only a few axons were observed at the SHi (Figure 9 C). Scarce labelling was found in the medial septum/diagonal band complex (Figure 9 C,D).

In the ventral striatum, very scarce labelling was observed in the nucleus accumbens, Tu and islands of Calleja (Figure 9 C,D). Also the SI presented moderately dense labelling (Figure 9 E-G) and very few fibres were observed in the IPAC (Figure 9 D).

4.4.2.6   *Hypothalamus*

None of our injections in the MePV showed dense labelled terminal fields in the hypothalamus (Table 2). At preoptic levels, moderately dense labelling was observed in the MPO and sparse anterograde labelling appeared in the MPA (Figure 9 D-F), with very few fibres in the LPO (Figure 9 D,E).

At anterior levels, the anterior hypothalamic area and LA showed a low density of anterograde labelling (Figure 9 F,G), while the Pe and Pa had very scarce labelling (Figure 9 E-H).

In the tuberal region, the VMHVL and VMHDM showed a moderately dense labelling (Figures 9 G-I and 6 C). Of note, dense labelling was observed just ventrolateral to the VMHVL (Figure 9 H,I). A few labelled axons could be also observed in the LH and Arc, and very few in the DM (Figure 9 F-J).

At mammillary levels, the premammillary nucleus showed a few labelled fibres in the PMD, but a dense terminal field was observed in the PMV (Figures 9 J and 6 F). Also, a few fibres appeared in the SuM and MM (Figure 9 K,L).

4.4.2.7   *Thalamus*

The injections in the MePV resulted in anterograde labelling in a few thalamic nuclei. Some axons gave rise to sparse terminal labelling in the PV and, to a lesser extent, in the Re and STh

(Figures 9 F-I). Axons progressing through the *stria medullaris* apparently provide a moderately dense innervation to the nucleus of the *stria medullaris* (Figure 9 F).

4.4.2.8 *Brainstem and midbrain*

Only a few axons from the MePV coursed caudally and gave rise to sparse anterograde labelling in the PAG and VTA (Figure 9 L).

4.4.3 *Contralateral labelling*

As in the other subnuclei of the Me, the anterograde labelling resulting from the injections in the MePV is mostly ipsilateral. Few labelled axons crossed the midline in the anterior commissure and the *sox*. In the contralateral hemisphere, anterograde labelling appeared generally in those structures that presented a dense ipsilateral projection. Thus, sparse anterograde labelling appeared in the ventral lateral septum, BST and the hypothalamus, mainly in the MPO, anterior hypothalamic area, ventromedial hypothalamic nucleus and PMV.

4.5 INJECTIONS IN THE *substantia innominata* AND THE OPTIC TRACT

We obtained one injection located in the SI, dorsal to the MeA. This injection resulted in fibre labelling in the telencephalon coursing through the *fmi*, with labelled axons present in the parietal insular cortex and CPu. In the diencephalon, anterograde labelling appeared in the lateral LHb, lateral geniculate complex, ventral posterior thalamic nuclei, Po, STh, and *sox*. Finally, in the brainstem some labelled fibres were located in the SN, both in its *pars compacta* and *pars reticulata*.

Another of our injections was restricted to the *opt*, medial to the MePV. As expected, in this case we observed anterograde labelling in the different structures composing the visual thalamus, the pretectum and the superior colliculus (not shown).

<div style="text-align: right; font-size: 3em;">5</div>

DISCUSSION

In the present work we have compared the pattern of efferent projections of the anterior, posteroventral and posterodorsal subdivisions of the medial amygdaloid nucleus in two different strains of mice, namely C57BL/6J and CD1. The efferent projections originated from all three subnuclei present a common component and a number of relevant differences, which confirm in female mice the heterogeneity of the efferent projections of the Me previously reported in other male rodents (Gomez and Newman, 1992; Canteras et al., 1995; Coolen and Wood, 1998). This cytoarchitectonic and hodological compartmentalization of the Me is consistent also with the heterogeneous developmental territories that give rise to neuronal populations of this nucleus (García-López et al., 2008; García-Moreno et al., 2010; Bupesh et al., 2011), as well as with the expression of the genes encoding different transcription factors of the Lhx family (Choi et al., 2005).

The comparison of the projections between the C57BL/6J (an inbred strain very often used in the generation of genetically modified animals) and CD1 (an outbred strain commonly used in behavioural studies) strains indicates that there are no relevant differences in the organisation of the efferent projections of the Me. In addition, the present work uses female mice as experimental subjects. As far as we know, all of the previous reports of the efferent projections of the Me used male subjects (rats: Canteras et al. 1995; hamsters: Gomez and Newman 1992; Coolen and Wood 1998; mice: Choi et al. 2005; Usunoff et al. 2009). The efferent projections of the Me subdivisions found in female mice are very similar to the previous results in male mice, rats and hamsters. These results suggest that the inter-strain and inter-species differences in reproductive (Vale et al., 1973, 1974; Burns-Cusato et al., 2004; Dominguez-Salazar et al., 2004) and defensive (Belzung et al., 2001; Yang et al., 2004) behaviours cannot be attributed to differences in the pattern of efferent projections originated from the Me. Instead they may be due to differences at molecular level (e.g., expression of neurotransmitters or their receptors in the relevant connections). Moreover, since

the Me, and specifically its MePD subdivision, has been shown to be sexually dimorphic (Cooke et al., 1999), the present results suggest that the sexual dimorphism does not include the pattern of organisation of its efferent projections (Simerly, 2002), at least as revealed by our qualitative study. Of course, quantitative analysis of particular pathways may uncover sexual differences in the magnitude of some of these efferent projections, or in their neurochemical features.

As described previously for the other amygdaloid efferents in the rat and mouse (Canteras et al., 1995; Petrovich et al., 1996; Novejarque et al., 2011) efferents from all three subnuclei of the Me course through the same tracts, namely the *stria terminalis* and the ventral amygdalofugal pathway (*ansa peduncularis*), which converge at rostral levels. Within the *stria terminalis*, the efferent projections from the Me course medially, as described also in rats (Canteras et al., 1995) and hamsters (Gomez and Newman, 1992). On the other hand, the MeA contributes to the ventral amygdalofugal pathway more than the posterior Me, as reported in rats (Canteras et al., 1995). Experimental evidence in hamsters suggests that the projection to the hypothalamus courses exclusively through the *stria terminalis* (Maragos et al., 1989). Consistent with this view, our results suggest that the ventral amygdalofugal pathway contains mainly fibres directed to the ventral striato-pallidum, some of which apparently continue rostrally to reach the AOB. In fact, the existence of a non-strial pathway from the vomeronasal amygdala to the AOB has been demonstrated in the mouse (Barber, 1982).

Another feature of the projections of the Me subnuclei is that they are mainly ipsilateral, with only a few axons observed crossing the midline through the anterior commissure, the supraoptic commissure and the supramammilary decussation. These contralateral axons lightly innervate the zones corresponding to the densest terminal fields observed in the ipsilateral hemisphere, as reported previously in rats (Canteras et al., 1995).

Those injections in which tracer leakage occurred along the pipette track showed additional labelling that does not interfere with the labelling found following restricted injections, since most of it terminates in different structures. The only target that probably receives a light projection from the Me and also an important one from the dorsally located SI is the LHb, as revealed by restricted injections in both MeA and SI (see 4). This is consistent with previous reports on the projections of the Me (Gomez and Newman, 1992; Canteras et al., 1995; Coolen and Wood, 1998) and of the SI (Grove, 1988). In addition, the SI also shows important projections to the VTA (Geisler and Zahm, 2005), and accordingly our injections in the Me and in the SI

result in anterograde labelling in the VTA. Nevertheless, retrograde tracing after injections in the VTA confirm that at least the MeA and MePD do project to the VTA (Martínez-Herández*et al.*, unpublished data).

5.1 DIFFERENTIAL CENTRIFUGAL PROJECTIONS TO THE AOB FROM THE MEDIAL AMYGDALOID SUBNUCLEI

Our results confirm and extend previous works showing that the Me gives rise to important feedback projections to the AOB (Figures 10 and 11; Barber 1982; Gomez and Newman 1992; Canteras et al. 1995 Coolen and Wood 1998; Fan and Luo 2009). However, a number of differences between the present results and previous works should be highlighted. First, we have found that the projection from the MeA innervates mainly the ventral aspect of the mitral cell layer, in agreement with the description in mice (Barber, 1982), rats (Canteras et al., 1995) and hamsters (Gomez and Newman, 1992; Coolen and Wood, 1998). However, a recent report in C57BL/6 male mice did not found this projection (Fan and Luo, 2009), maybe because the injections of retrograde tracers in the mitral cell layer of the AOB were too small. In fact, to confirm this projection we revised a collection of retrograde tracer injections in the AOB, which revealed labelled cells in both the MeA and MePV (our unpublished results). Nevertheless, sex differences cannot be currently discarded. In addition, we also found that tracer injections in the MeA resulted in a few fibres in the glomerular layer of the posterior AOB, a light projection that may have important functional significance as it might modulate the input to particular glomeruli.

Regarding the feedback projection from the MePV to the granular layer of the AOB, it was not found in previous works in rats (Canteras et al., 1995) or male hamsters (Gomez and Newman, 1992; Coolen and Wood, 1998), in the latter case probably because the injections in the posterior Me were located in a dorsal position. In contrast, this projection has been reported in male mice (Fan and Luo, 2009), and characterised as glutamatergic. Since the MePV contains a subpopulation of glutamatergic cells originated by the ventral pallium (Bupesh et al., 2011), it is likely that at least some of them give rise to the excitatory feedback projection to the granular layer of the AOB. This projection may modulate the increase in the inhibitory neurotransmitter GABA released by the granule cells, that regulates the mitral cell responsiveness to mating male chemosignals (Griffiths and Brennan, 2015).
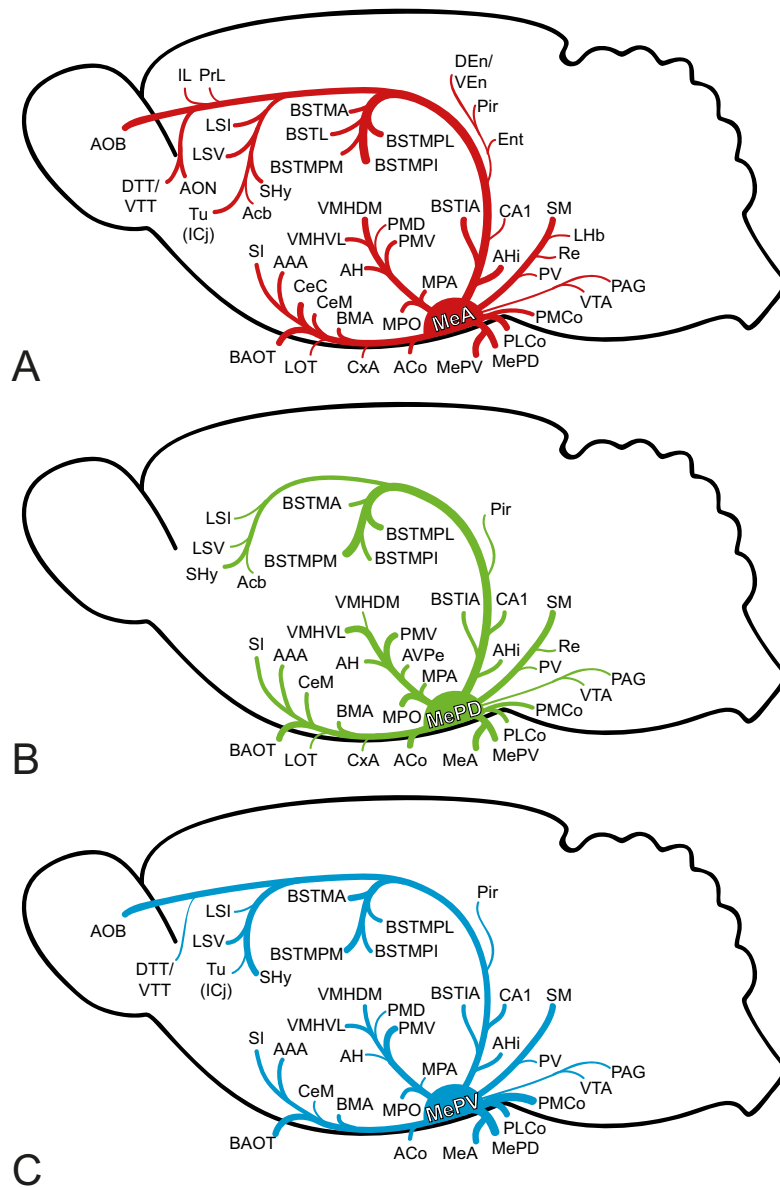
Figure 10: **Sagittal section of the mouse brain summarising the projections of the Me subnuclei**. **A,** Efferent projections of the MeA. **B,** Efferent projections of the MePD. **C,** Efferent projections of the MePV.

5.2 PROJECTIONS OF THE MEDIAL AMYGDALOID NUCLEUS TO THE VOMERONASAL SYSTEM

The efferent projections originated from all three subnuclei strongly innervate the other structures wich constitute the vomeronasal system, including the previously referred AOB, the BST and the vomeronasal amygdala.

The BST is a major recipient of efferent projections of the Me (Figure 11). Our results indicate that the different BST subdivi-
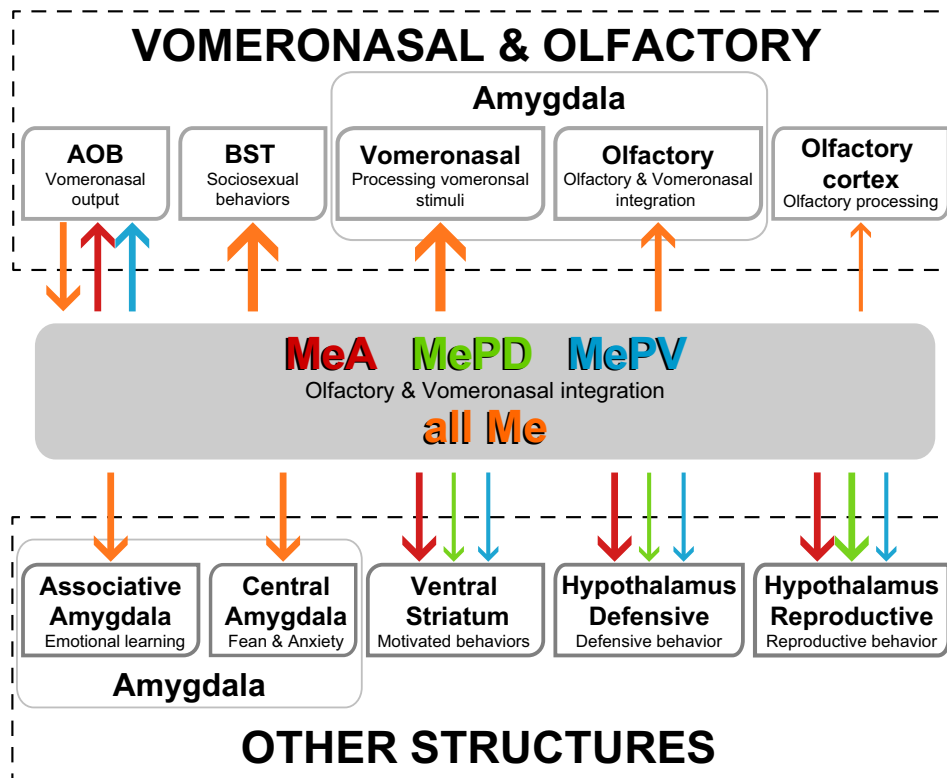
Figure 11: **Functional interpretation of the efferent projections arisen from the medial amygdaloid nucleus**. Schematic representation of the main efferent projections of the Me organised by functional systems. The differential projections are represented in red (MeA), green (MePD) and blue (MePV). The thickness of the arrows roughly represents the density of the projections.

sions display differential inputs from the subnuclei of the Me. Regarding the lateral BST, the MeA gives rise to moderate projections to these subdivisions of the BST, especially to the laterodorsal subnuclei of the BST (Figure 10 A). In contrast, the MePD and MePV originate only scarce projections to the lateral BST. This specific projection from the MeA to the lateral BST has not been reported in previous works (Gomez and Newman, 1992; Canteras et al., 1995), although a minor projection to lateral aspects of the anterior BST was illustrated by Coolen and Wood (1998). Nevertheless, this discrepancy may be partially explained by differences in the parcellation scheme of the BST: in the rat projections from the MeA have been described to the anterolateral, subcommissural and rhomboid subnuclei of the BST (Dong et al., 2001), which are included in the lateroventral BST and lateral posterior BST in our study (following the atlas of Paxinos and Franklin 2004). In fact, a moderate input from the MeA to the lateroventral BST has been confirmed by means of retrograde

tracing studies in the rat (Shin et al., 2008). In general, the lateral divisions of the BST are strongly interrelated with the central amygdaloid nucleus and are believed to be involved in eliciting fear and defensive or stress-related responses (Gray et al., 1993; Choi et al., 2007). In this sense, a recent study in mice has revealed that the vomeronasal organ has many more receptors for predator-derived stimuli than it was previously believed (Isogai et al., 2011) and, therefore, it is not surprising that the Me has direct projections to the these areas of the BST. Thus, the fact that mainly the MeA and, to a lesser extent, the MePV project to the lateral BST is consistent with the data showing that these subnuclei respond to predator-derived chemicals (Samuelsen and Meredith, 2009).

In contrast to the moderate and restricted projection to the lateral BST from the Me, the medial subnuclei of the BST are densely innervated by all three medial amygdaloid subdivisions. The density of the projections in the medial BST is different for each subnucleus and differs according to the Me subdivision of origin. The MeA innervates most densely the medial posterointermediate BST subdivision (Figure 10 A), whereas the MePD and MePV have their densest innervation in the medial posteromedial subdivision (Figure 10 B,C); also the MePV gives rise to a dense projection to the medial anterior BST (Figure 10 C). A similar pattern of projections has been reported previously for the MeA and MePD in several male rodents (hamsters: Gomez and Newman 1992; Coolen and Wood 1998; rats: Canteras et al. 1995; Dong et al. 2001; mice: Usunoff et al. 2009. However, the efferents of the MePV in our results differ from those previously studied in male rats (Canteras et al., 1995; Dong et al., 2001). Our results in female mice show a main projection from the MePV innervating the BSTMPM, whereas in male rats the main efferent from the MePV innervates the posterointermediate BST (interfascicular and transverse subnuclei of the posterior division in their nomenclature, see Dong et al. 2001). Although these discrepancies may be due to interspecies differences between rats and mice or sex differences between males and females, another possible explanation is the different interpretation of the nomenclature of this complex structure. Further research on the MePV efferents will be necessary to solve this question.

The pattern of projections to the medial divisions of the BST is consistent with the proposed functional roles of the different subnuclei of the Me. The MeA seems to filter and categorize the received chemosensory information, which would be relayed either to the neural circuit for socio-sexual behaviour (pheromones) through its projections to the MePD and BSTMPM or to the neural circuit for defensive behaviour (e.g., predator-derived

chemosignals) through its projections to the MePV and medial posterointermediate BST (Samuelsen and Meredith, 2009). In fact, the MePD projects massively to the BSTMPM and both nuclei are sexually dimorphic and enriched in steroid-sensitive cells involved in the control of sexual behaviour (Mitra et al., 2003; Swann et al., 2009). In contrast, the MePV has been said to project mainly to structures involved in defensive behaviour (Canteras, 2002; Choi et al., 2005). However, our results indicate that the MePV innervates the BSTMPM and the anteromedial BST. The latter gives rise to important projections to the hypo-thalamic neurosecretory system (Dong and Swanson, 2006), in-cluding the vasopressinergic and oxytocinergic neurons of the paraventricular nucleus. Since these neuropeptides in the Me have been shown to play a role in diverse social behaviours (Arakawa et al., 2010; Gabor et al., 2012), these data suggest that the MePV may be involved not only in defensive responses to predators, but also in the control of other non-sexual behaviours, such as agonistic encounters with same sex conspecifics or aver-sion to illness-derived social odours (Arakawa et al., 2010).

As described in previous works, our results confirm in fe-male mouse that the Me gives rise to important intramygdaloid projections, especially in the vomeronasal amygdala (Gutiérrez-Castellanos et al., 2010). The different subnuclei of the Me show dense bidirectional interconnections (Figure 10), in agreement with our previous retrograde study (Cádiz-Moretti et al., 2016b). Our material reveals that the projections of the MePD to the rest of the Me are more important than suggested by previous studies in male rats (Canteras et al. 1995; Figure 10 B). How-ever, in the male Syrian hamster Coolen and Wood (1998) and Gomez and Newman (1992) described a dense projection to the MeA from the posterior Me (without distinguishing between the MePD and MePV). By analysing the effects of lesions of the Me in the male Syrian hamster, Maras and Petrulis (2010a,b,c) proposed a functional interpretation for these anatomical data, which is fully supported by our findings in female mice. The MeA would filter the chemosensory information received from the olfactory bulbs that would then be relayed to the posterior Me. The abundant cells expressing receptors for sexual steroids in the MePD of the hamster (Wood et al., 1992) and the mouse (Mitra et al., 2003) make it a nodal center for the hormonal con-trol of the response to odours and pheromones in the context of reproductive behaviour. On the other hand, the projections from the MePD to the rest of the Me, which according to our results are very important in the female mouse, would allow an integra-tion of odour/ pheromone information with endocrine signals. In addition, it has been shown in male hamsters that the MeA

responds to heterospecific chemosensory stimuli, whereas the MePD appears to be inhibited by this type of stimuli (Meredith and Westberry, 2004). It has been suggested that the anatomical basis of this phenomenon include a projection from the MeA to the GABA-enriched intercalated cell mass, which in turn would inhibit the MePD cells (Meredith and Westberry, 2004). Our anatomical results indicate that the projection from the MeA to the intercalated cell mass located next to the MePD is present in female mice, and therefore a similar mechanism may operate so that the reproductive-related circuit is inhibited by heterospecific odours. However, a recent study in rats show that the exposure to a live cat induce c-fos expression in all subdivisions of the medial amygdala (Martínez et al., 2011), thus suggesting that, at least in this situation, heterospecific-induced inhibition of the MePD does not take place.

Among the projections innervating the rest of the vomeronasal amygdala (Kevetter and Winans 1981b; see Figure 11), projections from the three subnuclei terminate in the posteromedial cortical nucleus and in the anterior amygdaloid area, which also receives direct projections from the AOB (Cádiz-Moretti et al., 2013). In addition, the amygdalohippocampal transition area, which is not strictly chemosensory amygdala but it is strongly related to vomeronasal structures (see Swanson and Petrovich 1998; Martínez-García et al. 2012), is also interconnected with the Me, especially with the posterodorsal and posteroventral divisions (present results, Canteras et al. 1992, 1995).

5.3   PROJECTIONS OF THE MEDIAL AMYGDALOID NUCLEUS TO THE OLFACTORY SYSTEM

The olfatory system receives direct projections from the Me, mainly from the MeA, wich innervate a variety of structures: including the piriform and entorhinal cortices, endopiriform nucleus, anterior olfactory nucleus and *tenia tecta* (Figures 10 and 11). Only the MeA gives rise to significant projections to the Pir, particularly in its anterior region around the lateral olfactory tract, where they may converge with a light innervation directly originated by the mitral cells of the AOB (Cádiz-Moretti et al., 2013). Therefore, as suggested by Martínez-García et al. (2012), the Pir should not be viewed as a primary olfactory cortex, but as an associative chemosensory cortex.

In addition to the projections targeting vomeronasal amygdaloid nuclei already discussed, the Me gives rise to important the projections to the olfactory amygdala (Kevetter and Winans 1981a; Cádiz-Moretti et al. 2013; see Figures 10 and 11). All three subdivisions project to the anterior cortical and pos-

terolateral cortical nuclei, as it has been reported previously in different male rodents (hamsters: Coolen and Wood 1998; rats: Canteras et al. 1995; mice: Usunoff et al. 2009). Our results reveal also a previously unnoticed sparse projection of the Me to the cortex-amygdala transition zone and the LOT (only mentioned by Gomez and Newman 1992). The projection to the cortex-amygdala transition zone has been confirmed by means of retrograde tracer injections (Cádiz-Moretti et al., 2016a).

To summarise the connections with the vomeronasal and olfactory related structures, the Me not only receives direct projections from the main and accessory olfactory bulbs (Scalia and Winans, 1975; Pro-Sistiaga et al., 2007; Kang et al., 2009, 2011; Cádiz-Moretti et al., 2013), but also shows strong connections with both the olfactory and the vomeronasal components of the amygdala (Figure 11). These intra-amygdaloid connections are reciprocal in male rats (Pitkänen, 2000; Majak and Pitkänen, 2003), male hamsters (Coolen and Wood, 1998) and female mice (Cádiz-Moretti et al., 2016b), suggesting that the Me plays a relevant role in processing together the olfactory and vomeronasal chemical signals from conspecifics and heterospecifics (Baum and Kelliher, 2009; Keller et al., 2009; Martínez-García et al., 2009; Petrulis, 2013).

5.4 PROJECTIONS OF THE MEDIAL AMYGDALOID NUCLEUS TO THE NON-CHEMOSENSORY AMYGDALA

In contrast to the dense projection to the chemosensory cortical nuclei of the amygdala, the Me gives rise to relatively minor projections to the nuclei that compose the basolateral amygdaloid complex (Figure 11). Only the anterior basomedial nucleus apparently receives a moderate projection from all three medial amygdaloid subnuclei, although a minor projection to the lateral (ventral subnuclei) and basolateral nuclei also exists. These results are in agreement with the previous reports in several male rodents (Canteras et al., 1995; Coolen and Wood, 1998; Usunoff et al., 2009). Since the lateral and basolateral nuclei play a critical role in fear learning (Nader et al., 2001), the Me might play also a role in olfactory fear conditioning (Otto et al., 2000; Walker et al., 2005; Cousens et al., 2012). Of note, when cat odour is used as unconditioned stimulus, the contextual fear acquired is dependent of both the basolateral and the medial amygdaloid nuclei (Li et al., 2004). In addition, the projection to the basolateral nucleus might also be involved in attaching incentive value to olfactory stimuli. In fact, the basolateral nucleus densely innervates the ventral striatum (Novejarque et al., 2011), a projection that is known to play a critical role in many motivated be-

haviours (Shiflett and Balleine, 2010; Stuber et al., 2011). Meanwhile, the intricate set of intra-amygdaloid connections of the basomedial amygdaloid nucleus (Petrovich et al., 1996; Pitkänen et al., 1997), make this nucleus as a good candidate where vomeronasal information can be integrated with other kinds of emotionally labelled sensory information. Thus, the basomedial amygdaloid nucleus occupies a unique position to integrate a wealth of predator-derived cues, from olfactory to non-olfactory ones (such as visual and auditory sensory inputs) and to associate these cues with other stimuli gathered from the environment (Martínez et al., 2011).

Finally, the central nucleus of the amygdala receives substantial projections from the Me. The medial subdivision of the central nucleus receives moderate projections from all three Me subnuclei (Figure 11), but only the MeA gives rise to substantial projections to the capsular subdivision (Figure 10 A). These results agree with previous reports in male mice (Usunoff et al., 2009) and hamsters (Gomez and Newman, 1992; Coolen and Wood, 1998), although in hamsters the capsular subdivision was not considered. The results reported in male rats are slightly different, since all three subdivisions were found to moderately project to the capsular subdivision of the central nucleus and only the MeA gave rise to a moderate projection to the CeM (Canteras et al., 1995). The central amygdaloid nucleus has been considered to be primarily involved in the behavioural expression of conditioned fear responses (LeDoux, 2000; Davis, 2000) and in the modulation of appetitive behaviours (Parkinson et al., 2000; Robinson et al., 2014; Kim et al., 2017). Most of the ouput neurons of the central amygdaloid nucleus are located in its medial subdivision, that projects to hypothalamic and brainstem targets directly mediating emotional behaviours (Davis, 2000; Rosen et al., 1991), and is under inhibitory control originating in the lateral and capsular divisions (Ehrlich et al., 2009; Ciocchi et al., 2010; Kim et al., 2017). Therefore, the projections from the Me to the CeM and the CeC may modulate appetitive and aversive behaviours mediated by olfactory and vomeronasal stimuli. In this regard, a study by Cousens et al. (2012) shows that the Me is critically involved in the acquisition (and expression) of olfactory conditioned fear.

5.5 PROJECTIONS OF THE MEDIAL AMYGDALOID NUCLEUS TO THE SEPTUM, HIPPOCAMPUS AND VENTRAL STRIATUM

The three subdivisions of the Me give rise to moderate projections to the lateral septum, which target mainly its ventral and

intermediate divisions. Noteworthy, the ventral division is enriched in vasopressin innervation, and this projection is sexually dimorphic (Wang et al., 1993; Otero-García et al., 2014), with more density of vasopressinergic terminals in males. This pathway may convey sociosexual (and maybe also predator-derived) chemosensory information to the lateral septum so that it can be integrated with the spatial and contextual information relayed by the hippocampal formation. The convergence of sociosexual and contextual information would allow the animal to elicit appropriate reproductive/ defensive/ aggressive behaviours as a function of its contextual situation (Lanuza and Martínez-García, 2009). In this regard, we have observed a minor projection to the ventralmost tip of the ventral hippocampus, which is common to all three subdivisions of the Me (Figure 10). Although this projection is certainly a small one, it provides a direct route for the chemosensory stimuli processed in the Me to influence the contextual information processed in the ventral hippocampus. In rats, this same area of the ventral hippocampus has also been shown to receive substantial projections from the posteromedial cortical amygdaloid nucleus (Kemppainen et al., 2002) and to project back to AOB (de la Rosa-Prieto et al., 2009). Therefore, it is clearly a distinct subdivision of the ventral hippocampus that may be involved in integrating information about chemical signals with spatial or contextual cues.

According to our results, the Me displays scarce projections to some areas within the ventral striatum (Figure 10). This innervation reaches the ventromedial accumbens shell and adjacent Tu, as reported previously in male rats (Canteras et al., 1995) and hamsters (Gomez and Newman, 1992; Coolen and Wood, 1998). According to our results, the MePD and MePV contribute only with a few axons to this projection (Figure 11), although Usunoff et al. (2009) recently reported a significant projection from the MePD to the accumbens core, Tu and some islands of Calleja which we have not observed. The innervation in the medial Tu from the MeA reaches the vicinity of the ventromedial islands of Calleja (Figure 10 A). This area has also been reported to receive a direct input from the posteromedial cortical amygdala (Ubeda-Bañón et al., 2008; Novejarque et al., 2011), the other major target of the vomeronasal information. Therefore, this area of the ventral striato-pallidum may be specialized in processing the biological significance of pheromonal signals (Figure 11). In fact, the Tu is strongly related to the reward system of the brain (Ikemoto, 2007) and it may play a role in social odour processing (Wesson and Wilson, 2011).

5.6   PROJECTIONS OF THE MEDIAL AMYGDALOID NUCLEUS TO THE HYPOTHALAMUS

The hypothalamus is, together with the BST, the main target of the efferent projections of the Me. This fact has frequently led to the interpretation that the Me relays the information about pheromones, detected by the vomeronasal organ, to the hypothalamic circuits involved in the control of social and reproductive behaviour (Tirindelli et al., 1998; Luo and Katz, 2004). However, as we have already discussed, the Me has a more complex role and, accordingly, its projections to the hypothalamus show a complex pattern (Choi et al., 2005). In general, the MeA and MePV project to hypothalamic structures involved both in reproductive and defensive behaviours, whereas the MePD shows a much more delimitated pattern of projections, innervating mainly hypothalamic structures known to be involved in reproductive behaviours (Petrovich et al., 2001; Choi et al., 2005). Our results are consistent with this pattern of organisation (Figure 11), with some exceptions that are discussed below.

As described in male rats (Canteras et al., 1995; Petrovich et al., 2001) and hamsters (Gomez and Newman, 1992; Coolen and Wood, 1998), the hypothalamic targets of the MeA include not only the structures of the behavioural column controlling reproductive responses (Swanson, 2000), such as the MPO, ventrolateral VMH and PMV; but also the structures of the behavioural column controlling defensive responses (Swanson, 2000; Canteras, 2002), such as the anterior hypothalamic area, dorsomedial VMH and (lightly innervated) the dorsal premmamillary nucleus (Figure 10 A). In contrast, the main hypothalamic targets of the MePD are the nuclei involved in reproductive behaviour, thus the MPO, anteroventral periventricular nucleus, ventrolateral VMH and ventral premmamillary nucleus (Figure 10 B; Canteras et al. 1995; Petrovich et al. 2001). Regarding the hypothalamic projections of the MePV, our injections in this subdivision have resulted in relatively scarce anterograde labelling of hypothalamic structures (Figure 10 C). The major discrepancy of our results with those in male rats (Canteras et al., 1995; Petrovich et al., 2001) is the scarcity of the projection to the anterior hypothalamic area, which is part of the neural circuitry for defensive behaviours. This may be due either to interspecific differences or to the presence of sexual dimorphism in these particular efferent projections. In addition, we have found a very light projection to the dorsal premammillary nucleus originated mainly in the MeA, but also in the MePD and MePV, which has also been described in male rats using retrograde tracing by Comoli

et al. (2000), whose reanalysis of the material of a previous study (Canteras et al., 1995) showed few labelled fibres in this nucleus.

Another interesting result of our experiments is the presence of a relatively dense field of anterograde labelling in the PMV after tracer injections in the MePV. Although this confirms previous observations in the rat by Canteras et al. (1995), it does not fit a simple role of the MePV in anti-predatory defensive reactions, but suggests instead a possible modulation of socio-sexual behaviours mediated by this subnucleus. Since cells in the MePV are preferentially activated by predator-related chemosignals (Choi et al., 2005), this pathway might contribute to inhibiting sexual behaviour in threatening contexts, an issue that clearly requires further study.

5.7 PROJECTIONS OF THE MEDIAL AMYGDALOID NUCLEUS TO THE THALAMUS AND THE BRAINSTEM

The only thalamic nucleus that receives a dense input from all three subdivisions of the Me is the nucleus of the *stria medullaris* (Figure 10), as described previously by Usunoff et al. (2009) in male mice. In addition, a light projection common to the three medial amygdaloid subdivisions innervate the paraventricular and reuniens nuclei of the midline thalamus. The Re projects, among other targets, to the piriform and entorhinal cortices (Vertes et al., 2006). Therefore, this thalamic relay provides an additional indirect pathway for vomeronasal information to influence olfactory inputs to the hippocampal formation. On the other hand, the paraventricular nucleus projects back to the Me, as well as to other amygdaloid structures and to the nucleus accumbens, Tu and bed nucleus of *stria terminalis* (Vertes and Hoover, 2008). These connections suggest that the paraventricular nucleus is likely involved in the set of emotional behaviours controlled by the amygdala/ BST and the ventral striatum.

The Me provides only a light input to the brainstem, targeting the ventral tegmental area and the periaqueductal gray (Figure 10). The input to the VTA may be related to the reinforcing value that sexual pheromones have been shown to possess (Martínez-Ricós et al., 2007, 2008), although lesions of the dopaminergic cells of the VTA do not affect the attraction elicited by these sexual stimuli (Martínez-Hernández et al., 2006). In contrast, the projections of the PAG may be related to the elicitation of defensive behaviours by predator odours or chemical signals from dominant conspecifics (Motta et al., 2009). However, the few axons observed are not located in any of the longitudinal columnar regions of the periaqueductal grey described to be involved in

different emotional behaviours (Bandler and Shipley, 1994), but oriented dorsoventrally next to the ventricle.

Part III

PROJECTIONS FROM THE
POSTEROMEDIAL CORTICAL
AMYGDALOID NUCLEUS

6

MATERIALS AND METHODS

6.1 ANIMALS

The animals used for these experiments were 17 adult ($12-16$ weeks of age) female mice (*Mus musculus*), from the CD1 strain (Harlan, Spain) with body weights of $37.5 - 45.1$ g. Animals were housed in cages with water and food available *ad libitum*, in natural light conditions, at $21 - 22°C$. We treated them according to the EEC guidelines for European Communities Council Directives of 24th November 1986 (86/609/EEC), and experimental procedures were approved by the Committee of Ethics on Animal Experimentation of the University of Valencia.

6.2 SURGICAL PROCEDURES

The procedures employed to perform this experiment are similar to those described in the previous chapter, thus a brief description of the particular methods will be made.

6.2.1 *Tracer injections*

This experiment studied both the efferent and afferent projections from the posteromedial cortical amygdala. As anterograde tracer we used BDA (Molecular Probes, USA) diluted at 10% in saline PB (0.01 M, 0.9% NaCl, pH 7.6), while as retrograde tracer we used FluoroGold (FG, methanesulfonate hydroxystilbamidine; Biotium, USA) diluted at 2% in saline solution (0.9%). We delivered the tracers performing iontophoretic injections from glass micropipettes ($20 - 40$ μm inner diameter tips) by means of positive current pulses (7on/7off s, $3 - 5$ μA, $5 - 10$ min) using a current generator (Direlec, Spain). To reduce the leakage of tracer along the pipette track, a time lapse of $2 - 5$ minutes passed after the termination of each injection before the pipette was withdrawn. A continuous negative retentaining current (-0.9 μA) was applied during the entrance and withdrawal of the micropipette to avoid diffusion of the tracer. Some of the

tracer injections had been previously performed in the laboratory by Nicolás Gutiérrez Castellanos.

6.2.2   *Surgery*

Tracer injections were performed under deep anaesthesia with sodium pentobarbital (60 mg/kg, intraperitoneal; Sigma, USA), complemented with atropine (0.04 mg/kg, iperitoneal; Sigma). As the animals in the previous experiment, the depth of anaesthesia was monitored before and during the surgery. After fixing the mouse head in the stereotaxic apparatus (myNeurolab; Leica, Germany) a small incision was made in the skin revealing the skull surface, then the skull landmarks (Lambda and Bregma) were set in the same horizontal plane and we drilled two small holes above the postermedial cortical amygdala. Following tracer injection, we closed the wound with Histoacryl.

To minimise the number of animals, each animal received one injection per hemisphere. Thus, 11 animals received BDA injections and 6 animals FG injections. We adapted the coordinates in Paxinos and Franklin (2004) to CD1 mice and the resulting coordinates are shown in table 3.

Table 3: Coordinates of the injection sites (in mm) relative to Bregma.

	Antero Posterior	**Lateral**	**Depth**
PMCo	-2.6 to -2.8	±2.8 to ±3.2	-5.7 to -6.0

6.3   HISTOLOGY

After a survival of seven days the animals were deeply anaesthetised with an overdose of sodium pentobarbital and transcardially perfused with 20 ml of saline solution, followed by 60 ml of 4% paraformaldehyde diluted in PB. Brains were carefully removed from the skull and postfixed overnight in the same fixative. Then, they were cryoprotected with 30% sucrose solution in PB and we obtained frontal sections (40 μm) collected in four matching series.

6.3.1   *Tracer detection*

The detection of BDA was preformed as previously decrived. Briefly, we inactivated the endogenous peroxidase, then the sections were incubated overnight in ABC complex (Vectastain ABC

elite kit) diluted in TBS-Tx. The resulting peroxidase activity was visualised with diaminobenzidine, H_2O_2 and nickel ammonium sulphate to darken the reaction product.

The FG labelling was visualised with a fluorescence microscope using a wide-band ultraviolet excitation filter (Leica). The detailed analysis of the distribution of retrograde labelling required an immunohistochemical detection. To do so, we inactivated the endogenous peroxidase; then, sections were incubated overnight with a polyclonal rabbit anti-FG (Chemicon, Billerica, USA; cat. #AB153) diluted 1:5000 in TBS-Tx (0.1 M, 0.3% Triton X-100), followed by goat-anti-rabbit biotinylated secondary antibody (diluted 1:200 in the same buffer; Vector Laboratories). Immunodetection was completed with the ABC Elite kit and diaminobenzidine (without nickel) as described above for BDA.

In both cases the sections were mounted onto gelatinised slides,counterstained with the Nissl method, dehydrated with graded alcohols, cleared with xylene and coverslipped with Eukitt (Electron Microscopy Sciences, UK).

6.4 IMAGE ACQUISITION AND PROCESSING

Light and fluorescence microscopic images were photographed in a Leitz DMRB microscope equipped with a Leica DC 300FX digital camera (Leica Microsystems). Digital images were imported into Adobe Photoshop (Adobe Systems), brightness and contrast were adjusted and no additional filtering or manipulation of the images was performed. The final figures were composed and labeled with Adobe Photoshop. The design of the line drawings and their labelling was carried out with Adobe Illustrator (Adobe Systems).

7

RESULTS

For the description of the distribution of the afferent and efferent projections resulting from tracer injections in the posteromedial cortical amygdaloid nucleus (PMCo), we also followed the nomenclature of the atlas of the mouse brain by Paxinos and Franklin (2004). To simplify the description of the intramygdaloid projections, as in the Me, we use the terms "olfactory amygdala" and "vomeronasal amygdala" stablished by Kevetter and Winans (1981b,a). And, the term "chemosensory amygdala" which includes both the olfactory and the vomeronasal amygdala (Gutiérrez-Castellanos et al., 2010).

The labelling densities in the different nuclei projecting to or receiving projections from the PMCo, were subjectively classified as (see Table 4): very dense, dense, moderate, sparse and very sparse. We considered very dense the projection through the posteroventral amygdaloid nucleus and very sparse the areas where we could observe only $2-5$ labelled fibres/ cells.

The injection sites obtained in the PMCo are described below. In addition, we obtained a few injections in the adjacent PLCo, which were used as controls for the specificity of the anterograde labelling, together with the data from cited references (data summarised in Table 4; Majak and Pitkänen 2003; Jolkkonen et al. 2001; Shammah-Lagnado and Santiago 1999; Canteras et al. 1992).

Table 4: Semiquantitative rating of the density of the retrograde and anterograde labelling resulting after tracer injections in posteromedial cortical amygdaloid nucleus; the anterograde labelling was compared with that obtained following injections in adjacent structures (cited references and our unpublished results). IS = Injection site; nd = no data.

		FG PMCo (retrograde)	BDA PMCo (anterograde)	PLCo (affects the APir)[1]
Vomeronasal system and BST				
AOB	GrA/MiA	-/+++	++*/+↓	-
BST	BSTMA	-	+++*	+
	BSTMV	-	+	-
	BSTMPI	++	+++*	++
	BSTMPM	-	++*	+
	BSTMPL	+	++	+
	BSTLD	-	+↓	-
	BSTLP	+	+↓	-
Amygdala	BAOT	+++	+++*	nd
	MeA	++	+++*	+++
	MePD	++++	+++*	++
	MePV	++++	++++*	++
	AAA	++	+	++
	PMCo	IS*	IS*	+++
Olfactory system				
Tenia tecta	DTT/VTT	+/-	++/-	+/+
AON	AOM/AOP	-/-	++/+	+/+
Cortex	Pir	+++	++	++
	DEn/VEn	++++/++	+/++	++/++
	Ent	+++	+	+↓
Amygdala	LOT	++	+	+++
	CxA	++	+	+++
	ACo	++	++	++
	PLCo	++++	++	IS
	APir	++	+	IS
Non-chemosensory amygdala				
	BMA/BMP	+/+↓	+++/+	++/++
	BSTIA	+	++*	+

	AStr	-	+	nd
	I	-	+*	nd
	CeM	-	+	+↓
	CeC/CeL	-	+↓/-	+/-
	BLA/BLP	+↓ / ++	-/+	++/+
	La	+↓	+↓	++
	AHi	+	+	++

Other cortical structures

Prefrontal cortex	IL	-/+↓	-	+↓
	AIP	++	+↓	+↓
	Cl	+	-	nd
	PRh	+	+↓	+↓
Hippocampus	CA1/S	+++/-	+/+	+/+↓

Septum and Ventral striatum

Septum	LSV	-	++	+↓
	LSI	-	+	+↓
	LSD	-	+↓	-
	DB	+	+↓	+↓
Ventral striatum	AcbSh	-	+	+↓
	AcbC	-	+↓	+↓
	ICjM	-	++	+
	Tu	-	++	++
	ICjvm	-	+	+
	IPAC	-	+↓	+
	SI	+	++	++

Hypothalamus

	MPO	-	+↓	+
	AH	-	+↓	+↓
	LH	+	-	-

Very dense: ++++; Dense: +++; Moderate: ++; Sparse: +; Very sparse: +↓; No labelling: -.

* Contralateral labelling.

Data for PLCo/APir: our unpublished results and previous studies in the rat.

[1] PLCo: Canteras et al. (1992) and Majak and Pitkänen (2003); APir: Jolkkonen et al. (2001) and Shammah-Lagnado and Santiago (1999).
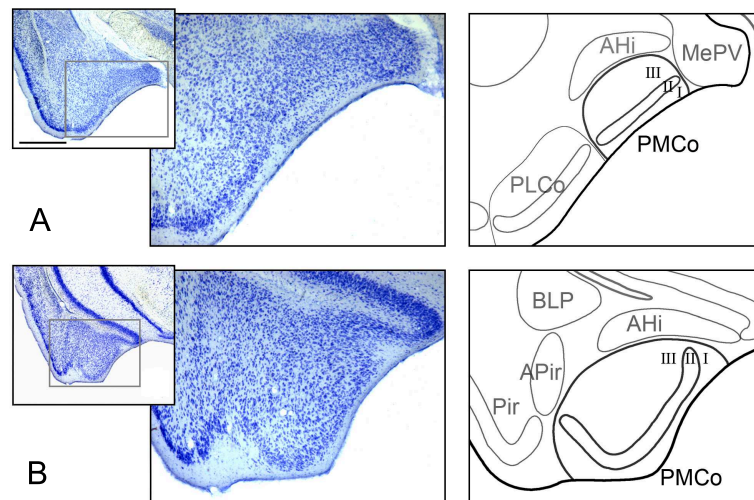
Figure 12: **Rostro-caudal organisation of the PMCo**. **A,** The rostral PMCo and surrounding amygdaloid structures. Left: low-power photomicrographs of Nissl staining of coronal sections through the amygdala in mice and higher magnification images to show the cytoarchitectonical organisation of the PMCo with its characteristic cortical lamination. Right: Schematic representation showing the general organisation of the PMCo and surrounding amygdaloid structures. **B,** Idem for the posterior PMCo. Scale bar in **A** (valid for **B**) = 500 μm.

7.1 ARCHITECTURE OF THE POSTEROMEDIAL CORTICAL AMYGDALOID NUCLEUS

The PMCo is a conspicuous cortical structure at the caudoventral aspect of the amygdala of mice, just superficial to the amygdalo-hippocampal area, with which it has somewhat diffuse boundaries in Nissl-stained sections. At rostral levels, the PMCo is interposed between the medially adjacent MePV and laterally adjacent PLCo (Figure 12 A). At caudal levels, it is medial to the APir and lateral to the ventral edge of the ventral hippocampus (Figure 12 B). As a cortical structure the PMCo shows a laminar organisation, with a superficial molecular layer (layer I), where the projection from the AOB terminates; an outer cell layer composed of relatively small, densely packed cells (layer II), easily recognised in Nissl-stained sections (Figure 12 A,B); and the deep cell layer (layer III), composed of relatively large and loosely organised somata.

7.2 FG INJECTIONS IN THE PMCO

7.2.1 *Injection sites*

Six female mice received FG injections aimed at the PMCo (Figure 13 A-D). Two of the injections were restricted to the target nucleus (Figure 13 B-D, injection Mo891). Another two injections encompassed the PMCo and partially affected the PLCo (Figure 13 A,B, injection Mo893). The other two affected the PMCo and a small part of the overlying AHi (Figure 13 A-C, injection Mo892). The results from these four injections, centered on but not restricted to the PMCo, confirmed the retrograde labelling described below (and summarised in Table 4), although they also showed retrogradely labelled cells that we attributed to the PLCo or the AHi.

7.2.2 *Retrograde labelling resulting from injections in the PMCo*

7.2.2.1 *Vomeronasal system*

All of the FG injections in the PMCo (Figures 14 I,J and 15 A) gave rise to abundant retrogradely labelled cells in the mitral cell layer of the ipsilateral AOB, in both its anterior (Figure 14 A and 15 B) and posterior divisions (Figure 14 B).

Retrograde labelling was also present in all of the secondary vomeronasal centres ipsilateral to the injection. Whithin the bed nucleus of the *stria terminalis*, its medial posterior division showed retrogradely labelled neurons, mainly located in the BST-MPI (Figures 14 C and 15 C). A few cells also appeared in the BSTMPL and in some injections scarce retrograde labelling appeared in the BSTLP.

In the vomeronasal amygdala, the labelling was dense in the BAOT (Figures 14 E and 15 D). Within the medial amygdaloid nucleus a very dense labelling was found in the posterior part (Figures 14 F,G and 15 E), both in the MePD and in the MePV; while the MeA showed a moderate density of retrogradely labelled cells, mainly restricted to its caudal aspect (Figure 14 E). Also, a moderate amount of retrogradely labelled cells was observed in the anterior amygdaloid area (Figure 14 D).

7.2.2.2 *Olfactory system*

As expected, the FG injections restricted to the PMCo did not yield retrograde labelling in the main olfactory bulb, but some cells could be found in secondary olfactory nuclei. The *tenia tecta*, mainly its dorsal part (not shown) displayed a few labelled neurons. In contrast, a dense population of retrogradely labelled
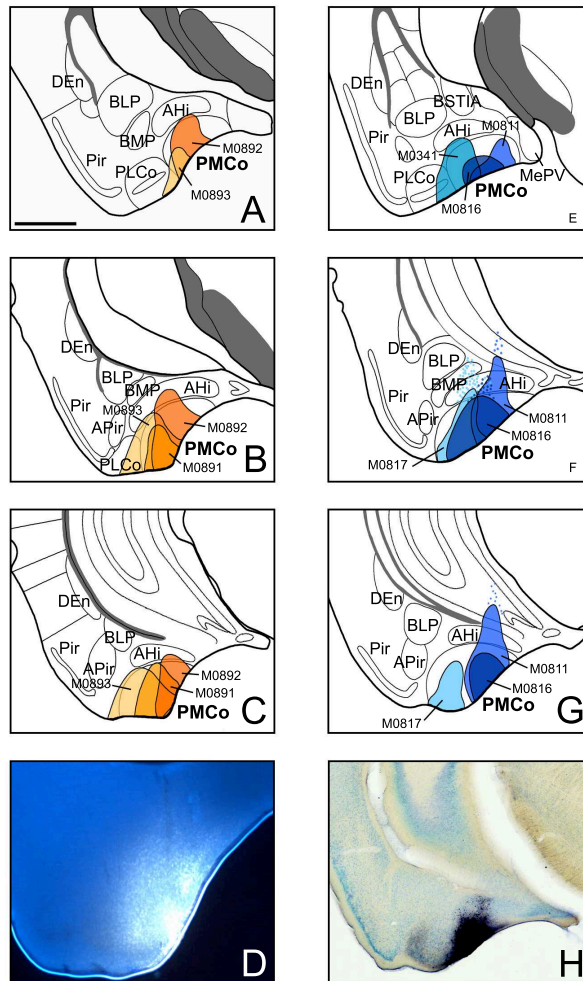
Figure 13: **Representative injections of Fluorogold (FG) and biotinilated dextran-amine (BDA) in the PMCo of mice.** Schematic representation of tracer injections encompassing the PMCo, different anteroposterior levels are shown to assess the rostrocaudal extension of the tracer deposits. FG injections are depicted in shades of orange (**A-C**), while BDA injections are shown in shades of blue (**E-G**). Injections M0891 (**B,C**) and M0816/ M0817 (**E-G**) are representative cases of restricted injections. Cases M0893 (**A-C**) and M0341 (**E**) are representative injections affecting the laterally adjacent PLCo. Injections M0892 (**A-C**) and M0811 (**E-G**) are representative injections which also affect the dorsally located AHi. Finally, low-magnification photomicrographs of representative injection sites of FG (**D**, case M0891) and BDA (**H**, case M0816). Scale bar in **A** (valid for **B-H**) = 500 μm.
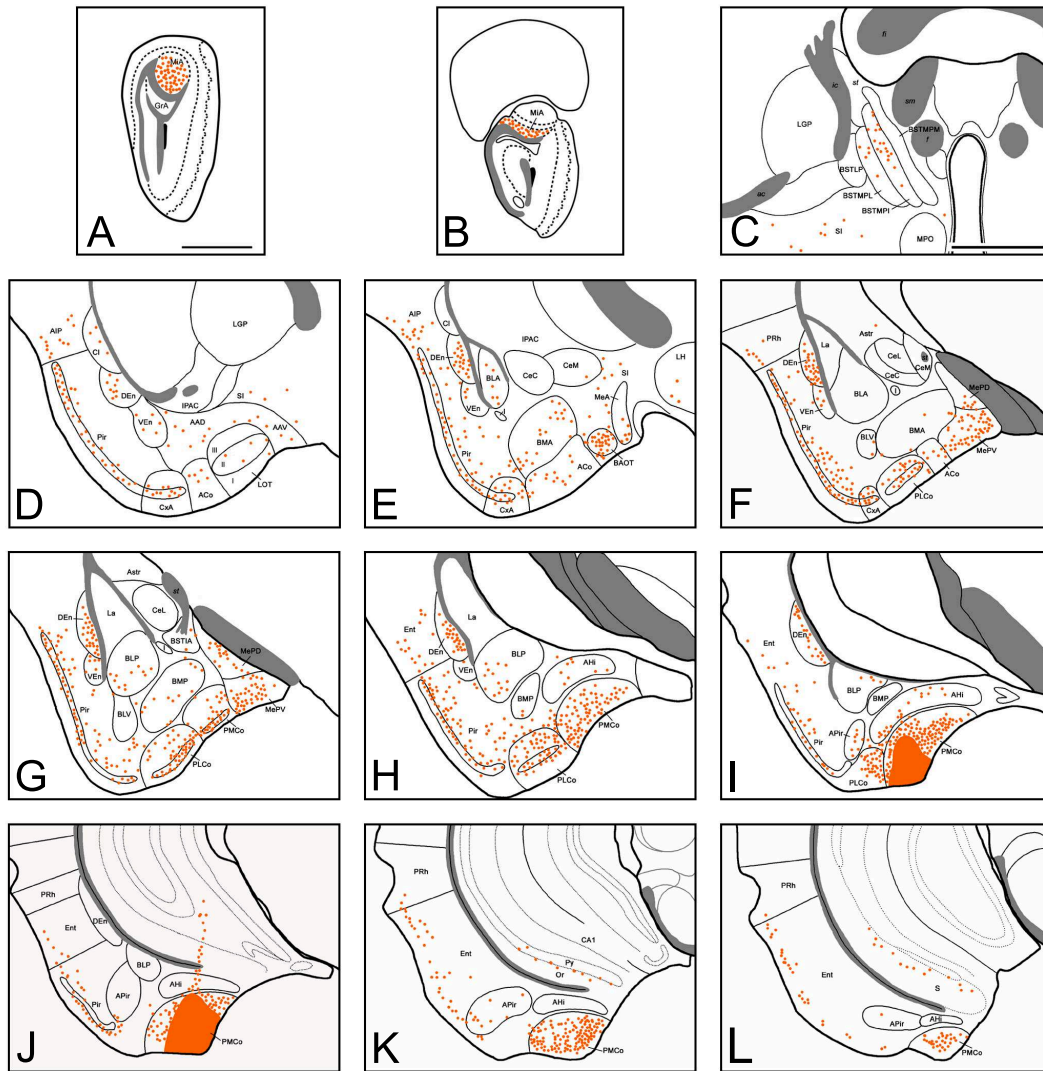
Figure 14: **Semi-schematic drawings of transverse sections through the mouse brain showing the ipsilateral afferent projections to the PMCo.** The injection site is depicted in panels **I** and **J**. **A** is rostral, **K** is caudal. The drawings were made based on injection M0891. For abbreviations, see list. Scale bar in **A** (valid for **B**) = 1 mm. Scale bar in **C** (valid for **D-L**) = 1 mm.
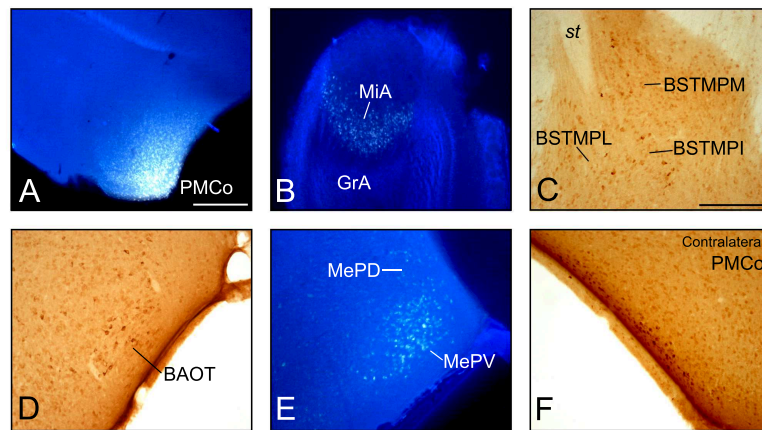
Figure 15: **Photomicrographs of representative vomeronasal-related structures containing retrograde labeled cells after an injection of FG affecting the PMCo.** Plates **A** and **E** are from experiment Mo891. Plates **B, C, D** and **F** are from experiment Mo890. Scale bar in **A** (valid for **B**) = 500 μm. Scale bar in **C** (valid for **D-F**) = 250 μm.

neurons was seen throughout the antero-posterior axis of the Pir, where the density of positive neurons was higher in layer II than in layer III (Figures 14 D-J and 16 A). Deep into the olfactory cortex, very dense retrograde labelling appeared in the dorsal endopiriform nucleus (DEn, Figures 14 D-I and 16 B). Although lower, a considerable number of labelled cells were also present in the ventral endopiriform nucleus (VEn, Figure 14 D-H). Retrograde labelling in the Pir extended caudally into the lateral Ent (Figures 14 H-L and 16 C), where abundant labelled cells were observed.

Within the olfactory amygdala, at rostral levels, the ACo (Figures 14 D-F and 16 D), the LOT (Figure 14 D) and the CxA (Figure 14 D-F) showed a moderate number of retrogradely labelled cells. In addition, very dense labelling was observed in the PLCo (Figures 14 F-I and 16 E), mainly in its layer II. Finally, at caudal levels, a moderate amount of labelled cells were present in the APir (Figure 14 I-L).

7.2.2.3 *Non-chemosensory amygdala*

Within the non-chemosensory amygdala, the FG injections in the PMCo resulted in a moderate labelling in the posterior part of the basolateral amygdaloid nucleus, whereas its anterior and ventral parts had very few stained cells (Figure 14 E-I). The basomedial amygdaloid nucleus showed scarce retrogradely labelled neurons in the anterior part and very few in the posterior part (Figure 14 E-H). A few labelled cells were also observed in the BSTIA (Figure 14 G). Lastly, only in two injections a few retro-
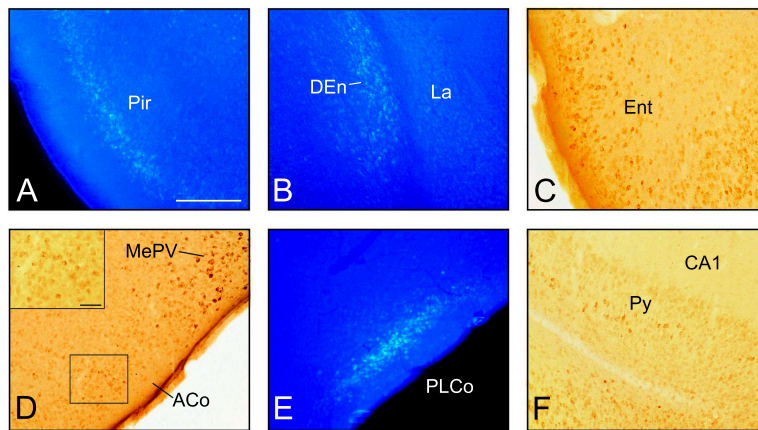
Figure 16: **Photomicrographs of olfactory-related structures and the hippo-campus containing retrograde labeled cells after an injection of FG affecting the PMCo.** Plates **A, B** and **E** are from experiment M0891. Plates **C** and **F** are from case M0893. Plate **D** is from experiment M0890. Scale bar in **A** (valid for **B-F**) = 250 μm. Scale bar in **C** inset = 50 μm.

gradely labelled cells were found in the La. In the AHi a number of retrogradely labelled cells were observed (Figure 14 H-L), although this result has to be taken with caution as the pipette track had to cross this area to reach the PMCo.

7.2.2.4 *Other telencephalic structures*

After tracer injections in the PMCo, very few retrogradely labelled neurons were observed in the infralimbic cortex (not shown), mainly located in its deep layers. In the posterior part of the agranular insular cortex (AIP) the tracer injections yielded a moderate density of labelled cells (Figure 14 D,E), while few labelled neurons were observed in the claustrum (Figure 14 D). In addition, a few retrogradely labelled cells were apparently present in the perirhinal cortex (PRh) just above the lateral Ent (Figure 14 F-L). Remarkably, the ventral hippocampus showed dense retrograde labelling in the pyramidal cell layer of the CA1 field (Figures 14 K,L and 16 F).

7.2.2.5 *Septum and ventral striatum*

FG injections in the PMCo barely resulted in any labelling in the septum and the ventral striatum. A few number of retrograde labelled cells were found in the nucleus of the diagonal band (not shown) and a few cells could also be found in the SI.

7.2.2.6 *Hypothalamus*

Within the hypothalamus, tracer injections in the PMCo resulted in few labelled neurons in the lateral hypothalamic area, almost reaching the ventromedial hypothalamic nucleus (Figure 14 E). In some (but not all) cases a few labelled cells appeared within the ventromedial nucleus and the dorsomedial hypothalamic nucleus.

7.2.3 *Contralateral labelling*

In the contralateral telencephalon the only labelled cells we observed were located in the contralateral PMCo, in particular superficially in layer II (Figure 15 F). Within the rostrocaudal extent of the contralateral PMCo, the labelled cells occupied a level similar to that of the injection site.

7.3 BDA INJECTIONS IN THE PMCO

7.3.1 *Injection sites*

Ten adult female mice received BDA injections affecting the PMCo (Figure 13 E-H). Four of these were centered and restricted to the PMCo (Figure 13 E-H, case M0816). The remaining injections were centred in the PMCo, but also involved small portions of the neighboring structures, such as the overlying AHi (Figure 13 E-G, injection M0811), the medial part of the PLCo (Figure 13 E-G, injection M0341) or the posterior part of the basomedial amygdaloid nucleus. The pattern of anterograde transport described below (and summarised in Table 4) is based on the observation of the restricted injections and was confirmed with the remaining injections.

7.3.2 *Anterograde labelling resulting from injections in the PMCo*

The injection of BDA in the PMCo gave rise to anterograde labelling in a complex range of cerebral nuclei. Intra-amygdalar axons spread directly from PMCo, while fibre labelling coursing outside the amygdala followed two main pathways: the *stria terminalis*, where labelled axons were located in the dorsal aspect (next to the ventricle) and, in a lesser extent, axons progressed across the SI. The output of the PMCo appeared mostly ipsilateral, with scarce fibre labelling present in contralateral nuclei, as described below.
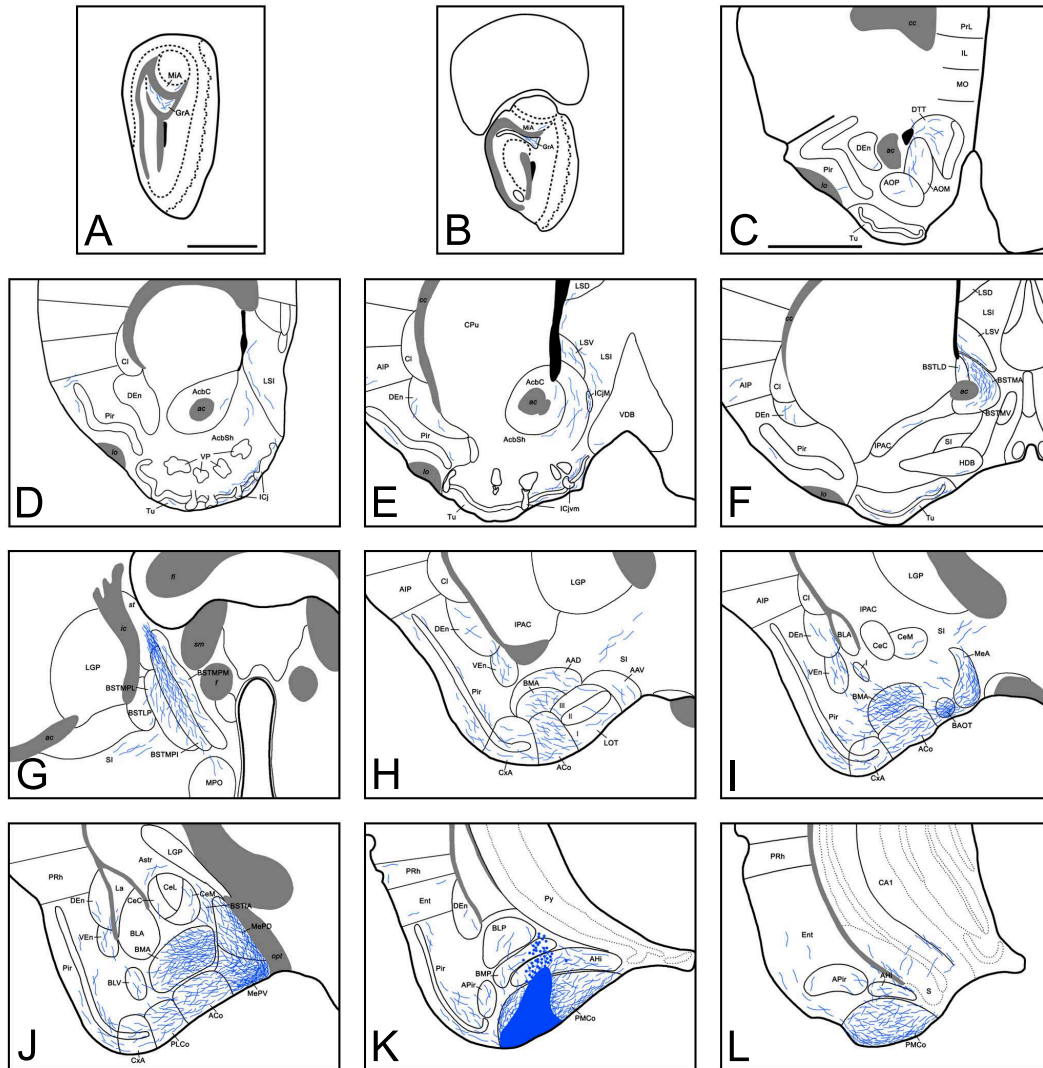
Figure 17: **Mapping of the ipsilateral anterograde labelling resulting after an injection of BDA centred in the PMCo**. The injection site is depicted in panels **K**. **A** is rostral, **L** is caudal. Scale bar in **A** (valid for **B**) = 1 mm. Scale bar in **C** (valid for **D-L**) = 1 mm.

Figure 18: **Photomicrographs of representative fields containing antero-
gradely labelled fibres in vomeronasal-related structures after a
BDA injection in the PMCo**. Plates **A, B** and **D** are from experi-
ment Mo816. Plates **C** and **F** are from experiment Mo811. Plate **E**
is from experiment Mo815. Scale bar in **A** = 500 μm. Scale bar in **B**
(valid for **C-F**) = 250 μm. Scale bars of the inset in **B** and in **F** = 50
μm.

7.3.2.1 *Vomeronasal system*

Tracer injections significantly affecting the three layers of the
nucleus (Figures 17 K and 18 A) showed anterogradely labelled
fibres next to the ventral sulcus of the lateral ventricle, in a jux-
taventricular location, that could be followed rostrally through
the subependymal layer of the olfactory ventricle, until the level
of the AOB (Figures 17 A,B and 18 B). These fibres gave rise to
a moderate labelling in the granular layer of this structure, both
in its anterior and in its posterior subdivisions. Also, very few
labelled axons appeared to enter the mitral cell layer of the AOB.

From the injection site some fibres ran medially to reach the
superficial part of the posterior medial amygdaloid nucleus and
finally entered the *stria terminalis*. This bundle of labelled axons
traveled in an anteromedial direction to reach the BST, where it
split into rostral and caudal branches. The rostral branch coursed
through the anterior BST to reach the lateral septum, while the
caudal branch gave rise to the anterograde labelling in the pos-
terior BST. Within the BST, a dense field of fibres was observed
in the BSTMA and a few axons reached the BSTMV (Figure 17 F).
In the posterior BST, dense labelling was present in the BSTMPI
and a moderate amount in the BSTMPL and BSTMPM (Figures
17 G and 18 C). The lateral division of the BST showed only very
scarce labelling located in the BSTLP and the laterodorsal part
(Figure 17 F,G).

Within the vomeronasal amygdala, a dense field of labelled fibres was found in the BAOT (Figures 17 I and 18 D). Axons from the injection site reached the Me, which showed dense labelling in its anterior and posterodorsal parts (Figures 17 I,J and 18 E) and even denser labelling in the MePV (Figures 17 J and 18 E). The majority of the anterogradely labelled fibres were located in the most superficial part of the nucleus. However, a remarkable innervation of fibres resembling fibers-on-passage was observed in the deep aspect of the MePD, which delineated the inner limit of this amygdaloid nucleus with the adjacent basomedial nucleus. In the anterior amygdaloid nucleus a sparse anterograde labelling was also observed (Figure 17 H). Finally, the smallest injection wich involved only the superficial part of the PMCo (Figure 13 H), mainly layer II, revealed a strong intranuclear connectivity targeting the whole extension of the nucleus (layers I and II).

7.3.2.2   *Olfactory system*

Tracer injections in the PMCo resulted in labelling in a number of olfactory-related structures. At rostral levels, labelled fibres could be found in the *tenia tecta*, which had a moderate density of labelling in its dorsal part but none in its ventral part (Figure 17 C). A moderate density of fibres appeared in the medial subdivision of the anterior olfactory nucleus, but the density was sparse in the posterior subdivision (Figure 17 C). The labelling observed in the Pir was moderately dense, but an heterogeneous distribution was observed rostrocaudally. The posterior part, next to the amygdala, had a denser labelling and it mainly affected layers I and III, with few fibres in layer II (Figures 17 C-K and 19 A). The endopiriform nucleus showed a differential labelling in its dorsal and ventral divisions; two of our restricted injections showed scarce labelling in the DEn and moderately dense in the VEn (Figures 17 C-K and 19 B), while another non-restricted injection showed a dense labelling in the DEn and scarce in the VEn (see 8). At more caudal levels, the labelled fibres in the Pir apparently extended into the Ent (Figures 17 K,L and 19 C).

In the olfactory amygdala, both the ACo and the PLCo showed a moderately dense fibre labelling (Figures 17 H-J and 19 D,E), whereas only scarce labelling was observed in the LOT (Figures 17 H and 19 F), CxA (Figure 17 H-J) and APir (Figure 17 K,L).

7.3.2.3   *Non-chemosensory amygdala*

Among the non-chemosensory amygdala several nuclei showed anterograde labelling. In the subpallial amygdala the central nuc-
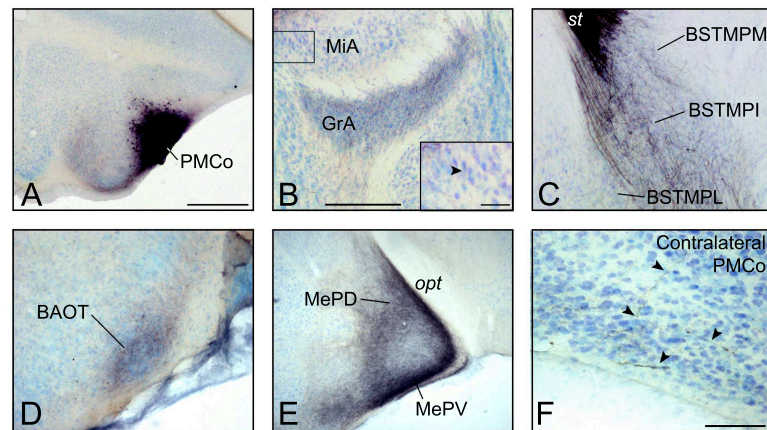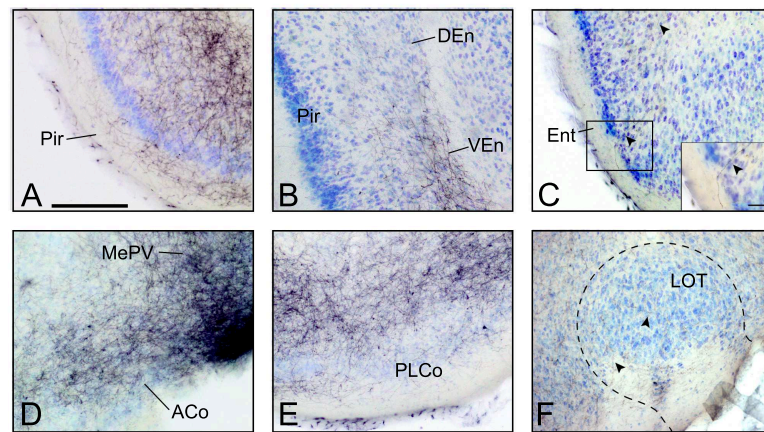
Figure 19: **Photomicrographs of representative fields containing antero-gradely labelled fibres in olfactory-related structures after a BDA injection in the PMCo**. Plates **A, D** and **E** are from experiment Mo811. Plates **B** and **C** are from experiment Mo816. Plate **F** is from case Mo81. Scale bar in **A** (valid for **B-F**) = 250 μm. Scale bar of the inset in **C** = 50 μm.

leus showed labelled axons ranging from sparse (CeM) to very sparse (CeC; Figure 17 I,J). The amygdalostriatal transition area and the BSTIA (Figure 17 J) presented a moderate density, although part of the labelling in the BSTIA is probably due to fibres that cross this nucleus in their course to the *stria terminalis*. In addition, a few fibres were observed in the intercalated mass (Figure 17 I). In the basolateral complex of the amygdala, the BMA showed the densest labelling (Figure 17 H-K). Additionally, sparse labelled fibres were observed in the posterior division of the basolateral nucleus (Figure 17 I-K) and portions of the La (Figure 17 J). In contrast, the AHi had a moderate density of anterograde labelling (Figure 17 K,L), but could be due to the small tracer deposits that appeared along the micropipette track.

7.3.2.4 *Other telencephalic structures*

As a rule, only injections affecting the deep layers of the PMCo showed anterograde labelling in the prefrontal cortex. In these injections, some scattered fibres were observed running dorsally from the *taenia tecta*, parallel to the midline, to reach the prefrontal cortex. Thus, a few scattered axons were observed in the dorsal part of the infralimbic cortex and the ventral portion of the prelimbic cortex (not shown). Tracer injections in the PMCo also presented very sparse labelling in the AIP (Figure 17 E,F). At caudal levels, the labelled fibres extended into in the PRh, where labelling was very scarce (Figure 17 K).
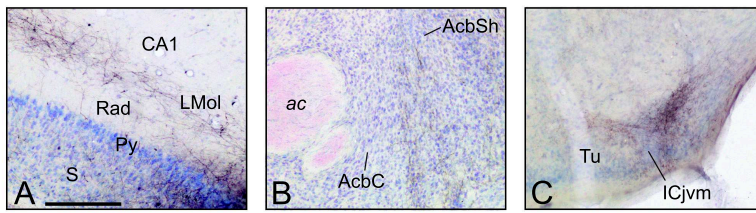
Figure 20: **Photomicrographs of representative fields containing antero- gradely labelled fibres in the hippocampus and ventral striatum after a BDA injection in the PMCo**. Plate **L** is from experiment Mo816. Plate **M** is from experiment Mo811. Plate **N** is from case Mo81. Scale bar in **A** (valid for **B, C**) = 250 μm.

Labelled fibres leaving the PMCo reached the hippocampal formation caudally, through the most superficial and ventral parts of the hippocampus, as illustrated in Figure 17 L. In the hippocampal formation the distribution of labelling varied sig- nificantly as a function of the intranuclear location of the injec- tion site. Those injections substantially affecting the deep PMCo (layer III) rendered a dense meshwork of anterograde labelling running between the ventral parts of the *stratum lacunosum mo- leculare* and the *stratum radiatum* of the CA1 field of the hippo- campus, densely innervating both strata at very caudal levels (Figure 20 A). The projection was restricted to this ventro-caudal position, and consequently no labelled fibres were observed in these same layers at anterior or dorsal coordinates. In addition, some of the fibres coming into the hippocampus were also ob- served in the most external part of the ventral subiculum. Also, small fibre bundles crossed perpendicularly the pyramidal layer of the CA1 field apparently connecting the two major terminal fields in the hippocampal formation. The superficial injections gave rise to a similar distribution of labelling, both in the CA1 and in the subiculum, but only a sparse labelling was observed in these cases.

7.3.2.5 *Septum and ventral striatum*

Part of the anterogradely labelled fibres running through the *stria terminalis* reached the lateral septum and continued rostrally next to the ventral sulcus of the lateral ventricle. Accord- ingly, anterograde labelling was present in the different parts of the lateral septum throughout their rostrocaudal extension (Fig- ure 17 D-F). The LSV showed a moderate density of labelling, while the LSI and LSD a low or very low density, respectively. Ventral to the septum, the nucleus of the diagonal band (both in its vertical and horizontal limbs) showed very scarce fibre la- belling (Figure 17 E,F).

Labelled fibres reached the ventral striatum through the *stria terminalis* and gave rise to anterograde labelling in the rostral and medial aspect of the ventral striatum (Figures 17 D,E and 20 B). Labelling density was low in the medial shell of the nucleus accumbens and very low in its medial core. In this nucleus the labelling appeared denser in those injections affecting the deep layers of the PMCo. Fibres coursing through the medial shell of the nucleus accumbens extended medially to the major island of Calleja (Figure 17 E) and the Tu, were the anterograde labelling was heterogeneous. Labelled fibres in the Tu were concentrated in the medial aspect of this structure, which showed a moderate density of labelling mainly in layers Ib end III, and the labelling gradually decreased laterally. In the medial Tu labelled axons were observed in close association with the ventromedial islands of Calleja, with some fibers apparently entering them (Figures 17 D-F and 20 C). In addition, the labelling in the Tu also extended into the adjacent striatal cell bridges that connect the shell of the nucleus accumbens with the Tu. Very few fibres were also found in the IPAC (Figure 17 F). Finally, a moderate density of labelled fibres could be found in the SI (Figure 17 H,I).

7.3.2.6   *Hypothalamus*

None of our injections in the PMCo showed dense labelled terminal fields in the hypothalamus. Only a few scattered fibres descending from the medial part of the ventral BST reached the MPO (Figure 17 G) and the anterior hypothalamic area (not shown). No labelling was observed in the rest of the hypothalamus, unless the injections affected the AHi or the basomedial amygdala.

7.3.3   *Contralateral labelling*

The anterograde labelling resulting from tracer injections in the PMCo was mainly ipsilateral. However, some fibres from the ipsilateral *stria terminalis* entered the anterior commissure, where they formed a compact dorsal bundle that crossed to the contralateral hemisphere. Although in some cases labelled fibres were also observed in other commissures (e.g. supraoptic), they could be attributed to the involvement of the AHi in the injection. From the anterior commissure, labelled fibres entered the contralateral *stria terminalis* from where they gave rise to anterograde labelling in the BST, rostrally in the AOB and caudally in the amygdaloid complex.

Labelling in AOB was restricted to the granular layer and appeared exclusively after injections involving the superficial

PMCo. In the BST, a moderate density of smooth and slightly varicose labelled axons was observed in the BSTMPI, a lower labelling could be seen in the BSTMA and very few fibres appeared in the BSTMPM. Within the amygdala, a low density of smooth (e.g. fibres-on-passage) and slightly varicose labelled fibres was observed in the BSTIA and the intercalated mass. Anterograde labelling was also present in other nuclei of the vomeronasal amygdala. In the Me the distribution of the labelling was similar to that of the ipsilateral hemisphere, but with a much lower density. Thus, all the subdivisions of the Me showed labelling, but the density was higher in the MePV than in the MeA or MePD. Some contralateral labelling was also found in the BAOT. Finally, the labelling extended caudally to give rise to a remarkable projection to the contralateral PMCo, where the labelled fibres occupied the deep part of layer I (Ib), as well as the superficial cell layer (layer II; Figure 18 F).

DISCUSSION

The present work describes for the first time the complete pattern of afferent and efferent projections of the posteromedial cortical amygdaloid nucleus in female mice. The results confirm and extend previous reports in other mammalian species, mainly in rats and hamsters, showing some of these connections (Kevetter and Winans 1981b; Canteras et al. 1992; Kemppainen et al. 2002; for a complete review, see Pitkänen 2000). In particular, the pattern of PMCo efferent projections presently described in female mice is very similar to that previously reported in male rats (Canteras et al., 1992). The fact that no relevant differences are found between the present results in female mice and previously reported data in male rats and hamsters indicates that no significant sexual dimorphism is present in the pattern of PMCo projections, and that this pattern of connections is common to the different rodent species.

The efferent projections from the PMCo follow the same tracts as other amygdaloid efferents in rat (Canteras et al., 1992; Petrovich et al., 1996), hamster (Kevetter and Winans, 1981b) and mouse (Novejarque et al. 2011; see 5). Intra-amygdalar axons spread directly from PMCo, while projections coursing outside the amygdala followed two main pathways: the *stria terminalis* and, in a lesser extent, axons progressed across the SI through the *ansa peduncularis*. As decribed in rats (Canteras et al., 1992), the labelled axons coursing through the *stria terminalis* were located in the dorsal aspect (next to the ventricle).

Another feature of the projections to and from the PMCo is that appears mostly ipsilateral. In fact, the PMCo only receives projections from the contralateral PMCo (Pitkänen 2000; Figure 21 C). Regarding the contralateral anterograde labelling, although it was light, extended to several nuclei. Axons were observed to cross through the anterior commissure and entered the contralateral *stria terminalis*, from where they gave rise to anterograde labelling in the BST, the AOB and the amygdaloid complex. The labelling in the granular layer of the AOB appears exclusively after injections involving the superficial PMCo and has been previously described in rats (de Olmos et al., 1978;

Barber, 1982). In the BST, labelled terminal fields are observed
in the BSTMPI (Canteras et al., 1992; Dong et al., 2001), but also
in the BSTMA and BSTMPM. Within the amygdala, as seen in
male rats (Canteras et al., 1992; Pitkänen, 2000), the vomerona-
sal amygdala shows labelling in the medial amygdaloid nucleus,
bed nucleus of the accessory olfactory tract and PMCo. Some
fibres appear in the intramygdaloid division of the BST and the
intercalated mass, which have not been previously reported. The
discrepant labelling between our results (in female mice) and
the contralateral labelling described in male rats (Canteras et al.,
1992) may be due to sexual dimorphism or inter-species differ-
ences.

Those experiments in which tracer injections affected adja-
cent amygdaloid areas, namely the posterolateral cortical amy-
gdaloid nucleus and the amygdalohippocampal area, were care-
fully examined and contrasted with the literature (Canteras et al.,
1992; Jolkkonen et al., 2001; Majak and Pitkänen, 2003) to con-
firm the labelling observed in the restricted injections.

8.1   THE POSTEROMEDIAL CORTICAL AMYGDALOID NUC-
LEUS IS THE VOMERONASAL PRIMARY CORTEX

Among the structures considered stricty vomeronasal, only the
PMCo shows characteristics that could make it be considered
as the primary vomeronasal cortex. The PMCo has a major in-
put from the AOB, first described in rats, rabbits and opossums
(Winans and Scalia, 1970; Scalia and Winans, 1975) and later
in mice (Von Campenhausen and Mori, 2000). This projection
originates in the mitral cells of the AOB and innervates the su-
perficial layer of the PMCo (rats: Scalia and Winans 1975; Pro-
Sistiaga et al. 2007; mice: Von Campenhausen and Mori 2000;
Cádiz-Moretti et al. 2013) and its terminal field coincides with
the calretinin, neuropilin-2 and acetyl cholinesterase innervation
(Kemppainen et al., 2002; Gutiérrez-Castellanos et al., 2010). The
presence of calretinin is a feature shared with the projection ori-
ginated by the mitral cells of the MOB to the piriform cortex and
the olfactory amygdala (Wouterlood and Härtig, 1995; Gutiérrez-
Castellanos et al., 2010), whereas the expression of neuropilin-2
and acetyl cholinesterase is specific to the AOB projection and,
therefore, clearly differentiates the vomeronasal from the olfact-
ory projection (Gutiérrez-Castellanos et al., 2010). The presence
of neuropilin-2 in the mitral cells of the AOB has been confirmed
by *in situ* hybridisation (Inaki et al., 2004; Huilgol et al., 2013),
confirming that this projection is enriched in neuropilin-2. The
projection originated by the AOB mitral cells is believed to be
glutamatergic (Wada et al., 1998; Jia et al., 1999; Park et al., 2014)
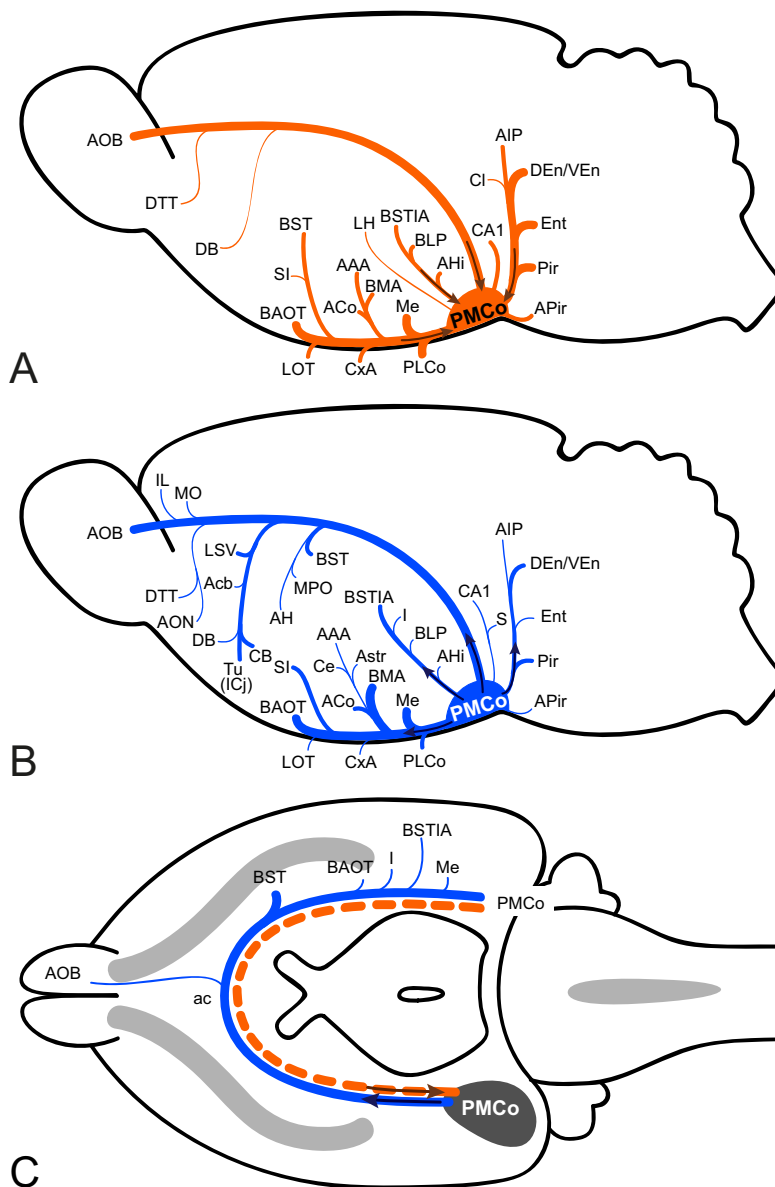
Figure 21: **Summary of the afferences and efferences of the PMCo. A,** Afferent projections of the PMCo. **B,** Efferent projections of the PMCo. **C,** Schematic representation of the main contralateral projections of the PMCo.

but, in contrast to most other glutamatergic telencephalic projections (Paoletti et al., 2009), it is not enriched in zinc (Kemppainen et al., 2002).

Among the structures targeted by the projection from the AOB, the PMCo is the only structure with a strict pallial origin, as revealed by the expression of the developmental regulatory genes Neurogenin 2 and Semaphorin 5A (Medina et al., 2004). Neurogenin 2 has been described to be characteristic of

the differentiation of pallial glutamatergic neurons (Guillemot et al., 2006). In addition, the laminar organisation of the PMCo is altered in reeler mice (Boyle et al., 2011). In contrast, the remaining targets of the AOB, the medial amygdala and bed nucleus of the *stria terminalis* are mainly of subpallial origin, although the posteroventral medial amygdala contains a small population of pallial cells (Bupesh et al., 2011; Martínez-García et al., 2012). Therefore, the PMCo should be considered the vomeronasal cortex.

An appealing hypothesis is that the PMCo, as the primary vomeronasal cortex, projects to the medial amygdala, which would be the "vomeronasal striatum". The Me, in turn, projects to the posteromedial BST (see 4), which would be the "vomeronasal pallidum", whom also receives a projection from the PMCo. However, the study of the embryonic origin of the medial amygdala and the posteromedial BST suggests that both of them contain neurons of different subpallial origins, including striatal and pallidal components (Bupesh et al., 2011), allowing the striato-pallidal circuits to be present within each of these two structures (McDonald, 2003).

When compared with the medial amygdala, the other major target of the AOB projection, the PMCo shows a noteworthy lack of intranuclear heterogeneity. The medial amygdala can be subdivided in anterior, posterodorsal and posteroventral subdivisions that show important differences in their efferent projections (Canteras et al. 1995; see 4). In contrast, our tracer injections in the PMCo revealed similar patterns of anterograde labelling regardless of the rostrocaudal or mediolateral location of the injection site within the nucleus. The only important differences appeared between the injections centered in the superficial layers (I and II) and those involving also the deep layer III. These differences indicate that layer II neurons innervate mainly the AOB and other rostral structures such as the dorsal *tenia tecta*, while the deeper neurons (layer III) mainly project to the ventral striatum and prefrontal cortex.

The light reciprocal projection with the prefrontal cortex, mainly with the infralimbic cortex, has also been reported in rats using anterograde (Hurley et al., 1991; Canteras et al., 1992; McDonald et al., 1996; Vertes, 2004) and retrograde tracers (Hoover and Vertes, 2007). In fact, tracer injections in the infralimbic and prelimbic cortices of the rat give rise to retrograde labelling in the deep cortical amygdaloid nucleus (see Figures 5 O,P and 8 O,P in Hoover and Vertes 2007), which is consistent with the differences observed between superficial and deep injections in the present work.

In conclusion, the PMCo is the main cortical target of the projection from AOB and therefore constitutes the primary vomeronasal cortex. Like other primary sensory cortices, the PMCo shows layered organisation of its inputs and outputs. Thus, its main sensory afferent terminates superficially (input to layer Ia) whereas the commissural projection from its contralateral counterpart terminates in layer Ib and deeper. In addition, the PMCo also shows a layered segregation of the cells giving rise to its main outputs, which are zinc-enriched glutamatergic neurons, a typical feature of cortical structures. Thus, cells projecting back to its main sensory input (AOB) and commissural cells projecting to the contralateral PMCo are located relatively superficially (layer II). In contrast, cells giving rise to associative cortico-cortical projections (e.g. olfactory cortex, frontal cortex) or to "descending" projections to subcortical targets (medial amygdala and BST, ventral striatopallidum) are located in deep layers (layer III) or distributed throughout the deepness of the cortex.

8.2 PROJECTIONS OF THE POSTEROMEDIAL CORTICAL AMY-GDALOID NUCLEUS TO THE VOMERONASAL SYSTEM

As summarised in Figures 21 and 22, the PMCo receives information from and projects back to each of the structures of the vomeronasal system, including the AOB, the medial amygdala, the bed nucleus of the accessory olfactory tract and the bed nucleus of the *stria terminalis*. The projection to the granular layer of the AOB was one of the first PMCo outputs to be reported (Barber and Field, 1975; Broadwell and Jacobowitz, 1976; de Olmos et al., 1978; Barber, 1982), and has been shown to originate from glutamatergic cells (Fan and Luo, 2009). Our results confirm that this projection is a bilateral one, although with clear ipsilateral dominance, and originates mainly in cells of layer II.

The PMCo has bidirectional connections with the BST (Figures 21 A,B), although the efferents are denser than the afferents. Our results indicate that the posteromedial subdivision of the BST displays both inputs and outputs from the PMCo, specially in the medial posterointermediate BST (Dong et al., 2001; Wood and Swann, 2005). Another substantial projection from the PMCo is observed in the medial anterior BST, as described previously in rats (Canteras et al., 1992; Dong et al., 2001). Regarding the lateral BST, only very scarce projections were found to this area, which have not been previously described. This discrepancy may be due to inter-species differences or to differences in the parcellation scheme of the BST.

In addition, the PMCo of mice gives rise to very dense projections to the BAOT, the medial amygdala and the contralateral PMCo, and receives significant inputs from these same structures (Figure 22), as previously reported in rats and hamsters (Kevetter and Winans, 1981b; Canteras et al., 1992). Therefore, there is a very dense network of interconnections among the different nodes of the vomeronasal system, which would mediate the processing of vomeronasal information. This processing is crucial for reproduction and survival as the vomeronasal system is involved in the detection of sexual pheromones (Martínez-Ricós et al., 2008; Haga et al., 2010; Roberts et al., 2010), chemical signals from competitors (Chamero et al., 2007), predators (Papes et al., 2010; Isogai et al., 2011), stress-related signals (Nodari et al., 2008) and illness signals (Rivière et al., 2009). Therefore, the information derived from these different classes of chemical signals requires an important amount of neural processing before an appropriate behavioural response may be generated. Note that all of the different vomeronasal stimuli named above elicit an emotional behavioural response, either appetitive (sexual pheromones), aggressive/ defensive (chemical signals from competitors), aversive (ill-related signals) or defensive (predators). Therefore, it is not surprising that vomeronasal information is processed in the amygdala, given the key role of the amygdala in emotional responses (LeDoux, 2000). From this point of view the amygdala may be considered a neural device to process emotional information (and learn about it) with different subdivisions for different sensory modalities (Martínez-García et al., 2012).

8.3   PROJECTIONS OF THE POSTEROMEDIAL CORTICAL AMYGDALOID NUCLEUS TO THE OLFACTORY SYSTEM

The PMCo also shows significant interconnections with the principal components of the main olfactory system, including the piriform cortex and endopiriform nucleus, the lateral entorhinal cortex and the olfactory amygdala (Figure 22). However, these connections with the olfactory system, specially the efferent projections, are not as dense as those with the vomeronasal structures (Figure 21 A,B). The description of these efferences has been previously reported in other rodents (Canteras et al., 1992; Kevetter and Winans, 1981b) and projections from the endopiriform are present in rats and cats (Krettek and Price, 1978). These connections would allow the integration of olfactory and vomeronasal information to compose a complete map of the chemical environment of the animal. In fact, electrophysiological recordings in the hamster's PMCo have revealed the existence
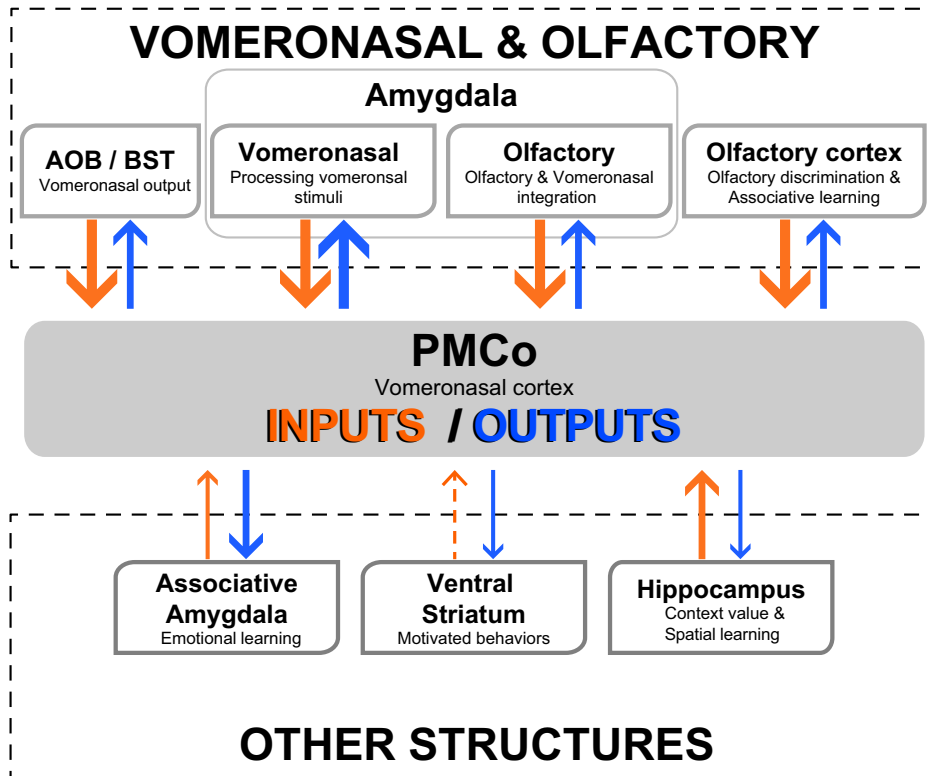
Figure 22: **Functional interpretation of the afferent and efferent projections of the posteromedial cortical amygdaloid nucleus**. Schematic representation of the main afferences and efferences of the PMCo organised by functional systems. The afferences are represented in orange and efferences in blue. The thickness of the arrows roughly represents the density of the projections.

of individual units activated by electrical stimulation of either the main olfactory bulb or the vomeronasal organ (Licht and Meredith, 1987).

In this regard, in rodents the main and accessory olfactory systems are known to play a complementary role in most behavioural responses driven by chemical senses (Baum and Kelliher, 2009; Martínez-García et al., 2009). This is reflected by olfactory-vomeronasal integration at two levels. First, convergence already occurs in the projections from the olfactory bulbs: the medial amygdala, the anterior cortical nucleus, the cortex-amygdala transition zone and the anterior amygdaloid area. These structures have been shown to receive direct projections from both the MOB and the AOB (Pro-Sistiaga et al., 2007; Kang et al., 2009; Cádiz-Moretti et al., 2013). And second, the reciprocal connections between the PMCo and secondary olfactory centers (Figure 22) might provide an anatomical substrate for olfactory-vomeronasal association that would occur not only in the PMCo itself, but also in the piriform and lateral entorhinal cortices that

receive direct projections from the PMCo. Therefore, as previously suggested, even the piriform cortex can be considered a chemosensory associative area rather than a primary sensory cortex (Haberly, 2001).

Our restricted injections reveal that the projection of the PMCo to the endopiriform nucleus targets mainly its ventral division. This is in agreement with previous reports in rats (Majak et al. 2002, see their Figure 5 E). The moderate projection to the dorsal endopiriform nucleus observed in some of our non-restricted injections is probably due to affected neurons of the amygdalo-hipocampal area (Canteras et al., 1992) or the posterior basomedial amygdaloid nucleus (Majak et al., 2002). However, the projection from the endopiriform nucleus to the PMCo is originated in its dorsal division (Krettek and Price 1978; present results).

As explained above, several vomeronasal stimuli are endowed with an intrinsic emotional valance (sexual pheromones, predator-derived signals, etc.) and therefore may act as unconditioned stimuli in Pavlovian associative learning. For instance, vomeronasal stimuli can be associated with neutral odorants (which would become the conditioned stimuli) that happen to be present at the same time. In fact, it has been shown that female mice are able to associate the attractive male sexual pheromones with male-derived odorants. In this way, male-derived odorants become attractive themselves (Moncho-Bogani et al., 2002; Martínez-Ricós et al., 2008), thus facilitating mate search. Data on c-fos expression strongly suggest that this kind of vomeronasal-olfactory associative learning takes place in the amygdala (Moncho-Bogani et al., 2005), where other forms of emotional learning also occur (e.g. fear conditioning; see LeDoux 2000). Given the convergence of olfactory and vomeronasal information on the piriform and/ or the entorhinal cortices, these two structures are also good candidates for this kind of association.

In this sense, the access of molecules to the vomeronasal organ requires the activation of an active pumping mechanism (Meredith and O'Connell, 1979; Wysocki et al., 1980) and the activation of the AOB has been shown to require direct nasal contact with the source of the molecules to be detected (Luo et al., 2003). In contrast, the main olfactory system detects volatile molecules at a distance. Therefore, the association of olfactory neutral odors with vomeronasal "emotional" stimuli would allow the animals to detect and react in advance to the proximity of conspecifics or predators, without the need of contacting them (nor their marks). Thus, the olfactory-vomeronasal associative learning would be an important advantage to track potential mates

or safely flee from potential predators (Martínez-García et al., 2009).

8.4 PROJECTIONS OF THE POSTEROMEDIAL CORTICAL AMY-GDALOID NUCLEUS TO THE NON-CHEMOSENSORY AMY-GDALA

In contrast to the dense connection with the chemosensory amygdala, the PMCo receives and gives rise to relatively minor projections to the nuclei that compose the basolateral amygdaloid complex (Figure 21). The PMCo receives sparse inputs from the basolateral and basomedial nuclei of the amygdala, and projects densely to the basomedial nucleus (Figure 22), in agreement with results previously reported in rats (Canteras et al., 1992). The basomedial amygdala also receives important afferents from the medial amygdala (Canteras et al. 1995; see 4), which in turn receives a direct projection from the AOB. Therefore, these anatomical data point to the basomedial nucleus as a good candidate where vomeronasal information can be integrated with other kinds of emotionally labelled sensory information, which would reach the nucleus through the intricate set of intra-amygdaloid connections (Pitkänen et al., 1997).

In contrast to previous reports in rats (Pitkänen et al., 1995), we did not consistently find a projection from the lateral nucleus to the PMCo. It is possible that this projection is very light in mice or restricted to the deep part of the nucleus, which was not affected in all of the FG injections. The reciprocal projection, from the PMCo to the lateral amygdaloid nucleus, is very light and restricted to the ventral aspect of the nucleus. In contrast with previous reports in rats (Kemppainen et al., 2002), labelled fibers show varicosities.

8.5 PROJECTIONS OF THE POSTEROMEDIAL CORTICAL AMY-GDALOID NUCLEUS TO THE HIPPOCAMPUS AND THE SEPTUM

The PMCo shows reciprocal projection with the ventral hippocampus, especially with the CA1 field (Figure 21 A,B). Similar results regarding the afferent (Ottersen, 1982; Cenquizca and Swanson, 2007) and efferent projections (Canteras et al., 1992; Kemppainen et al., 2002) have been reported in rats. In both rats and mice, the projection from the PMCo terminates specifically in the *stratum lacunosum-moleculare* and *stratum radiatum* of CA1, with the pyramidal layer being only lightly innervated (Canteras et al. 1992; Kemppainen et al. 2002; present results in mice). A similar innervation pattern of CA1 has been observed in the rat

arising from the amygdalo-hippocampal area and the posterolateral cortical amygdaloid nucleus (Canteras et al., 1992). In contrast, the posterior basomedial amygdaloid nucleus innervates the *stratum oriens* and the entire pyramidal layer (rats: Petrovich et al. 1996).

Field CA1 of the ventral hippocampus also receives a mild projection from the medial amygdala in rats (Canteras et al., 1995) and mice (see 4). In turn, the CA1 field of the ventral hippocampus projects to the AOB (de la Rosa-Prieto et al., 2009). Therefore, the ventral CA1 seems a highly specialised area of the hippocampus that is strongly interconnected with the vomeronasal system. An interesting hypothesis about the functional role of this vomeronasal-hippocampus interaction is that the information about vomeronasal stimuli contained in urine marks contributes to the spatial map generated by the hippocampus (Figure 22). The mouse is a territorial species and males delimitate their territory using urine marks (Hurst and Beynon, 2004). The vomeronasal stimuli contained in urine are critical in eliciting aggressive responses (Chamero et al., 2007, 2011) and a particular male-specific urinary pheromone named Darcin has recently been found to induce spatial learning (Roberts et al., 2012). The aggressive responses of males are dependent on the spatial location of the animals: the owner of the territory (resident male) strongly attacks intruder males, whereas the intruder generally adopts a defensive attitude (Miczek et al., 2001). The neural circuitry by which the territory modulates the aggressive/defensive responses is currently unknown (Adams, 2006). Given the key role of vomeronasal cues in this phenomenon, we suggest that the interconnections between the PMCo and the ventral hippocampus may play a critical role in constructing a territorial map based on vomeronasal cues.

The PMCo also gives rise to a projection to the ventrolateral septum (present results in mice, see Figure 21 A; Canteras et al. 1992 in rats). This is one of the two cases of efferent projections of the PMCo that are not reciprocated (the other one is the output to the ventral striatum, discussed below). The ventrolateral septum is also targeted by a projection arising from the ventral hippocampus (Risold and Swanson, 1997). This septal area receiving convergent projections from the ventral CA1 and the PMCo is part of the septal region that projects to the hypothalamic aggression area in male rats (Toth et al., 2010) and may gate the aggressive response in resident males when both the hippocampal and the PMCo inputs signal the presence of a competitor within the owned territory. In females, by contrast, the convergence of ventral CA1 and PMCo inputs to the ventrolateral septum may signal the presence of a dominant male in his

territory, and therefore the hypothalamic projections originated by the septum should activate, in this case, the hypothalamic circuits for reproductive behaviour. Although this hypothesis requires experimental support, it has recently been shown that hypothalamic subpopulations of neurons mediating aggression and reproductive behavior are located within the same structure, in such a way that neurons activated during aggressive encounters are inhibited during mating (Lin et al., 2011). Therefore, for the hypothesis stated above to hold true, the projection from the ventrolateral septum to the hypothalamus should innervate different target neurons in males (aggression-related neurons) and females (mating-related neurons).

8.6   PROJECTIONS OF THE POSTEROMEDIAL CORTICAL AMYGDALOID NUCLEUS TO THE VENTRAL STRIATUM

As shown in the summary of the PMCo connections (Figures 21 A,B and 22) most of the efferent projections of the PMCo target structures that project back to it. There are two major exceptions to this rule, the ventrolateral septum and the ventral striatum. The innervation of the ventral striatum is centered in the ventromedial aspect of the olfactory tubercle, and concentrates around the medial islands of Calleja (Ubeda-Bañón et al., 2008; Novejarque et al., 2011). The olfactory tubercle is part of the reward system of the brain (Ikemoto, 2007) and it has been suggested to be involved in processing the hedonic value of chemosensory stimuli (Wesson and Wilson, 2011). Among the vomeronasal stimuli putatively processed in the PMCo, those related to sexual attraction have reinforcing properties, as shown by its ability to induce conditioned place preference (Agustín-Pavón et al., 2007; Martínez-Ricós et al., 2007; Roberts et al., 2012). Therefore, the direct projection from the PMCo to the medial aspect of the olfactory tubercle, including the islands of Calleja, may constitute the anatomical pathway conveying information about the vomeronasal sexual pheromonesto the reward system of the brain (Novejarque et al., 2011). It should be noted that this direct projection is a relatively light one, and consequently it is possible that the dense projections from the PMCo to other amygdaloid structures, such as the basomedial nucleus, which in turn gives rise to dense projections to the ventral striatum (Petrovich et al., 1996; Novejarque et al., 2011), play an important role in the transfer of chemosensory information to the brain reward system.

Consequently, the vomeronasal cortex should be considered a key element in the emotional brain. It is interconnected with adjoining regions of the amygdala, thus allowing the associ-

ation of chemosensory cues (semiochemicals, pheromones and allomones) with other chemical and non-chemical stimuli, thus boosting the ability to establish emotional responses to previously neutral stimuli.

Part IV

OSCILLATORY ACTIVITY IN THE
VOMERONASAL SYSTEM

9

MATERIALS AND METHODS

9.1 ANIMALS

The animals used in the experiment were 9 adults, virgin female mice (*Mus musculus*) of the CD-1 strain (Janvier, France). Adult mice of the same strain provided urine-soiled bedding material (soft wood shavings, Souralit S.L., ref. 3000, Spain). All animals were housed at 23ºC with a natural light cycle and food and water were available *ad libitum*. The experimental procedures were approved by the Research Ethics and Animal Welfare Committee of the University of Valencia (A1431417790135 and A1283764105250) and are in accordance with European Communities Council Directive (2010/63/EU) on the protection of animals used for scientific purposes.

9.2 SURGICAL PROCEDURES

9.2.1 *Electrodes implantation*

The electrode implantation was performed under anaesthesia induced by an intraperitoneal injection of ketamine - medetomidine (75 mg/kg: 1 mg/kg, respectively; Merial laboratorios, Spain and Pfizer, Spain), with atropine (0.05 mg/kg, intraperitoneal; Sigma, USA) to reduce cardio-respiratory depression. The depth of anaesthesia was monitored before the surgery by assessing the loss of righting, palpebral and pedal reflexes, response to painful stimulation, and rate and depth of respiration; and during the surgery, by monitoring the rate and depth of respiration, eye blinking and whisker movements. When the animal was asleep, a subcutaneous injection of lidocaine (0.1 ml; B. Braun, Germany) was provided to disrupt the cranial sensitivity (ophthalmic and zygomatic nerves). To maintain normal body temperature the animals were on top of a thermic blanket and to prevent eye desiccation eye-drops (Siccafluid, Thea S.A Laboratories, Spain) were applied. The anaesthetised mice were secured to a stereotaxic frame (SR-6R; Narishige, Japan) and

maintained at $37-38$ºC with a heating pad. Following a midline sagittal incision, 7 trephine holes (4 electrodes, 1 reference, 2 screw holes) were drilled by adapting the stereotaxic coordinates from Paxinos and Franklin (2004) to CD-1 mice (Figure 23 B). The electrodes were implanted, as shown in Table 5 and Figure23 A, in the accessory olfactory bulb (at an angle of 45 rostral to the vertical), main olfactory bulb, medial amygdaloid nucleus and posteromedial cortical amygdaloid nucleus; antero-posterior coordinates (in mm) were measured from Bregma and depth from cranial surface. The field potential recordings were referenced against an indifferent electrode placed in the epidural cerebellar area. After the surgery, the mice received injections of atipamezol (5×10^{-4} mg/g, subcutaneous; Pfizer), to revert the anaesthesia effects, and butorphanol (0.02 mg/g, subcutaneous; Fort Dodge Veterinaria, Spain), as an analgesic.

Table 5: Coordinates of the electrodes implantation sites (in mm) relative to Bregma.

	Antero Posterior	Lateral	Depth
AOB	-4.75 (45º)	-1	$+2.4$
MOB	-4.75	$+1$	$+1.3$
Me	$+1.3$ to $+1.4$	-2.1	$+5.2$
PMCo	$+2.7$	-3	$+5.6$

9.2.2 *Recording electrodes*

The local field potential (LFP) was recorded with stainless steel polyimide-coated macroelectrodes, with an external diameter of 0.125 mm (E363/6/SPC; PlasticsOne, USA). The electrodes were fixed to the cranial surface with polymeric dental cement (Rapid Repair, Dentsply International, UK). To assure a proper fixation of the dental cement the skull surface was cleaned with sodium hypochlorite (40 g/L in distilled water), clean distilled water and acetone. The field potential recordings were referenced against an indifferent electrode placed in the epidural cerebellar area, which was directly screwed to the cranial surface (Figure 23). The electrodes were then connected to a six-channel electrode pedestal (PlasticsOne), which was fixed to the head using more dental cement.
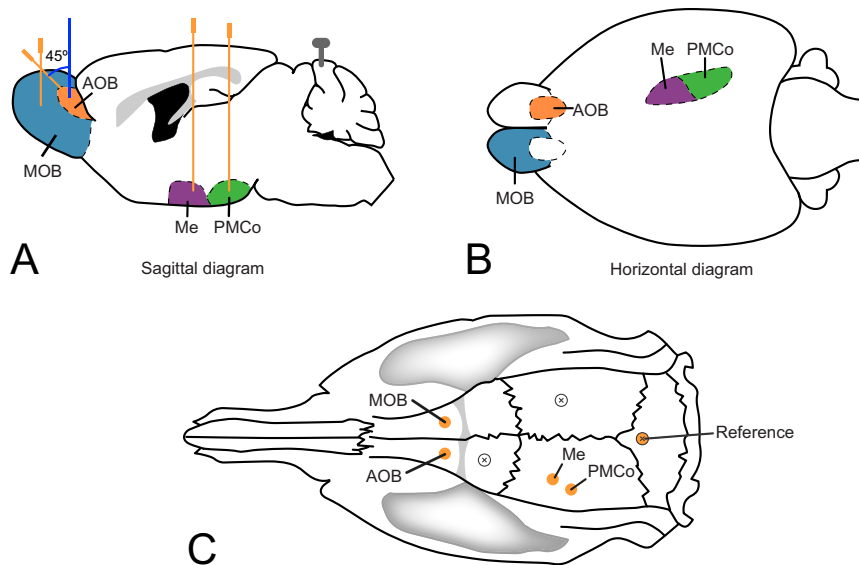
Figure 23: **Schematic diagram of the recording sites. A,** sagittal diagram
(left) and horizontal diagram (right) of the electrodes desired loc-
ations. **B,** Dorsal view of the skull of a mouse, with the position
of the 7 trephine holes: 4 electrodes, in orange; 1 reference, with a
grey outline; 2 screws, in orange with a grey outline.

9.2.3 *Post-surgical procedures*

The animals were housed in a transparent plastic cylindrical
cage (30 cm diameter) during the recovery and throughout the
whole period of study, except for the experimental tests (see
9.3.1). After the subjects had fully recovered (3 days), the mice
were trained to be able to sustain the weight of the recording
cable. To do so a screw was glued to the electrode pedestal tap
on the mouse's head and 3 nuts were gradually added in the
following 4−5 days. During this period, the animals were ha-
bituated to the experimenter and the recording procedure.

9.3 *in vivo* RECORDINGS

9.3.1 *Behavioural test*

Each animal was sequentially exposed to the following odour
stimuli:

> Neutral stimuli:
>> Clean bedding
>> Geraniol-scented bedding
>
> Conspecific-derived stimuli:

Castrated male-soiled bedding

Female-soiled bedding

Male-soiled bedding

All recordings took place in a methacrylate opaque box (42.5 × 26.5 × 18 cm), where the mouse could move freely. After at least 1 week of recovery after surgery, the animals were habituated to the experimenter and to the test conditions daily during four consecutive days. During this habituation, a glass dish containing clean bedding was placed to mimic the stimulus presentation.

During the test, a control period of 20 min was recorded before the presentation of each stimulus. For the stimulus presentation the mouse was transferred for 5 min to an identical box containing 15 ml of the stimulus, which was placed into a glass plate (6 cm diameter) to which the animal had full access. After the 5 min recording session, the animal was transferred back to the control box and allowed to rest for 20 min until the presentation of the next stimulus. The succession of control and stimulus-presentation periods was repeated until all five stimuli were presented.

Every test was video-recorded and after the experiment the animal behaviour was evaluated (see 9.4).

9.3.2 *Stimuli collection*

To obtain bedding soiled by gonadally intact males, the dominant males were housed individually in a clean plastic cage and the bedding was collected after 4 days. Castrated males (at least a month since the orchidectomy) and female mice were housed in groups of 6 animals to provide soiled bedding, which was also collected after 4 days. Geraniol-scented bedding was made by mixing artificial geraniol extract (1 μl/ 10 g; Ventós S.A., International Flavors and Fragrances, Spain) with clean bedding. To ensure that bedding soiled by a given kind of conspecifics was chemically homogeneous throughout the experiment, bedding from several cages containing the same kind of animals was mixed and stored at -20°C until the day of the test.

9.3.3 *Signal acquisition*

Raw field activity was amplified and online-filtered between 0.3 and 300 Hz (p55, Grass Technologies; Ampli 4G21, CIBERTEC, Spain). Then the signal was digitised (Power 1401; Cambridge Electronic Design, UK) for offline analysis (400 Hz sampling fre-

quency). The waveforms were continually monitored online using Spike 2 software (Cambridge Electronics Design).

Undesired signals may conceal or misrepresent the true underlying electrophysiological signal sought. These artefact signals may stem from light sources, alternating current systems frequency (50 Hz) or other electromagnetic sources. During the recording session, to avoid these artefacts, the test box was placed inside a Faraday cage connected to the building general ground.

9.4 EVALUATING THE CHEMOEXPLORATORY BEHAVIOUR

The behaviour of the animals was evaluated through the analysis of the recorded videos. We scored the time that the mouse approached the glass plate and investigated each stimulus, and these data were analysed to calculate the time spent exploring the provided stimuli.

Under exploratory behaviour, the activity sometimes became very rhythmic and concentrated in the theta band (see 10). To properly characterise this oscillation we double-checked the behaviour of the animal and the raw signal to accurately define the analysed time periods. Thus, for the stimuli comparison we only considered the times where, in the video, the animal actively touched the stimulus with the snout while their whiskers moved (as a sign of sniffing) and the raw signal showed a rhythmical theta-centred oscillation.

9.5 HISTOLOGY

When data acquisition ended, animals were deeply anaesthetised with sodium pentobarbital (100 mg/kg, intraperitoneal; Dolethal Vetoquinol, Spain) and transcardially perfused with 20 ml of saline solution (0.9%) followed by 60 ml of paraformaldehyde (4%) diluted in PB (0.1 M, pH 7.6). Then, brains were removed, postfixed overnight in the same fixative and cryoprotected in 30% sucrose in PB (0.1 M, pH 7.6) at 4ºC until they sank. We used a freezing microtome to obtain coronal sections (40 μm) which were collected in four parallel series.

The sections were mounted onto gelatinised slides, dehydrated with graded alcohols, cleared with xylene and coverslipped with Entellan (Merck, Germany). To facilitate the identification of the neural structures were the electrodes were placed, before the tissue was coverslipped, it was counterstained with the Nissl method.

We observed the sections using an Olympus CX41RF-5 microscopy and photographed them using a digital Olympus XC50 camera. Brightness and contrast were adjusted, but no addi-

tional filtering or manipulation of the photomicrographs was performed.

9.6   DATA ANALYSIS

Raw signals were imported to the MATLAB development environment (The MathWorks, USA) for the off-line analysis using self-developed code.

As a first approach, field potentials components were quantified using the fast Fourier transform (FFT), revealing the power distribution in the frequency domain. Power spectra estimation was done by means of the Welch's method (50% overlapping 4 s Hanning windows, with a resolution of 1.9 Hz and a nfft value of 2048). The frequency bands defined in the spectral analysis were: delta ($0.5 - 4$ Hz), theta ($4 - 12$ Hz), beta ($12 - 30$ Hz), low-gamma ($30 - 50$ Hz), high-gamma ($50 - 100$ Hz), and fast gamma (> 100 Hz).

9.6.1   *Wavelet analysis*

The wavelet transform has been found to be particularly useful for analysing signals which can best be described as non-stationary. Its ability to examine the signal simultaneously in both time and frequency domains in a distinctly different way from the traditional short time Fourier transform (STFT) has generated a number of wavelet-based methods for signal manipulation. The *continuous wavelet transform* is a method of converting a signal into another form which makes certain features of the original signal more tractable to study and enables the original data set to be described more succinctly. To perform a wavelet transform we need a wavelets function, $\psi(t)$, which satisfies certain mathematical criteria. These functions are manipulated through a process of translation (movements along the time axis) and dilation (spreading out of the wavelet) to transform the signal into another form, which unfolds it in time and scale.

In our case, to establish temporal correlations between pairs of neural signals from different locations, we need to separate the phase and amplitude components within the signals. Therefore, we consider complex or *analytic wavelets*, which have both real and imaginary parts. Among them we employed the most commonly used complex wavelet, the *Morlet wavelet* (Figure 24). Briefly, each signal was convoluted with the complex Morlet wavelet defined as:

$$\psi_0(t) = \frac{1}{\pi^{1/4}} e^{i\omega_0 t} e^{-t^2/2}$$
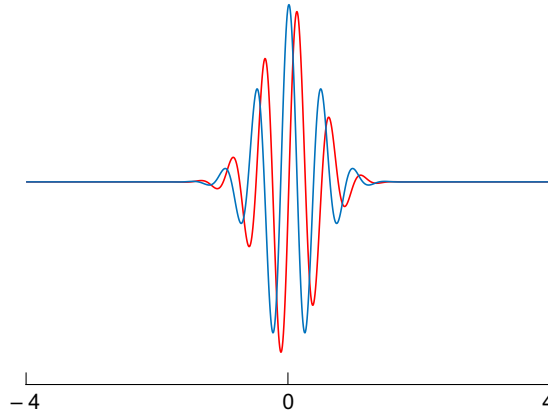
Figure 24: **Schematic diagram of the complex Morlet wavelet.** Real (blue line) and imaginary (red line) parts of the Morlet wavelet presented in the time domain.

This wavelet is a complex wave within a Gaussian envelope. The complex sinusoidal waveform is contained in the term $e^{i\omega_0 t}$, with a Gaussian window $e^{-t^2/2}$ of unit standard deviation, and normalised to unit energy with the term $\pi^{-1/4}$. The value of ω_0 represents the wavelet central angle frequency. Here, $\omega_0 = 2\pi$ is an optimal value for adjusting the time-frequency resolution of LFP signals (Farge, 1992). The continuous wavelet transform of the sampled time series χ_t is the result of the convolution of the signal with the wavelet function, with a scaled and translated version of the parent wavelet function $\psi_0(\eta)$,

$$W(t,s) = (\chi_t \otimes \psi(s,n))$$

where $\psi(s,n)$ are scaled and shifted versions of the parent wavelet,

$$W_{s,n}(t) = s^{-\frac{1}{2}} \psi \left(\frac{t-n}{s} \right)$$

The *Morlet wavelet* has a form very similar to the analysing function used for the short time Fourier transform within a Gaussian window. The important difference is that, for the *Morlet wavelet* transform, we scale the window and enclosed sinusoid together; whereas for the STFT we keep the window length constant and scale only the enclosed sinusoid. The wavelet can therefore localise itself in time for short duration (e.g. high frequency) fluctuations. However, the frequency distribution associated with wavelets of short duration is wide. Conversely, there is a spreading in temporal resolution at low frequencies. This is illustrated in Figure 25, where we represent the spread of the wavelets in the time-frequency plane by drawing boxes (Heisenberg boxes) of different lengths depending of the wavelet frequencies.
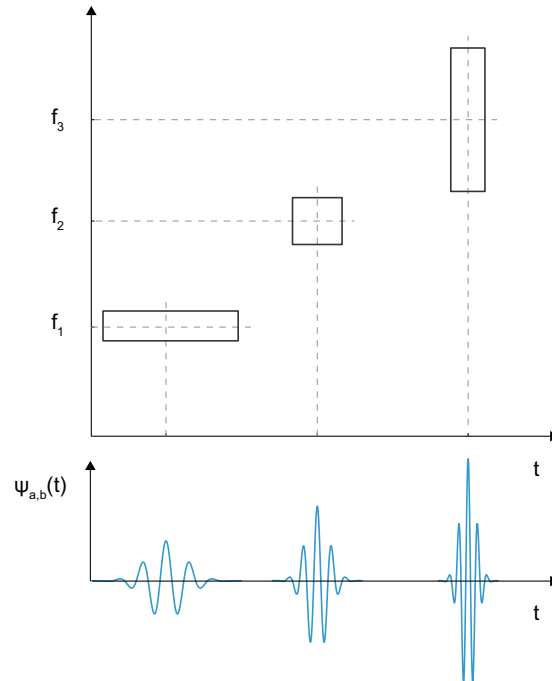
Figure 25: **Heisenberg boxes in the time-frequency plane**. The wavelet transform is scaled (or dilated) for better frequency fitting and translated (or shifted) for temporal fitting.

Under these considerations, to reveal temporal changes in the oscillatory activity of the LFP's time-series, the continuous wavelet transform was computed by using the MATLAB wavelet routines provided by Torrence and Compo (1998). The power of the signal at each wavelet scale s (frequency) was defined as the modulus of the wavelet coefficient, $|W(t,s)|^2$. The power values were normalised to scale, $s^{-1}(|W(t,s)|^2)$, to avoid scale-dependent biased values (Liu et al., 2007). Finally, the spectrograms in the time-frequency domain were extracted with the z-score normalised power spectra.

9.6.2 *Synchronisation measures*

9.6.2.1 *Phase to phase synchrony*

For detecting synchrony in a precise frequency range between two signals we used the methods purposed by Lachaux et al. (1999). The procedure computes a measure of phase-locking between the components of x_t and y_t signals at frequency f by means of the phase relationship between the two signals. The instantaneous phase difference between both signals, $\phi(t)$, was derived from the wavelet cross-spectrum (Borhegyi et al., 2004; Li et al., 2007). The wavelet cross-spectrum for the time series x_t and y_t is,

$$W_t^{xy}(s) = W_t^x(s)W^{y*}(s)$$

where $*$ is the complex conjugate. Then, the cross-wavelet phases were extracted as,

$$\phi(t,s) = \tan^{-1}\left(\frac{\Re\left\{W_t^{xy}(s)\right\}}{\Im\left\{W_t^{xy}(s)\right\}}\right)$$

where $\Re$ and $\Im$ are the real and imaginary parts, respectively.

The phase-locking value was defined for an epoch of length N as,

$$y = \frac{1}{N}\left|\sum_{n=1}^{N}\exp\left(i\phi_n\right)\right|$$

Phase synchrony was delimited to $y = 1$ for exact phase synchrony, e.g., $\phi_n = const$, and $y = 0$ for no phase synchrony.

Phase-difference values were selected from the cross-wavelet coefficients for the time-frequency regions isolated from the dominant frequency range for each time. In a first approach, the distributions of the phase difference values were represented on circular histograms with the radial extent of the circle segments representing the probability of the given phase-angles range. The Rayleigh's test for relative phase value uniformity was used to test uniform distribution (null hypothesis) or whether significant phase preference was present ($p < 0.05$).

9.6.2.2 *Phase-amplitude coupling*

Cross-frequency interactions between different frequencies of a signal were assessed by the modulation index (MI), purposed by Tort et al. (2010). In general, raw time-series is filtered in the two frequency ranges of interest. MI is a normalised measure that reflects how well the instantaneous amplitude of a faster oscillation (*amplitude modulated*) with frequency band f_A, is phase-locked to a underlying lower cycle (*phase modulating*) with frequency band f_p. First, the raw signal is filtered at the two frequency ranges under analysis, obtaining x_{f_p} and x_{f_A}. The instantaneous phase and amplitude of both processed signals are extracted by the Hilbert transform. Thus, amplitude envelope of x_{f_A} (expressed as $A_{f_A}(t)$) and the instantaneous phases of x_{f_p} (expressed as $\phi_{(f_p)}(t)$) gives the amplitude of the f_A oscillation at each phase of the f_p waves. Next, the binned phases and the mean of the amplitudes over each bin, the normalised mean amplitude is calculated:

$$P(j) = \frac{\langle A_{f_A} \rangle_{\phi_{f_p}}(j)}{\sum\limits_{k=1}^{N} \langle A_{f_A} \rangle_{\phi_{f_p}}(k)}$$

The MI value was determined to test the amplitude locking of frequencies of interest. Phase was converted to the range -2π and $+2\pi$, with wave trough as the 0 radians. In the case of phase-amplitude coupling between both filtered signals, the amplitude distribution over the phase bins is non-uniform. Following Tort's calculation, MI is defined as a measure that quantifies the deviation from the uniform distribution with an adaptation of the Kullback-Leibler distance (Kullback and Leibler, 1951). Modulation index assumes normalised values between 0 and 1. The MI was considered statistically significant whether its value was > 2 SD the mean surrogate MI, constructed by 200 random permutations of the amplitude distribution.

9.6.3 *Autocorrelation*

The analysis of the autocorrelation was computed for finding repeating patterns, such as the rhythmycity of a signal. Briefly, it is the correlation of a signal with a delayed copy of itself as a function of delay. The rhythmicity of the LPF is evidenced by multiple alternating peaks and troughs in the autocorrelogram. The coefficient is distributed between $+1$ and -1, indicating perfect correlation or anti-correlation between the two vectors respectively.

9.7 STATISTICAL ANALYSIS

Statistical analyses were performed using SPSS Statistics v20 (IBM, USA). Statistical comparisons were made using parametric or non-parametric tests wherever appropriate. We first checked whether the data fulfilled the conditions of normality (Kolmogorov-Smirnov test; $p < 0.05$ to reject) and homocedasticity (Levene's test; $p < 0.05$ to reject). For the chemoexploratory behaviour analysis the data was log-transformed ($\log[X]$) and an ANOVA (statistic F) was performed. The Kruskal-Wallis test (statistic K) was used as nonparametric method for comparisons between independent samples with pairwise comparisons when needed. To compare two independent samples the Mann-Whitney test (statistic U) was used, and for the related samples comparisons the Wilcoxon test (statistic W) was performed. The minimum significance level for all the tests was 0.05.

10

RESULTS

10.1 ELECTRODE LOCATION

Electrophysiological recordings were carried out in the brain of freely behaving adult mice under an olfactory exploration paradigm. After recording, only those cases in which the electrode tip was clearly positioned within the boundaries of the target areas were included for the study ($n = 6$; Figure 26). Within the olfactory bulbs, the electrodes in AOB ($n = 4$) were positioned in the anterior part of the granular or mitral/ glomerular layers (Figure 26 B); and in the MOB ($n = 6$), the electrode tip was generally located around the mitral layer (Figure 26 A). In the amygdaloid area, for the Me ($n = 4$), the electrodes were sited in the posterodorsal/ posteroventral subdivisions (Figure 26 C), with one case in which the electrode was placed in its anterior subdivision; in the PMCo ($n = 5$) the electrodes were mainly located in its anterior part (Figure 26 D), although in one case it was located in the posterior part (not shown).

10.2 CHEMOINVESTIGATORY BEHAVIOUR UNDER OLFACTORY EXPLORATION

Attending to our experimental paradigm, we first analysed the exploratory behaviour induced by the different olfactory stimuli. The analysis of the time spent investigating the different stimuli revealed significant differences ($F = 5.24$, $p < 0.05$). The post-hoc comparisons (Tukey test) revealed three homogeneous subsets of means (Figure 27): neutral stimuli (clean and geraniol-scented bedding, $p > 0.05$), conspecific-derived stimuli (female, castrated male and male-soiled bedding, $p > 0.05$) and a mixed group (geraniol-scented bedding and female-soiled bedding, $p > 0.05$). According to these results, the investigation time elicited by the conspecific stimuli was higher than that induced by neutral stimuli.
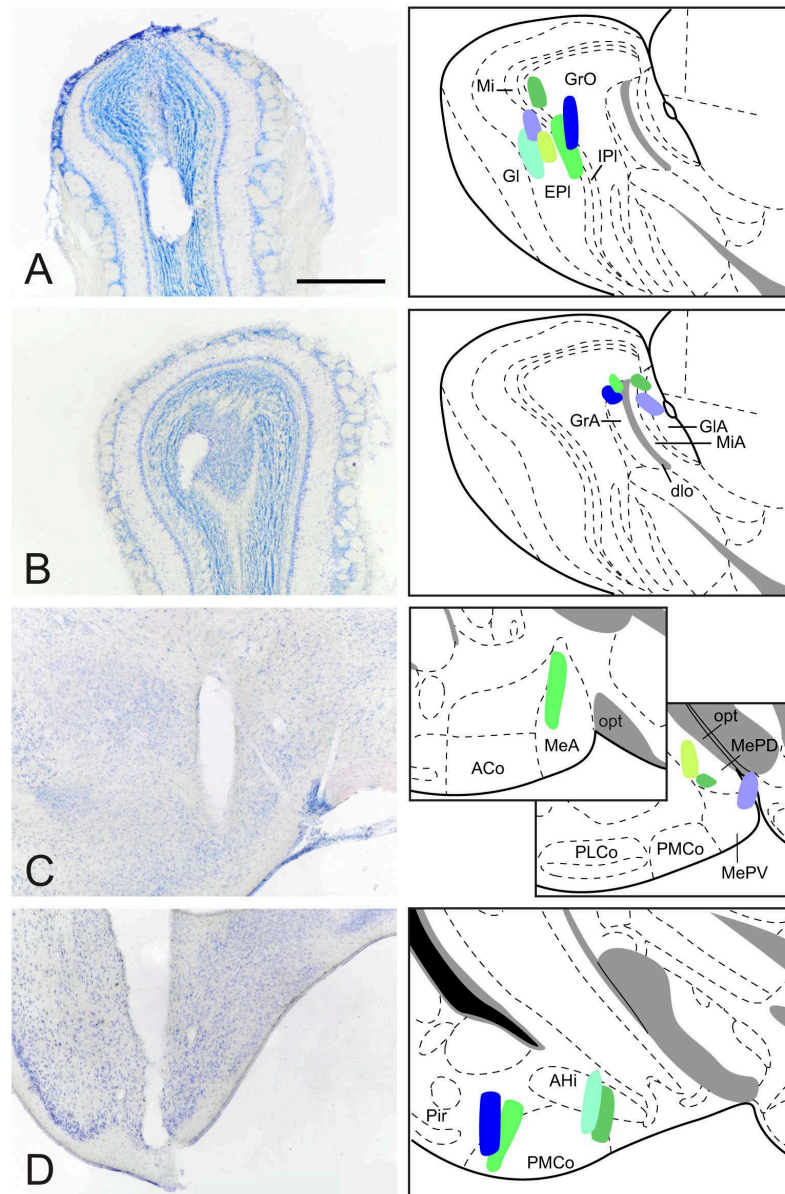
Figure 26: **Verification of the electrodes position. A,** Electrode position in the MOB; **B,** in the AOB; **C,** in the Me and **D,** in the PMCo. The actual recording site (electrode tip) should be along the trace of the electrode. Right: histological verification of the four electrodes properly placed on the same animal. Scale bar in **A** (valid **B-D**) = 500 μm. Left, schematic drawings of the recording regions on all the mice, each colour indicates a different animal.
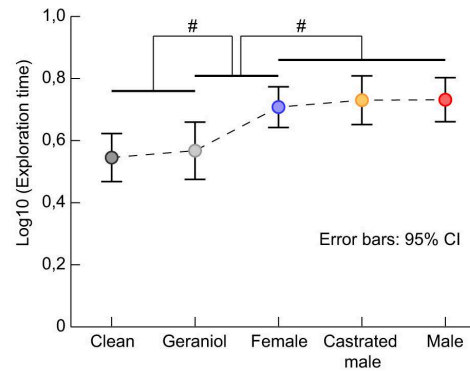
Figure 27: **Differences in the time spent exploring the presented stimuli.**
The differences in the means revealed three homogeneous subsets:
neutral stimuli (clean and geraniol-scented bedding), conspecific-
derived stimuli (female, castrated male and male-soiled bedding)
and a mixed group (geraniol-scented bedding and female-soiled
bedding).

10.3 THE CHARACTERISATION OF THE NEURONAL ACTIVITY PROFILE UNDER EXPLORATORY BEHAVIOUR IN THE OLFACTORY CIRCUITS REVEALS A SNIFFING-LIKE PATTERN

In general, the study of the neural activity in the different nodes
of the bulb-amygdaloid network showed a similar profile, where
the exploration periods could clearly be distinguished from
those in which a passive behaviour was prevailing.

First, we analysed the population activity under the pres-
ence of different stimuli evoking activation in the AOB. The
LFP showed distinguishable profiles in the absence and pres-
ence of stimuli (Figure 28 A,B). This pattern was recognisable,
even with clean bedding as stimulus, and was easily delimited in
the time-frequency domain by the wavelet spectrograms. Thus,
we began by identifying the neuronal activity under two con-
ditions (Figure 28 C): non-exploration (left, pre-stimulus; right,
post-stimulus) and exploratory behaviours (middle). As exem-
plified in the Figure 28 C, the oscillations in non-exploration
condition revealed a predominant field activity in delta waves
(< 2 Hz), with short incursions in slightly higher frequencies
(Figure 28 A,C left). However, the exploratory behaviour shifted
the activity pattern to theta frequencies ($4 - 10$ Hz; Figure 28
B,C middle). When the stimulus was removed from the arena
and the exploratory movements decreased, the predominant fre-
quencies fell gradually to slow pre-stimulus values (Figure 28 C
right). Furthermore, we detected, within the exploration periods,
short rhythmic epochs ($2 - 4$ s) where the oscillation temporally
remained in a stationary theta epoch (Figure 28 B,C in red). This

isolated theta pattern in the AOB recordings matched with the exploration of the stimulus area, even when a neutral stimulus, such as clean bedding, was presented.
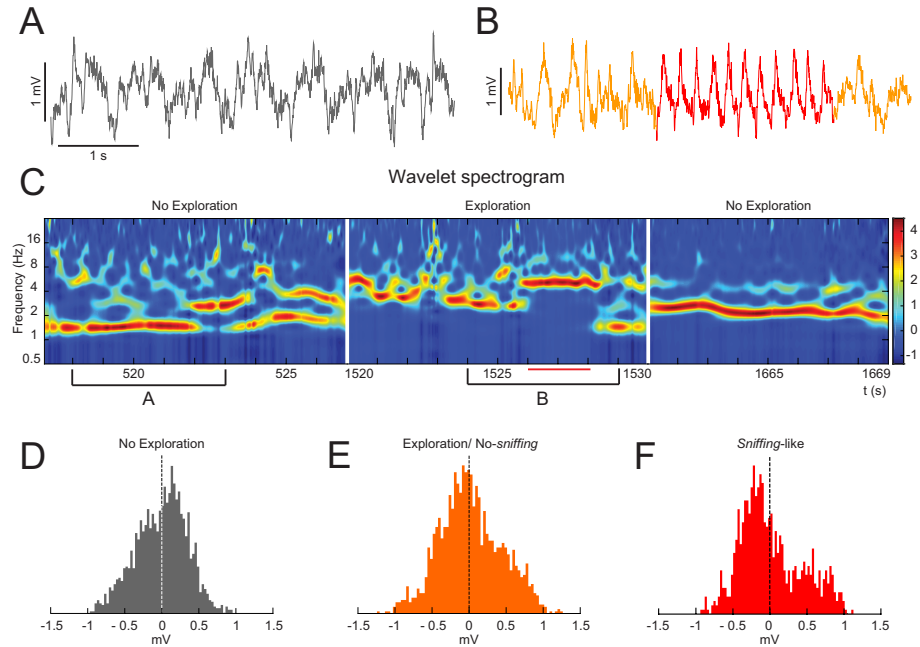
Figure 28: **Oscillatory changes in the AOB induced by clean bedding presentation. A,** Raw trace during non-exploration time. **B,** Raw trace during exploration time (in red indicating a sniffing-like oscillation). **C,** Wavelet spectrogram of three different time periods; left panel: non-exploration time; middle panel: exploration of a stimulus (red line indicating a sniffing-like oscillation); right panel: non-exploration after the stimulus. **D-F,** Distribution of the power asymmetry of the positive and negative parts of the waveform. **D,** In a non-exploration time. **E,** In an exploration/ no-sniffing time. **F,** In a sniffing-like oscillation present under exploratory behaviour.

We then wanted to distinguish the specific features of this pattern of theta activity within the exploratory epochs in the AOB. In a first approach, we represented the distribution of the amplitudes from the raw signal. A measure of the symmetry of this distribution evidenced differences between non-exploration and exploration periods (Figures 28 D-F and 29). In non-exploration epochs, the amplitude distribution showed a slight asymmetry centred at positive values (skewness $= -0.13 \pm 0.43$; Figure 28 D). In contrast, during exploration periods, the distribution showed a bimodal shape with a major peak for negative amplitudes and a minor peak in the positive counterpart (skewness $= -0.10 \pm 0.24$; Figure 28 E). This bimodal shape was more evident during the rhythmic theta epochs (skewness $= 0.34 \pm 0.09$; Figures 28 F and 29 -AOB-). The asymmetry in the amplitude distribution, as described above, indicates different temporal length
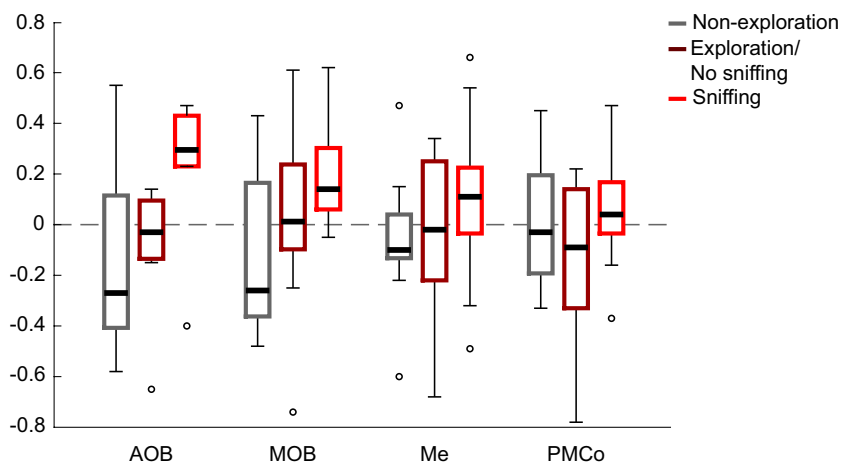
Figure 29: **Skewness values in the recorded nuclei for three different exploration paradigms**. The boxplot shows the measure of the asymmetry of the distribution of the amplitudes (skewness) for non-exploration (grey); exploration, but no-sniffing (dark red); and sniffing (red) in each nucleus. Negative values indicate that the tail on the left side of the distribution is longer or fatter than the right side, while positive values indicate the opposite.

of the negative and positive phases of the theta cycle. This aspect suggests that, under olfactory exploration, the theta cycles contain faster waves incrusted in its negative phase, as a putative sign of coupling between different rhythmical components. An overlapped representation of the filtered signals in the theta and gamma bands displayed the phase coupling of both components (Figure 30 A). In a detailed manner, the coupling between the amplitude of gamma oscillations with the phases defined in the theta band could be determined by means of the modulation index (MI). Thus, the MI showed significant values in the descending part of the theta phase (Figure 30 B).

The rhythmic nature of this sniffing-like oscillation was also characterised by periodicity measures. The autocorrelation of the raw signal in the sniffing-like periods showed high values in comparison with non-sniffing-like exploration epochs (Figure 30 C top). The time-course of the autocorrelation clearly demarked the entrance in a sniffing-like epoch with high autocorrelation values periodically distributed (Figure 30 C bottom). These measures, both the asymmetrical distribution and the rhythmicity profile of oscillation, helped us to identify the short theta segments correlated with chemoexploratory behaviour.

The analysis of the LFP under olfactory exploration in the MOB, as in the AOB, showed distinguishable profiles in the absence and presence of stimuli (Figure 31 A,B). This oscillation, analysed by the wavelet spectrograms in the time-frequency do-
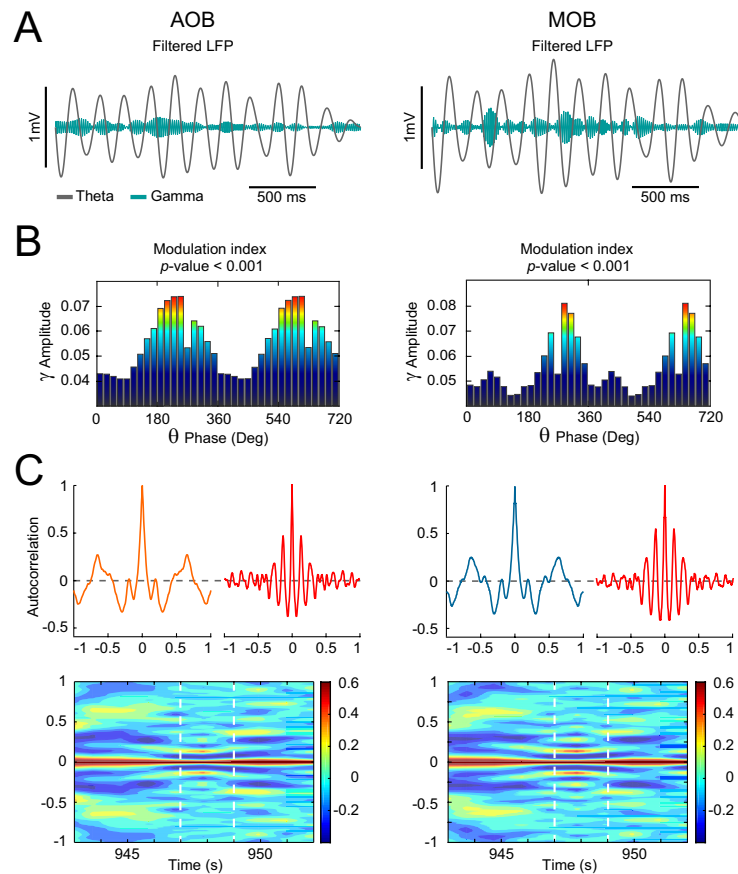
Figure 30: **Example of a sniffing-like time in the AOB (left column) and MOB (right column)**. **A,** filtered LFP for theta $(4 - 8\ Hz)$ and gamma $(55 - 68\ Hz)$ frequency bands. **B,** mean power between 60 and 80 Hz as a function of the waveform-based theta cycle phases (bin, 20°; peak of theta cycle, 180°). **C,** Top left: autocorrelation of a non-sniffing-like time; Top right: autocorrelation of a sniffing-like period; Bottom: evolution of the autocorrelation through time, the dashed white lines mark the sniffing-like period.

main, showed a predominant field activity in delta waves ($<$ 2 Hz), with short incursions in higher frequencies during non-exploration periods (Figure 31 A,C left). Whereas the exploration of a stimulus shifted the activity pattern to theta frequencies ($4 - 10$ Hz; Figure 31 B,C middle). When the stimulus was removed from the arena and the exploration ceased, the predominant frequencies reverted to slow pre-stimulus values (Figure 31 C right). In the MOB, we also detected short rhythmic epochs within the exploration periods where the oscillation remained in a stationary theta epoch (Figure 31 B,C in red). As for the AOB, we characterised the nature of this oscillation by means of the distribution of the amplitudes from the raw signal and its

Figure 31: **Oscillatory changes in the MOB induced by clean bedding presentation. A,** Raw trace during non-exploration time. **B,** Raw trace during exploration time (in red indicating a sniffing-like oscillation). **C,** Wavelet spectrogram of three different time periods; left panel: non-exploration time; middle panel: exploration of a stimulus (red line indicating a sniffing-like oscillation); right panel: non-exploration after the stimulus. **D-F,** Distribution of the power asymmetry of the positive and negative parts of the waveform. **D,** In a non-exploration time. **E,** In an exploration/ no-sniffing time. **F,** In a sniffing-like oscillation present under exploratory behaviour.

rhythmicity (Figures 31D-F, 29 -MOB- and 30 left column). First, for the amplitude distribution, during non-exploratory periods a slight asymmetry centred at positive values was observed (skewness $= -0.11 \pm 0.30$; Figure 31 D). During exploration epochs the distribution shifted its peak at negative amplitudes (skewness $= 0.05 \pm 0.32$; Figure 31 E), that during the rhythmic theta epochs showed a bimodal shape similar to that in the AOB (skewness $= 0.17 \pm 0.19$; Figures 31 F and 29 -MOB-). The analysis of the filtered signals in the theta and gamma bands reflected their phase relation (Figure 30 A) and the phase-amplitude MI between the gamma and theta oscillations showed significant values in the descending part of the theta phase (Figure 30 B). About the rhythmic nature of this oscillation, the autocorrelation of the raw signal in the non-sniffing-like periods was lower than in the sniffing-like exploration epochs (Figure 30 C top) and the time-course of the autocorrelation also demarked the entrance in a sniffing-like epoch (Figure 30 C bottom). Thus, this theta bouts, identified as short epochs in the exploratory behaviours

of the stimulus area, are compatible with previous descriptions of the LFP recordings in the MOB, where the olfactory activity is characterised by a sniffing process coupled to the respiratory rhythm (Wachowiak, 2011).

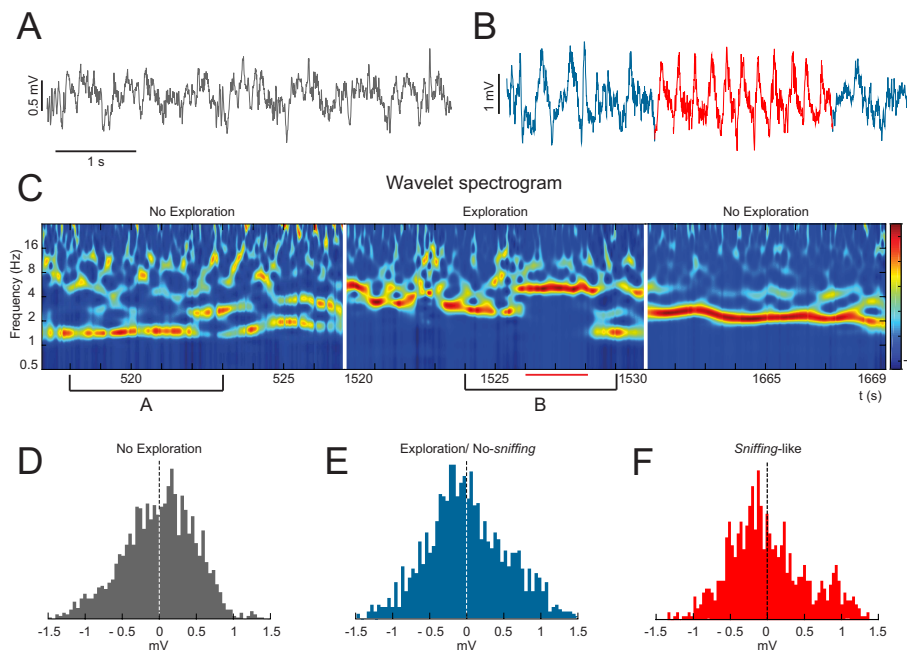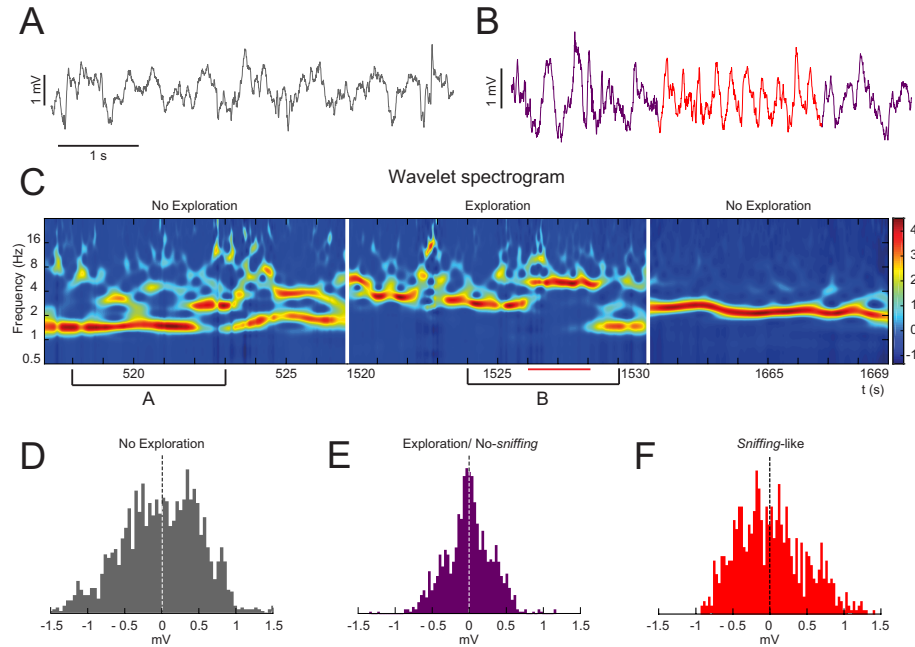Figure 32: **Oscillatory changes in the Me induced by clean bedding presentation. A,** Raw trace during non-exploration time. **B,** Raw trace during exploration time (in red indicating a sniffing-like oscillation). **C,** Wavelet spectrogram of three different time periods; left panel: non-exploration time; middle panel: exploration of a stimulus (red line indicating a sniffing-like oscillation); right panel: non-exploration after the stimulus. **D-F,** Distribution of the power asymmetry of the positive and negative parts of the waveform. **D,** In a non-exploration time. **E,** In an exploration/ no-sniffing time. **F,** In a sniffing-like oscillation present under exploratory behaviour.

In the amygdaloid nuclei, the analysis of the population activity in the absence and presence of stimuli showed distinguishable profiles (Figures 32 A,B and 33 A,B). In the wavelet spectrograms this oscillations showed, during non-exploration epochs a predominant activity in delta waves (< 2 Hz), with frequent incursions in higher frequencies both in the Me (Figure 32 A,C left) and the PMCo (Figure 33 A,C left). The exploration of a stimulus induced the activity pattern to shift to theta frequencies (Figures 32 B,C middle and 33 B,C middle). The removal of the stimulus from the arena shifted back to slow pre-stimulus values (Figures 32 C right and 33 C right). In the amygdala, the short rhythmic epochs within the exploration periods present in the olfactory bulbs, were observed in the Me (Figure 32 B,C in red), but they were not as clear in the PMCo (Figure

33 B,C in red). Thus, while studying the distribution of the amplitudes from the raw signal, some differences were found between these nulcei (Figure 29). The Me showed during non-exploratory periods a mostly symmetrycal distribution centred at positive values (skewness $= -0.07 \pm 0.23$; Figure 32 D). The distribution observed during exploration epochs was also symmetrycal (skewness $= -0.08 \pm 0.28$; Figure 32 E), but during the rhythmic theta epochs it showed a shift of the main peak to negative values (skewness $= 0.12 \pm 0.28$; Figures 32 F and 29 -Me-). As previously described, the PMCo did not show evident rythmic epochs during the exploration, which resulted in almost symmetrycal distributions in the power amplitudes during the three exploration paradigms: non-exploratory periods (skewness $= -0.02 \pm 0.23$; Figure 33 D), in this case centred at positive values; during exploration epochs (skewness $= -0.13 \pm 0.31$; Figure 33 E); and during the periords were rhythmic theta epochs
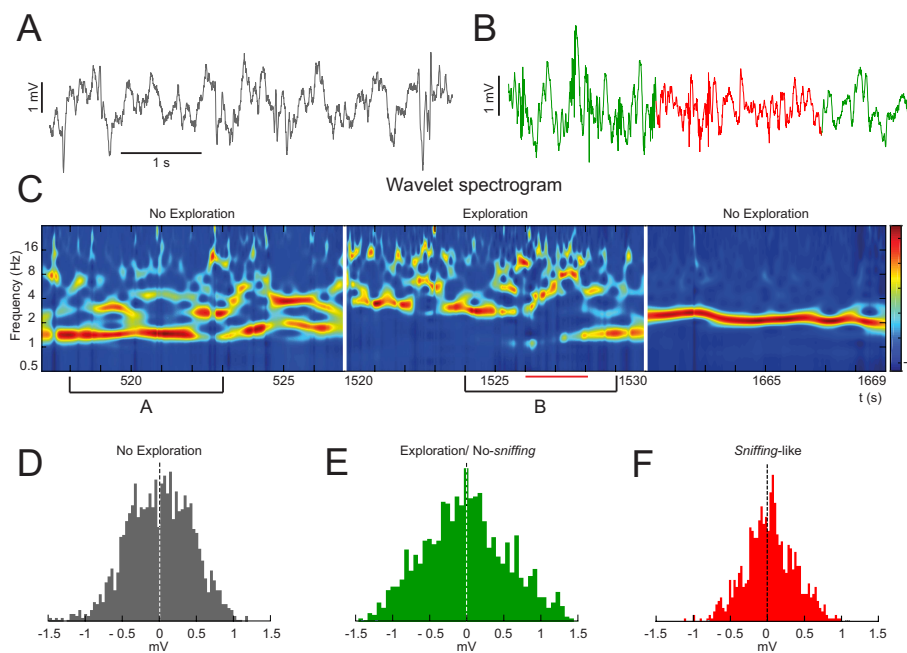
Figure 33: **Oscillatory changes in the PMCo induced by clean bedding presentation. A,** Raw trace during non-exploration time. **B,** Raw trace during exploration time (in red indicating a sniffing-like oscillation). **C,** Wavelet spectrogram of three different time periods; left panel: non-exploration time; middle panel: exploration of a stimulus (red line indicating a sniffing-like oscillation); right panel: non-exploration after the stimulus. **D-F,** Distribution of the power asymmetry of the positive and negative parts of the waveform. **D,** In a non-exploration time. **E,** In an exploration/ no-sniffing time. **F,** In a sniffing-like oscillation present under exploratory behaviour.

were present in the other nuclei (skewness $= 0.07 \pm 0.21$; Figures 33 F and 29 -PMCo-), in this case centered at negative values.

Altogether, the population activity under the presence of different stimuli evoking activation in the studied nuclei showed distinguishable profiles in the absence and presence of stimuli. The exploration of a sitimulus shifted the activity pattern to theta frequencies, with short rhythmic epochs ($2-4$ s) with an asymmetrical distribution and a rhythmicity profile of oscillation. This theta bouts were clearly identified in the olfactory bulbs and the Me, but were not as clear in the PMCo.

10.4 THE OLFACTORY EXPLORATION INDUCES A SPECIFIC THETA AND GAMMA OSCILLATORY PATTERN IN THE RECORDED STRUCTURES

We analysed the neural response of the olfactory circuit with the exploration of a neutral stimulus (clean bedding). The power spectral analysis displayed a prominent theta activity with a peak at $4-6$ Hz in the four target areas (Figure 34), according to the above description. However, a specific analysis of the gamma waves evidenced clear differences between the recording nodes in the theta epochs. Whereas AOB and MOB showed a power region in the high-gamma band ($60-80$ Hz; Figure 34 A,B); the AOB, Me and PMCo displayed prominent powers in the fast-gamma frequencies ($90-120$ Hz; Figure 34 A,C,D).

In a further step, we next carried out a detailed analysis of the spectral distributions comparing exploration (all stimuli) and non-exploration epochs. These results are represented in Figure 35 and summarised in Table 6. Overall, when analysing the wide frequency range ($0.5-120$ Hz) we observed a distinctive demeanor in the Me as compared to the other nuclei (Figure 35 A). Generally, the exploration induced a significant increase in the power ratio of the theta band accompanied by a decrease in the delta waves. Both bulbs did not exhibit significant differences in their gamma distribution attending to the exploratory behaviour, other than in the low-gamma oscillations which only showed differences in the MOB (Table 6). The PMCo activity followed a theta-band increase correlated to that of AOB but no delta decrease (Table 6). Remarkably, Me had a clear increase in the power ratio of the fast frequency segments during the exploration behaviours, while the delta, theta and low-gamma bands decreased its power (Figure 35 A -Me-); thus indicating that in the Me the dominant band is not the theta, but the gamma frequencies. A particular analysis of the theta ($0.5-30$ Hz power ratio) and gamma ($60-120$ Hz power ratio) oscillations allowed us a better understanding of the olfactory processing (Figure 35
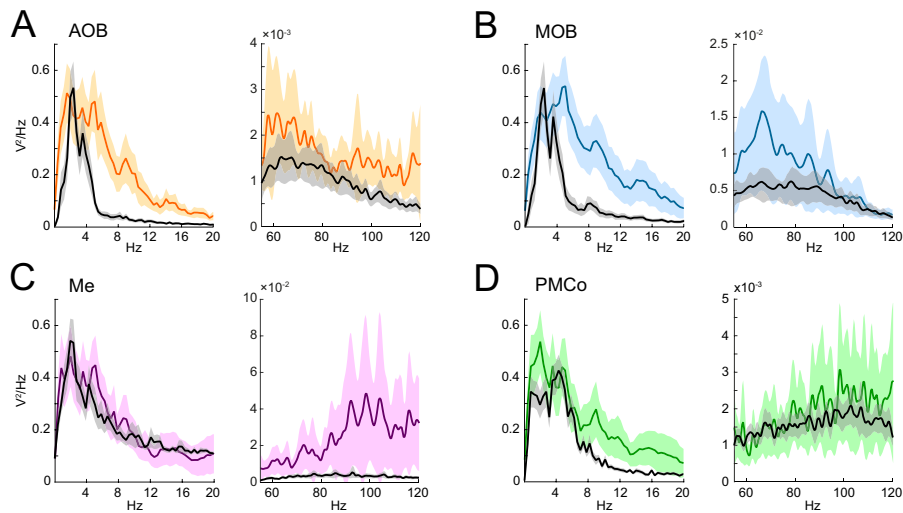
Figure 34: **Olfactory-induced changes in the recorded nuclei**. **A,** Power spectra in the AOB for clean bedding (in colour) and non-exploration (in black), showing the average (solid line) and standard deviation (shadowed area); Left: for the $0 - 20$ Hz frequency band; Right: for $55 - 120$ Hz frequency band. Idem in the MOB (**B**); the Me (**C**) and the PMCo (**D**).
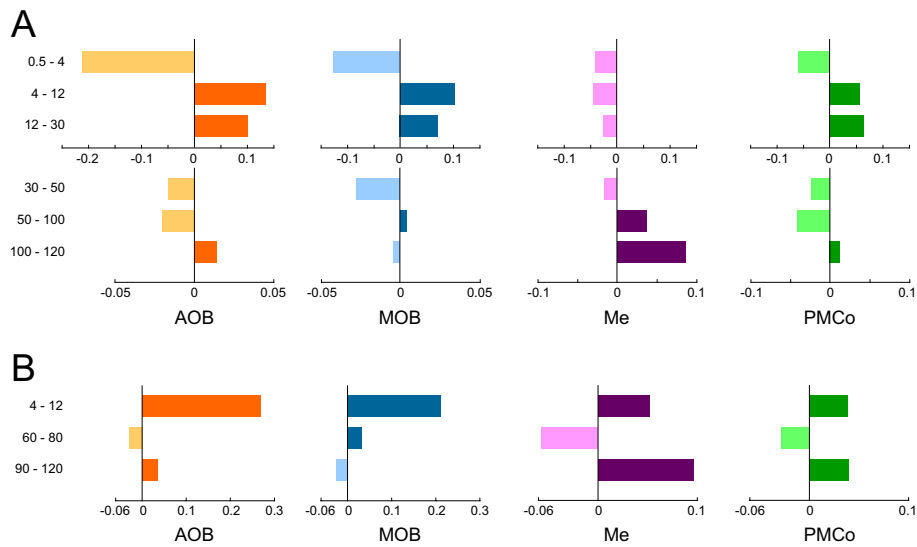
Figure 35: **Difference of the band power ratio means between the exploration (all stimuli) and the non-exploration conditions for different frequency bands**. **A,** Band power ratio analysed as the band power ratio within the $0.5 - 120$ Hz range. **B,** The theta $(4 - 12$ Hz) band power ratio was calculated within the $0.5 - 30$ Hz range. The high gamma $(60 - 80$ Hz) and fast gamma $(90 - 120$ Hz) bands were calculated within the $60 - 120$ Hz range.

B). Whereas the AOB evidenced an increase in the fast-gamma waves during the exploration, the MOB showed differences in the high-gamma band (Table 6). In contrast, high-gamma and fast-gamma oscillations exhibited a significant decrease in the MOB and AOB, respectively. Meanwhile, during the exploratory behaviours, the amygdaloid nuclei followed a gamma-band distribution correlated to that of AOB, the fast-gamma activity in PMCo showed a nearly significant increase (Table 6) and Me had a clear increase in the fast frequency segments.

These results suggest a differential gamma profile between nodes correlated to the olfactory theta activity. During the exploration epochs, the AOB and the amygdaloid nuclei showed fast-gamma frequency segments increase; whereas the MOB evidenced an increase in the high-gamma band.

Table 6: Results of the comparison of the power in the different frequency bands for exploration (all stimuli) and non-exploration times. ∗ Indicates significant differences.

Nucleus	Frequency band	W	N	p value	
AOB	$0.5 - 4$	-2.524	8	0.012	∗
	$4 - 12$	2.524	8	0.012	∗
	$12 - 30$	2.524	8	0.012	∗
	$30 - 50$	-1.542	8	0.123	
	$50 - 100$	-0.561	8	0.575	
	$100 - 120$	0.280	8	0.779	
	$4 - 12$	2.366	7	0.018	∗
	$60 - 80$	-2.197	7	0.028	∗
	$90 - 120$	2.028	7	0.043	∗
MOB	$0.5 - 4$	-1.992	13	0.046	∗
	$4 - 12$	2.971	13	0.003	∗
	$12 - 30$	3.111	13	0.002	∗
	$30 - 50$	-2.831	13	0.005	∗
	$50 - 100$	-0.051	10	0.959	
	$100 - 120$	0.513	10	0.878	
	$4 - 12$	3.181	13	0.001	∗
	$60 - 80$	2.091	10	0.037	∗
	$90 - 120$	-2.193	10	0.028	∗
	$0.5 - 4$	-2.103	8	0.035	∗
	$4 - 12$	-1.963	8	0.050	∗

Me

	$12 - 30$	-1.122	8	0.262	
	$30 - 50$	-1.963	8	0.050	$*$
	$50 - 100$	1.682	8	0.092	
	$100 - 120$	2.383	8	0.017	$*$
	$4 - 12$	2.524	8	0.012	$*$
	$60 - 80$	-1.823	8	0.068	
	$90 - 120$	2.383	8	0.017	$*$
	$0.5 - 4$	0.560	8	0.575	
	$4 - 12$	2.240	8	0.025	$*$
	$12 - 30$	0.700	8	0.484	
	$30 - 50$	-0.280	8	0.779	
PMCo	$50 - 100$	0.893	5	0.893	
	$100 - 120$	1.214	5	0.225	
	$4 - 12$	1.960	8	0.050	$*$
	$60 - 80$	-1.483	5	0.138	
	$90 - 120$	1.753	5	0.080	

10.5 DIFFERENTIAL THETA RHYTHMICITY INDUCED BY EXPLORATION OF NEUTRAL AND CONSPECIFIC STIMULI

As we described above, olfactory exploration leads to a prominent theta activity in the recorded sites, indicative of a sniffing-like process. The spectral profile of the neural activity showed a distinctive theta pattern with the exploration of specific stimulus (left panels in Figure 36). Moreover, the analysis of the main peak through the theta band seemed distinctive for each stimulus (right panels in Figure 36). With these data, we performed comparisons of the theta dominance for each recorded node and among stimuli: first, a pair-wise comparison of all the stimuli; second, a comparison of the neutral stimuli with the conspecific-derived stimuli; and third, a comparison among the conspecific stimuli.

The specific values of the theta peak frequencies are depicted at Table 7. In the AOB (Figure 36 A), the distribution of the main peak in the theta band was different among stimuli ($K = 12.042$, $p < 0.05$). Pairwise comparisons revealed significant differences between the geraniol-scented bedding and the castrated ($p < 0.05$) and female-soiled bedding ($p < 0.05$); and a tendency to differences between the geraniol-scented bedding and the male-soiled bedding was also evidenced ($p = 0.058$).
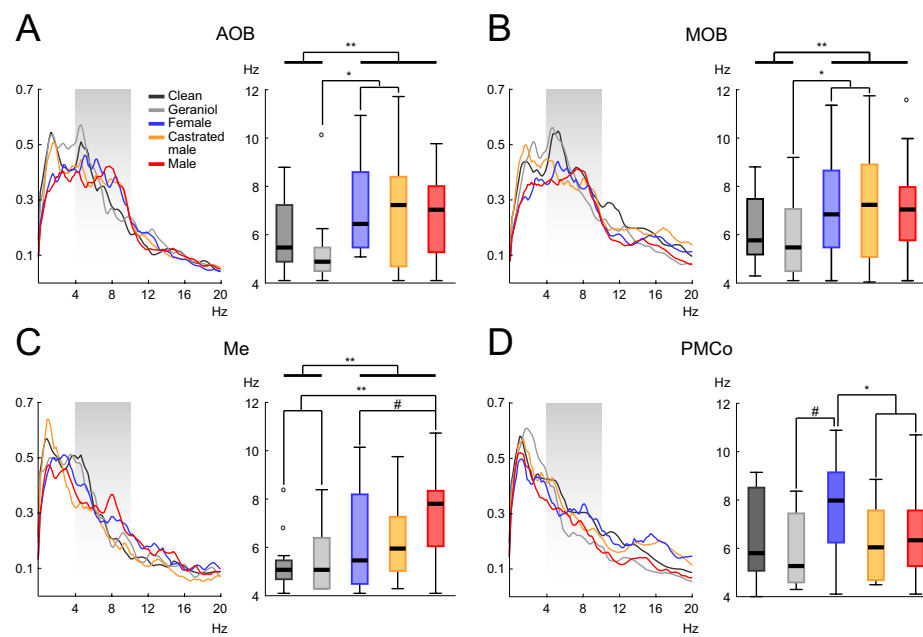
Figure 36: **Different stimuli induce unalike/ distinctive peaks in the theta range**. **A,** Right: mean normalised power spectra of the AOB field recordings, the shaded area points the theta frequency band; Left: main peak distribution for the different stimuli, the thick lines show the comparison between the neutral and the conspecific derived stimuli (♯ *p*-value ≈ 0.05; ∗ *p*-value < 0.05; ∗∗ *p*-value < 0.01). Idem for the MOB (**B**), the Me (**C**) and the PMCo (**D**).

A similar result was obtained in the MOB (Figure 36 B), where the comparison showed differences among stimuli ($K = 11.822$, $p < 0.05$) with pairwise differences between the geraniol-scented bedding and the castrated ($p < 0.05$) and female-soiled bedding ($p < 0.05$). The comparisons in the Me also showed clear differences (Figure 36 C; $K = 18.205$, $p < 0.01$), where male-soiled bedding presented significant differences with the clean ($p < 0.01$) and geraniol-scented bedding ($p < 0.05$). In the case of the PMCo (Figure 36 D), the statistical analysis revealed significant differences in the broad comparison ($K = 11.578$, $p = 0.021$), but no differences in the pairwise comparisons.

Comparing the neutral stimuli with the conspecific-derived stimuli, significant differences in the AOB were demonstrated ($U = 903.0$, $p < 0.01$), where the neutral stimuli had a mean theta peak of 5.74 ± 0.31 Hz, while in the case of the conspecific-derived stimuli the mean peak remained around 6.88 ± 0.18 Hz (Table 7). The MOB also showed such differences ($U = 2453.0$, $p < 0.01$), where the neutral a conspecific-derived stimuli had mean peaks with similar values to that of AOB (6.04 ± 0.15 Hz and 6.99 ± 0.20 Hz, respectively). In the Me recordings, the

Table 7: Results of main peak and standard deviation for the different stimuli as compared in Figure 36.

Nucleus	Stimulus	Mean	SD
AOB	Clean	6.29	1.33
	Geraniol-scented	5.79	1.47
	Female	7.07	1.93
	Castrated-male	7.13	2.11
	Male	6.85	1.56
	Neutral	5.74	1.70
	Conspecific	6.88	1.78
MOB	Clean	5.96	1.44
	Geraniol-scented	5.52	1.96
	Female	6.98	1.71
	Castrated-male	7.04	2.11
	Male	6.73	1.62
	Neutral	6.05	1.41
	Conspecific	6.99	1.83
Me	Clean	5.32	1.14
	Geraniol-scented	5.49	1.27
	Female	6.42	2.07
	Castrated-male	6.23	1.62
	Male	7.39	1.73
	Neutral	5.41	1.19
	Conspecific	6.85	1.89
PMCo	Clean	6.39	1.75
	Geraniol-scented	5.88	1.55
	Female	7.69	1.87
	Castrated-male	6.27	1.51
	Male	6.54	1.73
	Neutral	6.19	1.66
	Conspecific	6.81	1.79

mean frequency reached 5.4 ± 0.23 Hz for the neutral stimuli and 6.85 ± 0.22 Hz for the conspecific stimuli ($U = 592.0$, $p < 0.01$). No statistical differences were observed in the PMCo (Figure 36 D), where we detected peaks of 6.19 ± 0.33 Hz for the neutral and 6.81 ± 0.19 Hz for conspecific-derived stimuli.

Finally, the comparison among the conspecific-derived stimuli revealed no differences in the AOB and the MOB, but significant differences appeared in the amygdaloid nuclei. The Me showed differences in the conspecific comparison ($K = 6.581$, $p < 0.05$), but no differences in the pairwise comparisons (Figure 36 C), although the female to male-soiled bedding was close to significance (6.42 Hz and 7.39 Hz, respectively; $p = 0.065$). Furthermore, the analysis for the PMCo showed both differences in the general comparison ($K = 8.793$, $p < 0.05$) and in the pairwise comparisons (Figure 36 D), in this case with significant differences between the female and the castrated (7.69 Hz and 6.27 Hz, respectively; $p < 0.05$) and male-soiled beddings (6.54 Hz for the male; $p < 0.05$). In the PMCo, a particular analysis of the power ratio comparing the female and the non-exploration within the gamma frequencies ($60 - 120$ Hz power ratio), revealed now a significant increase in the fast-gamma oscillations ($W = 2.032$, $p < 0.05$).

Overall, these data suggest that the olfactory exploration leads to a particular theta oscillation whose profile is different attending to the node of the olfactory network and evidenced by specific stimuli.

10.6 THE OLFACTORY NETWORK SHOWED DIFFERENT LEVELS OF SYNCHRONY BETWEEN THEIR NEURONAL POPULATIONS

Attending to the previous results, the presence of theta oscillations in the olfactory network under exploration suggests that this particular activity could be a sign of communication among structures. For this purpose, we first determined the degree of temporary coincident activity between the AOB and the rest of the nuclei by analysing the wavelet cross-spectrum. The oscillatory patterns during non-exploratory periods are more similar at frequencies under 2 Hz in all comparisons (Figure 37 left). The exploration of a stimulus shifted the frequencies with high common power to higher, theta values. The exploration of geraniol-scented bedding induced coincident theta activity at around 6 Hz in the olfactory bulbs (Figure 37 A). In the vomeronasal amygdala, the cross-spectrum of the AOB whith both the Me (male-soiled bedding) and the PMCo (female-soiled bedding) showed coincident theta activity at around 8 Hz (Figure 37 B,C).

Then, we measured the phase synchronisation between pairs of signals by means of the phase-locking value (PLV, $0 - 1$ range). In Figure 38 we represent one case of synchronisation between the AOB and the rest of the nuclei. The phase analysis was performed filtering the individual raw signals in the main theta peak frequency (1 Hz wide) as calculated during the comparison between stimuli. Both in non-exploration and sniffing-like periods, the Rayleigh's test demonstrated non-uniform distributions with phase preference (control: $z = 426.75$, $p < 0.05$; sniffing: $z = 767.49$, $p < 0.05$). Regarding the synchronisation between the olfactory bulbs (Figure 38 A), we observed non-significant PLVs (0.55 ± 0.19) during non-exploration periods. However, the investigation of the geraniol-scented bedding increased the synchronisation values during the sniffing-like periods ($U = 13.00$, $p < 0.01$). As seen in Figures 28 C and 31 C, the signals of these two nuclei showed a remarkably similar profile with high PLVs (0.93 ± 0.07) in the theta band ($5 - 6$ Hz). The synchronisation between the AOB and the Me showed non-relevant values (0.50 ± 0.23, Figure 38 B) in the non-exploration times which significantly shifted to higher values during the sniffing-like periods (male-soiled bedding: 0.96 ± 0.03; $U = 1.50$,
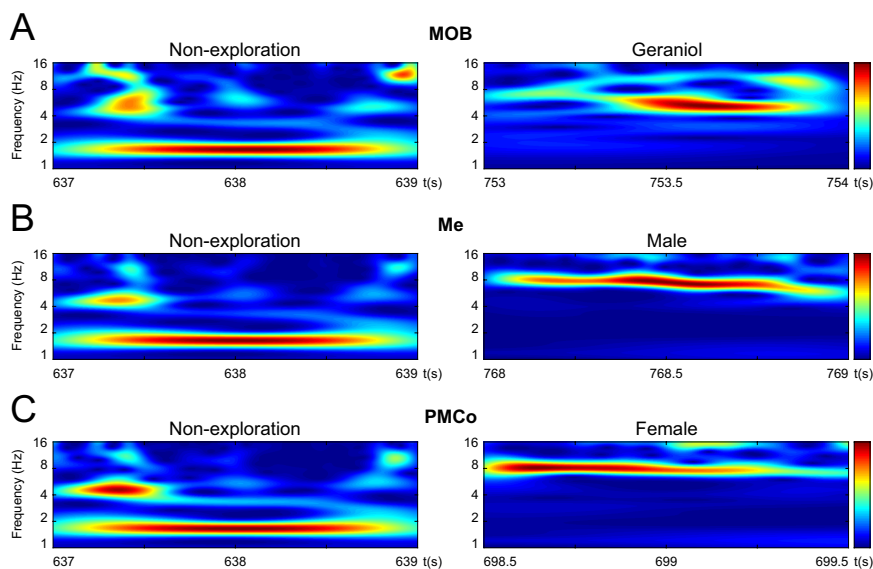
Figure 37: **Time-frequency analyses of the cross-spectrum between the AOB and the MOB, Me and PMCo**. **A,** Cross-spectrum of selected segments from a non-exploration (left) and geraniol-scented bedding exploration (right) between the AOB and MOB. Warmer colours indicate coexistence of similar oscillatory patterns at the same time and frequency. **B,** Idem between AOB and Me for the male-soiled bedding. **C,** Idem between AOB and PMCo for the female-soiled bedding.
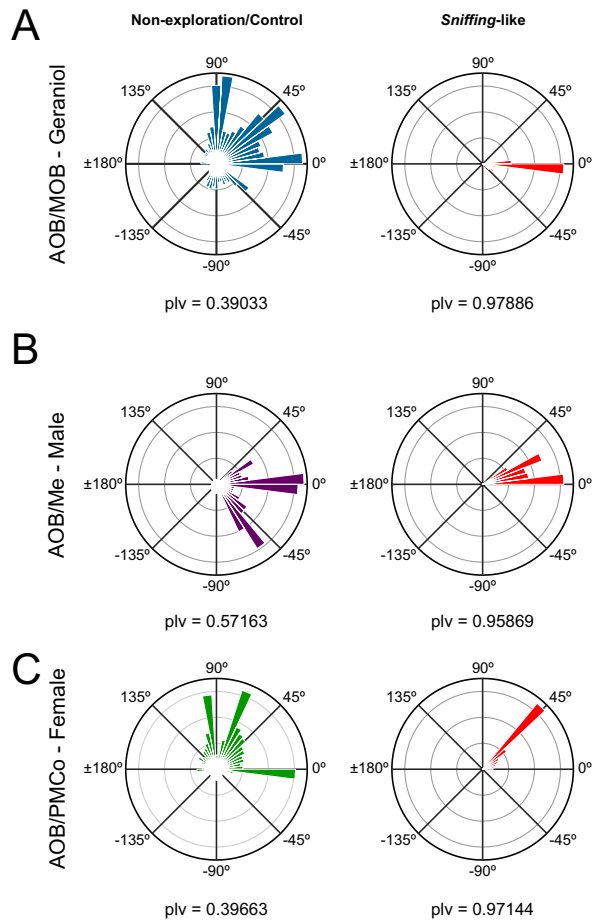
Figure 38: **Phase-locking values between the AOB and the MOB, Me and PMCo**. **A,** Phase to phase synchronisation between the AOB and the MOB for the geraniol-scented bedding, the PLV was calculated filtering the signal at the main theta peak frequency (1 Hz wide). Right, circular diagram showing a representative case for a non-exploration time; Left, a representative case for a sniffing-like period. **B,** Idem between AOB and Me for the male-soiled bedding. **C,** Idem between AOB and PMCo for the female-soiled bedding.

$p < 0.01$). The distribution of phase difference, as demostrated by the Rayleigh's test, was non-uniform both in the control and sniffing-like periods; still, the phase difference was more concentrated during sniffing-like periods (control: $z = 577.90$, $p < 0.05$; sniffing: $z = 1393.07$, $p < 0.05$). In the case of the coupling between the AOB and the PMCo, low PLVs were observed in the control periods (0.43 ± 0.13, Figure 38 C) and they significantly increased in sniffing-like periods (female-soiled bedding: 0.89 ± 0.09; PLVs comparison $U = 1.00$, $p < 0.01$). The phase-difference distribution during the control periods, although with significant values (Rayleigh's test control: $z = 451.76$, $p < 0.05$; sniffing: $z = 680.41$, $p < 0.05$), was quite widespread; whereas

the phase-difference was more delimited for the sniffing-like times.
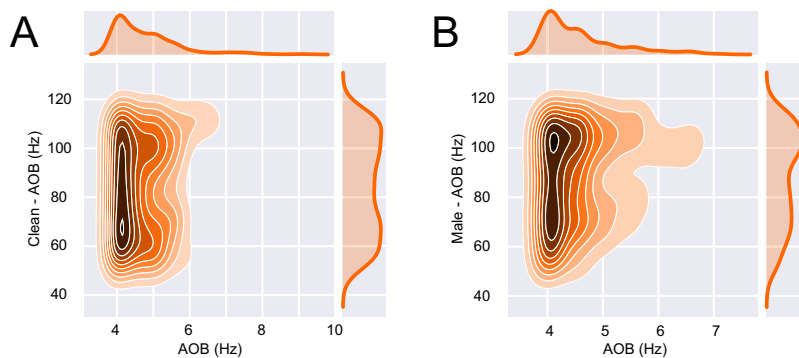
Figure 39: **Map of the theta-gamma modulation in the AOB**. **A,** Points of modulation in the gamma frequencies induced by the theta frequencies for clean bedding, calculated as the mean modulation for all times in each recording, only values over the 70th percentile are shown. **B,** Idem for the male-soiled bedding.

As we described above, gamma bursts seem driven by theta waves with particular frequency bands depending on stimulus. To examine whether this modulation is present between recording nodes, we assessed the phase-amplitude coupling between different frequencies and/or signals. For our study, we detected the frequency of the modulating oscillation in the AOB (theta frequencies with a 1 Hz range) driving the amplitude of the modulated oscillation (gamma frequencies with a 10 Hz range) in the AOB itself or in the other nuclei. Concerning the modulation induced in the AOB (Figure 39) we studied two different stimuli: a neutral stimulus (clean bedding) and a conspecific-derived stimulus (male-soiled bedding), each of them resulting in a different distribution of modulation. First, the clean bedding showed two modulator frequencies in the theta band. The frequecies around $4 - 5$ Hz showed a very high modulation over a wide range of gamma-frequencies (55 to 120) and the $5 - 7$ Hz present two main zones of modulation at $55 - 75$ Hz and $90 - 120$ Hz (Figure 39 A). Second, the male-soiled bedding also showed the wide modulation of gamma-frequencies by the $4 - 5$ Hz theta frequencies, but the $5 - 7$ Hz waves only induced modulation over the fast-gamma ($90 - 120$ Hz) frequencies (Figure 39 B). In the olfactory bulb (Figure 40 A) we analised the modulation in the case of the geraniol-scented bedding. Theta frequencies up to 6 Hz in the AOB overlapped with gamma oscillations ($55 - 85$ Hz) in the MOB. Within the amygdala, the Me (male-soiled bedding) and the PMCo (female-soiled bedding) showed distinctive distributions of the modulation. In the Me, the mod-

ulation map resembled that of the AOB for clean bedding. A large range of AOB's theta frequencies modulated gamma oscillations (Figure 40 B), frequencies between $4 - 5$ triggered a wide range of gamma-frequencies; while 5 to 7 Hz induced three gamma regions at $55 - 70$, $80 - 90$ Hz and $100 - 120$ Hz. In the PMCo the range of gamma-inducing theta frequencies is similar to that of the Me (Figure 40 C), while the gamma oscillations were clearly higher (> 85 Hz). In this sense the modulation map for the PMCo was similar to that of the AOB for male-soiled bedding.
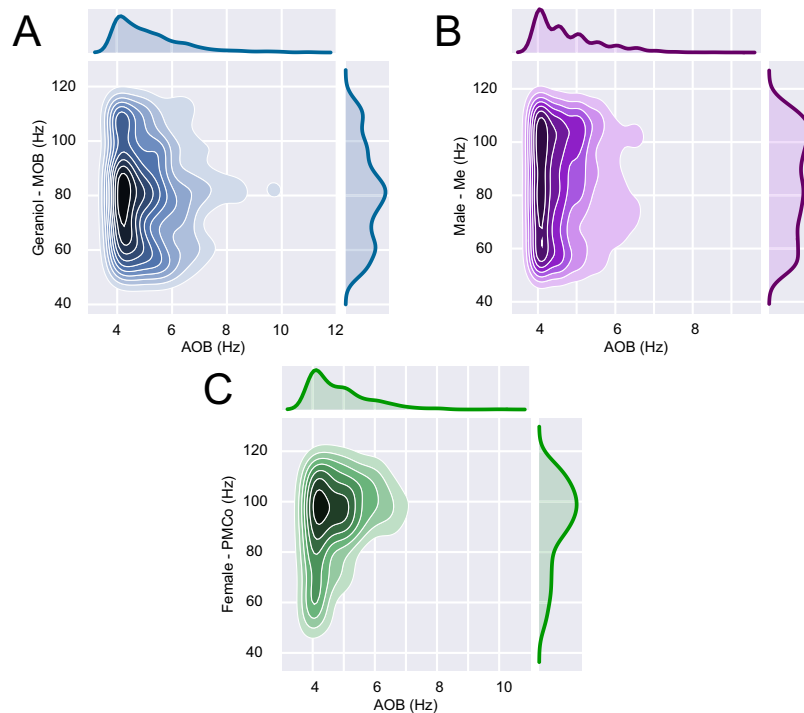
Figure 40: **Modulation index between the AOB and the MOB, Me and PMCo**. **A,** Points of modulation in the gamma frequencies (MOB) induced by the theta frequencies (AOB) for geraniol-scented bedding, calculated as the mean modulation for all times in each recording, only values over the 70th percentile are shown. **B,** Idem for the gamma frequencies (Me) induced by theta frequencies (AOB) for male-soiled bedding, showing the over 65th percentile values.**C,** Idem for the PMCo, showing the over 70th percentile values.

The results for the modulation suggest that the theta waves in the AOB drive the appearence of gamma oscillations, first in the AOB itself and later in the other nuclei. To test if this was indeed the case, we compared the normalised times for the start of the fast-gamma frequencies in the AOB and PMCo in non-exploration periods and female-exploration periods. Thus, we detected that the difference in the start time of the fast-gamma

was not significant for the non-exploration periods ($W = 848.00$, $p > 0.05$), but significant for the female-soiled bedding ($W = 460.00$, $p < 0.05$).
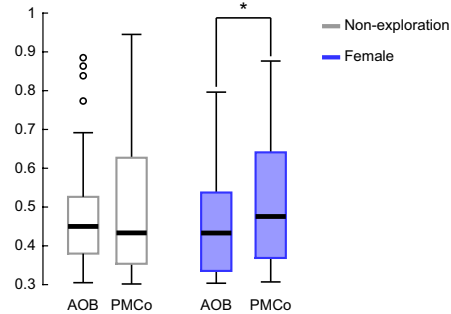
Figure 41: **Theta waves in the AOB drive the appearence of gamma oscillations in the PMCo**. Comparison of the normalised times for the begining of the fast-gamma frequencies in the AOB and PMCo, in non-exploration periods and female-soiled bedding periods ($*$ p-value < 0.05).

Altogether, the findings in the phase-to-phase synchronisation suggest that the AOB and the other nuclei are phase-locked at particular theta frequencies whose profile is specific attending to the stimulus and the recording node. Moreover, the results for the MI are consistent with the previously described power ratio analysis, suggesting a differential gamma profile between nodes correlated to their theta activity and the explored stimulus.

11

DISCUSSION

The present study investigates in awake, freely behaving female mice, the activity induced by the exposure to different chemical stimuli in the three main neural structures of the vomeronasal system and, for comparison, the simultaneous analysis of the activity in the main olfactory bulb. These chemicals include neutral odorants, detected by the main olfactory system, and three complex chemosensory stimuli, which contain both olfactory and vomeronasal chemical signals. As expected, the analysis of the behavioural response shows that the stimuli derived from conspecifics elicited a higher level of chemosensory investigation (Martínez-Ricós et al., 2007).

11.1 EXPLORATORY BEHAVIOUR OF NEUTRAL OLFACTORY STIMULI INDUCES OSCILLATORY ACTIVITY IN THE VOMERONASAL SYSTEM

The analysis of the electrophysiological recordings reveals that, during exploratory behaviour, neuronal activity in the vomeronasal system shows a clear theta rhythm even when only neutral olfactory stimuli are present, and so, without vomeronasal cues (Figure 42 B -neutral-). In contrast, in the absence of exploratory behaviour a predominant field activity in the delta frequencies (< 4 Hz) was observed (Figure 42 A). The theta oscillations observed during exploratory periods increases when the animals apparently focus in the chemoinvestigatory behaviour, we thus identified these periods with increased degrees of rhythmicity as episodes of sniffing-like patterns. In the AOB, during these sniffing-like periods, the theta oscillation modulates the appearance of particular gamma oscillations, located in the peak and descending parts of the theta cycle.

The oscillatory activity in the theta band observed in the MOB was relatively similar to that of the AOB, suggesting that the activity of both centres is synchronic during exploratory behaviour of olfactory stimuli (Figure 42 A). This aspect is confirmed by synchronisation measures, which show a significant increase during exploratory behaviour when exposed to geraniol, a pure

olfactory stimulus. Therefore, the presence of a neutral olfactory stimulus induces synchronic activity in the main and accessory olfactory bulbs. In this regard, the possibility of volumetric conduction of the LFP signals from the MOB to the AOB can be discarded based on several reasons. On the one hand, apart from the described peak in the theta band, the distribution of other frequency peaks in the power spectra is different. In addition, the phase-locking value is very low when the animals are not engaged in chemoexploratory behaviour. If the AOB and MOB recordings are affected by volumetric conduction, the phase-locking value should be relatively similar either in the absence or in the presence of exploration, which is not the case.

In the gamma frequency bands, the spectral analysis revealed differences between the MOB and the vomeronasal nuclei. In the AOB, Me and PMCo, the stimulus exploration gives rise to several peaks in the $90 - 120$ Hz frequencies, while activity in the MOB shows a prominent peak in the $60 - 80$ Hz band (Figure 42 B). When the activity in the gamma band is compared in the periods of exploratory activity induced by the different stimuli bedding (versus periods of no exploration) the medial amygdala stands out as the structure showing higher power in these same frequency bands. The activity in the gamma bands is thought to reflect local processing (Buzsáki and Wang, 2012), and in this regard, the local microcircuitry of the medial amygdala is very different from that of the bulbs and the PMCo. Whereas the olfactory bulbs and the PMCo are structures of major pallial origin (Huilgol and Tole, 2016), with glutamatergic projection neurons and inhibitory interneurons, the medial amygdala is a subpallial structure composed of different subpopulations of neurons of different embryological origin. The medial amygdala contains neurons originated in the caudal medial ganglionic eminence, in the preoptic region and in the hypothalamic supraoptoparaventricular domain, as well as neurons migrating into the medial amygdala from the adjacent ventral pallium (García-López et al., 2008; García-Moreno et al., 2010; Bupesh et al., 2011). Part of the projection neurons of the medial amygdala are GABAergic (Choi et al., 2005). Therefore, this organitsation could explain differencies between the local processing in the intrinsic circuits of the medial amygdala, which does not follow the same anatomical pattern observed in pallial structures. Although it is unknown how this different microcircuitry organisation affects the gamma oscillatory activity, the differences observed in the medial amygdala when compared to the bulbs or the PMCo may be related to the existence of different population of interneurons. These results are consistent with the PMCo being the primary vomeronasal cortex (see 7), while the medial amygdala corresponds

to the striato-pallidal output station (see 4; Cádiz-Moretti et al. 2016a).
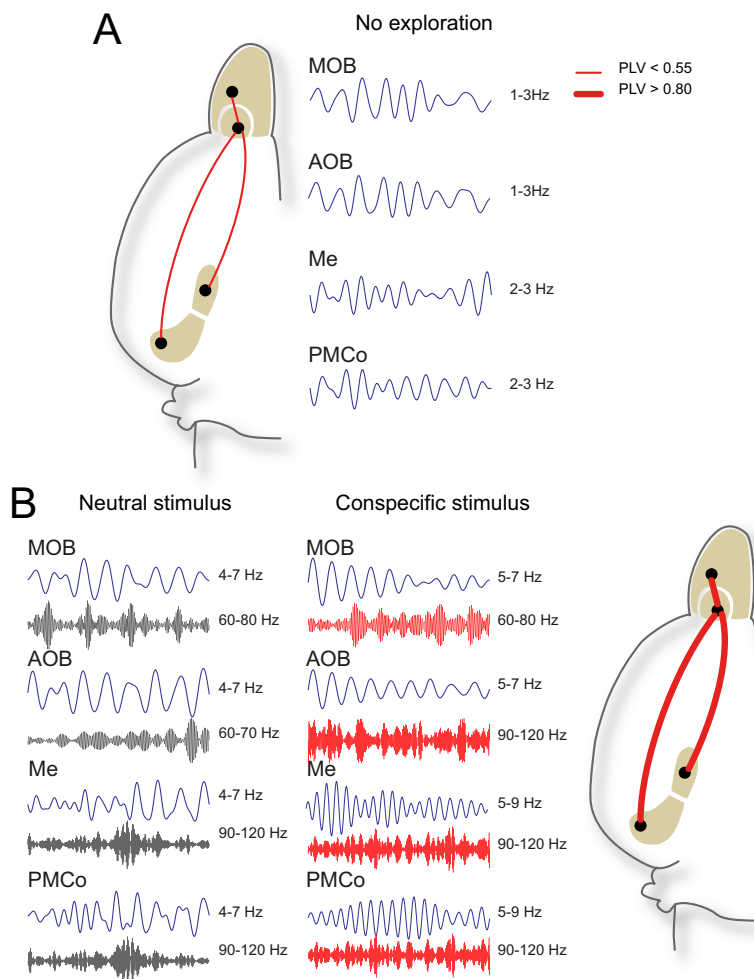
Figure 42: **Long-range interaction in the olfactory network**. **A,** Default network, synchrony level (Left) and representative LFP filtered in the dominant frequencies (Right) in non-exploration conditions. **B,** Representative LFP filtered in the dominant theta and dominant gamma frequencies in exploration conditions. Left: Neutral olfactory stimulus. Middle: Conspecific-derived stimulus. Right: Synchrony levels for neutral stimulus (AOB/ MOB) and conspecific stimuli (AOB/ Me and AOB/ PMCo).

11.2 SYNCHRONIC ACTIVITY IN THE MAIN AND ACCESSORY OLFACTORY BULBS SUGGESTS THAT SNIFFING AND VOMERONASAL PUMPING ARE COUPLED

Given that the projections from the main and the accessory olfactory bulbs are mainly independent (Scalia and Winans, 1975), and that the olfactory and vomeronasal systems have different internalisation mechanisms, it is possible that activity in the

main and the accessory olfactory bulbs followed different dynamics. However, the results show that oscillatory activity in both olfactory bulbs is strongly synchronic even when only pure olfactory stimuli are present (Figure 42 B -neutral-). This observation is consistent with previous reports analizing the simultaneous activity of the main and accessory olfactory system (Tendler and Wagner, 2015).

In the main olfactory system the rhythm of odour-sampling behaviour (sniffing) strongly drives activity in the sensory epithelium and in the olfactory bulb (Wachowiak, 2011). The neural control of sniffing is not completely understood, but it depends on muscles in the snout innervated by the motor neurons of the VII (facial) cranial nerve (Haidarliu et al., 2012), which in turn receive projections from the pre-Bötzinger, Bötzinger complex and parafacial respiratory group (Moore et al., 2014). This complex includes the central pattern generator of the respiratory rhythm.

On the other hand, vomeronasal pumping is under autonomic control by means of sympathetic neurons of the superior cervical ganglion (Meredith and O'Connell, 1979), whose preganglionic neurons are in the intermediolateral column of the cervical-toracic levels of the spinal cord(Rando et al., 1981). These spinal preganglionic neurons receive important projections from the lateral hypothalamus (Saper and Stornetta, 2015), which in turn is innervated by the Pir, the anterior olfactory nucleus, the olfactory tubercle and the anterior cortical amygdala (Price et al., 1991). Therefore, the detection of olfactory information may activate the vomeronasal pumping by this direct hypothalamo-spinal projection. A similar circuit through the lateral hypothalamus has been anatomically described in snakes (Martínez-Marcos et al., 2001), in this case to mediate the chemosensory modulation of the tongue-flick response, the mechanism for internalisation of chemical signals into the vomeronasal organ (Halpern and Kubie, 1980). The detection of airborne odours elicits an increase tongue-flick rate in snakes (Zuri and Halpern, 2003), suggesting that the role of the main olfactory system in activating vomeronasal sampling is general in terrestrial vertebrates. The lateral hypothalamus may be the interface between the chemosensory telencephalic structures and the motor control of the vomeronasal internalisation mechanism (Martínez-Marcos et al., 2002). The lateral hypothalamus projects also to the rostral ventrolateral reticular nucleus (Saper and Stornetta, 2015), where the pre-Bötzinger and Bötzinger complex are located. Consequently, the lateral hypothalamus would coordinate the detection of olfactory information with both olfactory (sniffing) and vomeronasal (vascular pumping) internalisation mechanisms, explaining the coupled oscillatory activity. In this regard,

chronic recordings of the activity of the vomeronasal pump in male hamsters showed that it is activated by novelty, and it keeps active during exploratory behaviour (Meredith, 1994). Although the induction of vomeronasal pumping by olfactory stimuli was not specifically investigated, the results reported by Meredith (1994) are consistent with synchronic internalisation of olfactory and vomeronasal stimuli by sniffing and vomeronasal pumping, respectively. Furthermore, lesions of the olfactory epithelium with zinc sulfate nasal lavage, leaving intact the vomeronasal organ, disturb vomeronasal-dependent behaviours (Slotnick et al., 2010), such as intermale aggression (Clancy et al., 1984) and puberty acceleration (Lomas and Keverne, 1982). These results also indicate that olfactory stimuli trigger the activation of the vomeronasal pumping mechanisms (Slotnick et al., 2010). Therefore, the profound behavioural deficits observed in some genetically modified mouse with null mutations of genes coding for essential proteins for olfactory signal transduction (e.g., cyclic nucleotide-gated channel alpha2, Mandiyan et al. 2005) may be reinterpreted as the result of the inability to detect both olfactory and vomeronasal information.

11.3 NEUTRAL VERSUS CONSPECIFIC CHEMOSENSORY PROCESSING IN THE OLFACTORY BULBS AND VOMERONASAL AMYGDALA

The rhythmic activity registered in the accessory olfactory bulb in the absence of vomeronasal stimuli is, to some extent, surprising. In any case, as expected, the conspecific-derived stimuli, which contain both olfactory and vomeronasal cues, induced particular changes in the oscillatory activity of the analysed structures. In the theta band, the investigation of chemical signals from either females, males or castrated males induced oscillatory activity at approximately 7 Hz in all four structures analysed (Figure 42 B -conspecific-). In contrast, as discussed before, the exploration of neutral stimuli induced a prominent theta activity with a peak at $4 - 6$ Hz in the olfactory bulbs, the Me and the PMCo (Figure 42 B -neutral-). The differences in the peaks induced by the exploration of neutral olfactory stimuli versus those induced by conspecific stimuli are significant in the AOB, MOB and Me, and approach significance in the PMCo. These results are similar to those reported by Tendler and Wagner (2015) in the olfactory bulbs and medial amygdala (they did not record in the PMCo) in a social recognition paradigm, although they use juvenile male rats as subjects, and either awake or anaesthetised male rats of similar age and different strain as stimuli. Therefore, in addition to chemosensory cues, visual

and somatosensory cues are available in this paradigm. The present results show that chemosensory cues from conspecifics are enough to induce this oscillatory activity, which appears common in rodents and independent of the gender of the subjects.

In the main and accessory olfactory bulbs, the main peak induced by female- and castrated male-soiled is also significantly different from that induced by geraniol-scented bedding. The peak induced by male-soiled bedding is similar to that elicited by female and castrated male cues. The lack of differences in the AOB activity induced by male- or female-derived chemical signals is consistent with the results obtained from multiunit and single unit recordings in the anaesthetised animals (Ben-Shaul et al., 2010; Bergan et al., 2014), which show a relatively low selectivity of AOB responses, due to the presence of individual neurons responsive to different types of stimuli. The presence of vomeronasal sensory neurons with broadly tuned responses, able to detect all of the major urinary proteins tested (Kaur et al., 2014), may be the reason underlying this low selectivity.

In contrast to the AOB, in the medial amygdala male-specific chemical signals elicited a rhythmic activity in the theta band with a peak near 8 Hz, which is different from that induced by female cues (as well as from those due to neutral olfactory stimuli). Among the chemical signals that may elicit this distinct activity, two non-volatile pheromones are strong candidates. On the one hand, the male-specific major urinary protein darcin, which elicits female attraction (Roberts et al., 2010), olfactory (Lanuza et al., 2014) and spatial learning (Roberts et al., 2012) and maternal aggression (Martín-Sánchez et al., 2015). On the other hand, the peptide ESP-1, secreted by the extraorbital gland of male mice, which induces lordosis (Kimoto et al., 2005; Haga et al., 2010). Both darcin and ESP-1 are detected by vomeronasal sensory neurons (darcin: Kaur et al. 2014; ESP-1: Kimoto et al. 2005, and are therefore processed by the accessory olfactory bulbs and the vomeronasal amygdaloid structures. The present results suggest that the medial amygdala is a key nucleus in the female brain involved in processing male-derived sexual signals, something consistent with previous electrophysiological (multiunit and single unit) data (Bergan et al., 2014) as well as data derived from c-Fos (Moncho-Bogani et al., 2005) and lesion studies (DiBenedictis et al., 2012).

In addition to darcin and ESP-1, several male-specific volatile molecules have been shown to influence sexual behaviour in females (Asaba et al., 2014), such as farnesenes, brevicomin and tiazoline, which are detected by the vomeronasal organ (Leinders-Zufall et al., 2000) and MTMT and (Z)-5-tetradecen-

1-ol, which are detected by the olfactory epithelium (Lin et al., 2005; Yoshikawa et al., 2013). The vomeronasal signals may obviously contribute to the male-specific activity of the Me. In addition, information about the olfactory cues may also reach directly from the MOB the anterior part of this nucleus (Scalia and Winans, 1975). Olfactory information may also reach the Me indirectly through afferents from the piriform cortex or the olfactory amygdala (Cádiz-Moretti et al., 2016a).

In contrast to the Me, in the PMCo the results show a peak of oscillatory activity in the theta band specifically induced by female-derived chemical signals. The female set of major urinary proteins also play a role in female aggressive behaviour, in the context of access to resources or reproductive opportunities (Stockley et al., 2013). In addition, a recent female-specific urinary signal has been identified (16-hydroxycorticosterone-20-hydroxy-21-acid) and named cortigynic acid (Fu et al., 2015). This molecule is a non-volatile vomeronasal signal that elicits male chemoinvestigation and induces mounting behaviour in males (Fu et al., 2015). Although it is not currently known whether cortigynic acid is also detected by females, it seems a likely possibility. It would be, therefore, interesting to investigate the role of the PMCo in female mice in processing vomeronasal signals derived from other females, in the context of female competition. To our knowledge, no information is available about this possible role of the PMCo.

11.4 THETA RHYTHM IN THE AOB MODULATES GAMMA OSCILLATIONS IN THE OLFACTORY NETWORK

The synchronic oscillatory activity between the different nodes of the olfactory network probably reflects a temporal coordination of the detected chemosensory information. During the exploration of either neutral stimuli (clean bedding) or conspecific-derived stimuli (male-soiled bedding) the theta activity in the AOB modulates gamma activity in the AOB itself. Furthermore, the exploration of geraniol-scented bedding by means of sniffing-like behaviour, induces a very high degree of coupling in the theta band between the MOB and AOB, and also theta activity in the AOB modulates gamma activity in the MOB. These results further reinforce the idea that the activity of the main and accessory olfactory bulbs is synchronised even during the detection of pure olfactory stimuli, as shown previously using high resolution fMRI in mice (Xu et al., 2005).

The Me shows a specific peak of theta activity during the exploration of male-derived chemicals. The analysis of the coupling values shows that the theta activity in the AOB and Me is

also strongly synchronic during the sniffing of male-soiled bedding. In addition, the theta oscillations in the AOB modulate the activity in the whole gamma band in the Me. These results are consistent with the Me processing information about male-specific vomeronasal signals, such as the attractive sexual pheromone darcin, relayed by the AOB.

Since the PMCo showed a specific peak of activity in the theta band when the animals were exposed to female-soiled bedding, we particularly analysed the coupling values among the AOB and PMCo in the theta band during the exploration of female stimuli. This analysis revealed a strongly synchronic activity in these two structures. Moreover, our data also indicate that theta activity in the AOB is able to modulate the high gamma oscillations in the PMCo.

Another interesting result is the particular gamma frequencies modulated by the AOB in the other nuclei. While neutral stimuli trigger high gamma waves ($60 - 80$ Hz), the conspecific-derived stimuli modulate higher fast-gamma frequencies ($90 - 120$ Hz).

Altogether, the synchronic theta activity between the MOB and AOB, and between the AOB and the vomeronasal amygdala, suggests that this particular rhythm, as showed for other brain regions, facilitates the coordination of the network activity for the transfer of information across these brain regions. Hierarchical operations in the olfactory network could explain the presence of a common theta oscillator with a feedforward processing between the olfactory bulbs and the amygdaloid nodes, and in this way, particular gamma oscillations emerge in the local circuits with a fine time-scale coordination. Thus, olfactory and vomeronasal information could be integrated into a complete representation of the chemosensory environment.

Part V

GENERAL DISCUSSION AND
CONCLUSIONS

12

GENERAL DISCUSSION

The presence of two olfactory systems with different sensory organs and central pathways in most tetrapods (Ubeda-Bañón et al., 2011) poses the question of whether they are redundant or complementary. The early discoveries of segregated and parallel projections of the olfactory and vomeronasal systems in vertebrates led to the enunciation of the dual olfactory system hypothesis (Scalia and Winans, 1975; Kevetter and Winans, 1981a,b). This hypothesis stated that there are two separate and distinct olfactory systems, the main and the accessory olfactory systems, with parallel pathways that subserve different functions. However, nowadays, there is an emerging consensus in that the two olfactory systems do not have independent functions but play complementary roles in mediating the behavioural responses to chemosensory cues (Brennan and Zufall, 2006; Kelliher, 2007; Restrepo et al., 2004; Zufall and Leinders-Zufall, 2007).

The different locations, anatomical structure and mechanisms of stimuli internalisation of the main olfactory epithelium and the vomeronasal organ led to the idea that the main olfactory system is specialised for detecting volatile, airborne molecules; whereas the vomeronasal system is specialised for the detection of non-volatile chemosignals, such as those in urine, scent glands and reproductive secretions. However, some findings indicate that this functional division is not as absolute as was once thought. There are urinary volatile chemosignals that activate the vomeronasal organ (Leinders-Zufall et al., 2000) and, reversely, non-volatile compounds that gain access to the main olfactory epithelium (Spehr et al., 2006b). In fact, there are molecules detected by both the olfactory and vomeronasal systems, as revealed by functional magnetic resonance imaging in anaesthetised mice which have shown robust changes in the activity of the AOB in response to urine odours delivered via the airstream (Xu et al., 2005). These data lead to another idea, which proposed that the main olfactory system detects odours, while the vomeronasal system would detect pheromones, substances which activate instinctive behaviours or autonomic physiological functions. This view is also at issue as newborn rabbits detect the mam-

mary pheromone, which generates nipple search, through the olfactory epithelium (Hudson and Distel, 1986). In addition, a subset of mitral cells of the main olfactory bulb has been described to respond exclusively to a male-specific pheromone ([methylthio]methanethiol) present in male urine (Lin et al., 2005). Finally, is has been described that the main olfactory epithelium also plays important roles in sensing predator and prey odours and in mediating innately aversive responses (Kobayakawa et al., 2007). These studies indicate that some olfactory neurones express special olfactory receptors that are likely narrowly tuned to detect specific pheromones or allomones (Spehr et al., 2006a). On the other hand, the non-overlapping projections of the olfactory bulbs have been call into question as even the earliest reports suggested areas of the amygdala where olfactory and vomeronasal inputs could converge (Scalia and Winans, 1975). This preliminary data has been corroborated by many groups (Kang et al., 2009; Pro-Sistiaga et al., 2007; Cádiz-Moretti et al., 2013) demostrating the integration of both types of chemosensory information in the amydala. Nevertheless, there is no consensus on how exactly this olfactory-vomeronasal interplay takes place.

Consequently, further understanding of the organisation and function of the olfactory and vomeronasal systems would allow us to comprehend how information from both systems is integrated and how appropriate behavioural responses are generated. This can be acquired through two experimental appraches, namely revealing the connectivity of fundamental nuclei, which can lead our reasoning about its function, and understanding how these two neuronal systems interact.

In a first approach, this work enquires the analysis of the connections of key amygdaloid nuclei involved in the processing of vomeronasal information, namely the medial and the posteromedial cortical amygdaloid nucleus, as part of the comprehensive analysis of the neural circuitry processing chemosensory information in the brain of female mice performed in our grup (Gutiérrez-Castellanos et al., 2010; Cádiz-Moretti et al., 2016b,a). Additionally, the pattern of connections gives us an static insight of the network, thus it is necessary to complement this with a dynamic counterpart. To understand the function of the olfactory and vomeronasal network it is of interest to investigate the neuronal population activity in these systems. Altoghether, these two approaches will allow us to understand how information from both systems is integrated to generate a complete picture of the chemical cues present in the environment and to generate appropriate behavioural responses.

12.1 INTRINSIC ORGANISATION AND PROCESSING IN THE VOMERONASAL CIRCUITS

Vomeronasal stimuli require a complex processing prior to its relay not only because of the complexity of these stimuli (Zufall and Leinders-Zufall, 2007), but also given to the fact that vomeronasal stimuli are related to different behaviours (i.e., sexual versus aggressive or defensive), and the neural circuits that should be activated in response to each one of these vomeronasal stimuli is different. Among the structures considered stricty vomeronasal, the PMCo should be considered as the primary vomeronasal cortex due to its distinguishing features. First, it has a major input from the AOB (Winans and Scalia, 1970; Scalia and Winans, 1975; Von Campenhausen and Mori, 2000) and is highly interconnected with each of the structures of the vomeronasal system. Second, the PMCo is the only structure with a strict pallial origin (Medina et al., 2004). And third, displays a characteristic cortical lamination and a layered organisation of its inputs and outputs. On the other hand, the Me would be the vomeronasal striatum, or the striato-pallidal output station of the vomeronasal system, as it strongly projects to hypothalamic behavioural circuits and the reward system. Regarding this, the embryonic origin of the Me suggests that it contains neurons of different subpallial origins, including striatal and pallidal components (Bupesh et al., 2011).

The processing of vomeronasal information is crucial for reproduction and survival as the vomeronasal system is involved in the detection of great variety of stimuli related to different behaviours. It was originaly thought that the vomeronasal system was involved in reproductive behaviours (Powers and Winans, 1975) as it detects sexual pheromones (Martínez-Ricós et al., 2008; Haga et al., 2010; Roberts et al., 2010). However, the vomeronasal organ detects also aggression-eliciting chemical signals from same-sex conspecifics (Clancy et al., 1984; Chamero et al., 2007); molecules derived from a wide range of predators, which induce defensive behaviours (Papes et al., 2010; Isogai et al., 2011); illness-related molecules (Rivière et al., 2009), which are likely to induce an avoidance response (Arakawa et al., 2010); and sulphated steroids present in the urine of conspecifics, which are likely to signal their physiological status (Nodari et al., 2008). Obviously, different neural circuits should be activated in response to each one of these vomeronasal stimuli.

Furthermore, depending on the perceived stimulus the three main neural structures of the vomeronasal system and the MOB show a distinctive activity. In the absence of exploratory behaviour the predominant field activity showed by the olfactory

network is centred in delta frequencies (< 4 Hz; Figure 42 A), a response tipically observed in the MOB (Welker, 1964; Kepecs et al., 2007). The exploration of a stimulus elicits an increase in the dominant activity to a theta rhythm, even when only neutral olfactory stimuli are present (Figure 42 B). Within the exploration periods we detected short rhythmic epochs ($2 - 4$ s) where the oscillation temporally remained in a stationary theta activity. The predominance of theta oscillations has been described for the MOB (Youngentob et al., 1987; Kepecs et al., 2006; Verhagen et al., 2007; Wesson et al., 2008) and the AOB (Binns and Brennan, 2005; Tendler and Wagner, 2015). However, neutral and conspecific-derived stimuli induce particular changes in the oscillatory activity of the analysed structures. Neutral stimuli (in absence of vomeronasal signals) induce a prominent theta activity with a peak at $4 - 6$ Hz; while the conspecific-derived stimuli (olfactory and vomeronasal cues) induce oscillatory activity at approximately 7 Hz in all four structures analysed. Similar frequencies have been described by Tendler and Wagner (2015) for the MOB, AOB and Me. In addition, the theta activity is highly synchronic between the MOB and AOB, and between the AOB and the vomeronasal amygdala, thus suggesting that this rhythm facilitates the coordination of the network activity for the transfer of information across these brain regions.

The oscillatory activity in the theta band observed in olfactory bulbs is quite similar and the measures of synchrony between the MOB and the AOB show a significant increase during exploratory behaviour when exposed to geraniol, a pure olfactory stimulus. These two facts suggest that the internalisation of the stimulus in the main olfactory epithelium (sniffing) is coupled with the internalisation of the stimulus in the vomeronasal organ (vomeronasal pumping). It is not clear the mechanisms that initiate the activation of the pumping, but our data suggest that the sniffing may drive vomeronasal sampling and, indirectly, the oscillatory pattern in the vomeronasal system.

During the exploration of a stimulus the Me stands out as the structure showing higher power in the gamma frequency bands. Moreover, the activity in these bands revealed differences between the MOB and the vomeronasal nuclei. The stimulus exploration gives rise to several peaks in the $90 - 120$ Hz frequencies in the AOB, Me and PMCo; while the MOB shows a prominent peak in the $60 - 80$ Hz band. This gamma activity in all nuclei is modulated by the theta oscillation in the AOB. Thus, the theta band in the AOB triggers, when a neutral stimulus is presented, high gamma waves ($60 - 80$ Hz) in the olfactory bulbs; while conspecific-derived stimuli modulate higher fast-gamma frequencies ($90 - 120$ Hz) in the AOB and the vomeronasal amy-

gdala. These results further reinforce the idea that the activity of the main and accessory olfactory bulbs is coupled even during the detection of pure olfactory stimuli.

From an olfactory perspective the piriform cortex is perhaps the most comparable to the PMCo and, among the olfactory cortices, is the most extensively studied and well understood. Like the PMCo, the Pir shows a trilaminar structure, receives direct olfactory information (from the MOB in this case) and is connected with other cortical olfactory structures and the chemosensory amygdala (Haberly and Price, 1978; Martínez-García et al., 2012). The activity of the Pir is also comparable to that of the PMCo. In the presence of an odour three rhythms dominate: theta, beta and gamma oscillations (Martin and Ravel, 2014; Beshel et al., 2007; Neville and Haberly, 2003). Furthermore, the theta rhythm in the Pir increases its coherence with that of the MOB in presence of an odour (Kay, 2005; Tendler and Wagner, 2015), thus indicating a coordinated processing of olfactory stimuli. This fact resembles the aforementioned phase-locking synchrony between the AOB and the PMCo. In contrast, the gamma oscillations observed in the Pir are similar to those in the MOB, showing an increase in the $\approx 60 - 90$ Hz high gamma band (Neville and Haberly, 2003; Mori et al., 2013).

The olfactory tubercle, in contrast, has received little attention in terms of elucidating its role in the processing and perception of odours, as the research has mostly focused on its relationship with the reward system. Among the neural structures through which olfactory sensory information flows, the Tu is perhaps the most similar to the Me. The Tu is considered part of the ventral striatum and shows a trilaminar and cortical-like structure that is interrupted by dense cell clusters (the islands of Calleja; Mori 2014). As the Me, contains cells from multiple developmental sites (García-Moreno et al., 2008) and is interconnected with numerous brain regions, especially with olfactory structures (Wesson and Wilson, 2011; Mori, 2014) and arousal/ reward centers (Ikemoto, 2007). However, its activity differs from that of the Me. Odour stimulation evokes increases in the power ratio in the theta, beta and gamma bands (Carlson et al., 2014), that are coherent with the MOB activity. Furthermore, Tu single-units respond in an odour-specific manner (Wesson and Wilson, 2010), thus contributing to odour discrimination or, more likely, to the integration of olfactory information with extramodal senses (Wesson and Wilson, 2011). The different activity as compared with the Me may be related to its laminar structure; nevertheless, as the Me, the Tu is a structure mediating the integration of chemosensory information.

12.2   THE ME COORDINATES THE BEHAVIOURAL RESPONSE TO OLFACTORY AND VOMERONASAL CUES

The efferent projections of the three subdivisions of the Me revealed by our results are summarised in Figure 11. The pattern of efferent projections of the medial amygdaloid subnuclei found in female mice is very similar to that reported in male rats and male hamsters. Thus suggesting that the inter-sexual and inter-species differences in reproductive (Vale et al., 1973, 1974; Burns-Cusato et al., 2004; Dominguez-Salazar et al., 2004) and defensive (Belzung et al., 2001; Yang et al., 2004) behaviours cannot be attributed to differences in the pattern of efferent projections originated from the Me. However, there are two relevant exceptions regarding the main projections originated from the MePV. First, we have found a very dense projection to the BSTMPM and a moderate projection to the BSTMPI, while the opposite pattern was found in male rats (Canteras et al., 1995). Second, the MePV gives rise to relatively lighter projections to the hypothalamus than those reported in male rats (Canteras et al., 1995), especially in the anterior region. Further research will be necessary to check whether these discrepancies are due to interspecific differences or to the presence of a certain degree of sexual dimorphism in these projections.

The strong connectivity of the Me with the other structures receiving vomeronasal information from the AOB and the dense intra-nucleus connections, suggests that the information detected by the vomeronasal system is subjected to a complex intrinsic processing before being relayed to other structures. Moreover, the Me (especially its anterior part) has strong interconnections with different structures of the main olfactory system, including the olfactory amygdala and the Pir. Therefore, there are anatomical pathways allowing for ample integration of olfactory and vomeronasal information in structures usually considered strictly as part of the olfactory or the vomeronasal systems (Gutiérrez-Castellanos et al., 2010), which strongly supports the complementary role of these systems (Baum and Kelliher, 2009; Martínez-García et al., 2009). In fact, the convergent inputs from the MOB and AOB induce classical long-term potentiation of the synapses in sagittal Me slices *in vitro* (Griffiths and Brennan 2015, unpublished results). The necessity of complex processing of vomeronasal stimuli prior to its relay may be related not only to the complexity of the vomeronasal stimuli (involving both volatile and involatile components, Zufall and Leinders-Zufall 2007), but also to the fact that these vomeronasal stimuli are related to different emotional, behavioural responses.

The anterior and posteroventral subdivisions of the Me project to key structures of the circuit involved in the defensive response against predators, that includes the BSTMPI, the AH, the VMHDM and the PMD (Canteras, 2002). As previously suggested, parts of the hypothalamic defensive circuit may also be involved in agonistic behaviours, such as aggressive responses against same-sex conspecific intruders (Motta et al., 2009), or avoidance of parasitised conspecifics (Arakawa et al., 2010). Furthermore, the Me has projections to the central amygdala and the basolateral complex. These anatomical data suggest a role of the Me not only in defensive responses to predators, but also in the modulation of appetitive and aversive behaviours mediated by olfactory and vomeronasal stimuli through the central amygdala and a minor role in fear learning (in the fear conditioning paradigm) mediated by the basolateral complex. Regarding this, the Me has been showed to be involved in both unconditioned (Li et al., 2004) and learned (Takahashi et al., 2007) fear responses to predator odours and is critically involved in the acquisition and expression of olfactory conditioned fear (Cousens et al., 2012). Further research is needed to clarify whether there are subsystems within this global defensive system for these different behavioural responses. In this context, the projections of the MePV to nuclei related to reproductive behaviours (e.g., PMV) can be interpreted as a pathway for inhibition of reproduction in the presence of predators or parasitised conspecifics.

The Me is involved in appetitive behaviours probably due to the rewarding properties of sexual behaviour and sexual pheromones (Moncho-Bogani et al., 2002, 2005). These rewarding properties are mediated by direct projections from the Me (especially the MeA) to the major structures of the brain system of reward, namely the VTA, the medial shell of the nucleus accumbens and the Tu (including the islands of Calleja). Indirect projections to the ventral striatum also exist through the basolateral amygdala. Previous work has shown that male pheromones are attractive to female mice and can be used as appetitive unconditioned stimuli to induce learning (Moncho-Bogani et al., 2002; Agustín-Pavón et al., 2007; Martínez-Ricós et al., 2007; Ramm et al., 2008; Roberts et al., 2010). Therefore, the projections from the Me to the reward system may be involved in processing the hedonic value of sexual pheromones. This hypothesis is consistent with data in hamsters showing that lesions of the Me abolish the female attraction toward male-derived chemical signals (Petrulis and Johnston, 1999). A recent report in mice has also shown that lesions of the Me blocked the preference of females for male urine, although in this case only lesions that included the posterior medial amygdala were effective (DiBenedictis et al., 2012);

whereas lesions restricted to the anterior subdivision had no effect, suggesting that the connections originated by the posterior subdivisions are sufficient to mediate the female preference for male-derived chemicals. Of note, the basolateral amygdala is known to play a relevant role in reward learning (Baxter and Murray, 2002), but the extent to which the Me (and other structures of the chemosensory amygdala) participate in the rewarding aspects of pheromones (or chemical signals with hedonic value) is unknown.

The response to odours and pheromones in the context of reproductive behaviour is mainly mediated by the MePD, which projects to the neural circuit for reproductive behaviours (Swanson, 2000), including the BSTMPM, the MPO, the VMHVL and the PMV. According to our results, in the Me, male-specic chemical signals elicit a rhythmic activity in the theta band with a peak near 8 Hz. In this sense Me neurons respond preferentially to stimuli from the opposite sex (Bergan et al., 2014), supporting the view that the Me mediates reroductive behaviours (for a review see Swann et al. 2009). Nevertheless, we want to point out that parts of this circuit may be involved in non-sexual aspects of reproductive behaviour, such as maternal aggression (Hasen and Gammie, 2006). In fact, a recent study has revealed the presence within the ventrolateral part of the VMH of male mice of mainly distinct neuronal subpopulations involved in fighting against male intruders and in mating (Lin et al., 2011). Therefore, the systems mediating reproductive and aggressive responses are not fully segregated.

Briefly, the Me would filter the chemosensory information received from the AOB and MOB that would then be relayed to different amygdaloid nuclei. The olfactory information requires a complex processing, as it is involved in a wide range of behaviours, and the pattern of projections from the Me reflects this complexity. Besides the strong intra-amygdaloid connections the main efferences of the Me are the BST and the hypothalamus, thus indicating a major role of this nucleus in the control of the neural circuits activated in response to different vomeronasal stimuli. The anterior division is, among the Me subnuclei, the main input and main output to the olfactory related nuclei, suggesting a key role of the MeA in the integration of the olfactory and vomeronasal signals. The MeA seems to filter and categorise the received chemosensory information, which would be relayed either to the neural circuit for socio-sexual behaviour or to the neural circuit for defensive behaviour. Information from sexual pheromones would be relayed to the socio-sexual neural circuit through the projections of the MePD to the BSTMPM and the hypothalamic reproductive nuclei. The MePD possesses abund-

ant cells expressing receptors for sexual steroids, which make it a nodal centre for the hormonal control of the response to odours and pheromones in the context of reproductive behaviour, and its projection to the rest of the Me would allow an integration of odour/ pheromone information with endocrine signals. Moreover, in the MePD heterospecific odours would inhibit reproductive-related circuits and facilitate defensive behaviours. In contrast, the MePV is mainly involved in defensive behaviours through its connections with the BSTMPl and the defensive hypothalamic circuit. Moreover, our results indicate that the MePV innervates the BSTMPM and the anteromedial BST, thus it may be involved in the control of other non-sexual behaviours, such as agonistic encounters with same sex conspecics or aversion to illness-derived social odours.

12.3 THE PMCO COORDINATES THE NEURAL PROCESSING OF VOMERONASAL CUES

The afferent and efferent projections of the PMCo revealed by our results are summarised in Figure 22. These results confirm and extend in female mice previous reports in other mammalian species, mainly in male rats and hamsters, which show some of these connections (Kevetter and Winans, 1981b; Canteras et al., 1992; Kemppainen et al., 2002; Pitkänen, 2000). As discussed for the Me efferents, the lack of relevant differences between our results (in female mice) and previously reported data (in male rats and hamsters) indicates that this pattern of connections is common to the different rodent species and that no significant sexual dimorphism is present in the pattern of PMCo projections. Noteworthy, most of the efferent projections of the PMCo target structures that project back to it, with two major exceptions to this rule, the ventrolateral septum and the ventral striatum.

The PMCo receives information from and projects back to each of the structures of the vomeronasal system, including the AOB, the Me, the bed nucleus of the accessory olfactory tract and the bed nucleus of the *stria terminalis*. It also shows significant interconnections with the principal components of the main olfactory system, including the piriform cortex, the endopiriform nucleus, the lateral entorhinal cortex and the olfactory amygdala. However, these connections, especially the efferences, are not as dense as those with the vomeronasal structures. These connections would allow the integration of olfactory and vomeronasal information to compose a complete map of the chemical environment of the animal. This integration is made at two levels: in the convergent projections of the olfactory bulbs (Pro-Sistiaga et al., 2007; Kang et al., 2009; Cádiz-Moretti et al., 2013); and in the re-

ciprocal connections between the PMCo and secondary olfactory centers. A further level of convergence would be the projections to the basomedial nucleus, where vomeronasal information can be integrated with other kinds of emotionally labelled sensory information.

Another relevant connection of the PMCo is that with the ventral CA1 and ventrolateral septum. The ventral hippocampus seems a specialised area strongly interconnected with the vomeronasal system, as it also receives projections from the Me (4). This suggests an interesting hypothesis: the information about vomeronasal stimuli could contribute to the spatial map generated by the hippocampus through this vomeronasal-hippocampus interaction. The neural circuitry by which the territory modulates the aggressive/ defensive responses of males against intruders is currently unknown (Adams, 2006), but it may be mediated by the projections from the PMCo to the ventrolateral septum (also targeted by the ventral hippocampus, Risold and Swanson 1997). In females, by contrast, the presence of a dominant male would activate the hypothalamic circuits for reproductive behaviour.

Toghether with the ventrolateral septum, the other neutral structure without reciprocal connections with the PMCo is the ventral striatum. The efferences from the PMCo to the medial aspect of the olfactory tubercle and the islands of Calleja, may constitute the anatomical pathway conveying information about the sexual pheromones processed in the vomeronasal system to the reward system of the brain (Novejarque et al., 2011). This direct projection and also indirect ones, like that through the basomedial nucleus, explain the reinforcing properties of sexual pheromones, which induce conditioned place preference (Agustín-Pavón et al., 2007; Martínez-Ricós et al., 2007; Roberts et al., 2012).

The vomeronasal amygdala seems to specifically respond to conspecific-derived stimuli. If the Me responds to male-derived chemical signals, the PMCo shows a peak of oscillatory activity in the theta band (up to 8 Hz) specifically induced by female-derived chemical signals. This might indicate that in female mice the PMCo processess vomeronasal signals derived from other females, thus playing a role in female aggressive behaviour.

12.4   COMPARATIVE AND EVOLUTIONARY REMARKS

The vomeronasal system is present, at least at some point during development, in virtually all amphibians, reptiles and mammals (Halpern, 2007). In these groups, separate main and accessory olfactory bulbs are recognized, with distinct targets in the foreb-

rain. Similar to mammals, the main olfactory bulbs innervate mainly the lateral (olfactory) cortex, whereas the accessory olfactory bulbs project mainly to amygdaloid areas (Scalia et al., 1991; Martinez-Garcia et al., 1991; Lanuza and Halpern, 1998). Within the vomeronasal amygdala, only a subpallial component can be recognized in amphibians (Moreno and González, 2007), whereas in reptiles pallial and subpallial components are present (Martínez-García et al., 2007), which can be compared to the medial amygdala and the posteromedial cortical amygdala in mammals. Therefore, the subpallial (striato-pallidal) part of the vomeronasal amygdala appears to be present in the anamniote ancestor of terrestrial vertebrates, whereas the "vomeronasal cortex" appears at some point in the anamniote-amniote transition. This cortical region in the amygdala of squamate reptiles takes the name of nucleus sphericus.

The connections of the medial amygdala and the nucleus sphericus are quite similar to those of the mammalian medial amygdala and PMCo (Lanuza and Halpern, 1997). In addition to the reciprocal connection with the AOB, the medial amygdala in reptiles gives rise to important projections to the hypothalamus (Martínez-Marcos et al., 1999). However, subregions of the reptilian medial amygdala, comparable to the posterodorsal and posteroventral subregions in mammals, have not been identified. With regard to the nucleus sphericus, as it happens with the PMCo, it shows an interconnection with the contralateral PMCo/nucleus sphericus through the anterior commissure, connections with the rest of the vomeronasal system, the olfactory cortex (lateral cortex in reptiles) and olfactory amygdala, the hippocampus (dorsal cortex in reptiles), the ventral striatum (olfactostriatum in snakes) and they also share a minor projection to the preoptic hypothalamus (Lanuza and Halpern, 1997; Lanuza et al., 1997). The vomeronasal cortex through its interconnections with adjoining regions of the amygdala would allow the association of chemosensory cues (semiochemicals, pheromones and allomones) with other chemical and non-chemical stimuli, thus boosting the ability to establish emotional responses to previously neutral stimuli.

Altogether, these data suggest that the vomeronasal system is an evolutionary ancient vomeronasal system in tetrapod vertebrates. Moreover, vomeronasal information is processed in the amygdala in all of the different vertebrate groups, indicating that probably vomeronasal signals mediate behaviours with a strong emotional component. A vomeronasal cortex is absent in amphibians but was very probably already present in the amygdala of the common ancestor of reptiles and mammals and,

consequently, is a key element in the evolution of the emotional brain in terrestrial vertebrates.

12.5   LARGE-SCALE INTEGRATION IN THE VOMERONASAL AND OLFACTORY SYSTEMS

The emergence of a coherent behaviour relies on the coordination of distributed brain regions that are functionally and anatomically specialised and, thus, in the modification of the communication dynamics between brain areas. Brain networks provide a basic structure for the integration of dynamic activity. Depending upon the current behavioural requirements, neural signals are differently routed or assessed though the network by transient reciprocal dynamic connections (Varela et al., 2001). Within a network we can distinguish two types of connections: the reciprocal connections within the same cortical area (or areas at the same level of the network) and connections that link different levels of the network in different brain regions. Connections of the latter type have been referred to as feedforward (or as bottom-up) and feedback (or top-down). Traditionally, the sensory end is taken as the starting point of a brain network, so that perception is described as a feedforward hierarchy from "lower" to "higher" stages of processing (Varela et al., 2001). Meanwhile, the endogenous activity, tipically provided by the states of preparation or attention, is referred to as feedback activity. When the brain engages in specific functions, such as processing sensory stimuli, the dynamics of the involved structures change and particular oscillation frequencies become dominant (Buzsáki et al., 2013). This means that the response of brain networks to different stimuli is encoded by changes in the oscillatory activity, and thus the recorded signals fluctuate at various frequencies, with dominant frequency components shifting according to behaviour (Salinas and Sejnowski, 2001). However, to describe the communication mechanisms of a network, as relevant as the individual activity of its components, is the dynamic nature of the links between them, since their interactions are the key for integration (Varela et al., 2001). The effective communication between two neuronal groups is carried out by the pattern of coherence (or synchrony) among neuronal groups. The term synchrony is applied when two signals have a common dominant oscillations, reflected by correlated amplitudes and/or frequency distribution, or with a common temporal structure reflected by the coincident phases for both oscillation patterns. The rhythmicity provided by the phase of the oscillation allows the communication through temporal windows, whose input and output are open at the same times (Fries, 2005). This could allow a network

to respond selectively to a task-relevant "target" signal while ignoring other intrinsic activity (Varela et al., 2001; Akam and Kullmann, 2012; Buzsáki et al., 2013).

Rhythms are a ubiquitous phenomenon in nervous systems, as neuronal groups have the intrinsic property to oscillate. Several rhythms can temporally coexist in the same or different structures and interact with each other. Within the same neuronal network frequency bands are typically associated with different brain states (Buzsáki et al., 2013). Still, the problem is that linking oscillations to behaviour has been difficult. To study the relationships between specific local field potential rhythms and behaviour or sensory processing, we first must understand that neural communication mechanisms are confined to the structure of the anatomical connections. However, behavioural (and cognitive) functions require flexibility in the routing of signals (Fries, 2005), as the same brain regions participate in divergent functions. Utterly understanding a neural circuit requires comprehension at many levels: the anatomical connections of the different nodes, the intrinsic oscillatory population activity provided by the network and the oscillatory fluctuation engaged by the processing of a sensory stimulus. Altogether, these aspects facilitate the understanding of the relationship between such oscillations and their behavioural correlates.

The olfactory neural circuits have unique characteristics that make the translation between odours or pheromones and the behavioural output an arduous task. Many of those have been previously mentioned, but the most relevant features will be briefly summarised. First, the most remarkable trait is the presence of two olfactory systems, the main olfactory system and the accessory or vomeronasal system. Second, the internalisation of stimuli so they reach the sensory organ depends on active mechanisms known as sniffing (main olfactory system) and vomeronasal pumping (accessory olfactory system). Third, the main olfactory epithelium can detect many tens of thousands of different odours with a relatively reduced number of receptors (Mombaerts, 2004), while vomeronasal neurons respond in an ultrasensitive extremely specific way (Leinders-Zufall et al., 2000) to the presence in the environment of a limited number (few hundreds) of chemical stimuli (Mombaerts, 2004). Fourth, the behavioural responses mediated by these systems are as variant as appetitive (sexual pheromones), defensive (predators), aggressive/ defensive (chemical signals from competitors) or aversive (ill-related signals). In fact, female mice change their behavioural response to male chemosignals (such as darcin), from attraction and mating facilitation (Roberts et al., 2010) to aggression after parturition (Martín-Sánchez et al., 2015).

Depending on the perceived stimulus and the internal state of the animal, different behavioural responses are issued. But how do stimuli modify the communication structure within the olfactory network? In general terms, sampling behaviour is a primary factor in shaping how the brain represents and processes olfactory inputs (Wachowiak, 2011). The odour sampling is mediated by an increase in the respiration rate to active odour incorporation, a mechanism known as sniffing (Youngentob et al., 1987; Kepecs et al., 2006; Verhagen et al., 2007; Wesson et al., 2008), that imposes a temporal structure that shapes how odour information is conveyed from the olfactory receptor neurons to the MOB. Delta waves are the predominant respiratory rhythm in absence of stimuli (Welker, 1964; Kepecs et al., 2007), while sniffing in rodents is usually at frequencies above 4 Hz (Wachowiak, 2011). Our results clearly show, in the MOB, this increase from < 2 Hz to $4 - 6$ Hz in the predominant frequencies when a neutral stimulus is preseted and slighty higher (7 Hz in our recordings) when exposed to conspecific-derived stimulus. Furthermore, within these exploration periods we observed very rhythmic epochs that last $2 - 4$ s, which would correspond to sniffing periods. Our results also show a similar increase in the predominat frequency in the AOB, during the exposure to a neutral stimulus (up to 6 Hz) or conspecific-derived stimuli (around 7 Hz), the latter values are similar to those observed in previous reports (Binns and Brennan, 2005; Tendler and Wagner, 2015). Nevertheless, the olfactory bulbs seem to lack the ability to distinguish among conspecific-derived stimuli, a result that is consistent whith previous reports showing that single units in the AOB respond to more than one type of stimulus (Ben-Shaul et al., 2010; Bergan et al., 2014). Therefore, a question arises about the activity observed under neutral stimulus exploration in the AOB, since the exposure to clean bedding does not induce Fos responses in the vomeronasal organ and only little response in the AOB (Halem et al., 1999). An interesting hypothesis is that neutral stimuli regulate the permissiveness of the olfactory network, providing a state of preparation, expectation and attention, which facilitates the communication dynamics in response to vomeronasal stimuli.

Moreover, the phase analysis of the MOB and the AOB shows high synchrony even when only pure olfactory stimuli are present (Figure 43). This simultaneous activity of the bulbs is consistent with previous reports (Tendler and Wagner, 2015) and suggests a coupled internalisation of olfactory and vomeronasal stimuli by sniffing and vomeronasal pumping, respectively. The results reported by Meredith (1994) show that the typical response when approaching an opposite-sex intruder was sniffing
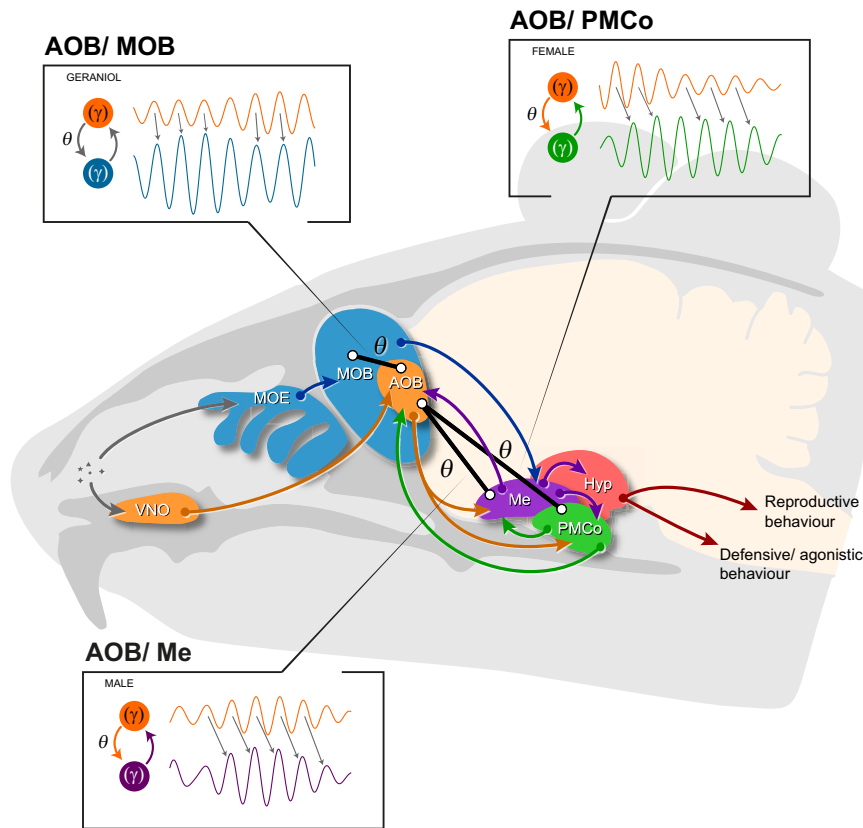
Figure 43: **Large-scale integration in the vomeronasal and olfactory systems**.
Basic structure of the studied network that allows the integration
of dynamic activity regulating the emergence of an appropriate be-
haviour. Theta rhythms (θ, thick black lines) show effective neur-
onal communication and coordinate specific gamma rhythms (γ)
related to the local processing.

the air and, in the vomeronasal organ, the oscillations increased
in frequency. Also, Slotnick et al. (2010) describe that in the ab-
sence of MOB input, trained mice were anosmic in olfactometric
tests using pheromonal stimuli and did not respond appropri-
ately to either species-specific social cues or pheromonal stimuli.
These results, together with our phase analysis result, indicate
that olfactory stimuli probably trigger the activation of vomero-
nasal pumping mechanisms. Although it is possible that mice en-
gage in spontaneous vomeronasal sampling (Meredith, 1994), in-
dependent of sniffing activity, that would increase in presence of
pheromones or pheromone-associated odours, this does not ex-
plain the increased activity in the AOB relative to neutral stimuli.
Nevertheless, this activity may be explained by the presence of a
small number of cells isolated in the vomeronasal organ that re-
spond to volatile compounds (Sam et al., 2001) and may express
odorant receptors (Lévai et al., 2006). In relation to this, garter
snakes do not engage in tongue-flick odour sampling (equival-

ent to vomeronasal pumping) in the presence of prey odours in the absence of input from the main olfactory epithelium (Zuri and Halpern, 2003). Furthermore, recently Vargas-Barroso et al. (2016) reported direct evidence for the existence of a physiological link between the anterior AOB and the dorsal MOB, providing an anatomical substrate for the functional overlap observed between both olfactory systems. Altogether, this rises the hypothesis that the initiation of vomeronasal sampling may be mostly dependent on the detection of odours by the main olfactory epithelium and that this be a general feature of vertebrates with dual olfactory systems.

The increase in the dominant theta rhythmicity is also present in the Me (Tendler and Wagner, 2015) and PMCo, thus suggesting that the temporal frame provided by the sniffing is being transmited along the olfactory circuit. The transmission to the Me is mainly direct through the projections from both the MOB and the AOB (Scalia and Winans, 1975; Pro-Sistiaga et al., 2007; Kang et al., 2009; Cádiz-Moretti et al., 2013); while the PMCo receives direct projection from the AOB (Winans and Scalia, 1970; Scalia and Winans, 1975; Von Campenhausen and Mori, 2000) and indirect ones from the MOB, mainly through its connections with the olfactory cortex and the olfactory amygdala (Canteras et al., 1992; Kevetter and Winans, 1981b). The amygdaloid nuclei perform specific processing of conspecific stimuli, as the Me shows a characteristic theta peak elicited by male-soiled bedding, while the PMCo has a distinctive peak driven by female-derived stimuli. A plausible interpretation is that the Me preferentially responds to opposite-sex derived stimuli (Bergan et al., 2014) and through its feedback projection to the AOB conveys information about opposite-sex odours and pheromones (Martel and Baum, 2009). As for the PMCo, it might be involved in the processing of vomeronasal signals derived from other females, thus playing a role in female aggressive behaviour. The analysis of the synchrony at specific theta peaks between the AOB and the amygdala strongly denotes an increase in the coherence between the oscillations in the sending group (AOB) and the receiving group (Me or PMCo), triggered by conspecific stimuli. This indicates an effective neuronal communication. Slow rhythms, such as theta waves, are robust for the establishment of long-distance synchrony (Varela et al., 2001), which facilitates grouping events and places together in time (Figure 43). Therefore, it coordinates the participating neuronal assemblies so they can be bound together in an appropiate temporal and spatial context (Buzsáki, 2005; Fries, 2005).

The nature of the interaction among oscillations is hierarchical, thus slow rhythms can coordinate specific neural assemblies by

temporarily binding higher frequency oscillations (Varela et al., 2001; Buzsáki et al., 2013). These fast oscillations, such as gamma rhythms, are more related to integration in local-circuits (Varela et al., 2001; Buzsáki and Wang, 2012) and are modulated by slow oscillations (Canolty et al., 2006; Buzsáki and Wang, 2012). Paying attention to local processing, gamma activity is intrinsic to the MOB (Adrian, 1950; Bressler and Freeman, 1980) and odour-evoked gamma-oscillations are one of the best studied olfactory oscillations (Rojas-Líbano and Kay, 2008). Previous studies report that odour sampling induces depression of gamma oscillatory activity (Freeman and Schneider, 1982; Kay and Freeman, 1998; Martin et al., 2004); however, according to our results, this can be explained as a decrase in the relative power of the gamma band due to the high increase in the power of the theta band, as their power analysis was performed over a broad range of frequencies (e.g. $2 - 100$ Hz, Martin et al. 2004). A specific analysis of the gamma oscillations does reflect a different odour-induced demeanour in separate gamma sub-bands. In the hippocampus, three distinct gamma bands have been identified by means of wavelet and cross-frequency analysis (Tort et al., 2010; Belluscio et al., 2012): low gamma ($30 - 50$ Hz), high gamma (or mid-frequency gamma, $50 - 90$ Hz) and fast gamma (or epsilon, $90 - 140$ Hz). The analysis of the high and fast gamma bands in the MOB reveals an increase in the high gamma ($60 - 80$ Hz), that has been reported during fine odour discrimination tasks (Beshel et al., 2007). This high gamma oscillation thus seems related to the odour processing. On the other hand, the analysis of the gamma band reveals distinctive characteristics in the vomeronasal system. The presentation of a stimuli modifies the gamma microstructure in the AOB, as in the amygdaloid nuclei, distinguished by a particular increase in the power of the fast gamma band ($90 - 120$ Hz), which may be related to the vomeronasal processing. Furthermore, the Me shows a distinctive demeanour, as the relative power of the gamma band conceals changes in other oscillations, that probably reflects its complex circuitry with three highly interconnected subdivisions and the connections with the behavioural hypothalamic centres. This high gamma activity reflects vast local processing in this structure, which together with its singular microcircuitry and its subpallial origin propose the medial amygdala as the striato-pallidal output station of the vomeronasal system (Cádiz-Moretti et al., 2016a). The prominent connectivity between neighbouring regions, as those shown by the dense intra-amygdaloid projections of the Me and PMCo, could be indicative of a rapid, efficient and local processing (Laughlin and Sejnowski, 2003) mediating the integration of the olfactory and vomeronasal information. Only

a small fraction of the computation that occurs locally can be transmitted to distant areas, but this may be enough to coordinate the processing along the olfactory network. The feedforward communication between the sensory structures and the amygdala is most likely mediated by theta oscillations (Figure 43). In this regard we study the synchrony over different frequency bands (theta and gamma oscillations), whose crosstalk states the different dimensions of the integration process. The theta wave in the AOB modulates stimuli-specific gamma activity in all the recorded nuclei: in the MOB modulates high gamma oscillations, in the Me both high and fast gamma oscillations and fast gamma in the PMCo. Thus, as suggested by Ben-Shaul et al. (2010), the AOB processing might maximise the efficiency of information transfer to other nuclei (amygdaloid structures), regardless of their ecological significance, where it is refined before appropiate behaviours emerge.

Chemosensory processing requires coordination between the olfactory and vomeronasal systems. The sensory input has to be accurately distinguished from the intrinsic activity, and other not-so-relevant inputs, and integrated to elicit suitable behaviours (Figure 43). The different nodes of the olfactory network examined in this work show complementary roles in the context of environmental perception. The vomeronasal system mediates identifying (knowing the identity of) a small number of biologically relevant molecules, whereas the olfactory system recognises mixtures of odours with which the animal has had previous experience (thus the term re-cognising) (Martínez-García et al., 2009). Specific gamma oscillations might be associated with the different roles of these two systems and communication through theta frequencies allows the individual to properly integrate the information collected by them. This is easily examplified in a territorial context, the individual enters an unfamiliar place where volatiles (MOB) will expose the presence of a conspecific, while the pheromones (AOB) will mediate identification of its gender. These chemosensory cues will then be relayed to the amygdala, where the integrated processing (PMCo and Me) takes place. The behavioural response (mediated by the Me) will depend on the nature of the intruder. An opposite-sex conspecific most likely will trigger socio-sexual behaviours (through the MePD), while same-sex conspecific will trigger aggresive/ defensive behaviours (through the MeA/ MePV).

In summary, all structures mediating appropiated behavioural responses to chemical cues, from the olfactory bulbs to the hypothalamic structures, are wired together. The different nodes show prominent coupled activity and effective communication, allowing the system to work as a distributed processor for the

integration of chemosensory cues. Overall, the present results expose the different levels of convergence of the olfactory and vomeronasal information, which promote a coordinated and integrated representation of the chemosensory environment.

13

CONCLUSIONS

The olfactory network provides the basic structure for the co-ordinated modification of the neural signals in response to both the perceived chemical stimuli and the behavioural requirements. The following conclusions describe how this coordination is accomplished.

I. The PMCo should be considered the vomeronasal primary cortex, based on its connections, its pallial origin and its cortical lamination; while the Me would be the striato-pallidal output station of the vomeronasal system, strongly connected to hypothalamic behavioural circuits and, although not as densely, with the reward system.

II. Depending on the perceived stimulus different oscillatory rhythms are issued. The predominant frequency in all the recorded areas shifts from delta to theta oscillations, even during the exposure to a neutral stimulus. However, neutral stimuli generally show lower theta peaks than conspecific-derived stimuli.

III. Communication between the AOB and the other nuclei is mediated by theta oscillations, as the AOB shows high phase synchrony with the MOB, Me and PMCo. Furthermore, the theta oscillation of the AOB modulates stimuli-specific gamma sub-bands in the olfactory network: in the MOB modulates high gamma oscillations (neutral stimuli), in the Me both high and fast gamma oscillations (male-derived stimuli), and fast gamma in the PMCo (female-derived stimuli). Finally, in the AOB itself induces both gamma oscillations in response to neutral stimuli and only fast gamma in response to male-derived stimuli. This fast gamma band ($90 - 120$ Hz) may be related to the vomeronasal processing, while the high gamma ($60 - 80$ Hz) band would be involved in the processing of olfactory stimuli.

IV. The high phase synchrony between the olfactory bulbs together with the remarkable similarity of their oscillatory

activity, even when only pure olfactory stimuli are present, suggest that the initiation of vomeronasal sampling and the olfactory sniffing are coupled, and probably the olfactory stimuli trigger the activation of vomeronasal pumping mechanisms.

V. The Me shows a distinctive high relative power of the gamma band, which reflects a vast local processing within its three highly interconnected subdivisions. This suggests that the Me coordinates the behavioural response to olfactory and vomeronasal cues.

VI. The strong connectivity of the Me with the other structures of the vomeronasal system, the dense intra-nucleus connections and interconnections with structures of the main olfactory system (especially from the MeA), suggests that the information from these systems is subjected to a complex intrinsic processing before being relayed to other structures.

VII. The behavioural responses mediated by the Me seem to be processed by different Me subdivisions. The MeA would relay chemosensory information either to the neural circuit for socio-sexual behaviour or to the neural circuit for defensive behaviour. The MePD would transfer the information from odours and pheromones to the neural circuit for reproductive behaviours (BSTMPM, MPO, VMHVL and PMV). The MeA and MePV are mainly connected to the defensive behaviour circuits as they project to the BSTMPI and the hypothalamic defensive circuit (AH, VMHDM and PMD). The MePV also projects to the BSTMPM and the BSTMA, and thus may be involved in other non-sexual behaviours, such as agonistic encounters with same sex conspecics or aversion to illness-derived social odours.

VIII. The PMCo coordinates the neural processing of vomeronasal cues, as it receives information from and projects back to each of the structures of the vomeronasal system, and it also shows significant interconnections with the principal components of the main olfactory system. These connections would allow the integration of olfactory and vomeronasal information.

IX. The PMCo indirectly affects behavioural responses, mainly through its porjections to the Me, but also by projecting to the hippocampal formation and the ventral striatum. The vomeronasal-hippocampus interaction would relay chemosensory information to the hippocampus and then contrib-

ute to the generation of the spatial map and to behavioural responses modulated by territory. The projections to the ventral striatum may constitute the anatomical pathway conveying information about the sexual pheromones to the reward system of the brain, involved in appetitive behaviours.

X. Although the olfactory bulbs seem to lack the ability to distinguish among conspecific-derived stimuli, the vomeronasal amygdala specifically responds to them. The Me shows a characteristic theta peak and fast gamma activity elicited by male-soiled bedding, thus suggesting that it preferentially responds to opposite-sex derived stimuli, what would be related to the role of this structure (especially the MePD) in reproductive responses. In contrast, the PMCo shows a characteristic theta peak and fast gamma oscillations in response to female-derived stimuli and might be involved in the processing of vomeronasal signals from other females, thus playing a role in female aggressive behaviour.

XI. The emergence of a coherent behaviour mediated by olfactory and vomeronasal cues relies on the coordination of several brain regions, from which we studied the MOB, AOB, Me and PMCo. The transient dynamic coherence between their connections are specifically driven by theta activity which modulates specific gamma sub-bands depending upon the perceived stimulus and the current behavioural requirements.

Part VI

RESUM EN VALENCIÀ

14

RESUM EN VALENCIÀ

La percepció de l'entorn és un procés actiu que requereix sistemes sensorials que detecten, recol·lecten i processen informació sobre un ambient en canvi continu. Aquesta detecció activa permet a l'animal mostrejar selectivament regions de l'espai a períodes de temps específics i aquest *input* ambiental dóna informació valuosa sobre les condicions externes en les que està vivint l'organisme, la qual cosa li permet generar respostes conductuals apropiades per a la seua supervivència.

En els rosegadors, com animals macrosmàtics, els estímuls olfactius tenen un paper fonamental en l'adquisició d'informació sobre conespecífics, possibles predadors o menjar proper. Com molts tetràpods (Ubeda-Bañón et al., 2011), tenen dos sistemes olfactius: el sistema olfactiu principal i l'acessori o vomeronasal. La informació olfactiva i vomeronasal és principalment processada per estructures anatòmicament separades, així i tot la informació d'ambdós sistemes ha de ser integrada per generar una imatge completa del senyals quimiosensorials presents a l'ambient i, per tant, generar respostes comportamentals adequades (Baum and Kelliher, 2009; Keller et al., 2009; Martínez-García et al., 2009). Entendre el funcionament d'aquests dos sistemes requereix una aproximació dual, ja que conéixer el patró de connexions físiques o transitòries no és suficient com per comprendre la forma en que donen lloc al comportament d'un animal. Encara que descobrir la connectivitat d'un nucli pot orientar el nostre raonament sobre la seua funció.

14.1 OBJECTIUS

L'objectiu principal d'aquesta tesi doctoral és ampliar el nostre coneixement de l'organització i funció dels sistemes olfactori i vomeronasal, i com la informació d'ambdós sistemes és integrada per permetre la generació d'un mapa complet dels senyals químics presents a l'ambient i la gereració de respostes comportamentals. Per això, primer aclarirem la connectivitat de les principals estructures amigdalines que reben projeccions dels bulbs olfactius principal i accessori. Entre elles ens centrem al

nucli medial de l'amígdala (Me), que rep projeccions considerables tant del bulb olfactiu principal (MOB) com de l'accessori (AOB; Scalia and Winans 1975; Pro-Sistiaga et al. 2007; Kang et al. 2009, 2011; Cádiz-Moretti et al. 2013), i al nucli posteromedial cortical (PMCo), que rep projeccions directes del AOB (Winans and Scalia, 1970; Scalia and Winans, 1975; Von Campenhausen and Mori, 2000). Després, intentarem entendre com aquests sistemes sensorials interactuen per assolir un comportament apropiat.

Aquest estudi s'ha desenvolupat emprant femelles de ratolí per diverses raons. Primer, els estudis comportamentals previs del nostre grup han estat centrats en l'atracció sexual que les femelles mostren front a feromones de mascle (Martínez-García et al., 2009). Segon, la majoria de les dades publicades en altres espècies (hàmsters i rates) han estat obtingudes en mascles, el que permetrà la comparació de les projeccions entre mascle i femella. Finalment, aquest treball està emmarcat en l'estudi del circuit neural que processa la informació vomeronasal en el cervell de femelles de ratolí (Cádiz-Moretti et al., 2013, 2016b).

Els objectius particulars són els següents:

1. Descripció de les connexions eferents de les diferents subdivisions del nucli medial de l'amígdala en ratolí.

   Donat que els ratolins són àmpliament emprats en estudis comportamentals, és d'interés obtindre dades anatòmiques en aquesta espècie. Les publicacions prèvies han estat realitzades en rates mascle (Canteras et al., 1995), hàmsters mascle (Gomez and Newman, 1992; Coolen and Wood, 1998; Maras and Petrulis, 2010a) o ratolins mascle (Usunoff et al., 2009), encara que aquest últim fa una descripció parcial de les projeccions centrades a la subdivisió posterodorsal del nucli medial. A més, hi ha diferències rellevants en el comportament reproductiu (Vale et al., 1973, 1974; Burns-Cusato et al., 2004; Dominguez-Salazar et al., 2004) i defensiu (Belzung et al., 2001; Yang et al., 2004) entre diferents soques de ratolí. Per tant, aquest estudi avaluarà les eferències de les diferents subdivisions de l'amígdala medial, fent a més una comparació del patró de connexions entre femelles de ratolí i els estudis previs en mascles i entre dos soques de ratolí diferents, a saber C57BL/6J i CD1.

2. Descripció de les connexions aferents i eferents del nucli posteromedial cortical de l'amígdala en ratolí.

   El PMCo, a més de rebre projeccions del AOB, també té una projecció *feedback* a la capa de les cèl·lules granulars

d'aquest nucli que modularia el processament de senyals vomeronasals (Fan and Luo, 2009; Martínez-Marcos and Halpern, 1999b). Aquest fet, junt a la seua organització en capes i el fet que entre els nuclis amb projecció directa des del AOB és l'únic amb origen palial, suggereixen la idea de que el PMCo deuria ser considerat el còrtex vomeronasal primari. Les seues connexions han estat estudiades de manera parcial en hàmsters mascle (Kevetter and Winans, 1981a), rates mascle (Canteras et al., 1992; Kemppainen et al., 2002) i ovella (Meurisse et al., 2009). Aquest estudi pretén, per tant, aportar una descripció comprensiva de les connexions aferents i eferents del nucli posteromedial cortical de l'amígdala en femelles de ratolí.

3. Avaluar les característiques de les oscil·lacions del sistemes olfactori i vomeronasal que permeten la integració d'ambdós tipus d'informació quimiosensorial.

Per això hem realitzat registres de l'activitat poblacional en el MOB, AOB, Me i PMCo, en ratolí despert mitjançant un paradigma d'exploració de diferents estímuls quimiosensorials. Aquestes substàncies inclouen dos estímuls neutres (borumballa neta i borumballa aromatitzada amb geraniol), detectats per sistema olfactiu principal, i tres estímuls complexes derivats de conspecífics (borumballa embrutada per mascles intactes, mascles castrats i femelles), que contenen senyals detectats pels dos sistemes. La borumballa embrutada per mascles conté feromones sexuals masculines atractives per les femelles (Martínez-Ricós et al., 2007), el que permetrà comparar l'activitat dels diferents nodes dels sistemes olfactius en el context de la comunicació sociosexual. A més, els llocs de registre triats permeten caracteritzar el patró oscil·latori del sistema vomeronasal i, alhora, avaluar si és diferent i independent del patró del sistema olfactiu principal. Aquesta descripció del processament de la informació olfactiva i vomeronasal facilitarà el enteniment de la integració d'aquests sistemes.

14.2 METODOLOGIA

14.2.1 *Animals*

Per la realització del experiments descrits anteriorment es va necessitar un total de 43 femelles de ratolí (*Mus musculus*) de les soques C57BL/J6 (Charles River, França) i CD-1 (Charles River o Janvier, França) amb edat superior a 2 mesos i pes entre 18.1 i 45.1 g. Els animals van estar allotjats en gàbies

Table 8: Nombre d'animals emprat en els diferents experiments.

Experiment	Soca	Nombre d'animals
Eferències de Me	C57BL/J6	9
	CD1	6
Connexions de PMCo	CD1	17
Activitat oscil·latòria	CD1	9

amb aigua i menjar disponibles *ad libitum*, en condicions de llum naturals o en un cicle llum: foscor de 12 h, a $21 - 23°C$ de temperatura. Els procediments experimentals per tots els estudis va ser aprovat pel Comitè d'Ètica i Benestar Animal de la Universitat de València i estan d'acord amb la directiva Europea per a la protecció d'animals d'ús científic del 24 de Novembre de 1986 (86/609/EEC) o la directiva actual (2010/63). Per al paradigma d'exploració d'estímuls quimiosensorials animals adults de la soca CD-1 van proveir la borumballa embrutada amb orina (serradura de fusta, Souralit S.L., ref. 3000, Espanya). El nombre específic d'exemplars emprat en cadascun dels experiments apareix a la taula 8.

14.2.2 *Procediments quirúrgics*

14.2.2.1 *Injecció de traçadors*

Per estudiar les projeccions sorgides de les diferents subdivisions del nucli medial de l'amígdala (anterior, posteroventral i posterodorsal) es van realitzar injeccions iontoforètiques de dos conjugats de dextranamines com a traçadors anterògrads: dextranamina conjugada amb biotina (BDA, 10000 MW; Invitrogen, EUA), diluïda al 5% en tampó fosfat (PB, 0.01 M, pH 8.0), i dextranamina conjugada amb tetrametilrodamina (RDA, fluoro-ruby, 10000 MW; Molecular Probes, EUA), diluïda al 5% en tampó fosfat (PB, 0.01 M, pH 7.6). Els traçadors van ser dipositats emprant micropipetes de vidre (amb un diàmetre intern a la punta de $10 - 50 \mu$m) mitjançant polsos de corrent positiva (7on/7off s, $3 - 5 \mu$A, $10 - 15$ min) utilitzant un generador de corrent (Midgard Precision Courrent Source, Stoelting, EUA). Per reduir les filtracions al llarg de rastre de la pipeta, es va deixar passar $2 - 5$ min des de la fi de la injecció fins a la retirada de la pipeta. A més, tant a l'entrada com a l'eixida de la micropipeta es va aplicar una corrent negativa continua (-0.8 μA) per evitar la difusió del traçador.

El procediment per estudiar les projeccions aferents i eferents del nucli posteromedial cortical de l'amigdala és semblant.

Com a traçador anterògrad s'ulititzà BDA (Molecular Probes) diluïda al 5% en PB salí (0.01 M, 0.9% NaCl, pH 7.6), mentre que com traçador retrògrad s'utilitzà FluoroGold (FG, metanosulfonat d'hidroxistilbamidina; Biotium, USA) diluït al 2% en solució salina (0.9% NaCl). El dipòsit dels traçadors es va realitzar també mitjançant injeccions inontoforètiques en les condicions següents: micropipetes ($20 - 40$ μm diàmetre intern), polsos de corrent positiva (7on/7off s, $3 - 5$ μA, $5 - 10$ min) amb un generador de corrent (Direlec, Spain) i corrent de retenció negativa (-0.9 μA).

14.2.2.2 *Cirurgia dels estudis de traçat de connexions*

Les cirurgies dels estudis de traçat de connexions són semblants, excepte per l'anestèsic utilitzat i algunes diferències menors. En general, una vegada els animals estaven profundament dormits rebien una injecció de butorfanol (5 mg/kg, subcutània; Fort Dodge Veterinaria, Espanya) com analgèsic. La profunditat de l'anestèsia es va supervisar abans de l'operació observant la disminució de la mobilitat, els reflexes palpebral i podal, la resposta a estímuls dolorosos i la freqüència i profunditat de la respiració; la supervisió durant la intervenció va consistir en controlar la freqüència i profunditat de la respiració, el parpelleig dels ulls i el moviment de les vibrisses. Pel manteniment de la temperatura corporal els animals es van possar sobre una manta tèrmica i per evitar la dessecació dels ulls es va aplicar gotes oculars (Siccafluid, Thea S.A Laboratories, Espanya). Després de fixar el cap de l'animal a l'aparell estereotàxic (Me: 963-A, David Kopf, EUA; PMCo: myNeurolab, Leica, Alemanya) es va realitzar una xicoteta incisió en la pell per observar la superfície cranial i després de alinear el crani es va realitzar un forat per damunt del Me o de PMCo. Al acabar la injecció del traçador el tall es va tancar amb Histoacryl (1050052; B.Braun, Alemanya).

En quant als anestèsics, 6 dels animals de l'estudi de connexions de Me van rebre injeccions intraperitoneals d'una solució 3:2 de quetamina (75 mg/kg; Merial laboratorios, Espanya) i medotomidina (1 mg/kg; Pfizer, Espanya), complementada amb atropina (0.04 mg/kg, intraperitoneal; Sigma, EUA) per reduir les secrecions bronquials i salivals i la depressió cardiorespiratòria; els altres 11 animals van ser anestesiats per inhalació d'isoflurà (1.5%) en oxigen (0.9 L/min; MSS Isoflurane Vaporizer, Medical Supplies and Services Int'l Ltd, Regne Unit) utilitzant una màscara d'anestèsia. Després de la cirurgia els animals anestesiats amb quetamina: medetomidina van rebre injeccions d'atipamezol (1 ml/kg, subcutànea; Pfizer) per revertir els efectes de la medetomidina. Els animals de l'estudi de connexions de PMCo van rebre injeccions de pentobarbital sòdic (60

mg/kg, intraperitoneal; Sigma, EUA), complementada amb atropina.

Els llocs d'injecció van estar determinats seguint el atlas del cervell de ratolí de Paxinos and Franklin (2004) realitzat en la soca C57BL/J6. Les coordenades relatives a Bregma emprades apareixen a la Taula 1 (Me) i a la taula 3 (PMCo), quan el ratolí pertanyia a la soca CD-1 van ser adaptades.

14.2.2.3   *Implantació d'elèctrodes de l'estudi de les oscil·lacions*

La implantació d'elèctrodes es va realitzar amb els animals anestesiats mitjançant una injecció intraperitoneal de quetamina: medetomidina (75 mg/kg: 1 mg/kg, respectivament), complementada amb atropina (0.05 mg/kg) i, quan el animal estava profundament dormit, una injecció d'anestèsia local (lidocaina, 0.1 ml; B. Braun, Alemanya) per reduir la sensibilitat cranial. Els animals dormits van ser traslladats al quadre estereotàxic (SR-6R; Narishige, Japó). Després de fer una incisió en la línia mitja del cap mostrant el crani es van fer 7 forats (4 elèctrodes, 1 referència, 2 caragols de subjecció) adaptant les coordenades de l'atlas de Paxinos and Franklin (2004) a ratolins CD-1 (Figura 23 B). Els elèctrodes van se implantats, com es mostra a la Taula 5 i la Figura 23 A, al AOB (amb un angle de 45 rostral a la vertical), MOB, Me i PMCo. Els registres es van referenciar front a un elèctrode indiferent col·locat sobre el cerebel. Després de la cirurgia els animals van rebre una injecció d'atipamezol, per revertir els efectes de l'anestèsia, i una altra de butorfanol, com analgèsic.

El registre de l'activitat de camp (local field potential; LFP) va ser captat mitjançant macroelèctrodes d'acer inoxidable recoberts amb poliimida, amb un diàmetre extern de 0.125 mm (E363/6/SPC; PlasticsOne, EUA). Els elèctrodes es fixaren a la superfície cranial amb ciment dental polimèric (Rapid Repair, Dentsply International, Regne Unit). Els 4 elèctrodes de registre i l'elèctrode de referència van ser connectats a un pedestal de 6 canals (PlasticsOne), que es va fixar al cap amb més ciment dental.

Durant la recuperació i al llarg de l'experiment els animals van ser allotjats en gàbies cilíndriques de plàstic transparent (30 cm diàmetre), excepte durant els períodes de test. Una vegada els animals s'havien recuperat completament (3 dies), els ratolins van ser entrenats per poder suportar el pes de cable de registre.

14.2.3   *Registres in vivo en l'estudi de les oscil·lacions*

Cada animal va ser exposat de manera seqüencial a diferents estímuls, uns de caràcter neutre (borumballa neta i borumballa aro-

matitzada amb geraniol) i altres derivats de conspecífics (borumballa embrutada per mascles castrats, per femelles o per mascles intactes).

Els registres es van realitzar en caixes opaques de metacrilat (42.5 × 26.5 × 18 cm), on l'animal es pot moure lliurement. Una setmana després de la cirurgia, els animals van ser habituats a l'experimentador i a les condicions del test durant 4 dies consecutius, en els quals l'estímul presentat va ser borumballa neta. Durant el test, es van gravar 20 min abans de la presentació de cada estímul. Per la presentació de l'estímul el ratolí va ser traslladat durant 5 min a una caixa idèntica amb 15 ml de l'estímul en una placa de vidre (6 cm diàmetre). Al finalitzar aquest període, el animal va ser traslladat de nou a la caixa control on va reposar durant 20 min abans de presentar el següent estímul. La successió de períodes controls i períodes de presentació d'estímul va repetir-se fins que els 5 estímuls van ser presentats. A més els test van ser gravats en vídeo per avaluar el comportament de l'animal posteriorment.

Per realitzar l'adquisició del senyal, l'activitat de camp va ser amplificada i filtrada *on-line* entre 0.3 i 300 Hz (p55, Grass Technologies; Ampli 4G21, CIBERTEC, Espanya). Posteriorment el senyal va ser digitalitzat (Power 1401; Cambridge Electronic Design, Regne Unit) per l'anàlisi *off-line* (400 Hz freqüència de mostreig). Durant el test el senyal va ser visualitzat utilitzant el *software* Spike 2 (Cambridge Electronics Design).

Posteriorment, el comportament de l'animal va ser avaluat analitzant els videos gravats. Per açò, registrarem el temps que l'animal s'aproximava a la placa de vidre i investigava cada estímul, amb aquestes dades es va calcular el temps que passava explorant cada estímul. Durant el comportament d'exploració, de vegades l'activitat es tornava molt rítmica i concentrada en la banda theta. Per caracteritzar aquesta osciľlació vam tornar a revisar el comportament de l'animal en el vídeo i el senyal per definir amb major precisió dels períodes de temps definits per a l'anàlisi.

14.2.4 *Histologia*

Per els experiments de traçat, entre sis a huit dies després de la cirurgia, els animals van ser anestesiats amb pentobarbital sòdic (90 mg/kg, intraperitoneal; Sigma). Quan estaven profundament dormits van ser perfosos amb 20 ml de solució salina seguida de 60 ml de paraformaldehid al 4% diluït en PB (0.1 M, pH 7.6). Després els cervells van ser postfixats durant 4 h en el mateix fixador i crioprotegits amb sacarosa al 30% en PB i es deixaren en nevera a 4°C fins que s'enfonsaren. Posteriorment, utilitzant un

micròtom de congelació vam obtindre seccions frontals (40 μm) de l'encèfal i, en alguns animals, els bulbs es van tallar a 30 μm. En el cas de l'experiment electrofisiològic, aquest procediment es va realitzar a la fi del test.

El mètode de detecció del traçador depén del taçador emprat. La detecció de BDA segueix el següent protocol: primer s'inactiva la peroxidasa endògena amb un 1% d'H_2O_2 amb tampó Tris salí (TBS, 0.05 M, pH 7.6), després les seccions van ser incubades amb un kit de detecció d'ABC (Vectastain ABC elite kit, Vector Labs, EUA) i la presència d'aquesta peroxidasa es va revelar amb diaminobencidina i H_2O_2. En la majoría dels casos es va afegir sulfat amònic de níquel per fer més fosc el precipitat.

Per la detecció inmunohistoquímica de RDA, després de la inhibició de la peroxidasa endògena, les seccions van ser incubades amb un anticós específic front a la tetrametilrodamina fet en conill (Molecular Probes, Cat. #A-6397) diluït 1:4000 in TBS-Tx TBS-Tx (0.1 M, 0.3% Triton X-100), seguit pel protocol estàndard de peroxidasa-antiperoxidasa (PAP; cabra anti-conill IgG, 1:100, Nordic Immunological Laboratories, Països Baixos; rabbit PAP, 1:800, Nordic Immunological Labs). Posteriorment es revelà la activitat peroxidasa con ja s'ha descrit, però sense afegir níquel.

El marcatge de FG va ser primer visualitzat al microscopi de fluorescència, encara que per l'anàlisi complet de la distribució del marcatge es va realitzar una detecció inmunohitoquímica. Després de la inactivació de la peroxidasa endògena, les seccions van ser incubades durant una nit amb un anticós anti-FG fet en conill (Chemicon, Billerica, EUA; cat. # AB153) diluït 1:5000 en TBS-Tx, seguit d'un anticòs secundari cabra anti-conill biotinilat (Vector Laboratories) diluït 1:200 en el mateix tampó. La detecció es va fer pel mètode descrit per la BDA sense níquel.

Les seccions es van muntar en portes gelatinitzats, deshidratats en un gradient d'alcohols i xilè i, per últim, cobertes amb Entellan (Merck, Alemanya). A les preparacions que durant la detecció van ser revelades amb níquel se'ls va realitzar una tinció de contrast (Nissl) per facilitar la identificació de les estructures neurals. Aquesta tinció és l'únic tractament que reberen les preparacions de l'experiment d'electrofisiologia per facilitar la visualització dels llocs on estaven els elèctrodes.

14.2.5 *Adquisició i processament d'imatges*

Les seccions van ser observades amb microscopi òptic (Olympus CX41RF-5) o de fluorescència (Leitz DMRB) i fotografiades amb una càmera digital (Olympus XC50 o Leica DC 300FX, respectivament). Les imatges van ser importades a l'Adobe Pho-

toshop (Adobe Systems, EUA), on es va ajustar el contrast i la lluentor, sense cap filtrat o manipulació addicional. Les composicions finals es van fer amb l'Adobe Photoshop i el disseny dels dibuixos del marcatge de projeccions amb Adobe Illustrator (Adobe Systems).

14.2.6 *Anàlisi de dades*

Els senyals en cru van ser importats al *software* MATLAB (The MathWorks, EUA) per l'anàlisi *off-line* utilitzant *scripts* propis.

El primer anàlisi realitzat dels LFP va ser la transformada ràpida de Fourier, que revela la distribució de potència en el domini de la freqüència. La estimació de l'espectre de potència es va realitzar pel mètode de Welch (finestres de Hanning de 4 s amb un solapament del 50%, amb una resolució de 1.9 Hz i un valor *nfft* de 2048). Per l'anàlisi espectral es van definir les següents bandes de freqüència: delta ($0.5 - 4$ Hz), theta ($4 - 12$ Hz), beta ($12 - 30$ Hz), gamma baix ($30 - 50$ Hz), gamma alt ($50 - 100$ Hz) i gamma ràpid (> 100 Hz).

14.2.6.1 *Anàlisi wavelet*

La transformada *wavelet* és particularment útil per l'anàlisi de senyals neurals, per la seua habilitat d'examinar el senyal simultàneament en els dominis del temps i la freqüècia. Per revelar els canvis en el temps de l'activitat oscil·latòria de l'LFP es van utilitzar les rutines *wavelet* de MATLAB proporcionades per Torrence and Compo (1998). En el nostre cas, per establir les relacions temporals entre senyals neurals obtinguts en nuclis diferents hem de separar les parts real (amplitud) i imaginària (fase), pel que hem utilitzat una *wavelet* complexa com la *wavelet* de Morlet. Les funcions concretes estan detallades a l'apartat de material i mètodes de la tercera part 9.

14.2.6.2 *Mesures de sincronització*

Sincronització de fases

Per la detecció de sincronia en un rang concret de freqüències entre dos senyals vam utilitzar els mètodes proposats per Lachaux et al. (1999). El procediment calcula el grau de acoblament de fase entre els components dels senyals x_t i y_t a freqüència f mitjançant la relació de fase entre els dos senyals, per al que es calcula la diferència de fase instantània entre ells. La sincronització de fases es delimita entre $y = 1$ per una sincronització perfecta, p. e. quan la diferència de fase instantànea és constant, i $y = 0$ quan no hi ha sincronia.

Acoblament fase-amplitud

El acoblament entre diferents freqüències d'un senyal va ser avaluat mitjançant el índex de modulació (MI), proposat per Tort et al. (2010). El MI és una mesura que indica el grau d'acoblament de l'amplitud d'una ona ràpida al cicle (o fase) d'una més lenta. En cas de que la fase-amplitud dels senyals filtrats estiguen acoblades, la distribució de les amplituds de la ona ràpida no serà uniforme al llarg de la fase de la ona lenta, el que es pot testar estadísticament.

14.2.6.3   *Autocorrelació*

El anàlisi de l'autocorrelació es realitzà per buscar patrons repetitius, com la ritmicitat d'un senyal. Breument, és la correlació d'un senyal amb una còpia desplaçada del mateix senyal en funció del desplaçament. Així, la ritmicitat de l'LFP s'observarà com una alternança de pics i valls en l'autocorrelograma. El coeficient té valors entre $+1$ i -1, que indicarien la perfecta correlació o l'absència de correlació entre els dos vectors, respectivament.

14.2.7   *Anàlisi estadístics*

Els anàlisi estadístics es van realitzar amb el SPSS Statistics v20 (IBM, EUA). Les comparacions estadístiques es van fer utilitzant test paramètrics o no paramètrics segons fóra necessari. Primer es va comprovar si les dades complien les condicions de normalitat (test de Kolmogorov-Smirnov; $p < 0.05$ per rebutjar) i homoscedasticitat (test de Levene; $p < 0.05$ per rebutjar). Per l'anàlisi del comportament exploratori les dades van ser transformades logarítmicament ($\log[X]$) i s'analitzaren amb un test ANOVA (estadístic F). Com a test no paramètric s'utilitzà el test de Kruskal-Wallis (estadístic K) per la comparació de mostres independents amb comparacions per parelles de ser necessari. Per la comparació de dos mostres independents s'utilitzà el test de Mann-Whitney test (estadístic U) i per la comparació de mostres relacionades el test de Wilcoxon (estadístic W). El nivell mínim de significació en tots els test és de 0.05.

14.3   DISCUSSIÓ GENERAL

Els rosegadors presenten dos sistemes olfactius, el sistema olfactiu principal (encarregat de la detecció de substàncies volàtils Buck 1996; Gutiérrez-Castellanos et al. 2010) i el sistema accessori o vomeronasal (que detecta substàncies no volàtils amb rellevància biològica Gutiérrez-Castellanos et al. 2010; Chamero et al. 2012). En el sistema olfactiu principal les olors arriben a l'epiteli olfactiu, que projecta al MOB, el qual connecta fona-

mentalment amb el còrtex olfactiu i nuclis de l'amígdala cortical (Martínez-Marcos, 2009). L'òrgan sensorial del sistema vomeronasal és l'òrgan vomeronasal i envia les seues projeccions al AOB, que projecta principalment als nuclis medial i posteromedial cortical de l'amígdala i el nucli llit de la *stria terminalis* (BST; Martínez-Marcos 2009). Si bé anatòmicament la informació olfactiva i vomeronasal és principalment processada en estructures separades, hi ha un cert grau de convergència especialment en nuclis amigdalins; entre ells destaca el Me, que rep denses projeccions d'ambdós bulbs (Scalia and Winans, 1975; Pro-Sistiaga et al., 2007; Kang et al., 2009, 2011; Cádiz-Moretti et al., 2013). D'altra banda, entre les estructures vomeronasals secundàries, el PMCo, a més de rebre projeccions directes des del AOB (Winans and Scalia, 1970; Scalia and Winans, 1975; Von Campenhausen and Mori, 2000), presenta característiques que apunten a podria ser considerat com el còrtex vomeronasal primari. La integració de la informació dels sistemes olfactius és necessària per la generació d'una imatge completa dels senyals químics presents a l'ambient, que permetrà la generació de respostes comportamentals adequades (Baum and Kelliher, 2009; Keller et al., 2009; Martínez-García et al., 2009). No obstant, no hi ha consens sobre com es produeix aquesta interacció olfactiva-vomeronasal.

Per tant, una comprensió més profunda de l'organització i funció dels sistemes olfactiu i vomeronasal ens permetrà entendre com es produeix la integració de la informació d'aquests sistemes i com açò condueix a desenvolupar comportaments apropiats. En una primera part, s'analitzarà les connexions dels principals nuclis amigdalíns involucrats en el processament de la informació vomeronasal: els nuclis medial i posteromedial cortical. A més, per entendre el funcionament d'aquesta xarxa neural, és necessari esclarir l'activitat neural poblacional d'ambdós sistemes olfactius.

14.3.1 *El Me coordina la resposta comportamental a senyals olfactòris i vomeronasals*

Les projeccions aferents de les tres subdivisions del Me mostrades pels nostres resultats apareixen resumides a la Figura 11. El patró de connexions observat en femelles de ratolí és similar entre soques i també és semblant a l'observat en mascles de rata i hàmster, el que suggereix que les diferències en el comportament reproductiu (Vale et al., 1973, 1974; Burns-Cusato et al., 2004; Dominguez-Salazar et al., 2004) i defensiu (Belzung et al., 2001; Yang et al., 2004) entre soques i entre espècies no pot ser atribuït a diferències en el patró d'eferències originades des

del Me. Així i tot, hi ha dos excepcions relatives a les projeccions de la divisió posteroventral del Me (MePV). Primer, hem observat una projecció densa a la divisió medial posteromedial del BST (BSTMPM) i moderada a la divisió medial posterointermèdia del BST (BSTMPI), encara que en rates s'observa el patró contrari (Canteras et al., 1995). Segon, el MePV dóna als nostres resultats projeccions més lleugeres a l'hipotàlem que les descrites en mascles de rata (Canteras et al., 1995), especialment les de la regió anterior. Per saber si aquestes discrepàncies són degudes a diferències interspecífiques o a la presència d'un cert grau de dimorfisme sexual serà necessària més investigació.

La important connectivitat del Me amb les altres estructures que reben projeccions del AOB i les denses connexions intranuclears, suggereixen que la informació detectada pel sistema vomeronasal es sotmesa a un processament intrínsec complex abans de ser transmesa a altres estructures. A més, el Me (especialment la seua part anterior; MeA) té connexions importants amb nuclis del sistema olfactiu principal com l'amígdala olfactòria o el còrtex piriforme. Açò estableix les vies anatòmiques per a una àmplia integració de la informació olfactiva i vomeronasal, el que recolza el paper complementari que representen aquests dos sistemes (Baum and Kelliher, 2009; Martínez-García et al., 2009). La necessitat d'un processament complex de la informació vomeronasal abans de ser transmesa està relacionada tant amb la complexitat dels estímuls (amb components volàtils i no volàtils, Zufall and Leinders-Zufall 2007) com a la complexitat dels comportaments mediats per aquests estímuls. A més de comportaments reproductius (Powers and Winans, 1975), també detecta senyals de conspecífics del mateix sexe que poden induir comportaments d'agressió (Clancy et al., 1984; Chamero et al., 2007), senyals de depredadors que indueixen comportaments defensius (Papes et al., 2010; Isogai et al., 2011) o molècules relacionades amb l'estat de salut de l'individu (Rivière et al., 2009). Els circuits neurals activats en resposta a cadascun d'aquests estímuls ha de ser diferent.

Les subdivisions anterior i posteroventral projecten majoritàriament a estructures del circuit neural que media les respostes defensives front a depredadors, que inclou el BSTMPI i els nuclis hipotalàmics: anterior, la divisió dorsomedial del nucli ventromedial i el premamil·lar dorsal (Canteras, 2002). Part del circuit hipotalàmic defensiu també podria estar implicat en comportaments agonístics, com l'agressió front a conespecífics intrusos del mateix sexe (Motta et al., 2009) o l'evitació de conspecífics parasitats (Arakawa et al., 2010). A més, les projeccions des del Me a l'amígdala central i al complex basolateral suggereixen que, a més d'estar implicat en respostes defensives front a depre-

dadors, el Me modularia comportaments apetitius i aversius mediats per estímuls olfactius i vomeronasals a través de nucli central de l'amígdala i en l'aprenentatge a la por (en el paradigma de por condicionada) mediat pel complex basolateral. No obstant, es necessita més inverstigació per saber si les diferents respostes comportamentals es deuen a subsistemes diferents dins del circuit defensiu. En aquest context, les projeccions del MePV sobre nuclis del sistema reproductiu (com el premamil·lar ventral de l'hipotàlem) poden interpretar-se com una via per inhibir comportaments reproductius en presència de depredadors o conpecífics parasitats.

El Me està implicat en comportaments apetitius probablement degut a les propietats reforçants de les feromones sexuals (Moncho-Bogani et al., 2002, 2005), mediades per les projeccions directes (especialment des de MeA) a les principals estructures del circuit del reforç: l'àrea ventral tegmental, el nucli accumbens i el tubercle olfactiu (i els illots de Calleja); i les projeccions indirectes a través de l'amígdala basolateral. Les feromones masculines són atractives per les femelles de ratolí i poden utilitzar-se com a estímul incondicionat per induir aprenentatge (Moncho-Bogani et al., 2002; Agustín-Pavón et al., 2007; Martínez-Ricós et al., 2007; Ramm et al., 2008; Roberts et al., 2010). Per tant les projeccions del Me al sistema de reforç poden estar implicades en el processament del valor hedònic de les feromones sexuals. Encara que el grau de participació del Me en els aspectes reforçants de les feromones (o d'altres senyals amb valor hedònic) es desconeix.

D'altra banda, la resposta a olors i feromones en el context del comportament reproductiu està fonamentalment mediat per la subdivisió posterodorsal del Me (MePD), que projecta principalment a nuclis del circuit reproductiu, el BSTMPM i els nuclis hipotalàmics: preòptic medial, la divisió ventrolateral del nucli ventromedial (VMHVL) i el premamil·lar ventral. Hi ha nombroses evidències experimentals a favor d'aquesta interpretació (veure la revisió de Swann et al. 2009), però hem d'assenyalar que parts d'aquest circuit podrien estar implicades en aspectes no sexuals del comportament reproductiu, com l'agressió maternal (Hasen and Gammie, 2006). De fet, un estudi mostra la presència dins del VMHVL de ratolins mascle d'una subpoblació neuronal que estaria implicada en la lluita front a mascles intrusos i l'aparellament (Lin et al., 2011). Açò implicaria que els sistemes que medien les respostes reproductives i agressives no estan completament segregats.

En resum, el Me faria de filtre de la informació rebuda des del AOB i el MOB abans de transferir-la a altres nuclis. La informació olfactòria requereix un processament complex, donat

l'espectre de comportaments en el que està implicada, i el patró d'eferències del Me reflecteix aquesta complexitat. A més de les denses connexions intra-amigdalines, les principals eferències del Me són el BST i l'hipotàlem, el que indica que té un paper important en el control dels circuits neurals activats en resposta a estímuls vomeronasals. La subdivisió anterior és, entre els subnuclis del Me, el que major *input* i *output* té cap a nuclis olfactius, el que suggereix que el MeA té una funció integradora dels senyals olfactives i vomeronasals. El MeA filtra i cataloga la informació quimiosensorial, que serà transmesa ja siga al circuit neural que controla els comportaments socio-sexuals o al circuit neural que controla els comportaments defensius. La informació de les feromones sexuals passaria al circuit socio-sexual a través de projeccions directes, però sobretot per la projecció del MePD al BSTMPM i als nuclis reproductius hipotalàmics. El MePD conté gran quantitat de cèl·lules que expressen receptors per esteroides sexuals, el que fa d'aquest nucli un centre clau per al control hormonal de la resposta a olors i feromones en el context del comportament reproductiu. A més, les projeccions a la resta del Me i l'amígdala permetrien la integració de la informació olfactiva i vomeronasal amb la informació endocrina. També a través del MePD, les olors d'heterospecífics, inhibirien el circuit reproductiu facilitant els comportaments defensius. Per contra, el MePV està principalment implicat en comportaments defensius a través de les seues connexions amb el BSTMPI i el circuit hipotalàmic defensiu. Els nostres resultats també mostren projeccions al BSTMPM i el BST anteromedial, el que podria indicar que també està implicat en el control de comportaments no sexuals, com respostes agonístiques amb conespecífics del mateix sexe o aversió a olors derivats de conspecífics parasitats.

14.3.2   *El PMCo coordina el processament neural de senyals vomeronasals*

El PMCo té característiques que fan que puga ser considerat el còrtex vomeronasal primari. Primer, té un *input* considerable des del AOB, originat a les cèl·lules mitrals (Winans and Scalia, 1970; Scalia and Winans, 1975; Von Campenhausen and Mori, 2000). Aquesta projecció innerva la capa superficial del PMCo, on coincideix amb diferents marcadors: calretinina, marcador d'*inputs* quimiosensorials (Wouterlood and Härtig, 1995); neuropilina-2 i la innervació d'acetil colinesterasa, específica del AOB (Kemppainen et al., 2002; Gutiérrez-Castellanos et al., 2010). Segon, entre les projeccions del AOB és l'única estructura amb origen estrictament palial, com mostra l'expressió de gens reguladors del desenvolupament Neurogenina 2 i Semaforina 5A (Medina

et al., 2004). Tercer, presenta una laminació cortical, que depén de la Reelina (Boyle et al., 2011), i una organització laminada dels *inputs* i *outputs*. A més, l'amígdala és una estructura amb una organització nuclear, connexions i neuroquímica molt conservades (Martínez-García et al., 2007) i dins de l'amígdala es pot observar una estructura vomeronasal homòloga al PMCo. En rèptils *squamata* aquesta regió s'anomena *nucleus sphericus*. Les connexions d'aquest nucli revelen una elevada similaritat amb les del PMCo: connexions recíproques del AOB, interconnexions amb el PMCo/ *nucleus sphericus* contralateral a través de la comissura anterior, amb la resta del sistema vomeronasal, el còrtex olfactiu (còrtex lateral en rèptils) i l'amígdala olfactiva, l'hipocamp (còrtex dorsal en rèptils), l'estriat ventral (olfacto-striat en serps) i una projecció menor a l'hipotàlem preòptic (Lanuza and Halpern, 1997; Lanuza et al., 1997). En general, aquestes dades suggereixen que el PMCo deuria ser considerat el còrtex comeronasal, que ja estava present en l'amígdala de l'avantpassat comú a mamífers i rèptils, per tat és un element essencial de l'evolució del cervell emocional en vertebrats terrestres.

Les aferècies i eferències del PMCo mostrades pels nostres resultats estan resumides a la Figura 22. Aquests resultat confirmen i amplien els estudis previs en altres mamífers, principalment en mascles de rata i hàmter (Kevetter and Winans, 1981b; Canteras et al., 1992; Kemppainen et al., 2002; Pitkänen, 2000). Com en el cas del Me, la falta de diferències rellevants entre els nostres resultats (en femelles de ratolí) i dades prèvies (en mascles de rata i hàmster) indiquen que el patró de connexions és comú en rosegadors i que no hi ha dimorfisme sexual en les projeccions de PMCo. En general, la majoria de les projeccions són recíproques, però hi ha dos excepcions, les eferències al septum ventrolateral i a l'estriat ventral.

El PMCo rep informació des de i projecta a cadascuna de les estructures del sistema vomeronasal: el AOB, Me, nucli del llit del tracte olfactori accessori i el BST. També presenta interconnexions significatives amb els principals components del sistema olfactori prncipal: els nuclis que composen el còrtex olfactiu i l'amígdala olfactiva; encara que aquestes connexions, especialment les eferències, no són tan denses com les del sistema vomeronasal. Aquestes connexions podrien permetre la integració de la informació olfactòria i vomeronasal. La integració seria a dos nivells: en les projeccions convergents dels bulbs olfactoris (Pro-Sistiaga et al., 2007; Kang et al., 2009; Cádiz-Moretti et al., 2013) i en les connexions recíproques entre el PMCo i els centres olfactoris secundaris. Un nivell més d'integració serien les projeccions

del PMCo al nucli basomedial de l'amígdala, on la informació vomeronasal s'integra amb altres tipus d'informació sensorial.

Una altra connexió important del PMCo és la que té amb l'hipocamp ventral i el septum ventrolateral. El hipocamp ventral pareix una àrea especialitzada i densament interconnectada amb el sistema vomeronasal, ja que també rep projeccions del Me. Açò suggereix una hipòtesi interessant: la informació dels estímuls vomeronasals continguda en els rastres d'orina contribueix al mapa espacial generat per l'hipocamp a través d'aquesta interacció entre l'amígdala vomeronasal i l'hipocamp. D'altra banda, el circuit neural pel qual el territori indueix en mascles respostes agressives o defensives front a mascles intrusos, encara que actualment es desconeix (Adams, 2006), podria estar mediada per les connexions del PMCo amb el septum ventrolateral (al que també projecta l'hipocamp ventral, Risold and Swanson 1997). En femelles, per contra, la presència d'un mascle activaria els circuits hipotalàmics que controlen els comportaments reproductius.

L'altra estructura neural sense connexions recíproques amb el PMCo és l'estriat ventral. Les eferències del PMCo a la regió medial del tubercle olfactiu i els illots de Calleja, pot constituir part de la via anatòmica que transfereix la informació vomeronasal al sistema de reforç (Novejarque et al., 2011). Aquesta projecció directa junt a altres indirectes, com a través del nucli basolateral de l'amígdala, explicaria les propietats reforçants de les feromones sexuals que indueixen preferència condicionada de lloc (Agustín-Pavón et al., 2007; Martínez-Ricós et al., 2007; Roberts et al., 2012).

14.3.3   *Els sistemes olfactiu i vomeronasal tenen una activitat complementària i coordinada*

El nostre estudi investiga, en un paradigma exploratori en animal despert, l'activitat induïda per estímuls olfactius i vomeronasals en tres nuclis fonamentals del sistema vomeronasal i, simultàneament, del MOB. Açò, permet investigar tant l'activitat del sistema vomeronasal com la integració de la informació olfactiva i vomeronasal.

Quan no hi ha exploració l'activitat predominant en tota la xarxa es centra en freqüències delta (< 4 Hz; Figura 42 A), una resposta típicament observada al MOB (Welker, 1964; Kepecs et al., 2007). L'exploració de l'estímul indueix un augment de l'activitat theta, fins i tot quan es presenta un estímul neutre (Figura 42 B). Durant els períodes d'exploració es van detectar trams curts ($2-4$ s) en els que l'oscil·lació és més rítmica temporalment i es manté en theta constant. La predominància d'oscil-

lacions theta s'ha observat en el MOB (Youngentob et al., 1987; Kepecs et al., 2006; Verhagen et al., 2007; Wesson et al., 2008) i en el AOB (Binns and Brennan, 2005; Tendler and Wagner, 2015). Tanmateix, els estímul neutres i de conespecífics produeixen canvis particulars en l'activitat oscil·latòria de les estructures analitzades. El estímuls neutres (sense senyals vomeronasals) indueix activitat theta amb un pic a $4 - 6$ Hz; mentre que els estímuls de conspecífics (senyals vomeronasals i olfactives) indueixen un pic a uns 7 Hz, similars a les freqüències descrites per Tendler and Wagner (2015) en MOB, AOB i Me. No obstant, els bulbs olfactius no són capaços de distingir entre els estímuls de conspecífics, el que és consistent amb estudis previs fent registre unitari en el AOB mostren que les neurones responen a més d'un estímul (Ben-Shaul et al., 2010; Bergan et al., 2014). Per contra, l'amígdala vomeronasal pereix respondre de manera específica a estímuls de conspecífics. En el Me, els senyals de mascle indueixen una activitat rítimica a freqüències theta amb un pic de 8 Hz, en aquests sentit les neurones del Me pareixen respondre a estímuls de conspecífics del mateix sexe (Bergan et al., 2014). El PMCo, mostra un pic semblant induït per senyals derivats de femella.

L'activitat oscil·latòria en banda theta observada en els bulbs és molt semblant, i el grau de sincronització entre AOB i MOB mostra un augment significatiu durant l'exploració de geraniol, un estímul olfactiu pur. Aquestes dades suggereixen que la internalització de l'estímul en la cavitat nasal (*sniffing*) està acoblada amb la internalització de l'estímul a l'òrgan vomeronasal (bombeig vomeronasal). No es coneix el mecanisme pel que s'inicia el bombeig, però les nostres dades suggereixen que l'*sniffing* podria dirigir el mostreig vomeronasal i, indirectament, el patró oscil·latori del sistema vomeronasal.

Durant l'exploració d'un estímul el Me destaca com l'estructura que mostra més potència en les bandes de freqüència gamma. A més, l'activitat d'aquestes bandes revela diferències entre el MOB i els nuclis vomeronasals. L'exploració indueix un augment de la potència de les freqüències de $90 - 120$ Hz en AOB, Me i PMCo, mentre que el MOB mostra un augment en les freqüències de $60 - 80$ Hz. L'activitat gamma induïda per l'exploració està modulada per l'oscil·lació theta del AOB. Així, la banda theta del AOB genera, quan hi ha un estímul neutre, gamma alt ($60 - 80$ Hz) en els bulbs; mentre que els estímuls de conspecífics modulen freqüències més altes, gamma ràpid ($90 - 120$ Hz), en l'amígdala vomeronasal.

El desenvolupament d'un comportament coherent mediat per senyals olfactoris i vomeronasals depén de la coordinació de nombroses regions cerebrals, entre les quals hem estudiat

el MOB, AOB, Me i PMCo. Els canvis transitoris i dinàmics
de la coherència entre les seues connexions estan dirigits per
l'activitat theta que modula sub-bandes específiques de freqüèn-
cies gamma, que depenen de l'estímul percebut i dels requeri-
ments comportamentals.

REFERENCES

A. Abellán, B. Vernier, S. Rétaux, and L. Medina. Similarities and differences in the forebrain expression of Lhx1 and Lhx5 between chicken and mouse: Insights for understanding telencephalic development and evolution. *Journal of Comparative Neurology*, 518(17): 3512–3528, may 2010. ISSN 10969861. doi: 10.1002/cne.22410. URL http://doi.wiley.com/10.1002/cne.22410.

D. B. Adams. Brain mechanisms of aggressive behavior: An updated review. *Neuroscience and Biobehavioral Reviews*, 30(3):304–318, 2006. ISSN 01497634. doi: 10.1016/j.neubiorev.2005.09. 004. URL http://www.sciencedirect.com/science/article/pii/S0149763405001466.

E. Adrian. The electrical activity of the mammalian olfactory bulb. *Electroencephalography and Clinical Neurophysiology*, 2(1-4):377–388, jan 1950. ISSN 00134694. doi: 10.1016/0013-4694(50)90075-7. URL http://linkinghub.elsevier.com/retrieve/pii/0013469450900757.

C. Agustín-Pavón, J. Martínez-Ricós, F. Martínez-García, and E. Lanuza. Effects of dopaminergic drugs on innate pheromone-mediated reward in female mice: A new case of dopamine-independent "liking.". *Behavioral Neuroscience*, 121(5):920–932, 2007. ISSN 1939-0084. doi: 10.1037/0735-7044.121.5.920. URL http://doi.apa.org/getdoi.cfm?doi=10.1037/0735-7044.121.5.920.

T. E. Akam and D. M. Kullmann. Efficient "Communication through Coherence" Requires Oscillations Structured to Minimize Interference between Signals. *PLoS Computational Biology*, 8(11):e1002760, nov 2012. ISSN 1553-7358. doi: 10.1371/journal.pcbi.1002760. URL http://dx.plos.org/10.1371/journal.pcbi.1002760.

H. Arakawa, K. Arakawa, and T. Deak. Oxytocin and vasopressin in the medial amygdala differentially modulate approach and avoidance behavior toward illness-related social odor. *Neuroscience*, 171(4):1141–1151, dec 2010. ISSN 03064522. doi: 10.1016/j.neuroscience.2010.10.013. URL http://linkinghub.elsevier.com/retrieve/pii/S0306452210013436.

A. Asaba, T. Hattori, K. Mogi, and T. Kikusui. Sexual attractiveness of male chemicals and vocalizations in mice. *Frontiers in neuroscience*, 8(8 JUL), aug 2014. ISSN 1662453X. doi: 10.3389/fnins.2014.00231. URL http://journal.frontiersin.org/article/10.3389/fnins.2014.00231/abstract.

R. Bandler and M. T. Shipley. Columnar organization in the midbrain periaqueductal gray: modules for emotional expression? *Trends in Neurosciences*, 17(9):379–389, jan 1994. ISSN 01662236. doi: 10.1016/0166-2236(94)90047-7. URL http://linkinghub.elsevier.com/retrieve/pii/0166223694900477.

P. C. Barber. Adjacent laminar terminations of two centrifugal afferent pathways to the accessory olfactory bulb in the mouse. *Brain Research*, 245(2):215–221, aug 1982. ISSN 00068993. doi: 10.1016/0006-8993(82)90803-4. URL http://linkinghub.elsevier.com/retrieve/pii/0006899382908034.

P. C. Barber and P. Field. Autoradiographic demonstration of afferent connections of the accessory olfactory bulb in the mouse. *Brain Research*, 85(2):201–203, feb 1975. ISSN 00068993. doi: 10.1016/0006-8993(75)90070-0. URL http://linkinghub.elsevier.com/retrieve/pii/0006899375900700.

P. C. Barber and G. Raisman. An Autoradiographic Investigation Of The Projection Of The Vomeronasal Organ To The Accessory Olfactory Bulb In The Mouse. *Brain Research*, 81:119–132, 1974.

B. Bathellier, D. L. Buhl, R. Accolla, and A. Carleton. Dynamic Ensemble Odor Coding in the Mammalian Olfactory Bulb: Sensory Information at Different Timescales. *Neuron*, 57(4):586–598, feb 2008. ISSN 08966273. doi: 10.1016/j.neuron.2008.02.011. URL http://linkinghub.elsevier.com/retrieve/pii/S0896627308001347.

M. J. Baum and K. R. Kelliher. Complementary roles of the main and accessory olfactory systems in mammalian mate recognition. *Annual Review of Physiology*, 71(September 2008):141–160, jan 2009. ISSN 0066-4278. doi: 10.1146/annurev.physiol.010908.163137. URL http://www.annualreviews.org/doi/10.1146/annurev.physiol.010908.163137.

M. G. Baxter and E. A. Murray. The amygdala and reward. *Nature Reviews Neuroscience*, 3(7):563–573, jul 2002. ISSN 14710048. doi: 10.1038/nrn875. URL http://www.nature.com/doifinder/10.1038/nrn875.

M. A. Belluscio, K. Mizuseki, R. Schmidt, R. Kempter, and G. Buzsáki. Cross-Frequency Phase-Phase Coupling between Theta and Gamma Oscillations in the Hippocampus. *Journal of Neuroscience*, 32(2):423–435, jan 2012. ISSN 0270-6474. doi: 10.1523/JNEUROSCI.4122-11.2012. URL http://www.pubmedcentral.nih.gov/articlerender.fcgi?artid=3293373{&}tool=pmcentrez{&}rendertype=abstract.

C. Belzung, W. El Hage, N. Moindrot, and G. Griebel. Behavioral and neurochemical changes following predatory stress in mice. *Neuropharmacology*, 41(3):400–408, sep 2001. ISSN 00283908. doi: 10.1016/S0028-3908(01)00072-7. URL http://linkinghub.elsevier.com/retrieve/pii/S0028390801000727.

Y. Ben-Shaul, L. C. Katz, R. Mooney, and C. Dulac. In vivo vomeronasal stimulation reveals sensory encoding of conspecific and allospecific cues by the mouse accessory olfactory bulb. *Proceedings of the National Academy of Sciences*, 107(11):5172–5177, mar 2010. ISSN 0027-8424. doi: 10.1073/pnas.0915147107. URL http://www.pnas.org/cgi/doi/10.1073/pnas.0915147107.

D. Benson, P. Isackson, C. Gall, and E. Jones. Contrasting patterns in the localization of glutamic acid decarboxylase and Ca2+ /calmodulin protein kinase gene expression in the rat centrat nervous system. *Neuroscience*, 46(4):825–849, feb 1992. ISSN 03064522. doi: 10.1016/0306-4522(92)90188-8. URL http://linkinghub.elsevier.com/retrieve/pii/0306452292901888.

J. Bergan, Y. Ben-Shaul, and C. Dulac. Sex-specific processing of social cues in the medial amygdala. *eLife*, 3:22, jan 2014. ISSN 2050-084X. doi: 10.7554/eLife.02743. URL http://elifesciences.org/content/3/e02743.abstract.

J. Beshel, N. Kopell, and L. M. Kay. Olfactory Bulb Gamma Oscillations Are Enhanced with Task Demands. *Journal of Neuroscience*, 27(31):8358–8365, aug 2007. ISSN 0270-6474. doi: 10.1523/JNEUROSCI.1199-07.2007. URL http://www.jneurosci.org/cgi/doi/10.1523/JNEUROSCI.1199-07.2007.

K. E. Binns and P. A. Brennan. Changes in electrophysiological activity in the accessory olfactory bulb and medial amygdala associated with mate recognition in mice. *European Journal of Neuroscience*, 21(9):2529–2537, may 2005. ISSN 0953-816X. doi: 10.1111/j.1460-9568.2005.04090.x. URL http://www.ncbi.nlm.nih.gov/pubmed/15932610.

Z. Borhegyi, V. Varga, N. Szilagyi, D. Fabo, and T. F. Freund. Phase Segregation of Medial Septal GABAergic Neurons during Hippocampal Theta Activity. *Journal of Neuroscience*, 24(39):8470–8479, 2004. ISSN 0270-6474. doi: 10.1523/JNEUROSCI.1413-04.2004. URL http://www.jneurosci.org/cgi/doi/10.1523/JNEUROSCI.1413-04.2004.

M. P. Boyle, A. Bernard, C. L. Thompson, L. Ng, A. Boe, M. Mortrud, M. J. Hawrylycz, A. R. Jones, R. F. Hevner, and E. S. Lein. Cell-type-specific consequences of reelin deficiency in the mouse neocortex, hippocampus, and amygdala. *The Journal of Comparative Neurology*, 519(11):2061–2089, aug 2011. ISSN 00219967. doi: 10.1002/cne.22655. URL http://doi.wiley.com/10.1002/cne.22655.

P. A. Brennan and F. Zufall. Pheromonal communication in vertebrates. *Nature*, 444(7117):308–315, nov 2006. ISSN 0028-0836. doi: 10.1038/nature05404. URL http://www.nature.com/doifinder/10.1038/nature05404.

S. C. Bressler and M. J. Baum. Sex comparison of neuronal fos immunoreactivity in the rat vomeronasal projection circuit after chemosensory stimulation. *Neuroscience*, 71(4):1063–1072, apr 1996. ISSN 03064522. doi: 10.1016/0306-4522(95)00493-9. URL http://linkinghub.elsevier.com/retrieve/pii/0306452295004939.

S. L. Bressler and W. J. Freeman. Frequency analysis of olfactory system EEG in cat, rabbit, and rat. *Electroencephalography and clinical neurophysiology*, 50(1-2):19–24, 1980. ISSN 0013-4694. doi: 10.1016/0013-4694(80)90319-3. URL http://www.ncbi.nlm.nih.gov/pubmed/6159187.

R. D. Broadwell and D. M. Jacobowitz. Olfactory relationships of the telencephalon and diencephalon in the rabbit. III. The ipsilateral centrifugal fibers to the olfactory bulbar and retrobulbar formations. *Journal of Comparative Neurology*, 170(3):321–345, dec 1976. ISSN 10969861. doi: 10.1002/cne.901700305. URL http://doi.wiley.com/ 10.1002/cne.901700305.

L. B. Buck. Information Coding in the Vertebrate Olfactory System. *Annual Review of Neuroscience*, 19(1):517–544, mar 1996. ISSN 0147-006X. doi: 10.1146/annurev.ne.19.030196.002505. URL http://www. annualreviews.org/doi/10.1146/annurev.ne.19.030196.002505.

M. Bupesh, I. Legaz, A. Abellán, and L. Medina. Multiple telencephalic and extratelencephalic embryonic domains contribute neurons to the medial extended amygdala. *Journal of Comparative Neurology*, 519(8):1505–1525, jun 2011. ISSN 00219967. doi: 10.1002/cne.22581. URL http://doi.wiley.com/10.1002/cne.22581.

M. Burns-Cusato, E. M. Scordalakes, and E. F. Rissman. Of mice and missing data: What we know (and need to learn) about male sexual behavior, nov 2004. ISSN 00319384. URL http://linkinghub. elsevier.com/retrieve/pii/S0031938404003531.

G. Buzsáki. Theta rhythm of navigation: Link between path integration and landmark navigation, episodic and semantic memory. *Hippocampus*, 15(7):827–840, 2005. ISSN 10509631. doi: 10.1002/hipo. 20113.

G. Buzsáki. *Rhythms of the Brain*. Oxford University Press, 2006. ISBN 9780199828234. URL https://global.oup.com/academic/product/ rhythms-of-the-brain-9780199828234?cc=es{&}lang=en{&}.

G. Buzsáki and X.-J. Wang. Mechanisms of Gamma Oscillations. *Annual Review of Neuroscience*, 35(1):203–225, jul 2012. ISSN 0147-006X. doi: 10.1146/annurev-neuro-062111-150444. URL http://www. annualreviews.org/doi/10.1146/annurev-neuro-062111-150444.

G. Buzsáki, N. Logothetis, and W. Singer. Scaling Brain Size, Keeping Timing: Evolutionary Preservation of Brain Rhythms. *Neuron*, 80(3):751–764, oct 2013. ISSN 08966273. doi: 10.1016/j.neuron. 2013.10.002. URL http://linkinghub.elsevier.com/retrieve/ pii/S0896627313009045.

B. Cádiz-Moretti, F. MartÍnez-GarcÍa, and E. Lanuza. Neural substrate to associate odorants and pheromones: Convergence of projections from the main and accessory olfactory bulbs in mice. In M. L. East and M. Dehnhard, editors, *Chemical Signals in Vertebrates 12*, pages 3–16. Springer Science, New York, 2013. ISBN 9781461459279. doi: 10.1007/9781461459279. URL https://link. springer.com/chapter/10.1007/978-1-4614-5927-9_1.

B. Cádiz-Moretti, M. Abellán-Álvaro, C. Pardo-Bellver, F. Martínez-García, and E. Lanuza. Afferent and Efferent Connections of the Cortex-Amygdala Transition Zone in Mice. *Frontiers in Neuroanatomy*, 10:125, dec 2016a. ISSN 1662-5129. doi: 10.3389/fnana.2016.

00125. URL http://journal.frontiersin.org/article/10.3389/fnana.2016.00125/full.

B. Cádiz-Moretti, M. Otero-García, F. Martínez-García, and E. Lanuza. Afferent projections to the different medial amygdala subdivisions: a retrograde tracing study in the mouse. *Brain Structure and Function*, 221(2):1–33, mar 2016b. ISSN 18632661. doi: 10.1007/s00429-014-0954-y. URL http://link.springer.com/10.1007/s00429-014-0954-y.

A. R. Caffé, F. W. van Leeuwen, and P. G. M. Luiten. Vasopressin cells in the medial amygdala of the rat project to the lateral septum and ventral hippocampus. *Journal of Comparative Neurology*, 261(2):237–252, jul 1987. ISSN 00219967. doi: 10.1002/cne.902610206. URL http://doi.wiley.com/10.1002/cne.902610206.

R. T. Canolty, E. Edwards, S. S. Dalal, M. Soltani, S. S. Nagarajan, M. S. Berger, N. M. Barbaro, R. T. Knight, H. E. Kirsch, M. S. Berger, N. M. Barbaro, and R. T. Knight. High Gamma Power is Phase-Locked to Theta Oscillations in Human Neocortex. *Science (New York, N.Y.)*, 313(5793):1626–1628, 2006. ISSN 0036-8075. doi: 10.1126/science.1128115.High.

N. S. Canteras. The medial hypothalamic defensive system: Hodological organization and functional implications. *Pharmacology Biochemistry and Behavior*, 71(3):481–491, mar 2002. ISSN 0091-3057. doi: 10.1016/S0091-3057(01)00685-2. URL http://linkinghub.elsevier.com/retrieve/pii/S0091305701006852.

N. S. Canteras, R. B. Simerly, and L. W. Swanson. Connections of the posterior nucleus of the amygdala. *The Journal of Comparative Neurology*, 324(2):143–179, oct 1992. ISSN 0021-9967. doi: 10.1002/cne.903240203. URL http://doi.wiley.com/10.1002/cne.903240203.

N. S. Canteras, R. B. Simerly, and L. W. Swanson. Organization of projections from the medial nucleus of the amygdala: A PHAL study in the rat. *Journal of Comparative Neurology*, 360(2):213–245, sep 1995. ISSN 10969861. doi: 10.1002/cne.903600203. URL http://doi.wiley.com/10.1002/cne.903600203.

K. S. Carlson, M. R. Dillione, and D. W. Wesson. Odor- and state-dependent olfactory tubercle local field potential dynamics in awake rats. *Journal of Neurophysiology*, 111(10):2109–2123, 2014. ISSN 0022-3077. doi: 10.1152/jn.00829.2013. URL http://jn.physiology.org/cgi/doi/10.1152/jn.00829.2013.

L. A. Cenquizca and L. W. Swanson. Spatial organization of direct hippocampal field CA1 axonal projections to the rest of the cerebral cortex. *Brain Research Reviews*, 56(1):1–26, nov 2007. ISSN 01650173. doi: 10.1016/j.brainresrev.2007.05.002. URL http://linkinghub.elsevier.com/retrieve/pii/S0165017307000732.

P. Chamero, T. F. Marton, D. W. Logan, K. Flanagan, J. R. Cruz, A. Saghatelian, B. F. Cravatt, and L. Stowers. Identification of protein pheromones that promote aggressive behaviour. *Nature*, 450(7171):

899–902, dec 2007. ISSN 1476-4687. doi: 10.1038/nature05997. URL http://www.nature.com/doifinder/10.1038/nature05997.

P. Chamero, V. Katsoulidou, P. Hendrix, B. Bufe, R. Roberts, H. Matsunami, J. Abramowitz, L. Birnbaumer, F. Zufall, and T. Leinders-Zufall. G protein G(alpha)o is essential for vomeronasal function and aggressive behavior in mice. *Proceedings of the National Academy of Sciences of the United States of America*, 108(31):12898–903, aug 2011. ISSN 1091-6490. doi: 10.1073/pnas.1107770108. URL http://www.pnas.org/cgi/doi/10.1073/pnas.1107770108.

P. Chamero, T. Leinders-Zufall, and F. Zufall. From genes to social communication: molecular sensing by the vomeronasal organ. *Trends in neurosciences*, 35(10):597–606, oct 2012. ISSN 1878-108X. doi: 10.1016/j.tins.2012.04.011. URL http://www.ncbi.nlm.nih.gov/pubmed/22658923.

D. C. Choi, A. R. Furay, N. K. Evanson, M. M. Ostrander, Y. M. Ulrich-Lai, and J. P. Herman. Bed Nucleus of the Stria Terminalis Subregions Differentially Regulate Hypothalamic-Pituitary-Adrenal Axis Activity: Implications for the Integration of Limbic Inputs. *Journal of Neuroscience*, 27(8):2025–2034, feb 2007. ISSN 0270-6474. doi: 10.1523/JNEUROSCI.4301-06.2007. URL http://www.jneurosci.org/cgi/doi/10.1523/JNEUROSCI.4301-06.2007.

G. B. Choi, H.-w. Dong, A. J. Murphy, D. M. Valenzuela, G. D. Yancopoulos, L. W. Swanson, and D. J. Anderson. Lhx6 Delineates a Pathway Mediating Innate Reproductive Behaviors from the Amygdala to the Hypothalamus. *Neuron*, 46(4):647–660, may 2005. ISSN 0896-6273. doi: 10.1016/j.neuron.2005.04.011. URL http://linkinghub.elsevier.com/retrieve/pii/S0896627305003478.

S. Ciocchi, C. Herry, F. Grenier, S. B. E. Wolff, J. J. Letzkus, I. Vlachos, I. Ehrlich, R. Sprengel, K. Deisseroth, M. B. Stadler, C. Müller, and A. Lüthi. Encoding of conditioned fear in central amygdala inhibitory circuits. *Nature*, 468(7321):277–282, nov 2010. ISSN 0028-0836. doi: 10.1038/nature09559. URL http://www.nature.com/doifinder/10.1038/nature09559.

A. N. Clancy, A. Coquelin, F. Macrides, R. A. Gorski, and E. P. Noble. Sexual behavior and aggression in male mice: involvement of the vomeronasal system. *The Journal of neuroscience : the official journal of the Society for Neuroscience*, 4(9):2222–2229, 1984. ISSN 0270-6474. URL http://www.jneurosci.org/content/jneuro/4/9/2222.full.pdf.

E. Comoli, É. R. Ribeiro-Barbosa, and N. S. Canteras. Afferent connections of the dorsal premammillary nucleus. *Journal of Comparative Neurology*, 423(1):83–98, jul 2000. ISSN 0021-9967. doi: 10.1002/1096-9861(20000717)423:1<83::AID-CNE7>3.0.CO;2-3. URL http://doi.wiley.com/10.1002/1096-9861%2820000717%29423%3A1%3C83%3A%3AAID-CNE7%3E3.0.CO%3B2-3.

E. Comoli, É. R. Ribeiro-Barbosa, N. Negrão, M. Goto, and N. S. Canteras. Functional mapping of the prosencephalic systems involved in organizing predatory behavior in rats. *Neuroscience*, 130

(4):1055–67, jan 2005. ISSN 0306-4522. doi: 10.1016/j.neuroscience. 2004.10.020. URL http://www.ncbi.nlm.nih.gov/pubmed/15653000.

B. M. Cooke. Steroid-dependent plasticity in the medial amygdala, mar 2006. ISSN 03064522. URL http://linkinghub.elsevier.com/ retrieve/pii/S0306452205006548.

B. M. Cooke, G. Tabibnia, and S. M. Breedlove. A brain sexual dimorphism controlled by adult circulating androgens. *Proceedings of the National Academy of Sciences of the United States of America*, 96(13): 7538–40, jun 1999. ISSN 0027-8424. doi: 10.1073/pnas.96.13.7538. URL http://www.pnas.org/cgi/doi/10.1073/pnas.96.13.7538.

L. M. Coolen and R. I. Wood. Bidirectional connections of the medial amygdaloid nucleus in the Syrian hamster brain: Simultaneous anterograde and retrograde tract tracing. *The Journal of Comparative Neurology*, 399(2):189–209, sep 1998. ISSN 0021-9967. doi: 10.1002/(SICI)1096-9861(19980921)399:2<189::AID-CNE4>3.0.CO; 2-X. URL http://doi.wiley.com/10.1002/%28SICI%291096-9861% 2819980921%29399%3A2%3C189%3A%3AAID-CNE4%3E3.0.CO%3B2-X.

G. A. Cousens, A. Kearns, F. Laterza, and J. Tundidor. Excitotoxic lesions of the medial amygdala attenuate olfactory fear-potentiated startle and conditioned freezing behavior. *Behavioural Brain Research*, 229(2):427–432, 2012. ISSN 01664328. doi: 10.1016/j.bbr.2012.01.011. URL http://dx.doi.org/10.1016/j.bbr.2012.01.011.

M. Davis. The role of the amygdale in conditioned and unconditioned fear and anxiety. In J. P. Aggleton, editor, *The Amygdala: A Functional Analysis*, pages 213–287. Oxford University Press, Oxford, UK, 2000.

C. de la Rosa-Prieto, I. Ubeda-Bañón, A. Mohedano-Moriano, P. Pro-Sistiaga, D. Saiz-Sanchez, R. Insausti, and A. Martínez-Marcos. Subicular and CA1 hippocampal projections to the accessory olfactory bulb. *Hippocampus*, 19(2):124–129, feb 2009. ISSN 1098-1063. doi: 10.1002/hipo.20495. URL http://doi.wiley.com/10. 1002/hipo.20495.

J. de Olmos, H. Hardy, and L. Heimer. The afferent connections of the main and the accessory olfactory bulb formations in the rat: An experimental HRP???study. *Journal of Comparative Neurology*, 181(2): 213–244, sep 1978. ISSN 10969861. doi: 10.1002/cne.901810202. URL http://doi.wiley.com/10.1002/cne.901810202.

B. T. DiBenedictis, K. L. Ingraham, M. J. Baum, and J. A. Cherry. Disruption of urinary odor preference and lordosis behavior in female mice given lesions of the medial amygdala. *Physiology & Behavior*, 105(2):554–559, jan 2012. ISSN 00319384. doi: 10. 1016/j.physbeh.2011.09.014. URL http://linkinghub.elsevier. com/retrieve/pii/S003193841100463X.

R. A. Dielenberg, G. E. Hunt, and I. S. McGregor. "When a rat smells a cat": the distribution of Fos immunoreactivity in rat brain following exposure to a predatory odor. *Neuroscience*, 104(4): 1085–1097, jul 2001. ISSN 03064522. doi: 10.1016/S0306-4522(01)

00150-6.   URL http://linkinghub.elsevier.com/retrieve/pii/S0306452201001506.

E. Dominguez-Salazar, H. L. Bateman, and E. F. Rissman.   Background matters: The effects of estrogen receptor α gene disruption on male sexual behavior are modified by background strain. *Hormones and Behavior*, 46(4):482–490, nov 2004. ISSN 0018506X. doi: 10.1016/j.yhbeh.2004.05.006.   URL http://linkinghub.elsevier.com/retrieve/pii/S0018506X04001333.

H.-W. Dong and L. W. Swanson. Projections from bed nuclei of the stria terminalis, anteromedial area: Cerebral hemisphere integration of neuroendocrine, autonomic, and behavioral aspects of energy balance. *Journal of Comparative Neurology*, 494(1):142–178, jan 2006. ISSN 00219967. doi: 10.1002/cne.20788. URL http://doi.wiley.com/10.1002/cne.20788.

H.-W. Dong, G. D. Petrovich, and L. W. Swanson. Topography of projections from amygdala to bed nuclei of the stria terminalis. *Brain Research Reviews*, 38(1-2):192–246, dec 2001. ISSN 01650173. doi: 10.1016/S0165-0173(01)00079-0. URL http://linkinghub.elsevier.com/retrieve/pii/S0165017301000790.

I. Ehrlich, Y. Humeau, F. Grenier, S. Ciocchi, C. Herry, and A. Lüthi. Amygdala Inhibitory Circuits and the Control of Fear Memory. *Neuron*, 62(6):757–771, 2009. ISSN 08966273. doi: 10.1016/j.neuron.2009.05.026. URL http://www.sciencedirect.com/science/article/pii/S0896627309004267.

S. Fan and M. Luo. The organization of feedback projections in a pathway important for processing pheromonal signals. *Neuroscience*, 161(2):489–500, jun 2009. ISSN 1873-7544. doi: 10.1016/j.neuroscience.2009.03.065. URL http://linkinghub.elsevier.com/retrieve/pii/S0306452209004928.

M. Farge.   Wavelet transforms and their applications to Turbulence. *Annual Review of Fluid Mechanics*, 24(1):395–457, jan 1992.   ISSN 00664189.   doi: 10.1146/annurev.fl.24.010192.002143. URL http://www.annualreviews.org/doi/10.1146/annurev.fl.24.010192.002143.

G. D. Fernandez-Fewell and M. Meredith. C-Fos Expression in Vomeronasal Pathways of Mated or Pheromone-Stimulated Male Golden Hamsters: Contributions From Vomeronasal Sensory Input and Expression Related To Mating Performance. *The Journal of Neuroscience*, 14(6):3643–3654, 1994. ISSN 0270-6474. URL http://www.jneurosci.org/content/14/6/3643.long.

W. J. Freeman and W. Schneider. Changes in spatial patterns of rabbit olfactory EEG with conditioning to odors. *Psychophysiology*, 19(1):44–56, 1982. ISSN 00485772 (ISSN). doi: 10.1111/j.1469-8986.1982.tb02598.x.

P. Fries. A mechanism for cognitive dynamics: Neuronal communication through neuronal coherence. *Trends in Cognitive Sciences*, 9(10):474–480, 2005. ISSN 13646613. doi: 10.1016/j.tics.2005.08.011.

X. Fu, Y. Yan, P. S. Xu, I. Geerlof-Vidavsky, W. Chong, M. L. Gross, and T. E. Holy. A Molecular Code for Identity in the Vomeronasal System. *Cell*, 163(2):313–323, 2015. ISSN 10974172. doi: 10.1016/j.cell.2015.09.012. URL http://dx.doi.org/10.1016/j.cell.2015.09.012.

C. S. Gabor, A. Phan, A. E. Clipperton-Allen, M. Kavaliers, and E. Choleris. Interplay of oxytocin, vasopressin, and sex hormones in the regulation of social recognition. *Behavioral Neuroscience*, 126(1):97–109, 2012. ISSN 1939-0084. doi: 10.1037/a0026464. URL http://doi.apa.org/getdoi.cfm?doi=10.1037/a0026464.

M. García-López, A. Abellán, I. Legaz, J. L. Rubenstein, L. Puelles, and L. Medina. Histogenetic compartments of the mouse centromedial and extended amygdala based on gene expression patterns during development. *The Journal of Comparative Neurology*, 506(1):46–74, jan 2008. ISSN 00219967. doi: 10.1002/cne.21524. URL http://doi.wiley.com/10.1002/cne.21524.

F. García-Moreno, L. López-Mascaraque, and J. A. De Carlos. Early telencephalic migration topographically converging in the olfactory cortex. *Cerebral Cortex*, 18(6):1239–1252, 2008. ISSN 10473211. doi: 10.1093/cercor/bhm154.

F. García-Moreno, M. Pedraza, L. G. Di Giovannantonio, M. Di Salvio, L. López-Mascaraque, A. Simeone, and J. A. De Carlos. A neuronal migratory pathway crossing from diencephalon to telencephalon populates amygdala nuclei. *Nature Neuroscience*, 13(6):680–689, jun 2010. ISSN 1097-6256. doi: 10.1038/nn.2556. URL http://dx.doi.org/10.1038/nn.2556.

S. Geisler and D. S. Zahm. Afferents of the ventral tegmental area in the rat-anatomical substratum for integrative functions. *Journal of Comparative Neurology*, 490(3):270–294, sep 2005. ISSN 00219967. doi: 10.1002/cne.20668. URL http://doi.wiley.com/10.1002/cne.20668.

D. M. Gomez and S. W. Newman. Differential projections of the anterior and posterior regions of the medial amygdaloid nucleus in the Syrian hamster. *The Journal of Comparative Neurology*, 317(2):195–218, mar 1992. ISSN 0021-9967. doi: 10.1002/cne.903170208. URL http://doi.wiley.com/10.1002/cne.903170208.

A. González, R. Morona, J. M. López, N. Moreno, and R. G. Northcutt. Lungfishes, like tetrapods, possess a vomeronasal system. *Frontiers in neuroanatomy*, 4(September):1–11, 2010. ISSN 1662-5129. doi: 10.3389/fnana.2010.00130.

T. S. Gray, R. A. Piechowski, J. M. Yracheta, P. A. Rittenhouse, C. L. Bethea, and L. D. Van de Kar. Ibotenic Acid Lesions in the Bed Nucleus of the Stria terminalis Attenuate Conditioned Stress-Induced Increases in Prolactin, ACTH and Corticosterone. *Neuroendocrinology*, 57(3):517–524, apr 1993. ISSN 0028-3835. doi: 10.1159/000126400. URL http://www.karger.com/?doi=10.1159/000126400.

P. R. Griffiths and P. A. Brennan. Roles for learning in mammalian chemosensory responses. *Hormones and Behavior*, 68:91–102, feb 2015. ISSN 0018506X. doi: 10.1016/j.yhbeh.2014.08.010. URL http://linkinghub.elsevier.com/retrieve/pii/S0018506X14001834.

E. A. Grove. Efferent connections of the substantia innominata in the rat. *The Journal of Comparative Neurology*, 277(3):347–364, nov 1988. ISSN 0021-9967. doi: 10.1002/cne.902770303. URL http://doi.wiley.com/10.1002/cne.902770303.

F. Guillemot, Z. Molnár, V. Tarabykin, and A. Stoykova. Molecular mechanisms of cortical differentiation. *European Journal of Neuroscience*, 23(4):857–868, feb 2006. ISSN 0953816X. doi: 10.1111/j.1460-9568.2006.04626.x. URL http://doi.wiley.com/10.1111/j.1460-9568.2006.04626.x.

N. Gutiérrez-Castellanos, A. Martínez-Marcos, F. Martínez-García, and E. Lanuza. Chemosensory Function of the Amygdala. In G. Litwack, editor, *Vitamins and hormones*, volume 83, pages 165–196. Elsevier Academic Press, jan 2010. doi: 10.1016/S0083-6729(10)83007-9. URL http://linkinghub.elsevier.com/retrieve/pii/S0083672910830079.

L. B. Haberly. Parallel-distributed processing in olfactory cortex: new insights from morphological and physiological analysis of neuronal circuitry. *Chemical Senses*, 26(5):551–76, jun 2001. ISSN 0379-864X. URL http://www.ncbi.nlm.nih.gov/pubmed/11418502.

L. B. Haberly and J. L. Price. Association and commissural fiber systems of the olfactory cortex of the rat. I. Systems originating in the piriform cortex and adjacent areas. *The Journal of Comparative Neurology*, 178(4):711–740, apr 1978. ISSN 0021-9967. doi: 10.1002/cne.901780408. URL http://doi.wiley.com/10.1002/cne.901780408.

S. Haga, T. Hattori, T. Sato, and K. Sato. The male mouse pheromone ESP1 enhances female sexual receptive behaviour through a specific vomeronasal receptor. *Nature*, 466(7302):118–122, jul 2010. ISSN 1476-4687. doi: 10.1038/nature09142. URL http://www.nature.com/nature/journal/v466/n7302/abs/nature09142.html.

S. Haidarliu, D. Golomb, D. Kleinfeld, and E. Ahissar. Dorsorostral Snout Muscles in the Rat Subserve Coordinated Movement for Whisking and Sniffing. *Anatomical Record*, 295(7):1181–1191, jul 2012. ISSN 19328486. doi: 10.1002/ar.22501. URL http://doi.wiley.com/10.1002/ar.22501.

H. A. Halem, J. A. Cherry, and M. J. Baum. Vomeronasal neuroepithelium and forebrain Fos responses to male pheromones in male and female mice. *Journal of Neurobiology*, 39(2):249–263, may 1999. ISSN 0022-3034. doi: 10.1002/(SICI)1097-4695(199905)39:2<249::AID-NEU9>3.0.CO;2-R. URL http://doi.wiley.com/10.1002/%28SICI%291097-4695%28199905%2939%3A2%3C249%3A%3AAID-NEU9%3E3.0.CO%3B2-R.

M. Halpern. The evolution of the vomeronasal system. *Evolution of Nervous Systems*, 2:407–415, 2007. doi: 10.1016/B0-12-370878-8/00143-9.

M. Halpern and J. L. Kubie. Chemical access to the vomeronasal organs of garter snakes. *Physiology & Behavior*, 24(2):367–371, feb 1980. ISSN 00319384. doi: 10.1016/0031-9384(80)90100-6. URL http://linkinghub.elsevier.com/retrieve/pii/0031938480901006.

M. Halpern and A. Martínez-Marcos. Structure and function of the vomeronasal system: An update. *Progress in Neurobiology*, 70(3):245–318, jun 2003. ISSN 03010082. doi: 10.1016/S0301-0082(03)00103-5. URL http://linkinghub.elsevier.com/retrieve/pii/S0301008203001035.

N. S. Hasen and S. C. Gammie. Maternal aggression: New insights from Egr-1. *Brain Research*, 1108(1):147–156, sep 2006. ISSN 00068993. doi: 10.1016/j.brainres.2006.06.007. URL http://linkinghub.elsevier.com/retrieve/pii/S0006899306017100.

M. Heeb and P. Yahr. C-Fos immunoreactivity in the sexually dimorphic area of the hypothalamus and related brain regions of male gerbils after exposure to sex-related stimuli or performance of specific sexual behaviors. *Neuroscience*, 72(4):1049–1071, jun 1996. ISSN 03064522. doi: 10.1016/0306-4522(95)00602-8. URL http://linkinghub.elsevier.com/retrieve/pii/0306452295006028.

C. J. Herrick. The connections of the vomeronasal nerve, accessory olfactory bulb and amygdala in amphibia. *Journal of Comparative Neurology*, 33(3):213–280, 1921. ISSN 10969861. doi: 10.1002/cne.900330303.

T. Hirata, P. Li, G. M. Lanuza, L. A. Cocas, M. M. Huntsman, and J. G. Corbin. Identification of distinct telencephalic progenitor pools for neuronal diversity in the amygdala. *Nature Neuroscience*, 12(2):141–149, feb 2009. ISSN 1097-6256. doi: 10.1038/nn.2241. URL http://www.nature.com/doifinder/10.1038/nn.2241.

T. E. Holy, C. Dulac, and M. Meister. Responses of Vomeronasal Neurons to Natural Stimuli. *Science*, 289(5484):1569–1572, sep 2000. ISSN 00368075. doi: 10.1126/science.289.5484.1569. URL http://www.sciencemag.org/cgi/doi/10.1126/science.289.5484.1569.

W. B. Hoover and R. P. Vertes. Anatomical analysis of afferent projections to the medial prefrontal cortex in the rat. *Brain Structure and Function*, 212(2):149–179, sep 2007. ISSN 1863-2653. doi: 10.1007/s00429-007-0150-4. URL http://link.springer.com/10.1007/s00429-007-0150-4.

R. Hudson and H. Distel. Pheromonal release of suckling in rabbits does not depend on the vomeronasal organ. *Physiology & Behavior*, 37(1):123–128, jan 1986. ISSN 00319384. doi: 10.1016/0031-9384(86)90394-X. URL http://linkinghub.elsevier.com/retrieve/pii/003193848690394X.

D. Huilgol and S. Tole. Cell migration in the developing rodent olfactory system. *Cellular and Molecular Life Sciences*, 73(13):2467–2490, 2016. ISSN 14209071. doi: 10.1007/s00018-016-2172-7.

D. Huilgol, S. Udin, T. Shimogori, B. Saha, A. Roy, S. Aizawa, R. F. Hevner, G. Meyer, T. Ohshima, S. J. Pleasure, Y. Zhao, and S. Tole. Dual origins of the mammalian accessory olfactory bulb revealed by an evolutionarily conserved migratory stream. *Nature Neuroscience*, 16(2):157–165, jan 2013. ISSN 1097-6256. doi: 10.1038/nn.3297. URL http://www.nature.com/doifinder/10.1038/nn.3297.

K. Hurley, H. Herbert, M. M. Moga, and C. B. Saper. Efferent projections of the infralimbic cortex of the rat. *Journal of Comparative Neurology*, 308:249–276, 1991. URL http://onlinelibrary.wiley.com/doi/10.1002/cne.903080210/abstract.

J. L. Hurst and R. J. Beynon. Scent wars: the chemobiology of competitive signalling in mice. *BioEssays*, 26(12):1288–1298, dec 2004. ISSN 0265-9247. doi: 10.1002/bies.20147. URL http://doi.wiley.com/10.1002/bies.20147.

S. Ikemoto. Dopamine reward circuitry: Two projection systems from the ventral midbrain to the nucleus accumbens-olfactory tubercle complex. *Brain Research Reviews*, 56(1):27–78, nov 2007. ISSN 01650173. doi: 10.1016/j.brainresrev.2007.05.004. URL http://linkinghub.elsevier.com/retrieve/pii/S0165017307000756.

K. Inaki, S. Nishimura, T. Nakashiba, S. Itohara, and Y. Yoshihara. Laminar organization of the developing lateral olfactory tract revealed by differential expression of cell recognition molecules. *The Journal of Comparative Neurology*, 479(3):243–256, nov 2004. ISSN 0021-9967. doi: 10.1002/cne.20270. URL http://doi.wiley.com/10.1002/cne.20270.

Y. Isogai, S. Si, L. Pont-Lezica, T. Tan, V. Kapoor, V. N. Murthy, and C. Dulac. Molecular organization of vomeronasal chemoreception. *Nature*, 478(7368):241–245, oct 2011. ISSN 1476-4687. doi: 10.1038/nature10437. URL http://www.nature.com/doifinder/10.1038/nature10437.

C. Jia, W. R. Chen, and G. M. Shepherd. Synaptic organization and neurotransmitters in the rat accessory olfactory bulb. *Journal of Neurophysiology*, 81(1):345–55, jan 1999. ISSN 0022-3077. URL http://www.ncbi.nlm.nih.gov/pubmed/9914294.

E. Jolkkonen, R. Miettinen, and A. Pitkänen. Projections from the amygdalo-piriform transition area to the amygdaloid complex: A PHA-L study in rat. *Journal of Comparative Neurology*, 432(4):440–465, 2001. ISSN 00219967. doi: 10.1002/cne.1113.

N. Kang, M. J. Baum, and J. A. Cherry. A direct main olfactory bulb projection to the "vomeronasal" amygdala in female mice selectively responds to volatile pheromones from males. *European Journal of Neuroscience*, 29(3):624–634, feb 2009. ISSN 0953816X. doi: 10.1111/j.1460-9568.2009.06638.x. URL http://doi.wiley.com/10.1111/j.1460-9568.2009.06638.x.

N. Kang, M. J. Baum, and J. A. Cherry. Different profiles of main and accessory olfactory bulb mitral/tufted cell projections revealed in mice using an anterograde tracer and a whole-mount, flattened cortex preparation. *Chemical Senses*, 36(3):251–60, mar 2011. ISSN 1464-3553. doi: 10.1093/chemse/bjq120. URL https://academic.oup.com/chemse/article-lookup/doi/10.1093/chemse/bjq120.

A. W. Kaur, T. Ackels, T. H. Kuo, A. Cichy, S. Dey, C. Hays, M. Kateri, D. W. Logan, T. F. Marton, M. Spehr, and L. Stowers. Murine pheromone proteins constitute a context-dependent combinatorial code governing multiple social behaviors. *Cell*, 157(3):676–688, 2014. ISSN 10974172. doi: 10.1016/j.cell.2014.02.025. URL http://dx.doi.org/10.1016/j.cell.2014.02.025.

L. M. Kay. Theta oscillations and sensorimotor performance. *Proceedings of the National Academy of Sciences*, 102(10):3863–3868, 2005. ISSN 0027-8424. doi: 10.1073/pnas.0407920102. URL http://www.pnas.org/cgi/doi/10.1073/pnas.0407920102.

L. M. Kay and J. Beshel. A beta oscillation network in the rat olfactory system during a 2-alternative choice odor discrimination task. *Journal of Neurophysiology*, 104(2):829–839, 2010. ISSN 1522-1598. doi: 10.1152/jn.00166.2010. URL http://jn.physiology.org/content/jn/104/2/829.full.pdf.

L. M. Kay and W. J. Freeman. Bidirectional processing in the olfactory-limbic axis during olfactory behavior. *Behavioral Neuroscience*, 112 (3):541–53, 1998. ISSN 0735-7044. doi: 10.1037/0735-7044.112.3.541. URL http://www.ncbi.nlm.nih.gov/pubmed/9676972.

L. M. Kay, J. Beshel, J. Brea, C. Martin, D. Rojas-Líbano, and N. Kopell. Olfactory oscillations: The what, how and what for. *Trends in Neurosciences*, 32(4):207–214, 2009. ISSN 0166-2236. doi: 10.1016/j.tins.2008.11.008. URL http://linkinghub.elsevier.com/retrieve/pii/S0166223609000253.

M. Keller, M. J. Baum, O. Brock, P. A. Brennan, and J. Bakker. The main and the accessory olfactory systems interact in the control of mate recognition and sexual behavior. *Behavioural brain research*, 200 (2):268–76, jun 2009. ISSN 1872-7549. URL http://www.ncbi.nlm.nih.gov/pubmed/19374011.

K. R. Kelliher. The combined role of the main olfactory and vomeronasal systems in social communication in mammals. *Hormones and Behavior*, 52(5):561–570, 2007. doi: 10.1016/j.yhbeh.2007.08.012. The. URL http://www.sciencedirect.com/science/article/pii/S0018506X07001985.

S. Kemppainen, E. Jolkkonen, and A. Pitkänen. Projections from the posterior cortical nucleus of the amygdala to the hippocampal formation and parahippocampal region in rat. *Hippocampus*, 12(6):735–755, jan 2002. ISSN 1050-9631. doi: 10.1002/hipo.10020. URL http://doi.wiley.com/10.1002/hipo.10020.

A. Kepecs, N. Uchida, and Z. F. Mainen. The Sniff as a Unit of Ol-
factory Processing. *Chemical Senses*, 31:167–179, 2006. doi: 10.1093/
chemse/bjj016.

A. Kepecs, N. Uchida, and Z. F. Mainen. Rapid and precise control
of sniffing during olfactory discrimination in rats. *Journal of neuro-
physiology*, 98(1):205–213, 2007. ISSN 0022-3077. doi: 10.1152/jn.
00071.2007.

G. A. Kevetter and S. S. Winans. Connections of the corticomedial
amygdala in the golden hamster. II. Efferents of the "olfactory amy-
gdala". *The Journal of Comparative Neurology*, 197(1):99–111, mar
1981a. ISSN 0021-9967. doi: 10.1002/cne.901970108. URL http:
//doi.wiley.com/10.1002/cne.901970108.

G. A. Kevetter and S. S. Winans. Connections of the corticomedial
amygdala in the golden hamster. I. Efferents of the "vomeronasal
amygdala". *The Journal of comparative neurology*, 197(1):81–98, mar
1981b. ISSN 0021-9967. doi: 10.1002/cne.901970107. URL http://
doi.wiley.com/10.1002/cne.901970107.

J. Kim, X. Zhang, S. Muralidhar, S. A. LeBlanc, and S. Tonegawa.
Basolateral to Central Amygdala Neural Circuits for Appetitive Be-
haviors. *Neuron*, 93(6):1464–1479.e5, mar 2017. ISSN 08966273. doi:
10.1016/j.neuron.2017.02.034. URL http://www.cell.com/neuron/
fulltext/S0896-6273(17)30142-3.

H. Kimoto, S. Haga, K. Sato, and K. Touhara. Sex-specific peptides
from exocrine glands stimulate mouse vomeronasal sensory neur-
ons. *Nature*, 437(7060):898–901, oct 2005. ISSN 0028-0836. doi:
10.1038/nature04033. URL http://www.nature.com/doifinder/10.
1038/nature04033.

K. Kobayakawa, R. Kobayakawa, H. Matsumoto, Y. Oka, T. Imai,
M. Ikawa, M. Okabe, T. Ikeda, S. Itohara, T. Kikusui, K. Mori, and
H. Sakano. Innate versus learned odour processing in the mouse
olfactory bulb. *Nature*, 450(7169):503–508, nov 2007. ISSN 1476-
4687. doi: 10.1038/nature06281. URL http://www.nature.com/
doifinder/10.1038/nature06281.

S. Kollack-Walker and S. W. Newman. Mating-induced ex-
pression of c-fos in the male Syrian hamster brain: Role of
experience, pheromones, and ejaculations. *Journal of Neuro-
biology*, 32(5):481–501, may 1997. ISSN 0022-3034. doi:
10.1002/(SICI)1097-4695(199705)32:5<481::AID-NEU4>3.0.CO;2-1.
URL http://doi.wiley.com/10.1002/%28SICI%291097-4695%
28199705%2932%3A5%3C481%3A%3AAID-NEU4%3E3.0.CO%3B2-1.

J. E. Krettek and J. L. Price. A description of the amygdaloid com-
plex in the rat and cat with observations on intra-amygdaloid ax-
onal connections. *The Journal of Comparative Neurology*, 178(2):255–
279, mar 1978. ISSN 0021-9967. doi: 10.1002/cne.901780205. URL
http://doi.wiley.com/10.1002/cne.901780205.

S. Kullback and R. Leibler. On information and sufficiency. *The Annals of Mathematical Statistics*, 22(1):79–86, 1951. doi: doi:10.1214/aoms/1177729694.

J. P. Lachaux, E. Rodriguez, J. Martinerie, and F. J. Varela. Measuring phase synchrony in brain signals. *Human Brain Mapping*, 8(4):194–208, 1999. ISSN 10659471. doi: 10.1002/(SICI)1097-0193(1999)8:4<194::AID-HBM4>3.0.CO;2-C. URL http://doi.wiley.com/10.1002/%28SICI%291097-0193%281999%298%3A4%3C194%3A%3AAID-HBM4%3E3.0.CO%3B2-C.

E. Lanuza and M. Halpern. Afferent and efferent connections of the nucleus sphericus in the snake Thamnophis sirtalis: Convergence of olfactory and vomeronasal information in the lateral cortex and the amygdala. *The Journal of Comparative Neurology*, 385(4):627–640, sep 1997. ISSN 0021-9967. doi: 10.1002/(SICI)1096-9861(19970908)385:4<627::AID-CNE8>3.0.CO;2-5. URL http://doi.wiley.com/10.1002/%28SICI%291096-9861%2819970908%29385%3A4%3C627%3A%3AAID-CNE8%3E3.0.CO%3B2-5.

E. Lanuza and M. Halpern. Efferents and centrifugal afferents of the main and accessory olfactory bulbs in the snake Thamnophis sirtalis. *Brain, Behavior and Evolution*, 51(1):1–22, 1998. ISSN 0006-8977. URL http://www.ncbi.nlm.nih.gov/pubmed/9435967.

E. Lanuza and F. Martínez-García. Evolution of septal nuclei. In M. D. Binder, N. Hirokawa, and D. Windhorst, editors, *Encyclopedia of Neurocience*, pages 1270–1278. Springer, Berlin, 2009.

E. Lanuza, C. Font, A. Martínez-Marcos, and F. Martínez-García. Amygdalo-hypothalamic projections in the lizard-Podarcis hispanica: A combined anterograde and retrograde tracing study. *The Journal of Comparative Neurology*, 384(4):537–555, aug 1997. ISSN 0021-9967. doi: 10.1002/(SICI)1096-9861(19970811)384:4<537::AID-CNE4>3.0.CO;2-3. URL http://doi.wiley.com/10.1002/%28SICI%291096-9861%2819970811%29384%3A4%3C537%3A%3AAID-CNE4%3E3.0.CO%3B2-3.

E. Lanuza, A. Martín-Sánchez, P. Marco-Manclús, B. Cádiz-Moretti, L. Fortes-Marco, A. Hernández-Martínez, L. McLean, R. J. Beynon, J. L. Hurst, and F. Martínez-García. Sex pheromones are not always attractive: Changes induced by learning and illness in mice. *Animal Behaviour*, 97:265–272, 2014. ISSN 00033472. doi: 10.1016/j.anbehav.2014.08.011.

J. A. Larriva-Sahd. The accessory olfactory bulb in the adult rat: A cytological study of its cell types, neuropil, neuronal modules, and interactions with the main olfactory system. *The Journal of Comparative Neurology*, 510(3):309–350, sep 2008. ISSN 1096-9861. doi: 10.1002/cne.21790. URL http://doi.wiley.com/10.1002/cne.21790.

S. B. Laughlin and T. J. Sejnowski. Communication in Neuronal Networks. *Science*, 301(5641):1870–1874, sep 2003. ISSN 0036-8075. doi: 10.1126/science.1089662. URL http://www.sciencemag.org/cgi/doi/10.1126/science.1089662.

J. E. LeDoux. Emotion Circuits in the Brain. *Annual Review of Neuroscience*, 23(1):155–184, mar 2000. doi: 10.1146/annurev.neuro.23.1.155. URL http://www.ncbi.nlm.nih.gov/pubmed/10845062.

T. Leinders-Zufall, A. P. Lane, A. C. Puche, W. Ma, M. V. Novotny, M. T. Shipley, and F. Zufall. Ultrasensitive pheromone detection by mammalian vomeronasal neurons. *Nature*, 405(6788):792–796, jun 2000. ISSN 00280836. doi: 10.1038/35015572. URL http://www.nature.com/doifinder/10.1038/35015572.

O. Lévai, T. Feistel, H. Breer, and J. Strotmann. Cells in the vomeronasal organ express odorant receptors but project to the accessory olfactory bulb. *The Journal of Comparative Neurology*, 498(4):476–490, oct 2006. ISSN 0021-9967. doi: 10.1002/cne.21067. URL http://doi.wiley.com/10.1002/cne.21067.

C.-I. Li, T. L. Maglinao, and L. K. Takahashi. Medial Amygdala Modulation of Predator Odor-Induced Unconditioned Fear in the Rat. *Behavioral Neuroscience*, 118(2):324–332, apr 2004. ISSN 0735-7044. doi: 10.1037/0735-7044.118.2.324. URL http://doi.apa.org/getdoi.cfm?doi=10.1037/0735-7044.118.2.324.

X. Li, X. Yao, J. Fox, and J. G. Jefferys. Interaction dynamics of neuronal oscillations analysed using wavelet transforms. *Journal of Neuroscience Methods*, 160(1):178–185, 2007. ISSN 01650270. doi: 10.1016/j.jneumeth.2006.08.006. URL http://linkinghub.elsevier.com/retrieve/pii/S0165027006003979.

G. Licht and M. Meredith. Convergence of main and accessory olfactory pathways onto single neurons in the hamster amygdala. *Experimental Brain Research*, 69:7–18, 1987. URL http://link.springer.com/article/10.1007/BF00247024.

D. Lin, M. P. Boyle, P. Dollar, H. Lee, P. Perona, E. S. Lein, and D. J. Anderson. Functional identification of an aggression locus in the mouse hypothalamus. *Nature*, 470(7333):221–226, feb 2011. ISSN 1476-4687. doi: 10.1038/nature09736. URL http://www.nature.com/doifinder/10.1038/nature09736.

D. Y. Lin, S.-Z. Zhang, E. Block, and L. C. Katz. Encoding social signals in the mouse main olfactory bulb. *Nature*, 434(7032):470–477, 2005. ISSN 0028-0836. doi: 10.1038/nature03414. URL http://www.nature.com/nature/journal/v434/n7032/pdf/nature03414.pdf.

Y. Liu, X. S. Liang, and R. H. Weisberg. Rectification of the bias in the wavelet power spectrum. *Journal of Atmospheric and Oceanic Technology*, 24(12):2093–2102, 2007. ISSN 07390572. doi: 10.1175/2007JTECHO511.1. URL http://journals.ametsoc.org/doi/abs/10.1175/2007JTECHO511.1.

A. H. Lohman and W. J. Smeets. Overview of the Main and Accessory Olfactory Bulb Projections in Reptiles. *Brain, Behavior and Evolution*, 41(3-5):147–155, jan 1993. ISSN 0006-8977. doi: 10.1159/000113832. URL http://www.karger.com/?doi=10.1159/000113832.

D. E. Lomas and E. B. Keverne. Role of the vomeronasal organ and prolactin in the acceleration of puberty in female mice. *Journal of reproduction and fertility*, 66(1):101–107, sep 1982. ISSN 1470-1626. doi: 10.1530/jrf.0.0660101. URL http://www.ncbi.nlm.nih.gov/pubmed/6889647.

M. Luo and L. C. Katz. Encoding pheromonal signals in the mammalian vomeronasal system. *Current Opinion in Neurobiology*, 14(4): 428–434, 2004. ISSN 09594388. doi: 10.1016/j.conb.2004.07.001.

M. Luo, M. S. Fee, and L. C. Katz. Encoding Pheromonal Signals in the Accessory Olfactory Bulb of Behaving Mice. *Science*, 299(5610): 1196–1201, feb 2003. ISSN 1095-9203. doi: 10.1126/science.1082133. URL http://linkinghub.elsevier.com/retrieve/pii/S0959438.

F. Macrides and S. L. Chorover. Olfactory Bulb Units: Activity Correlated with Inhalation Cycles and Odor Quality. *Science*, 175(4017): 84–87, jan 1972. ISSN 0036-8075. doi: 10.1126/science.175.4017. 84. URL http://www.sciencemag.org/cgi/doi/10.1126/science.175.4017.84.

K. Majak and A. Pitkänen. Projections from the periamygdaloid cortex to the amygdaloid complex, the hippocampal formation, and the parahippocampal region: A PHA-L study in the rat. *Hippocampus*, 13(8):922–942, 2003. ISSN 10509631. doi: 10.1002/hipo.10134. URL http://doi.wiley.com/10.1002/hipo.10134.

K. Majak, M. Pikkarainen, S. Kemppainen, E. Jolkkonen, and A. Pitkänen. Projections from the amygdaloid complex to the claustrum and the endopiriform nucleus: a Phaseolus vulgaris leucoagglutinin study in the rat. *The Journal of comparative neurology*, 451 (3):236–49, sep 2002. ISSN 0021-9967. doi: 10.1002/cne.10346. URL http://www.ncbi.nlm.nih.gov/pubmed/12210136.

V. S. Mandiyan, J. K. Coats, and N. M. Shah. Deficits in sexual and aggressive behaviors in Cnga2 mutant mice. *Nature Neuroscience*, 8 (12):1660–1662, dec 2005. ISSN 1097-6256. doi: 10.1038/nn1589. URL http://www.nature.com/doifinder/10.1038/nn1589.

W. F. Maragos, S. W. Newman, M. N. Lehman, and J. B. Powers. Neurons of origin and fiber trajectory of amygdalofugal projections to the medial preoptic area in syrian hamsters. *The Journal of Comparative Neurology*, 280(1):59–71, feb 1989. ISSN 0021-9967. doi: 10.1002/cne. 902800106. URL http://doi.wiley.com/10.1002/cne.902800106.

P. M. Maras and A. Petrulis. The posteromedial cortical amygdala regulates copulatory behavior, but not sexual odor preference, in the male Syrian hamster (Mesocricetus auratus). *Neuroscience*, 156(3):425–35, oct 2008. ISSN 0306-4522. doi: 10.1016/j. neuroscience.2008.08.004. URL http://linkinghub.elsevier.com/retrieve/pii/S0306452208011858.

P. M. Maras and A. Petrulis. Anatomical connections between the anterior and posterodorsal sub-regions of the medial amygdala: Integration of odor and hormone signals. *Neuroscience*, 170(2):

610–622, oct 2010a. ISSN 03064522. doi: 10.1016/j.neuroscience. 2010.06.075. URL http://linkinghub.elsevier.com/retrieve/pii/S0306452210009474.

P. M. Maras and A. Petrulis. The anterior medial amygdala transmits sexual odor information to the posterior medial amygdala and related forebrain nuclei. *European Journal of Neuroscience*, 32(3):469–482, aug 2010b. ISSN 0953816X. doi: 10.1111/j.1460-9568.2010.07289.x. URL http://doi.wiley.com/10.1111/j.1460-9568.2010.07289.x.

P. M. Maras and A. Petrulis. Lesions that functionally disconnect the anterior and posterodorsal sub-regions of the medial amygdala eliminate opposite-sex odor preference in male Syrian hamsters (Mesocricetus auratus). *Neuroscience*, 165(4):1052–1062, feb 2010c. ISSN 03064522. doi: 10.1016/j.neuroscience.2009.11.024. URL http://linkinghub.elsevier.com/retrieve/pii/S0306452209018703.

K. L. Martel and M. J. Baum. A centrifugal pathway to the mouse accessory olfactory bulb from the medial amygdala conveys gender-specific volatile pheromonal signals. *European Journal of Neuroscience*, 29(2):368–376, 2009. ISSN 0953816X. doi: 10.1111/j.1460-9568.2008.06564.x. URL http://onlinelibrary.wiley.com/doi/10.1111/j.1460-9568.2008.06564.x/full.

C. Martin and N. Ravel. Beta and gamma oscillatory activities associated with olfactory memory tasks: different rhythms for different functional networks? *Frontiers in behavioral neuroscience*, 8 (June):218, jun 2014. ISSN 1662-5153. doi: 10.3389/fnbeh.2014.00218. URL http://journal.frontiersin.org/article/10.3389/fnbeh.2014.00218/abstract.

C. Martin, R. Gervais, E. Hugues, B. Messaoudi, and N. Ravel. Learning Modulation of Odor-Induced Oscillatory Responses in the Rat Olfactory Bulb: A Correlate of Odor Recognition? *Journal of Neuroscience*, 24(2):389–397, jan 2004. ISSN 0270-6474. doi: 10.1523/JNEUROSCI.3433-03.2004. URL http://www.jneurosci.org/cgi/doi/10.1523/JNEUROSCI.3433-03.2004.

A. Martín-Sánchez, L. McLean, R. J. Beynon, J. L. Hurst, G. Ayala, E. Lanuza, and F. Martínez-García. From sexual attraction to maternal aggression: when pheromones change their behavioural significance. *Hormones and Behavior*, 68:65–76, feb 2015. ISSN 10956867. doi: 10.1016/j.yhbeh.2014.08.007. URL http://linkinghub.elsevier.com/retrieve/pii/S0018506X14001640.

R. C. R. Martínez, E. F. Carvalho-Netto, É. R. Ribeiro-Barbosa, M. V. C. Baldo, and N. S. Canteras. Amygdalar roles during exposure to a live predator and to a predator-associated context. *Neuroscience*, 172:314–328, jan 2011. ISSN 03064522. doi: 10.1016/j.neuroscience.2010.10.033. URL http://linkinghub.elsevier.com/retrieve/pii/S0306452210013631.

F. Martinez-Garcia, F. E. Olucha, V. Teruel, M. J. Lorente, and W. K. Schwerdtfeger. Afferent and efferent connections of the olfactory bulbs in the lizardPodarcis hispanica. *The Journal of Comparative Neurology*, 305(2):337–347, mar 1991. ISSN 0021-9967. doi:

10.1002/cne.903050214. URL http://doi.wiley.com/10.1002/cne.903050214.

F. Martínez-García, F. E. Olucha, V. Teruel, and M. J. Lorente. Fiber connections of the amygdaloid formation of the lizard podarcis. *Brain, Behavior and Evolution*, 41(3-5):156–162, jan 1993. ISSN 00068977. doi: 10.1159/000113833. URL http://www.karger.com/?doi=10.1159/000113833.

F. Martínez-García, A. Novejarque, and E. Lanuza. Evolution of the amygdala in vertebrates. In J. H. Kaas, editor, *Evolution of Nervous Systems*, chapter 15, pages 313–392. Academic Press, Oxford, 2007. ISBN 9780123750808. doi: 10.1016/B0-12-370878-8/00139-7. URL http://www.sciencedirect.com/science/article/pii/B0123708788001397.

F. Martínez-García, J. Martínez-Ricós, C. Agustín-Pavón, J. Martínez-Hernández, A. Novejarque, and E. Lanuza. Refining the dual olfactory hypothesis: Pheromone reward and odour experience. *Behavioural Brain Research*, 200(2):277–286, jun 2009. ISSN 01664328. doi: 10.1016/j.bbr.2008.10.002. URL http://linkinghub.elsevier.com/retrieve/pii/S016643280800555X.

F. Martínez-García, A. Novejarque, N. Gutiérrez-Castellanos, and E. Lanuza. Piriform Cortex and Amygdala. In C. Watson, G. Paxinos, and L. Puelles, editors, *The Mouse Nervous System*, chapter 6, pages 140–172. Elsevier, 2012. ISBN 9780123694973. doi: 10.1016/B978-0-12-369497-3.10006-8. URL http://linkinghub.elsevier.com/retrieve/pii/B9780123694973100068.

J. Martínez-Hernández, E. Lanuza, and F. Martínez-García. Selective dopaminergic lesions of the ventral tegmental area impair preference for sucrose but not for male sexual pheromones in female mice. *European Journal of Neuroscience*, 24(3):885–893, aug 2006. ISSN 0953816X. doi: 10.1111/j.1460-9568.2006.04944.x. URL http://doi.wiley.com/10.1111/j.1460-9568.2006.04944.x.

A. Martínez-Marcos. On the organization of olfactory and vomeronasal cortices. *Progress in Neurobiology*, 87(1):21–30, jan 2009. ISSN 0301-0082. doi: 10.1016/j.pneurobio.2008.09.010. URL http://www.ncbi.nlm.nih.gov/pubmed/18929620.

A. Martínez-Marcos and M. Halpern. Differential projections from the anterior and posterior divisions of the accessory olfactory bulb to the medial amygdala in the opossum, Monodelphis domestica. *The European journal of neuroscience*, 11(11):3789–99, nov 1999a. ISSN 0953-816X. URL http://www.ncbi.nlm.nih.gov/pubmed/10583468.

A. Martínez-Marcos and M. Halpern. Differential centrifugal afferents to the anterior and posterior accessory olfactory bulb. *Neuroreport*, 10(10):2011–5, jul 1999b. ISSN 0959-4965. URL http://www.ncbi.nlm.nih.gov/pubmed/10424666.

A. Martínez-Marcos and M. Halpern. Efferent connections of the main olfactory bulb in the opossum (Monodelphis domestica): A

characterization of the olfactory entorhinal cortex in a marsupial. *Neuroscience Letters*, 395(1):51–56, feb 2006. ISSN 03043940. doi: 10. 1016/j.neulet.2005.10.052. URL http://linkinghub.elsevier.com/ retrieve/pii/S0304394005012334.

A. Martínez-Marcos, E. Lanuza, and M. Halpern. Organization of the ophidian amygdala: Chemosensory pathways to the hypothalamus. *Journal of Comparative Neurology*, 412(1):51–68, 1999. ISSN 00219967. doi: 10.1002/(SICI)1096-9861(19990913)412:1<51:: AID-CNE4>3.0.CO;2-M.

A. Martínez-Marcos, I. Ubeda-Bañón, and M. Halpern. Neural substrates for tongue-flicking behavior in snakes. *Journal of Comparative Neurology*, 432(1):75–87, mar 2001. ISSN 00219967. doi: 10.1002/cne.1089. URL http://doi.wiley.com/10.1002/cne.1089.

A. Martínez-Marcos, E. Lanuza, and M. Halpern. Neural substrates for processing chemosensory information in snakes. In *Brain Research Bulletin*, volume 57, pages 543–546, 2002. ISBN 0361-9230 (Print)\n0361-9230 (Linking). doi: 10.1016/S0361-9230(01) 00686-4. URL http://linkinghub.elsevier.com/retrieve/pii/ S0361923001006864.

J. Martínez-Ricós, C. Agustín-Pavón, E. Lanuza, and F. Martínez-García. Intraspecific communication through chemical signals in female mice: Reinforcing properties of involatile male sexual pheromones. *Chemical Senses*, 32(2):139–148, 2007. ISSN 0379864X. doi: 10.1093/chemse/bjl039. URL https://academic.oup.com/chemse/ article-lookup/doi/10.1093/chemse/bjl039.

J. Martínez-Ricós, C. Agustín-Pavón, E. Lanuza, and F. Martínez-García. Role of the vomeronasal system in intersexual attraction in female mice. *Neuroscience*, 153(2):383–395, may 2008. ISSN 03064522. doi: 10.1016/j.neuroscience.2008.02.002. URL http://linkinghub. elsevier.com/retrieve/pii/S0306452208002145.

R. E. McCotter. The Connection Of The Vomeronasal Nerves With The Accessory Olfactory Bulb In The Opossum And Other Mammals. *The Anatomical Record*, 6(8):299–318, 1912.

A. J. McDonald. Is There an Amygdala and How Far Does It Extend? *Annals of the New York Academy of Sciences*, 985(1):1–21, jan 2003. ISSN 00778923. doi: 10.1111/j.1749-6632.2003.tb07067.x. URL http://doi. wiley.com/10.1111/j.1749-6632.2003.tb07067.x.

A. J. McDonald, F. Mascagni, and L. Guo. Projections of the medial and lateral prefrontal cortices to the amygdala: a Phaseolus vulgaris leucoagglutinin study in the rat. *Neuroscience*, 71:55–75, 1996. URL http://www.sciencedirect.com/science/article/pii/ 0306452295004173.

A. J. McDonald, J. F. Muller, and F. Mascagni. GABAergic innervation of alpha type II calcium/calmodulin-dependent protein kinase immunoreactive pyramidal neurons in the rat basolateral amygdala. *Journal of Comparative Neurology*, 446(3):199–218, may 2002. ISSN

00219967. doi: 10.1002/cne.10204. URL http://www.ncbi.nlm.nih.gov/pubmed/11932937.

L. Medina, I. Legaz, G. González, F. De Castro, J. L. Rubenstein, and L. Puelles. Expression of Dbx1 , Neurogenin 2 , Semaphorin 5A , Cadherin 8 , and Emx1 distinguish ventral and lateral pallial histogenetic divisions in the developing mouse claustroamygdaloid complex. *Journal of Comparative Neurology*, 474(4):504–523, jul 2004. ISSN 00219967. doi: 10.1002/cne.20141. URL http://doi.wiley.com/10.1002/cne.20141.

J. P. Meeks, H. A. Arnson, and T. E. Holy. Representation and transformation of sensory information in the mouse accessory olfactory system. *Nature Neuroscience*, 13(6):723–730, jun 2010. ISSN 1097-6256. doi: 10.1038/nn.2546. URL http://dx.doi.org/10.1038/nn.2546.

M. Meredith. Chronic recording of vomeronasal pump activation in awake behaving hamsters. *Physiology & Behavior*, 56(2):345–354, aug 1994. ISSN 00319384. doi: 10.1016/0031-9384(94)90205-4. URL http://linkinghub.elsevier.com/retrieve/pii/0031938494902054.

M. Meredith and R. J. O'Connell. Efferent control of stimulus access to the hamster vomeronasal organ. *The Journal of Physiology*, 286(1):301–316, jan 1979. ISSN 0022-3751. doi: 10.1113/jphysiol.1979.sp012620. URL http://doi.wiley.com/10.1113/jphysiol.1979.sp012620.

M. Meredith and J. M. Westberry. Distinctive responses in the medial amygdala to same-species and different-species pheromones. *The Journal of Neuroscience*, 24(25):5719–5725, jun 2004. ISSN 0270-6474. doi: 10.1523/JNEUROSCI.1139-04.2004. URL http://www.jneurosci.org/cgi/doi/10.1523/JNEUROSCI.1139-04.2004.

M. Meurisse, E. Chaillou, and F. Lévy. Afferent and efferent connections of the cortical and medial nuclei of the amygdala in sheep. *Journal of Chemical Neuroanatomy*, 37(2):87–97, mar 2009. ISSN 1873-6300. doi: 10.1016/j.jchemneu.2008.09.001. URL http://www.ncbi.nlm.nih.gov/pubmed/18835351.

K. A. Miczek, S. C. Maxson, E. W. Fish, and S. Faccidomo. Aggressive behavioral phenotypes in mice. *Behavioural Brain Research*, 125 (1-2):167–181, 2001. ISSN 01664328. doi: 10.1016/S0166-4328(01)00298-4. URL http://www.sciencedirect.com/science/article/pii/S0166432801002984.

S. W. Mitra, E. Hoskin, J. Yudkovitz, L. Pear, H. A. Wilkinson, S. Hayashi, D. W. Pfaff, S. Ogawa, S. P. Rohrer, J. M. Schaeffer, B. S. McEwen, and S. E. Alves. Immunolocalization of Estrogen Receptor β in the Mouse Brain: Comparison with Estrogen Receptor α. *Endocrinology*, 144(5):2055–2067, may 2003. ISSN 0013-7227. doi: 10.1210/en.2002-221069. URL https://academic.oup.com/endo/article-lookup/doi/10.1210/en.2002-221069.

P. Mombaerts. Genes and ligands for odorant, vomeronasal and taste receptors. *Nature Reviews Neuroscience*, 5(4):263–78, apr 2004. ISSN 1471-003X. doi: 10.1038/nrn1365. URL http://www.ncbi.nlm.nih.gov/pubmed/15034552.

J. Moncho-Bogani, E. Lanuza, A. Hernández-Martínez, A. Novejarque, and F. Martínez-García. Attractive properties of sexual pheromones in mice. *Physiology & Behavior*, 77(1):167–176, sep 2002. ISSN 00319384. doi: 10.1016/S0031-9384(02)00842-9. URL http://linkinghub.elsevier.com/retrieve/pii/S0031938402008429.

J. Moncho-Bogani, F. Martínez-García, A. Novejarque, and E. Lanuza. Attraction to sexual pheromones and associated odorants in female mice involves activation of the reward system and basolateral amygdala. *European Journal of Neuroscience*, 21(8):2186–2198, apr 2005. ISSN 0953816X. doi: 10.1111/j.1460-9568.2005.04036.x. URL http://doi.wiley.com/10.1111/j.1460-9568.2005.04036.x.

J. D. Moore, D. Kleinfeld, and F. Wang. How the brainstem controls orofacial behaviors comprised of rhythmic actions. *Trends in Neurosciences*, 37(7):370–380, 2014. ISSN 1878108X. doi: 10.1016/j.tins.2014.05.001. URL http://linkinghub.elsevier.com/retrieve/pii/S0166223614000769.

N. Moreno and A. González. Evolution of the amygdaloid complex in vertebrates, with special reference to the anamnio-amniotic transition. *Journal of Anatomy*, 211(2):151–163, aug 2007. ISSN 00218782. doi: 10.1111/j.1469-7580.2007.00780.x. URL http://doi.wiley.com/10.1111/j.1469-7580.2007.00780.x.

K. Mori. Piriform Cortex and Olfactory Tubercle. In K. Mori, editor, *The Olfactory System*, chapter 8, pages 161–175. Springer Japan, Tokyo, 2014. doi: 10.1007/978-4-431-54376-3_8. URL http://link.springer.com/10.1007/978-4-431-54376-3{_}8.

K. Mori, H. Manabe, K. Narikiyo, and N. Onisawa. Olfactory consciousness and gamma oscillation couplings across the olfactory bulb, olfactory cortex, and orbitofrontal cortex. *Frontiers in Psychology*, 4(October):1–13, 2013. ISSN 1664-1078. doi: 10.3389/fpsyg.2013.00743. URL http://journal.frontiersin.org/article/10.3389/fpsyg.2013.00743/abstract.

S. C. Motta, M. Goto, F. V. Gouveia, M. V. C. Baldo, N. S. Canteras, and L. W. Swanson. Dissecting the brain's fear system reveals the hypothalamus is critical for responding in subordinate conspecific intruders. *Proceedings of the National Academy of Sciences of the United States of America*, 106(12):4870–5, mar 2009. ISSN 1091-6490. doi: 10.1073/pnas.0900939106. URL http://www.pnas.org/cgi/doi/10.1073/pnas.0900939106.

K. Nader, P. Majidishad, P. Amorapanth, and J. E. LeDoux. Damage to the Lateral and Central, but Not Other, Amygdaloid Nuclei Prevents the Acquisition of Auditory Fear Conditioning. *Learning & Memory*, 8(3):156–163, may 2001. ISSN 10720502. doi: 10.1101/lm.38101. URL http://www.learnmem.org/cgi/doi/10.1101/lm.38101.

K. R. Neville and L. B. Haberly. Beta and gamma oscillations in the olfactory system of the urethane-anesthetized rat. *Journal of Neurophysiology*, 90(6):3921–3930, 2003. ISSN 0022-3077. doi: 10.1152/jn.00475.2003. URL http://www.ncbi.nlm.nih.gov/pubmed/12917385.

S. W. Newman. The medial extended amygdala in male reproductive behavior. A node in the mammalian social behavior network. *Annals of the New York Academy of Sciences*, 877(1):242–257, jun 1999. ISSN 00778923. doi: 10.1111/j.1749-6632.1999.tb09271.x. URL http://doi.wiley.com/10.1111/j.1749-6632.1999.tb09271.x.

K. Niimi, S. Horie, M. Yokosuka, F. Kawakami-Mori, K. Tanaka, H. Fukayama, and Y. Sahara. Heterogeneous electrophysiological and morphological properties of neurons in the mouse medial amygdala in vitro. *Brain Research*, 1480:41–52, oct 2012. ISSN 00068993. doi: 10.1016/j.brainres.2012.08.050. URL http://www.ncbi.nlm.nih.gov/pubmed/22960119.

F. Nodari, F.-F. Hsu, X. Fu, T. F. Holekamp, L.-F. Kao, J. Turk, and T. E. Holy. Sulfated steroids as natural ligands of mouse pheromone-sensing neurons. *The Journal of neuroscience : the official journal of the Society for Neuroscience*, 28(25):6407–6418, jun 2008. ISSN 0270-6474. doi: 10.1523/JNEUROSCI.1425-08.2008. URL http://www.jneurosci.org/cgi/doi/10.1523/JNEUROSCI.1425-08.2008.

A. Novejarque, N. Gutiérrez-Castellanos, E. Lanuza, and F. Martínez-García. Amygdaloid projections to the ventral striatum in mice: direct and indirect chemosensory inputs to the brain reward system. *Frontiers in Neuroanatomy*, 5(August):1–20, jan 2011. ISSN 1662-5129. doi: 10.3389/fnana.2011.00054. URL http://journal.frontiersin.org/article/10.3389/fnana.2011.00054/abstract.

R. J. O'Connell and M. Meredith. Effects of volatile and nonvolatile chemical signals on male sex behaviors mediated by the main and accessory olfactory systems. *Behavioral Neuroscience*, 98(6):1083–1093, dec 1984. ISSN 0735-7044. doi: 10.1037/0735-7044.98.6.1083. URL http://content.apa.org/journals/bne/98/6/1083.

M. Otero-García, A. Martín-Sánchez, L. Fortes-Marco, J. Martínez-Ricós, C. Agustín-Pavón, E. Lanuza, and F. Martínez-García. Extending the socio-sexual brain: Arginine-vasopressin immunoreactive circuits in the telencephalon of mice. *Brain Structure and Function*, 219(3):1055–1081, may 2014. ISSN 18632661. doi: 10.1007/s00429-013-0553-3. URL http://link.springer.com/10.1007/s00429-013-0553-3.

O. P. Ottersen. Connections of the amygdala of the rat. IV: Corticoamygdaloid and intraamygdaloid connections as studied with axonal transport of horseradish peroxidase. *The Journal of Comparative Neurology*, 205(1):30–48, feb 1982. ISSN 0021-9967. doi: 10.1002/cne.902050104. URL http://doi.wiley.com/10.1002/cne.902050104.

T. Otto, G. Cousens, and C. Herzog. Behavioral and neuropsychological foundations of olfactory fear conditioning. *Behavioural Brain Research*, 110(1-2):119–128, jun 2000. ISSN 01664328. doi: 10.1016/S0166-4328(99)00190-4. URL http://linkinghub.elsevier.com/retrieve/pii/S0166432899001904.

P. Paoletti, A. M. Vergnano, B. Barbour, and M. Casado. Zinc at glutamatergic synapses. *Neuroscience*, 158(1):126–136, jan 2009. ISSN

03064522. doi: 10.1016/j.neuroscience.2008.01.061. URL http://dx.doi.org/10.1016/j.neuroscience.2008.01.061.

F. Papes, D. W. Logan, and L. Stowers. The vomeronasal organ mediates interspecies defensive behaviors through detection of protein pheromone homologs. *Cell*, 141(4):692–703, may 2010. ISSN 1097-4172. doi: 10.1016/j.cell.2010.03.037. URL http://linkinghub.elsevier.com/retrieve/pii/S0092867410003557.

S. K. Park, J. H. Kim, E. S. Yang, D. K. Ahn, C. Moon, and Y. C. Bae. Ultrastructure and synaptic connectivity of main and accessory olfactory bulb efferent projections terminating in the rat anterior piriform cortex and medial amygdala. *Brain Structure and Function*, 219(5):1603–1613, sep 2014. ISSN 1863-2653. doi: 10.1007/s00429-013-0588-5. URL http://link.springer.com/10.1007/s00429-013-0588-5.

J. A. Parkinson, T. W. Robbins, and B. J. Everitt. Dissociable roles of the central and basolateral amygdala in appetitive emotional learning. *European Journal of Neuroscience*, 12(1):405–413, 2000. ISSN 0953816X. doi: 10.1046/j.1460-9568.2000.00960.x.

G. Paxinos and K. B. J. Franklin. *Mouse Brain in Stereotaxic Coordinates*, volume 2nd. Academic Press, 2004. ISBN 0125476361. doi: 10.1016/S0306-4530(03)00088-X. URL http://dx.doi.org/10.1016/S0306-4530(03)00088-X.

G. D. Petrovich, P. Y. Risold, and L. W. Swanson. Organization of projections from the basomedial nucleus of the amygdala: A PHAL study in the rat. *The Journal of Comparative Neurology*, 374(3):387–420, oct 1996. ISSN 0021-9967. doi: 10.1002/(SICI)1096-9861(19961021)374:3<387::AID-CNE6>3.0.CO;2-Y. URL http://onlinelibrary.wiley.com/doi/10.1002/(SICI)1096-9861(19961021)374:3%3C387::AID-CNE6%3E3.0.CO;2-Y/abstract.

G. D. Petrovich, N. S. Canteras, and L. W. Swanson. Combinatorial amygdalar inputs to hippocampal domains and hypothalamic behavior systems. *Brain Research Reviews*, 38(1-2):247–289, dec 2001. ISSN 01650173. doi: 10.1016/S0165-0173(01)00080-7. URL http://linkinghub.elsevier.com/retrieve/pii/S0165017301000807.

A. Petrulis. Neural mechanisms of individual and sexual recognition in Syrian hamsters (Mesocricetus auratus). *Behavioural Brain Research*, 200(2):260–267, jun 2009. ISSN 01664328. doi: 10.1016/j.bbr.2008.10.027. URL http://linkinghub.elsevier.com/retrieve/pii/S0166432808005949.

A. Petrulis. Chemosignals, hormones and mammalian reproduction. *Hormones and Behavior*, 63(5):723–741, may 2013. ISSN 0018506X. doi: 10.1016/j.yhbeh.2013.03.011. URL http://linkinghub.elsevier.com/retrieve/pii/S0018506X13000731.

A. Petrulis and R. E. Johnston. Lesions centered on the medial amygdala impair scent-marking and sex-odor recognition but spare dis-

crimination of individual odors in female golden hamsters. *Behavioral Neuroscience*, 113(2):345–357, 1999. ISSN 0735-7044. doi: 10.1037/0735-7044.113.2.345. URL http://doi.apa.org/getdoi.cfm?doi=10.1037/0735-7044.113.2.345.

A. Pitkänen. Connectivity of the rat amygdaloid complex. In J. P. Aggleton, editor, *The Amygdala: A Functional Analysis*, pages 31–115. Oxford University Press, Oxford, UK, 2000.

A. Pitkänen, L. Stefanacci, C. R. Farb, G.-G. Go, J. E. Ledoux, and D. G. Amaral. Intrinsic connections of the rat amygdaloid complex: Projections originating in the lateral nucleus. *Journal of Comparative Neurology*, 356(2):288–310, may 1995. ISSN 00219967. doi: 10.1002/cne.903560211. URL http://doi.wiley.com/10.1002/cne.903560211.

A. Pitkänen, V. Savander, and J. E. LeDoux. Organization of intra-amygdaloid circuitries in the rat: an emerging framework for understanding functions of the amygdala. *Trends in Neurosciences*, 20 (11):517–523, nov 1997. ISSN 01662236. doi: 10.1016/S0166-2236(97) 01125-9. URL http://linkinghub.elsevier.com/retrieve/pii/S0166223697011259.

J. B. Powers and S. S. Winans. Vomeronasal organ: critical role in mediating sexual behavior of the male hamster. *Science*, 187(4180):961–963, mar 1975. ISSN 0036-8075. doi: 10.1126/science.1145182. URL http://www.sciencemag.org/cgi/doi/10.1126/science.1145182.

J. L. Price, B. M. Slotnick, and M.-F. Revial. Olfactory projections to the hypothalamus. *The Journal of Comparative Neurology*, 306(3):447–461, apr 1991. ISSN 0021-9967. doi: 10.1002/cne.903060309. URL http://doi.wiley.com/10.1002/cne.903060309.

P. Pro-Sistiaga, A. Mohedano-Moriano, I. Ubeda-Bañón, M. del mar Arroyo-Jimenez, P. Marcos, E. Artacho-Pérula, C. Crespo, R. Insausti, and A. Martínez-Marcos. Convergence of olfactory and vomeronasal projections in the rat basal telencephalon. *The Journal of Comparative Neurology*, 504(4):346–362, oct 2007. ISSN 00219967. doi: 10.1002/cne.21455. URL http://doi.wiley.com/10.1002/cne.21455.

S. A. Ramm, S. A. Cheetham, and J. L. Hurst. Encoding choosiness: female attraction requires prior physical contact with individual male scents in mice. *Proceedings of the Royal Society B: Biological Sciences*, 275(1644):1727–1735, aug 2008. ISSN 0962-8452. doi: 10.1098/rspb.2008.0302. URL http://rspb.royalsocietypublishing.org/cgi/doi/10.1098/rspb.2008.0302.

S. Ramón y Cajal. Estudios sobre la corteza cerebral humana. lV. Estructura de la corteza cerebral olfativa del hombre y mamíferos. *Trabajos del Laboratorio de Investigaciones Biológicas*, 1:1–140, 1901.

T. A. Rando, C. W. Bowers, and R. E. Zigmond. Localization of neurons in the rat spinal cord which project to the superior cervical ganglion. *The Journal of comparative neurology*, 196(1):73–83, feb 1981. ISSN 0021-9967. doi: 10.1002/cne.901960107. URL http://doi.wiley.com/10.1002/cne.901960107.

N. Ravel, P. Chabaud, C. Martin, V. Gaveau, E. Hugues, C. Tallon-Baudry, O. Bertrand, and R. Gervais. Olfactory learning modifies the expression of odour-induced oscillatory responses in the gamma (60-90 Hz) and beta (15-40 Hz) bands in the rat olfactory bulb. *European Journal of Neuroscience*, 17(2):350–358, jan 2003. ISSN 0953816X. doi: 10.1046/j.1460-9568.2003.02445.x. URL http://doi.wiley.com/10.1046/j.1460-9568.2003.02445.x.

D. Restrepo, J. Arellano, A. M. Oliva, M. L. Schaefer, and W. Lin. Emerging views on the distinct but related roles of the main and accessory olfactory systems in responsiveness to chemosensory signals in mice. *Hormones and Behavior*, 46(3):247–56, sep 2004. ISSN 0018-506X. doi: 10.1016/j.yhbeh.2004.02.009. URL http://www.ncbi.nlm.nih.gov/pubmed/15325226.

P. Y. Risold and L. W. Swanson. Connections of the rat lateral septal complex. *Brain Research Reviews*, 24(2-3):115–195, sep 1997. ISSN 01650173. doi: 10.1016/S0165-0173(97)00009-X. URL http://linkinghub.elsevier.com/retrieve/pii/S016501739700009X.

S. Rivière, L. Challet, D. Fluegge, M. Spehr, and I. Rodriguez. Formyl peptide receptor-like proteins are a novel family of vomeronasal chemosensors. *Nature*, 459(7246):574–577, may 2009. ISSN 1476-4687. doi: 10.1038/nature08029. URL http://www.nature.com/nature/journal/v459/n7246/pdf/nature08029.pdf.

S. A. Roberts, D. M. Simpson, S. D. Armstrong, A. J. Davidson, D. H. Robertson, L. McLean, R. J. Beynon, and J. L. Hurst. Darcin: a male pheromone that stimulates female memory and sexual attraction to an individual male's odour. *BMC Biology*, 8(1):75, 2010. ISSN 1741-7007. doi: 10.1186/1741-7007-8-75. URL http://www.biomedcentral.com/1741-7007/8/75.

S. A. Roberts, A. J. Davidson, L. McLean, R. J. Beynon, and J. L. Hurst. Pheromonal Induction of Spatial Learning in Mice. *Science*, 338(6113):1462–1465, 2012. ISSN 0036-8075. doi: 10.1126/science.1225638. URL http://www.sciencemag.org/cgi/doi/10.1126/science.1225638.

M. J. F. Robinson, S. M. Warlow, and K. C. Berridge. Optogenetic Excitation of Central Amygdala Amplifies and Narrows Incentive Motivation to Pursue One Reward Above Another. *Journal of Neuroscience*, 34(50):16567–16580, 2014. ISSN 0270-6474. doi: 10.1523/JNEUROSCI.2013-14.2014. URL http://www.jneurosci.org/cgi/doi/10.1523/JNEUROSCI.2013-14.2014.

D. Rojas-Líbano and L. M. Kay. Olfactory system gamma oscillations: The physiological dissection of a cognitive neural system. *Cognitive Neurodynamics*, 2(3):179–194, sep 2008. ISSN 18714080. doi: 10.1007/s11571-008-9053-1. URL http://link.springer.com/article/10.1007/s11571-008-9053-1.

P. R. Romero, C. A. Beltramino, and H. F. Carrer. Participation of the olfactory system in the control of approach behavior of the female rat to the male. *Physiology & Behavior*, 47(4):685–690, apr

1990. ISSN 00319384. doi: 10.1016/0031-9384(90)90078-I. URL http://linkinghub.elsevier.com/retrieve/pii/003193849090078I.

J. B. Rosen, J. M. Hitchcock, C. B. Sananes, M. J. Miserendino, and M. Davis. A direct projection from the central nucleus of the amygdala to the acoustic startle pathway: anterograde and retrograde tracing studies. *Behavioral neuroscience*, 105(6):817–25, dec 1991. ISSN 0735-7044. URL http://www.ncbi.nlm.nih.gov/pubmed/1777104.

E. Salinas and T. J. Sejnowski. Correlated neuronal activity and the flow of neural information. *Nature Reviews Neuroscience*, 2(8):539–550, aug 2001. ISSN 1471-003X. doi: 10.1038/35086012. URL http://www.nature.com/doifinder/10.1038/35086012.

M. Sam, S. Vora, B. Malnic, W. Ma, M. V. Novotny, and L. B. Buck. Odorants may arouse instinctive behaviours. *Nature*, 412(6843):142–142, jul 2001. ISSN 00280836. doi: 10.1038/35084137. URL http://www.nature.com/doifinder/10.1038/35084137.

C. L. Samuelsen and M. Meredith. Categorization of biologically relevant chemical signals in the medial amygdala. *Brain Research*, 1263:33–42, mar 2009. ISSN 00068993. doi: 10.1016/j.brainres.2009.01.048. URL http://linkinghub.elsevier.com/retrieve/pii/S0006899309002236.

C. B. Saper and R. L. Stornetta. Central Autonomic System. In G. Paxinos, editor, *The Rat Nervous System*, chapter Chapter 23, pages 629–673. Elsevier, fourth edi edition, 2015. ISBN 9780123742452. doi: 10.1016/B978-0-12-374245-2.00023-1. URL http://linkinghub.elsevier.com/retrieve/pii/B9780123742452000231.

F. Scalia and S. S. Winans. The differential projections of the olfactory bulb and accessory olfactory bulb in mammals. *Journal of Comparative Neurology*, 161(1):31–55, may 1975. ISSN 10969861. doi: 10.1002/cne.901610105. URL http://doi.wiley.com/10.1002/cne.901610105.

F. Scalia, G. Gallousis, and S. Roca. Differential projections of the main and accessory olfactory bulb in the frog. *Journal of Comparative Neurology*, 305(3):443–461, 1991. ISSN 10969861. doi: 10.1002/cne.903050308.

S. J. Shammah-Lagnado and A. C. Santiago. Projections of the amygdalopiriform transition area (APir): A PHA-L study in the rat. *Annals of the New York Academy of Sciences*, 877:655–660, 1999. ISSN 00778923. doi: 10.1111/j.1749-6632.1999.tb09295.x.

M. W. Shiflett and B. W. Balleine. At the limbic-motor interface: disconnection of basolateral amygdala from nucleus accumbens core and shell reveals dissociable components of incentive motivation. *European Journal of Neuroscience*, 32(10):1735–1743, nov 2010. ISSN 0953816X. doi: 10.1111/j.1460-9568.2010.07439.x. URL http://doi.wiley.com/10.1111/j.1460-9568.2010.07439.x.

J.-W. Shin, J. C. Geerling, and A. D. Loewy. Inputs to the ventrolateral bed nucleus of the stria terminalis. *The Journal of Comparative Neurology*, 511(5):628–657, dec 2008. ISSN 00219967. doi: 10.1002/cne.21870. URL http://doi.wiley.com/10.1002/cne.21870.

R. B. Simerly. WIRED FOR REPRODUCTION: Organization and Development of Sexually Dimorphic Circuits in the Mammalian Forebrain. *Annual Review of Neuroscience*, 25(1):507–536, mar 2002. ISSN 0147-006X. doi: 10.1146/annurev.neuro.25.112701.142745. URL http://www.annualreviews.org/doi/10.1146/annurev.neuro.25.112701.142745.

R. B. Simerly, L. W. Swanson, C. Chang, and M. Muramatsu. Distribution of androgen and estrogen receptor mRNA-containing cells in the rat brain: An in situ hybridization study. *The Journal of Comparative Neurology*, 294(1):76–95, apr 1990. ISSN 0021-9967. doi: 10.1002/cne.902940107. URL http://doi.wiley.com/10.1002/cne.902940107.

B. Slotnick, D. Restrepo, H. Schellinck, G. Archbold, S. Price, and W. Lin. Accessory olfactory bulb function is modulated by input from the main olfactory epithelium. *European Journal of Neuroscience*, 31(6):1108–1116, mar 2010. ISSN 0953816X. doi: 10.1111/j.1460-9568.2010.07141.x. URL http://doi.wiley.com/10.1111/j.1460-9568.2010.07141.x.

M. Spehr, K. R. Kelliher, X.-H. Li, T. Boehm, T. Leinders-Zufall, and F. Zufall. Essential role of the main olfactory system in social recognition of major histocompatibility complex peptide ligands. *The Journal of neuroscience : the official journal of the Society for Neuroscience*, 26(7):1961–70, 2006a. ISSN 1529-2401. doi: 10.1523/JNEUROSCI.4939-05.2006. URL http://www.ncbi.nlm.nih.gov/pubmed/16481428.

M. Spehr, J. Spehr, K. Ukhanov, K. R. Kelliher, T. Leinders-Zufall, and F. Zufall. Parallel processing of social signals by the mammalian main and accessory olfactory systems. *Cellular and Molecular Life Sciences*, 63(13):1476–1484, 2006b. ISSN 1420682X. doi: 10.1007/s00018-006-6109-4.

M. Spehr, J. Spehr, K. Ukhanov, K. R. Kelliher, T. Leinders-Zufall, and F. Zufall. Signaling in the Chemosensory Systems. *Cellular and Molecular Life Sciences*, 63(13):1476–1484, 2006c. ISSN 1420-682X. doi: 10.1007/s00018-006-6109-4. URL http://link.springer.com/10.1007/s00018-006-6109-4.

P. Stockley, L. Bottell, and J. L. Hurst. Wake up and smell the conflict: odour signals in female competition. *Philosophical transactions of the Royal Society of London. Series B, Biological sciences*, 368(1631):20130082, 2013. ISSN 1471-2970. doi: 10.1098/rstb.2013.0082. URL http://dx.doi.org/10.1098/rstb.2013.0082.

G. D. Stuber, D. R. Sparta, A. M. Stamatakis, W. A. van Leeuwen, J. E. Hardjoprajitno, S. Cho, K. M. Tye, K. A. Kempadoo, F. Zhang, K. Deisseroth, and A. Bonci. Excitatory transmission from the amygdala

to nucleus accumbens facilitates reward seeking. *Nature*, 475(7356): 377–380, jun 2011. ISSN 0028-0836. doi: 10.1038/nature10194. URL http://www.nature.com/doifinder/10.1038/nature10194.

J. Swann, C. Fabre-Nys, and R. Barton. Hormonal and Pheromonal Modulation of the Extended Amygdala: Implications for Social Behavior. In *Hormones, Brain and Behavior*, pages 441–474. Elsevier, 2009. ISBN 9780080887838. doi: 10.1016/B978-008088783-8. 00012-7. URL http://linkinghub.elsevier.com/retrieve/pii/B9780080887838000127.

L. W. Swanson. Cerebral hemisphere regulation of motivated behavior. *Brain research*, 886(1-2):113–164, dec 2000. ISSN 0006-8993. doi: 10.1016/S0006-8993(00)02905-X. URL http://linkinghub.elsevier.com/retrieve/pii/S000689930002905X.

L. W. Swanson and G. D. Petrovich. What is the amygdala? *Trends in Neurosciences*, 21(8):323–331, aug 1998. ISSN 01662236. doi: 10.1016/S0166-2236(98)01265-X. URL http://linkinghub.elsevier.com/retrieve/pii/S016622369801265X.

L. K. Takahashi. Olfactory systems and neural circuits that modulate predator odor fear. *Frontiers in behavioral neuroscience*, 8:72, mar 2014. ISSN 1662-5153. doi: 10.3389/fnbeh.2014. 00072. URL http://journal.frontiersin.org/article/10.3389/fnbeh.2014.00072/abstract.

L. K. Takahashi, D. T. Hubbard, I. Lee, Y. Dar, and S. M. Sipes. Predator odor-induced conditioned fear involves the basolateral and medial amygdala. *Behavioral Neuroscience*, 121(1):100–110, 2007. ISSN 1939-0084. doi: 10.1037/0735-7044.121.1.100. URL http://doi.apa.org/getdoi.cfm?doi=10.1037/0735-7044.121.1.100.

K. Taniguchi, S. Saito, T. Oikawa, and K. Tanigushi. Phylogenic Aspects of the Amphibian Dual Olfactory System. *Journal of Veterinary Medical Science*, 70(1):1–9, 2008. ISSN 0916-7250. doi: 10.1292/jvms.70. 1. URL http://joi.jlc.jst.go.jp/JST.JSTAGE/jvms/70.1?from=CrossRef.

A. Tendler and S. Wagner. Different types of theta rhythmicity are induced by social and fearful stimuli in a network associated with social memory. *eLife*, 4(4):1–22, 2015. ISSN 2050084X. doi: 10.7554/eLife.03614.

R. Tirindelli, C. Mucignat-Caretta, and N. J. Ryba. Molecular aspects of pheromonal communication via the vomeronasal organ of mammals. *Trends in Neurosciences*, 21(11):482–486, nov 1998. ISSN 01662236. doi: 10.1016/S0166-2236(98)01274-0. URL http://linkinghub.elsevier.com/retrieve/pii/S0166223698012740.

C. Torrence and G. P. Compo. A Practical Guide to Wavelet Analysis. *Bulletin of the American Meteorological Society*, 79(1):61–78, 1998. ISSN 00030007. doi: 10.1175/1520-0477(1998)079<0061:APGTWA>2.0.CO; 2.

A. B. L. Tort, R. Komorowski, H. Eichenbaum, and N. Kopell. Measuring Phase-Amplitude Coupling Between Neuronal Oscillations of Different Frequencies. *Journal of Neurophysiology*, 104(2):1195–1210, aug 2010. ISSN 0022-3077. doi: 10.1152/jn.00106.2010. URL http://jn.physiology.org/cgi/doi/10.1152/jn.00106.2010.

M. Toth, T. Fuzesi, J. Halasz, A. Tulogdi, and J. Haller. Neural inputs of the hypothalamic "aggression area" in the rat. *Behavioural Brain Research*, 215(1):7–20, 2010. ISSN 01664328. doi: 10.1016/j.bbr.2010.05.050. URL http://www.sciencedirect.com/science/article/pii/S0166432810004249.

D. Trotier and K. B. Doving. "Anatomical description of a new organ in the nose of domesticated animals" by Ludvig Jacobson (1813). *Chemical Senses*, 23(6):743, 1998. ISSN 0379-864X. doi: 10.1093/chemse/23.6.743.

I. Ubeda-Bañón, A. Novejarque, A. Mohedano-Moriano, P. Pro-Sistiaga, R. Insausti, F. Martínez-García, E. Lanuza, and A. Martínez-Marcos. Vomeronasal inputs to the rodent ventral striatum. *Brain Research Bulletin*, 75(2-4):467–473, mar 2008. ISSN 03619230. doi: 10.1016/j.brainresbull.2007.10.028. URL http://linkinghub.elsevier.com/retrieve/pii/S0361923007003334.

I. Ubeda-Bañón, P. Pro-Sistiaga, A. Mohedano-Moriano, D. Saiz-Sanchez, C. de la Rosa-Prieto, N. Gutiérrez-Castellanos, E. Lanuza, F. Martínez-García, and A. Martínez-Marcos. Cladistic analysis of olfactory and vomeronasal systems. *Frontiers in neuroanatomy*, 5(January):3, 2011. ISSN 1662-5129. doi: 10.3389/fnana.2011.00003. URL http://journal.frontiersin.org/article/10.3389/fnana.2011.00003/abstract.

P. S. Ulinski. *Dorsal ventricular ridge: a treatise on forebrain organization in reptiles and birds*. WILEY SERIES in NEUROBIOLOGY Series. John Wiley & Sons, Incorporated, 1983. ISBN 9780471876120. URL https://books.google.es/books?id=yyOLAAAAIAAJ.

K. G. Usunoff, O. Schmitt, D. E. Itzev, S. J.-P. Haas, N. E. Lazarov, A. Rolfs, and A. Wree. Efferent projections of the anterior and posterodorsal regions of the medial nucleus of the amygdala in the mouse. *Cells Tissues Organs*, 190(5):256–85, jan 2009. ISSN 1422-6421. doi: 10.1159/000209233. URL http://www.karger.com/doi/10.1159/000209233.

J. R. Vale, D. Ray, and C. A. Vale. Interaction of genotype and exogenous neonatal estrogen: Aggression in female mice. *Physiology & Behavior*, 10(2):181–183, jul 1973. ISSN 00319384. doi: 10.1016/0031-9384(73)90294-1. URL http://doi.wiley.com/10.1002/dev.420060405.

J. R. Vale, D. Ray, and C. A. Vale. Neonatal Adrogen Treatment and Sexual Behavior in Males of Three Inbred Strains of Mice. *Developmental Psychobiology*, 7(March):483–488, sep 1974. ISSN 10982302. doi: 10.1002/dev.420070512. URL http://doi.wiley.com/10.1002/dev.420070512.

F. J. Varela, J. P. Lachaux, E. Rodriguez, and J. Martinerie. The brain-web: phase synchronization and large-scale integration. *Nature reviews. Neuroscience*, 2(4):229–239, 2001. ISSN 1471-003X. doi: 10.1038/35067550. URL http://www.ncbi.nlm.nih.gov/pubmed/11283746.

V. Vargas-Barroso, B. Ordaz-Sánchez, F. Peña-Ortega, and J. A. Larriva-Sahd. Electrophysiological Evidence for a Direct Link between the Main and Accessory Olfactory Bulbs in the Adult Rat. *Frontiers in Neuroscience*, 9:518, jan 2016. ISSN 1662-453X. doi: 10.3389/fnins.2015.00518. URL http://journal.frontiersin.org/Article/10.3389/fnins.2015.00518/abstract.

J. V. Verhagen, D. W. Wesson, T. I. Netoff, J. A. White, and M. Wachowiak. Sniffing controls an adaptive filter of sensory input to the olfactory bulb. *Nature neuroscience*, 10(5):631–639, 2007. ISSN 1097-6256. doi: 10.1038/nn1892.

R. P. Vertes. Differential projections of the infralimbic and prelimbic cortex in the rat. *Synapse*, 51(1):32–58, jan 2004. ISSN 0887-4476. doi: 10.1002/syn.10279. URL http://doi.wiley.com/10.1002/syn.10279.

R. P. Vertes and W. B. Hoover. Projections of the paraventricular and paratenial nuclei of the dorsal midline thalamus in the rat. *The Journal of Comparative Neurology*, 508(2):212–237, may 2008. ISSN 00219967. doi: 10.1002/cne.21679. URL http://doi.wiley.com/10.1002/cne.21679.

R. P. Vertes, W. B. Hoover, A. C. Do Valle, A. Sherman, and J. Rodriguez. Efferent projections of reuniens and rhomboid nuclei of the thalamus in the rat. *The Journal of Comparative Neurology*, 499(5):768–796, dec 2006. ISSN 00219967. doi: 10.1002/cne.21135. URL http://doi.wiley.com/10.1002/cne.21135.

H. Von Campenhausen and K. Mori. Convergence of segregated pheromonal pathways from the accessory olfactory bulb to the cortex in the mouse. *European Journal of Neuroscience*, 12(1):33–46, jan 2000. ISSN 0953816X. doi: 10.1046/j.1460-9568.2000.00879.x. URL http://doi.wiley.com/10.1046/j.1460-9568.2000.00879.x.

M. Wachowiak. All in a Sniff: Olfaction as a Model for Active Sensing. *Neuron*, 71(6):962–973, 2011. ISSN 08966273. doi: 10.1016/j.neuron.2011.08.030. URL http://linkinghub.elsevier.com/retrieve/pii/S0896627311007859.

M. Wachowiak and L. B. Cohen. Representation of odorants by receptor neuron input to the mouse olfactory bulb. *Neuron*, 32(4):723–735, 2001. ISSN 08966273. doi: 10.1016/S0896-6273(01)00506-2.

E. Wada, R. Shigemoto, A. Kinoshita, H. Ohishi, and N. Mizuno. Metabotropic glutamate receptor subtypes in axon terminals of projection fibers from the main and accessory olfactory bulbs: A light and electron microscopic immunohistochemical study in the rat. *The Journal of Comparative Neurology*, 393(4):493–504, apr 1998. ISSN 0021-9967. doi: 10.1002/

(SICI)1096-9861(19980420)393:4<493::AID-CNE8>3.0.CO;2-W.
URL   http://doi.wiley.com/10.1002/%28SICI%291096-9861%
2819980420%29393%3A4%3C493%3A%3AAID-CNE8%3E3.0.CO%3B2-W.

D. L. Walker, G. Y. Paschall, and M. Davis. Glutamate receptor ant-
agonist infusions into the basolateral and medial amygdala reveal
differential contributions to olfactory vs. context fear conditioning
and expression. *Learning & Memory*, 12(2):120–9, mar 2005. ISSN
1072-0502. doi: 10.1101/lm.87105. URL http://www.learnmem.org/
cgi/doi/10.1101/lm.87105.

Z. Wang, N. A. Bullock, and G. J. De Vries. Sexual differentiation
of vasopressin projections of the bed nucleus of the stria termin-
als and medial amygdaloid nucleus in rats. *Endocrinology*, 132
(6):2299–2306, jun 1993. ISSN 0013-7227. doi: 10.1210/en.132.6.
2299. URL https://academic.oup.com/endo/article-lookup/doi/
10.1210/en.132.6.2299.

W. I. Welker. Analysis of Sniffing of the Albino Rat. *Beha-
viour*, 22(3):223–244, jan 1964. ISSN 0005-7959. doi: 10.1163/
156853964X00030. URL http://booksandjournals.brillonline.
com/content/10.1163/156853964x00030.

D. W. Wesson and D. A. Wilson. Smelling Sounds: Olfactory-Auditory
Sensory Convergence in the Olfactory Tubercle. *Journal of Neur-
oscience*, 30(8):3013–3021, 2010. ISSN 0270-6474. doi: 10.1523/
JNEUROSCI.6003-09.2010. URL http://www.jneurosci.org/cgi/
doi/10.1523/JNEUROSCI.6003-09.2010.

D. W. Wesson and D. A. Wilson. Sniffing out the contributions
of the olfactory tubercle to the sense of smell: Hedonics, sens-
ory integration, and more? *Neuroscience and Biobehavioral Re-
views*, 35(3):655–668, jan 2011. ISSN 01497634. doi: 10.1016/
j.neubiorev.2010.08.004. URL http://linkinghub.elsevier.com/
retrieve/pii/S0149763410001338.

D. W. Wesson, R. M. Carey, J. V. Verhagen, and M. Wachowiak. Rapid
encoding and perception of novel odors in the rat. *PLoS Biology*, 6(4):
717–729, 2008. ISSN 15449173. doi: 10.1371/journal.pbio.0060082.

S. S. Winans and F. Scalia. Amygdaloid Nucleus: New Afferent Input
from the Vomeronasal Organ. *Science*, 170(3955):330–332, oct 1970.
ISSN 0036-8075. doi: 10.1126/science.170.3955.330. URL http://
www.sciencemag.org/cgi/doi/10.1126/science.170.3955.330.

R. I. Wood and J. M. Swann. The bed nucleus of the stria terminalis
in the Syrian hamster: subnuclei and connections of the posterior
division. *Neuroscience*, 135(1):155–79, jan 2005. ISSN 0306-4522. doi:
10.1016/j.neuroscience.2005.05.029. URL http://www.ncbi.nlm.nih.
gov/pubmed/16084647.

R. I. Wood, R. K. Brabec, J. M. Swann, and S. W. Newman. Androgen
and estrogen concentrating neurons in chemosensory pathways of
the male Syrian hamster brain. *Brain Research*, 596(1-2):89–98, nov
1992. ISSN 00068993. doi: 10.1016/0006-8993(92)91536-N. URL http:
//linkinghub.elsevier.com/retrieve/pii/000689939291536N.

F. G. Wouterlood and W. Härtig. Calretinin-immunoreactivity in mitral cells of the rat olfactory bulb. *Brain Research*, 682(1-2):93–100, jun 1995. ISSN 00068993. doi: 10.1016/0006-8993(95)00326-L. URL http://linkinghub.elsevier.com/retrieve/pii/000689939500326L.

C. J. Wysocki, J. L. Wellington, and G. K. Beauchamp. Access of urinary nonvolatiles to the mammalian vomeronasal organ. *Science*, 207(4432):781–783, feb 1980. ISSN 0036-8075. doi: 10.1126/science.7352288. URL http://www.ncbi.nlm.nih.gov/pubmed/7352288.

F. Xu, M. Schaefer, I. Kida, J. Schafer, N. Liu, D. L. Rothman, F. Hyder, D. Restrepo, and G. M. Shepherd. Simultaneous activation of mouse main and accessory olfactory bulbs by odors or pheromones. *The Journal of Comparative Neurology*, 489(4):491–500, sep 2005. ISSN 0021-9967. doi: 10.1002/cne.20652. URL http://doi.wiley.com/10.1002/cne.20652.

M. Yang, H. Augustsson, C. M. Markham, D. T. Hubbard, D. Webster, P. M. Wall, R. J. Blanchard, and D. C. Blanchard. The rat exposure test: A model of mouse defensive behaviors. *Physiology & Behavior*, 81(3):465–473, may 2004. ISSN 00319384. doi: 10.1016/j.physbeh.2004.02.010. URL http://linkinghub.elsevier.com/retrieve/pii/S003193840400054X.

K. Yoshikawa, H. Nakagawa, N. Mori, H. Watanabe, and K. Touhara. An unsaturated aliphatic alcohol as a natural ligand for a mouse odorant receptor. *Nature chemical biology*, 9(3):160–2, jan 2013. ISSN 1552-4469. doi: 10.1038/nchembio.1164. URL http://www.nature.com/doifinder/10.1038/nchembio.1164.

S. L. Youngentob, M. M. Mozell, P. R. Sheehe, and D. E. Hornung. A quantitative analysis of sniffing strategies in rats performing odor detection tasks. *Physiology and Behavior*, 41(1):59–69, 1987. ISSN 00319384. doi: 10.1016/0031-9384(87)90131-4.

F. Zufall and T. Leinders-Zufall. Mammalian pheromone sensing. *Current Opinion in Neurobiology*, 17(4):483–489, aug 2007. ISSN 09594388. doi: 10.1016/j.conb.2007.07.012. URL http://linkinghub.elsevier.com/retrieve/pii/S0959438807000955.

I. Zuri and M. Halpern. Differential effects of lesions of the vomeronasal and olfactory nerves on garter snake (Thamnophis sirtalis) responses to airborne chemical stimuli. *Behavioral Neuroscience*, 117(1):169–183, 2003. ISSN 0735-7044. doi: 10.1037/0735-7044.117.1.169. URL http://doi.apa.org/getdoi.cfm?doi=10.1037/0735-7044.117.1.169.